

ORGANOSCANDIUM COMPLEXES AS MECHANISTIC PROBES IN THE  
ZIEGLER-NATTA POLYMERIZATION OF  $\alpha$ -OLEFINS AND DIENES

Thesis by  
W. Donald Cotter

In Partial Fulfillment of the Requirements  
for the Degree of  
Doctor of Philosophy

California Institute of Technology  
Pasadena, CA

1993

(Submitted December 11, 1992)

*For Deborah Pyle*



## FEAR AND TREMBLING

The sun now angles downward, and southward.  
The summer, that is, approaches its final fulfillment.  
The forest is silent, no wind-stir, bird-note, or word.  
It is time to reflect on what the season has meant.

But what is the meaningful language for such meditation?  
What is a word but wind through the tube of the throat?  
Who defines the relation between the word *sun* and the sun?  
What word has glittered on whitecap? Or lured blossom out?

Walk deeper, foot soundless, into the forest.  
Stop, breath bated. Look southward, and up, where high leaves  
Against sun, in vernal translucence, yet glow with the freshest  
Young tint of the lost spring. Here now nothing grieves.

Can one, in fact, meditate in the heart, rapt and wordless?  
Or find his own voice in the towering gust now from northward?  
When boughs toss—is it in joy or pain and madness?  
The gold leaf—is it whirled in anguish or ecstasy skyward?

Can the heart's meditation wake us from life's long sleep,  
And instruct us how foolish and fond was our labor spent—  
Us who now know that only at death of ambition does the deep  
Energy crack crust, spurt forth and leap

From grottoes, dark—and from the caverned enchainment?

Robert Penn Warren

## ACKNOWLEDGEMENTS

I have perceiv'd that to be with those I like is enough,  
 To stop in company with the rest at evening is enough,  
 ...  
 All things please the soul well, but these please the soul well.

Walt Whitman  
 "I Sing the Body Electric"

**Warning to the Consumer:** I'm not going to make any attempt to keep this section brief. As it began to get long, I decided to stick it in back of the thesis so that it could be easily avoided by the general reader. Unfortunately, the powers that be nixed this idea, so you have that many more pages to flip through up front. Sorry, but that's just the way it has to be. I promise not to be offended if you don't wade through it. This section is for me and, frankly, I intend to indulge myself. Shamelessly.

By my estimate, I walked my 500th mile in the Sierra Nevada sometime on Labor Day of this year, in the company of LeRoy Whinnery and Jim Toth. It seems appropriate to mention this at the beginning of this section, since my thoughts about many of the people who have contributed to my scientific and personal life at Caltech are tied to my thoughts about those mountains, and it was hard not to feel a certain sense of completeness upon reaching what I considered a significant personal milestone (the number 500 when applied to miles has a set of folk song-like connotations which I find appealing) in the company of two of the people with whom I first experienced the Sierra Nevada. *That* was five summers ago now, and I can still remember my fellow novice Jim rather pathetically asking John Bercaw, as we were all being mercilessly pelted with cold rain and hail on our first evening out, "It doesn't get any worse than this, does it?" Well—"No, it doesn't," was John's appropriate response though, as I (and, I'm sure, Jim) learned very quickly, it does get much, much better.

My own memories of that first day in the Sierras actually center less now on the miserable weather than on a magnificent view of Shadow Lake from Agnew Meadows, with the rain making the air in the gorge between almost translucent rather than transparent, and washing everything with a uniform gray tint which

made that lake much more beautiful, I imagined, than it could possibly be in the sunlight. I remember suggesting something to that effect to John, and if he was paying attention this may have been his first real clue that, as he has started to tell me with some frequency in the last several months, I'm something of a romantic. Well, that may be, but by introducing me to the Sierra Nevada, John has certainly given that tendency toward romanticism an awful lot of fuel. I mention all this (since this is nominally an acknowledgements section and not a travel memoir) because it illuminates part of why I am so grateful to have had John Bercaw as my thesis advisor and mentor for the last five years. Life is bigger than science, and the ability to comprehend that the image of a weather-beaten subalpine lake can carry at least as much meaning as an isotope effect, and to somehow convey a rich appreciation of each which does not exclude the other--that to me is one of John's real strengths. If I have been able to learn from John--and I think I have--it is because I have always been able to like and admire him.

The aforementioned LeRoy taught me high-vacuum techniques back in the old days when 213 was a two-man lab. Regrettably, not even LeRoy, an extremely orderly person who always carried spare flashlight bulbs on the trail, could curb my tendency toward slovenliness in lab, but I hope I learned well from him otherwise. LeRoy also taught me a lot about organizing and leading backpacking trips, though I was to learn the really important lessons, as one always does, through my own mistakes. Mark Treeeeeeimmer introduced me to the arcane mysteries of the IBM-PC; a decidedly mixed blessing (thank God for the Macintosh!). Trim was eventually among those who suffered for my enthusiasm on the first group hike I put together on my own, the Emigrant-to-Hetch Hetchy hike (a.k.a. "Bataan Death March"--which *should* have been the Emigrant-to-Tuolumne trip; not that I'm bitter or anything), so I may have gotten some of my own back in the long run . . . LeRoy and Trim may not remember this, but the night after my entering class took our placement exams, I found myself in the Ath shooting tequila with the two of them and Claudia Barner. I have never considered it coincidental that I subsequently wound up in the Bercaw group (EQG, if you've read this far: it's all *their* fault).

Marty St. Clair, whose puns were worse than mine, Claudia Barner, who had the grace to laugh at our puns, and I occupied the northeast corner of the clubhouse,

back when it was a proper office, as opposed to a garden maze. Ged Parkin, the *enfant terrible* of organometallic chemistry, taught me that one can in fact handle organoscandium complexes using Schlenk techniques. Kaspar Evertz, who joined up soon after I did, was a good friend, and Helmut (f\*\*king kripple!) Schmidt introduced me to the aromatic wonders of Pernod. Pat Anderson pretends to be amused by me, which always makes me feel better. Among latter-day Bercavians (Bercawites? Cheese-heads?) to whom I owe particular debts (aside from the literal ones to the coffee and soda clubs) are Tim Herzog, who did some  $^2\text{H}$ -NMR work I refer to in Chapter 5 and graciously gave me a mL of deuterium-labeled hexadiene, and Gerrit Luinstra, who encouraged me to do the labeled isobutyl experiments in Chapter 6 when I was seriously tempted to just cut my losses and write up. Eugene Mueller shocked me by being an even more ruthless proofreader than I am—probably a more helpful one, too. Sharad Hajela, besides putting up with me as a suck-buddy for the last few months, helped me deal with the ugly bureaucratic hoops I had to jump through after I totaled my car—a favor I have not forgotten. Last (in this paragraph) but not least, Andy Kiely taught me that there is adequate whisky distilled on *both* sides of the Atlantic. I think we all know where the world's finest gin is distilled, and I'm counting on Andy to keep the tradition alive.

If there's an incarnation of the Bercaw group that I have missed the most keenly, it's the one which more or less existed during my second and third years, when I was blessed with the company and friendship of Warren, Marrian, and Jeff "mon petit chou-chou" Piers, Sally Proshek and especially John Power. I have no clever remarks with which to summarize the extent of my personal indebtedness and affection for them. They have left me wordless.

Over in the Lewis group or thereabouts, Gail Ryba, Teri Longin, and Gary and Nancy "the pine cone lady" Shreve have been good hiking companions and good friends. Is there a difference, guys? Gary and Nancy provided many of us with a warm home every year at Thanksgiving. Teri aspires to be a "crazy cat lady," and she will succeed unless she winds up living next door to Gail! I hope Bruce Tufts knows what I mean when I thank him for doing the dishes! Sonbinh Nguyen sets an example for me up to which I cannot live but which I cherish nevertheless.

The Kaweah Gap is the most beautiful place on earth. Few people know this, and I wouldn't know it either if it were not for Jim Toth and Dave Wheeler. Dave's a hard person to impress, or at least he wants you to think so. So when Dave and Jim came back from the Gap one summer raving about its equivalency to Yosemite Valley, one had to take it seriously. Dave also taught me my first lessons in practical NMR, and tried to instill in me a skepticism about the inherent accuracy of NMR integrations which, as a few of the chapters of this thesis will attest, did not entirely take—to my sorrow. Along with LeRoy and Trim, Dave and Jim were probably the older (no offense intended, Jim) graduate students I most looked up to as a first-year . . . well, what can I say? I was young and foolish then. . . .

Pat Kearney, my roommate for four years at the Starlite Villa (where Gig looks just like Phyllis Dilla), got off to an inauspicious start in the Sierras (at least the water in Pioneer Basin was less *invigorating* than the water at Rock Creek trailhead), but these days he is able to dust me if he so chooses. I'm sure it can't have been easy putting up with a roommate like me, and I'm grateful for the fact that our friendship survived that pressure. I've certainly relied on it over the years. The first time I ever saw Kaweah Gap and Hamilton Lakes, it was with Pat. I think that probably says as much as anything.

The Metastable Mountaineers are gone now, and I suppose there's no point in mourning their passing. But Dean Willberg, Elizabeth Burns, Gene Spears, K.-T. Lim, Josh Jacobs, Pat Kearney and I (not to mention the innocent victims we literally led to Hell and back) had a lot of good times in the San Gabriel mountains back in our first year. I regret never having been to the Sierras with Dean, but we have been to Point Sal a few times over the years, haven't we? That counts for much. And Gene, wherever you are, I hope your delognish always remains deleaved down. And that's a whump!

I'll miss the real musical fellowship of the Cantores Atri Mortis and Byrd's Recusants. I don't think my wildest imaginings about Caltech would have included a group of people who just liked to hang around, drink beer and sing 15th- and 16th-century choral music! It was really something else. I'm grateful for Helen Johnston's knowledge, taste and dedication, which kept us going for so long. I think Joel Schwartz, aka Smog-man, finally knows the difference between a madrigal and a motet. Chris Tinney's oddly refreshing cynicism and



Jamie Schlessman's mothering instincts have been welcome, if contrasting, sources of succor. Neill Reid and I spent the last several months working together on a set of folksong arrangements (I use the term somewhat loosely). Since I've gone and broken my finger, it remains unclear that we'll ever perform them, but with that kind of music more than any other, perhaps, the real rewards lie not in who hears you but in the pleasure of making music with a friend.

Don Caldwell and Frank Brownstead provided me with opportunities to sing in more formalized environments. I'm grateful to each of them--to Don, perhaps more than anything, for tolerating my increasing acerbity and decreasing reliability as I became more desperate to finish my research, and to Frank and the St. Philip's choir for providing a real refuge from the environs and attitudes of Caltech.

I'm several pages in and have wandered well away from the Bercaw group. One builds up so many personal debts over the course of five years. . . What sort of a debt, then, does one build up over eight years? It's hard to measure, but that's how long I've been privileged to know and work with Bryan Coughlin. I have come to take his companionship and his deeply intuitive chemical sense almost for granted, and I really cannot imagine what life will be like without him nearby. Roger Quan, who is the nicest man in chemistry, put up with me in 213 for more than two years. His facility at ordering dim sum is only one of the traits which have made it so great to have him for a lab-mate. Pirate Radio, less so! Gui Bazan was highly unusual and, usually, obscure. An enigma, you might say. He and Marie O'Regan did much to make the last two years tolerable (Thank God one of them is rational--no, Gui, it's not you). Viva Señor Fish!

Strictly speaking, Jay Labinger is not, I suppose, a member of the Bercaw group, but that has not prevented many of us--myself quite obviously included--from benefiting from his knowledge and insight. I owe him particular thanks for help with the quantitative analyses in Chapters 2, 3, and 6. Frankly, I owe him a no less important debt for exemplifying the extent to which one can be a scientist and retain the generalist's perspective--an example I hope to be able to emulate to some degree.

Of course, I picked up an early sense of that possibility from Gene Wubbels, Luther Erickson, and Jim Swartz years ago at Grinnell College, but that--thank

God!--is a different world entirely. I guess the trick now is to see if I can find my way back to that world (*Auntie Em! Auntie Em!*). . . Speaking of Grinnell, it is somewhat paradoxical but nevertheless true that I would not have finished this degree had it not been for Ellen Mease's encouragement and willingness to support me regardless of the directions my intellectual development has taken. If I make it back to where I want to be, it will also be due to the encouragement I've received from Harry Gray.

I have always been thankful for the love and support of my family (which means you, too, MR), though like most sons, grandsons and brothers I am sure I have too frequently taken them for granted. The value my parents always placed on education has perhaps helped them to understand what I've been up to out here. If I still believe that education has a redemptive value for the life of an individual, I owe the germ of that belief to them and to the people who taught me science in high school--my father, Ken Kramme, and Deborah Pyle. Pyle, I cannot express how deeply I wish you could be reading this.

Oops . . . oh, yeah--money. I was supported at various times by the National Science Foundation, the Department of Education, and Amoco. During the last year or so, I've been supported by the John Bercaw "Get the Hell Out of My Labs and Start Your Life" Scholarship Fund. I am very grateful for all of this.

**Abstract:** Measurement of the molecular-weight distributions of alkanes prepared by treatment of permethylscandocene alkyl complexes at  $-78^{\circ}\text{C}$  reveals that under the reaction conditions the reaction may be described as "living."

The stoichiometric insertion of 2-butyne across the scandium-carbon  $\sigma$ -bond in  $\text{Cp}^*_2\text{ScCH}_3$  proceeds without a visible kinetic deuterium isotope effect, either for substitution at the alkyne methyl groups or at the scandium-methyl group. The first result reveals that steric isotope effects are not important in this reaction, which models the propagation step in Ziegler-Natta polymerization. The second result suggests that an  $\alpha$ -agostic interaction is likely not present in the transition state for 2-butyne insertion.

The polymerization of conjugated dienes with organoscandium complexes of the type  $[(\eta^5\text{-C}_5\text{Me}_4)\text{SiMe}_2\text{NCMe}_3]\text{ScR}]_2$  ( $\text{R} = n\text{-propyl}, n\text{-butyl}$ ) leads to polymers with very narrow molecular-weight distributions and microstructures rich in 1,2-repeat units and an unusual cyclic repeat unit derived from two sequential 1,2-insertions. The 1,4-repeat unit characteristic of rubber account for about 40 mass-% of the products. Allyl complexes are readily prepared from treatment of alkylscandium complexes with conjugated dienes, or from treatment of the scandium hydride complex  $[(\eta^5\text{-C}_5\text{Me}_4)\text{SiMe}_2\text{NCMe}_3]\text{ScH}(\text{PMe}_3)_2$  with allenes. This hydride complex, however, reacts with butadiene to form an ethylene-bridged complex and ethane.

Both the hydride complex  $[(\eta^5\text{-C}_5\text{Me}_4)\text{SiMe}_2\text{NCMe}_3]\text{ScH}(\text{PMe}_3)_2$  and the alkyl complex  $[(\eta^5\text{-C}_5\text{Me}_4)\text{SiMe}_2\text{NCMe}_3]\text{Sc}(\text{CH}_2\text{CH}_2\text{CH}_3)_2$  catalyze the cyclopolymerization of 1,5-hexadiene. Although polymers with narrow molecular weight distributions (1.1-1.2) can be obtained, the polydispersity index is very sensitive to the presence of trimethylphosphine and, to a lesser extent, to the nature of the initiating group. Chain-transfer processes could not be studied directly due to deleterious reactivity with scandium-hydride trapping reagents. Cyclopolymerization is not accompanied by a measurable  $\alpha$  deuterium isotope effect on the cyclization step, which suggests that trans-fused [5,4]-bicyclic transition states are allowed for this step.

Variable-temperature NMR spectroscopy was used to examine the dynamic solution behavior of several *ansa*-(cyclopentadienyl)amidoscandium alkyl complexes. On the basis of these studies, it is proposed that the primary equilibrium when trimethylphosphine is present is between a phosphine-bound scandium alkyl and a free, 12-electron monomeric scandium alkyl.



## TABLE OF CONTENTS

|   |     |
|---|-----|
| Acknowledgements  | iii |
| Abstract  | ix  |
| Table of Contents   | x   |
| List of Figures   | xi  |
| List of Tables  | xiv |
| Chapter 1: Introduction   | 1   |
| Chapter 2: Ethylene Oligomerization by Permethylscandocene<br>Complexes. Product Studies of Ethylene Oligomers  | 11  |
| Chapter 3: Investigations of the Magnitude of Steric and $\alpha$ Deuterium<br>Isotope Effects in a Carbon-Carbon Bond Forming Reaction<br>of a Permethylscandocene Complex | 28  |
| Chapter 4: Polymerization of Conjugated Dienes with (Cyclopentadienyl)-<br>amidoscandium Alkyl Complexes  | 53  |
| Chapter 5: Studies in the Mechanism of 1,5-Hexadiene<br>Cyclopolymerization by Single-component Organoscandium<br>Catalysts   | 87  |
| Chapter 6: Examination of the Solution Dynamics of Intermediates in<br>Organoscandium-catalyzed Ziegler-Natta Polymerization  | 130 |

## LIST OF FIGURES

## CHAPTER 2

- Figure 1.** (a) Sample chromatogram of alkane standards 16  
 (b) Sample chromatogram of reaction mixture
- Figure 2.** Molecular weight distribution of alkanes prepared by treatment 17  
 of **3** with varying amounts of ethylene
- Figure 3.** Molecular weight distribution of alkanes prepared by treatment 17  
 of **1** and **3** with approximately equal amounts of ethylene
- Figure 4.** Molecular weight distribution of alkanes prepared by treatment 18  
 of **2** with two equivalents of ethylene

## CHAPTER 3

- Figure 1.** Methane isotopomer composition as a function of C-H/C-D 42  
 bending ratios
- Figure 2.** Methane isotopomer composition as a function of C-H/C-D 43  
 stretching ratios

## CHAPTER 4

- Figure 1.** Gel permeation chromatograph of polydienes prepared with 61  
 scandium alkyl complex **2**
- Figure 2.** Partial  $^1\text{H}$ -NMR of polybutadiene showing the olefinic region 64
- Figure 3.** Partial  $^1\text{H}$ -NMR of the product of reaction between 73  
 $\text{Cp}^*_2\text{ScD}(\text{THF})$  and butadiene

## CHAPTER 5

- Figure 1.** Gel permeation chromatographs of poly(hexadiene) prepared 91  
 with **1** as catalyst precursor

|  |     |
|--|-----|
| <b>Figure 2.</b> Gel permeation chromatograph of poly(hexadiene) prepared with <b>2</b> as catalyst precursor  | 93  |
| <b>Figure 3.</b> Gel permeation chromatographs of poly(hexadiene) prepared with <b>3</b> (a) and <b>3</b> + PMe <sub>3</sub> (b) as catalyst precursor                 | 94  |
| <b>Figure 4.</b> <sup>13</sup> C{ <sup>1</sup> H}-NMR spectrum of low-dispersity poly(hexadiene)   | 96  |
| <b>Figure 5.</b> Monomer consumption kinetics for 1,5-hexadiene and 1-pentene with scandium hydride <b>1</b> at T = 31 ± 1°C   | 100 |
| <b>Figure 6.</b> Partial <sup>13</sup> C{ <sup>1</sup> H}-NMR spectra of (a) deuterated and (b) undeuterated polymers  | 109 |
| <b>CHAPTER 6</b>   |     |
| <b>Figure 1a.</b> Dependence of polymerization rate on catalyst concentration  | 133 |
| <b>Figure 1b.</b> Dependence of polymerization rate on catalyst concentration, with restored data points   | 135 |
| <b>Figure 2.</b> <sup>1</sup> H-NMR spectrum of <b>4</b> at -60°C  | 137 |
| <b>Figure 3.</b> <sup>1</sup> H-NMR spectrum of <b>4</b> + one equivalent PMe <sub>3</sub> at -85°C  | 137 |
| <b>Figure 4.</b> 125 MHz <sup>13</sup> C{ <sup>1</sup> H}-NMR spectrum of <b>4</b> - <sup>13</sup> C <sub>3</sub> (0.042 M) at 200 K                                   | 139 |
| <b>Figure 5.</b> 125 MHz <sup>13</sup> C{ <sup>1</sup> H}-NMR spectrum of <b>4</b> - <sup>13</sup> C <sub>3</sub> in dilute solution at 200 K                          | 140 |
| <b>Figure 6.</b> Equilibrium composition of phosphine-bound scandium alkyl complexes as a function of total scandium concentration                                     | 141 |
| <b>Figure 7.</b> 125 MHz <sup>13</sup> C{ <sup>1</sup> H}-NMR spectrum of <b>5</b> - <sup>13</sup> C <sub>3</sub> at room temperature                                  | 142 |
| <b>Figure 8.</b> 125 MHz <sup>13</sup> C{ <sup>1</sup> H}-NMR spectra of <b>5</b> - <sup>13</sup> C <sub>3</sub> in dilute solution at 200 K                           | 143 |
| <b>Figure 9.</b> <sup>1</sup> H <sup>13</sup> C{ <sup>1</sup> H}-NMR spectrum of <b>6</b> •P( <sup>13</sup> CH <sub>3</sub> ) <sub>3</sub> in dilute solution at 200 K | 144 |

|  |     |
|--|-----|
| <b>Figure 10.</b> Equilibrium composition of phosphine-bound scandium propyl complex as a function of total scandium concentration                   | 145 |
| <b>Figure 11.</b> Equilibrium compositions predicted from kinetic studies  | 149 |
| <b>Figure 12.</b> Equilibrium data for $\beta$ -branched alkyl complexes, plotted with fits to monomeric and dimeric equilibrium expressions         | 153 |
| <b>Figure 13.</b> The effect on Figure 1a of altering $[\text{Sc}]_0$  | 154 |
| <b>Figure 14.</b> Equilibrium data for $6 \bullet \text{P}(^{13}\text{CH}_3)_3$ , plotted with fits to monomeric and dimeric equilibrium expressions | 155 |
| <b>Figure 15.</b> Equilibrium data for $6 \bullet \text{P}(^{13}\text{CH}_3)_3$ , plotted with fits to monomeric and coupled equilibrium expressions | 155 |

## LIST OF TABLES

## CHAPTER 2

|  |    |
|--|----|
| Table I. Second-order rate constants for the reaction of ethylene with $\text{Cp}^*_2\text{ScR}$ complexes | 13 |
|--|----|

|   |    |
|---|----|
| Table II. IR Data for $\text{Cp}^*_2\text{Sc}(\text{C}(\text{CH}_3)\text{C}(\text{X})\text{CH}_3)$ , X = H, D | 21 |
|---|----|

## CHAPTER 3

|   |    |
|---|----|
| Table I. Normalized methyl integrations for 2-methylbutenes obtained from hydrolysis of <b>2c</b> and <b>2d</b> | 40 |
|---|----|

|   |    |
|---|----|
| Table II. Relative concentrations of methanes obtained from hydrolysis of <b>2c</b> and <b>2d</b> | 42 |
|---|----|

|  |    |
|--|----|
| Table III. $^1\text{H}$ -NMR data for selected compounds | 45 |
|--|----|

## CHAPTER 4

|   |    |
|---|----|
| Table I. Stereochemical assignments for polybutadiene | 65 |
|---|----|

|   |    |
|---|----|
| Table II. NMR data for selected compounds | 76 |
|---|----|

## CHAPTER 5

|  |     |
|--|-----|
| Table I. NMR data for selected compounds | 112 |
|--|-----|

|   |     |
|---|-----|
| Table II. $^{13}\text{C}\{^1\text{H}\}$ -NMR stereochemical analysis of a representative poly(hexadiene) sample | 118 |
|---|-----|

## CHAPTER 6

|  |     |
|--|-----|
| Table I. $^1\text{H}$ and $^{13}\text{C}$ -NMR data for selected compounds | 157 |
|--|-----|

## **Chapter 1**

### **Introduction**

**Abstract:** A brief overview of mechanistic progress in Ziegler-Natta catalysis provides context for the experiments described in Chapters 2 through 6.

Since the fortuitous discovery by Ziegler<sup>1</sup> in 1953 that ethylene reacts with  $\text{AlEt}_3$  and zirconium acetylacetonate to form linear polyethylene, the chemistry of ethylene and other  $\alpha$ -olefins with early transition metals has been vigorously explored and production of poly( $\alpha$ -olefins) by Ziegler-type catalysts has become one of the most important industrial organometallic processes.<sup>2</sup> The catalyst systems currently employed for industrial applications are generally composed of  $\text{TiCl}_3$  or  $\text{TiCl}_4$  supported on solid  $\text{MgCl}_2$  and treated with an aluminum cocatalyst.<sup>3</sup> Such systems are notoriously difficult to study. Few of the many types of sites at the catalyst surface are active for polymerization, and the nature of these active sites remains a subject of debate. Indeed, the overwhelming variety of effective heterogeneous catalysts probably precludes the development of a single, grand mechanistic picture applicable to all cases. However, several of the best catalysts share a number of attributes, and while progress in this field has some of the traits of a random walk, hindsight allows the imposition of a more or less linear pattern upon the most important developments. (For the purposes of this discussion, the term "Ziegler-Natta" catalyst is confined to the description of early transition metal-based catalyst systems, industrially dominated by titanium; late transition metal systems and the equally important chromium/silica "Philips' catalyst" are not necessarily comparable).

"First-generation" Ziegler-Natta catalysts were simple mixtures of metal halides (*e.g.*,  $\text{TiCl}_3$  or  $\text{TiCl}_4$ ) with large excesses of alkylaluminum compounds. The addition of various Lewis-basic compounds such as esters (*e.g.*, ethyl acetate) was found to enhance or alter the stereoselectivities of the basic catalyst mixtures; exploration of such effects led to what can be broadly perceived as a second generation of catalysts. A third generation of catalysts can be considered to have emerged with the innovation of ball-milling these mixtures with  $\text{MgCl}_2$ , leading to greatly increased activities--over a million grams of polymer can now be routinely prepared per gram of catalyst. Within each of these categories, the precise nature of the components of the catalyst mixture and the relative amounts of each component are subject to extensive variation. The patent literature and a great deal of academic literature are glutted with descriptive reports of the molecular weight and stereochemical properties of polymers derived from treatment of  $\alpha$ -olefins with a seemingly endless barrage of nearly

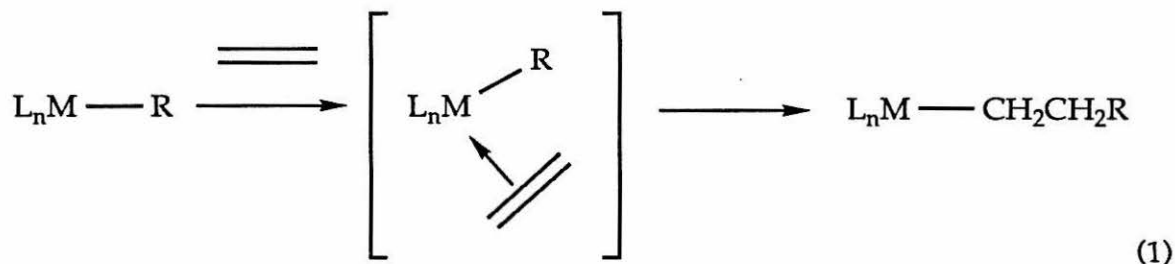
alchemical preparations. It is hardly surprising that detailed, experimentally meaningful mechanistic interpretations were long in coming.

This is not to suggest that early workers in this field were without insight; merely that the material they had to work with by its nature defied precise observation. On the contrary, it is impressive how far back the lineage of many of the current mechanistic ideas about Ziegler-Natta catalysis extends. The Cossee-Arlman mechanism (*vide infra*) proposed in 1964, eleven years after Ziegler's first report, has remained the basis of most interpretations of Ziegler-Natta reactivity. Even earlier than this, Shilov<sup>4</sup> had made the important suggestion that chain propagation might occur at cationic group IV metal sites. Furthermore, the study of "homogeneous" catalyst systems--which was ultimately to lead to the experimental achievements which form the basis of the current understanding of Ziegler-Natta catalysis--very quickly became an important area of organometallic chemistry, in part because it was recognized that the heterogeneous systems so convenient for industrial application were going to be difficult to study at the molecular level. The chemist's ability to probe structure and mechanism in solution was then, and remains, much more fully developed than corresponding methods for solid-state work.

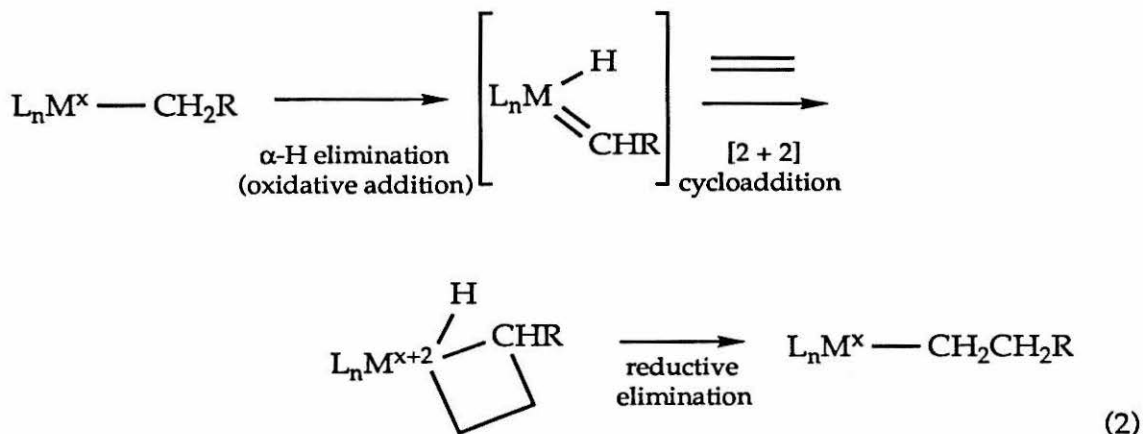
Soluble, heterogeneous Ziegler-Natta catalysts have themselves undergone a meaningful evolution of sorts, which has led to an understanding of some of the characteristics of the active sites and mechanisms involved in Ziegler olefin polymerization. Evidence for the presence of titanium aluminate ion pairs in homogeneous titanocene-based catalysts was first obtained by Breslow in 1959.<sup>5</sup> For the most part, though, these early soluble systems based on titanocene dichloride and alkylaluminum cocatalysts proved in many ways as resistant to study as their heterogeneous counterparts. Since large excesses of alkylaluminum reagent are still required to activate the transition metal centers, the latter are typically present only in minute quantities. This effectively negates many of the advantages of removing the active sites from the surface/solution interface. The synthesis of metallocene derivatives which could catalyze ethylene polymerization in the absence of an activator thus constituted a major experimental breakthrough. Cossee and Arlman<sup>6</sup> had suggested that the active species contains a metal-carbon  $\sigma$ -bond and that propagation occurs by direct insertion of olefin across this bond, presumably *via* a prior metal-olefin adduct



(depicted in Equation 1 for ethylene polymerization). This fundamental reaction remained unobserved until 1982, when Watson<sup>7</sup> used deuterium labeling studies to demonstrate the insertion of propylene into the lutetium-carbon bond of  $\text{Cp}^*_2\text{LuCH}_3$  ( $\text{Cp}^* = \text{C}_5\text{Me}_5$ ).



Up until Watson's work, a number of early transition metal complexes which seemed to be reasonable models for Ziegler-Natta reactive sites had been synthesized. While olefin insertion into metal-hydride bonds was well-known<sup>8</sup> the failure of related alkyl compounds to exhibit olefin insertion<sup>9</sup> led Rooney and Green<sup>10</sup> to propose a mechanism which did not rely on direct insertion as a fundamental step. In the "Green-Rooney" mechanism, which strongly resembles that for olefin metathesis,<sup>11</sup>  $\alpha$ -hydride elimination occurs, leading to the reactive intermediate, a metal carbene. Reaction with ethylene to form a metallacyclobutane is proposed to be the carbon-carbon bond forming step (Equation 2).



This mechanism has also been demonstrated to be experimentally viable. In 1983, Schrock<sup>12</sup> reported that certain tantalum alkylidene complexes polymerize ethylene, and presented evidence for the operation of the Green-Rooney mechanism in such systems.

Of course, a certain amount of risk accompanies attempts to extrapolate from the chemistry of extremely simplified systems such as these back to the chemistry of the complex systems they are intended to model. Nevertheless, evidence favoring direct insertion as the predominant mode of propagation is strong. If one assumes that the solid-state active sites resemble the soluble models in having  $d^0$  electron configurations, one is required to discard the Green-Rooney mechanism out of hand, since oxidative addition at a  $d^0$  metal center would involve removal of core electrons and is thermodynamically unfavorable. Since most industrial systems rely on titanium, which has three relatively accessible oxidation states, it can be argued that the model chemistry is irrelevant and that a  $d^1$  or  $d^2$  center may be important in the complex mixtures typical of alkylaluminum-cocatalyzed polymerizations. These objections have more than gadfly significance. Many classical Ziegler-Natta catalysts are also effective olefin metathesis catalysts and it was certainly reasonable to wonder whether the two processes might be closely related. Noting that the Green mechanism involves making and breaking C-H and M-H bonds whereas the Cossee-Arlman mechanism does not, Grubbs<sup>13</sup> looked for kinetic H/D isotope effects in the operation of the soluble Ziegler analogue system  $\text{Cp}_2\text{TiCl}_2/\text{Et}_2\text{AlCl}$ , and found none. His experiments clearly demonstrate that the rate-determining step does not involve bond cleavage or formation at hydrogen and thus implicate the operation of the Cossee-Arlman mechanism.

While these issues concerning the viability of certain fundamental mechanistic steps were being addressed, a parallel thread of research was beginning to provide important insights into the steric and electronic nature of homogeneous reactive sites. In a 1975 paper<sup>14</sup> that turned out to be something of a watershed, Long and Breslow reported that small amounts of water greatly increase the reactivity of titanocene-based catalyst systems. Shortly thereafter, a new family of two-component homogeneous catalysts appeared. Kaminsky<sup>15</sup> used a partial hydrolysis product of trimethylaluminum, "aluminoxane", as an activator for zirconocene derivatives, and produced olefin polymers with a product-to-transition metal ratio competitive with the best heterogeneous catalysts. Subsequently, it was shown that use of the chiral, linked zirconocenes developed by Brintzinger<sup>16</sup> led to the production of highly stereoregular polyolefins.<sup>17</sup> The commercial potential of methylaluminoxane catalysts is currently a topic of furious research in some industrial circles. More to the point

at hand, studies of this family of compounds have provided much of the basis of the current understanding of structure/function activity in Ziegler-Natta catalysis, particularly with regard to stereoselection. The simple "quadrant" model advanced by Pino<sup>18</sup>--which uses the four-center Cossee transition state geometry as its basis--has dominated discussion of this topic. Assuming a four-center transition state geometry for the carbon-carbon bond-forming step, Pino constructed a model for stereochemical induction invoking simple steric repulsions between the various substituents at the olefin, polymer chain, and transition metal ligand array. Intricate relationships between the transition metal ligand array and the stereochemical integrity of the polymeric product are still being elucidated.<sup>19</sup>

Concurrently, experimentalists firmly established the importance of group IV alkyl cations in homogeneous Ziegler-Natta catalysis. Using a classical model system,  $\text{Cp}_2\text{TiCl}_2/\text{MeAlCl}_2$ , Eisch<sup>20</sup> isolated a cationic complex resulting from the formal insertion of a bulky alkyne into a  $\text{Ti-CH}_3$  bond. He proposed that the reactive intermediate was  $\text{Cp}_2\text{TiCH}_3^+$ . Most convincingly, in 1986 Jordan<sup>21</sup> reported the polymerization of ethylene by well-characterized cationic zirconium alkyl complexes,  $[\text{Cp}_2\text{ZrR}]^+$ . In the light of this and subsequent work by Turner<sup>22</sup> and Marks<sup>23</sup> there seems little room for doubt that the Kaminsky catalysts involve cationic zirconium centers. While some investigators of the heterogeneous  $\text{MgCl}_2$ -supported system still maintain that the active sites are based on lower oxidation states of titanium<sup>24</sup> this work has been challenged.<sup>25</sup> Other workers have demonstrated that titanium reduction correlates, at least qualitatively, with reduced catalytic activity.<sup>26</sup>

In spite of (or because of) the progress outlined above, research in Ziegler-Natta catalysis remains vigorous. Chemists are now able to ask increasingly subtle questions about the mechanism of carbon-carbon bond formation in Ziegler-Natta catalysis. The "modified Green-Rooney" mechanism, discussed in detail in Chapter 3, is one example of the level of refinement which mechanistic inquiry has reached. This deceptively simple variation of the Cossee-Arman mechanism carries important consequences for both the electronic requirements of the catalytic metal center and the steric configurations of the growing polymer chain.

The Bercaw group's interest in the organometallic chemistry of early transition metals has produced several systems well-suited to the study of olefin polymerization. Several stable olefin hydride complexes of niobocene and tantalocene and the permethyl analogs have been prepared which undergo olefin insertion into the metal-hydride bond upon heating, allowing for thorough investigation of steric and electronic effects on this important mechanistic step.<sup>27</sup> These complexes do not polymerize ethylene. However, permethylscandocene alkyl complexes,  $\text{Cp}^*\text{ScR}$ ,<sup>28</sup> are efficient ethylene polymerization agents. These neutral, coordinatively unsaturated,  $d^0$  complexes have proven to be excellent models for the study of elementary reaction steps at an active polymerization site in the absence of counter-ion or cocatalyst effects. Chapter 2 describes experiments<sup>28b</sup> which explore the relationship between propagation and termination in this reaction, and which illustrate the mechanistic relationship between the behavior of single-component group 3 catalysts and homogeneous group 4/alkylaluminum catalysts.

Chapters 4 through 6 extend our investigations of the polymerization reactivity of the *ansa*-cyclopentadienyl(amido)scandium derivatives, abbreviated " $(\text{Cp}^*\text{SiNR})\text{ScR}(\text{PMe}_3)$ ". Chapter 4 veers away from simple olefin polymerizations to the mechanistically more complex polymerization of conjugated dienes. The surprising importance of cyclization events in this reaction relate it to the chemistry reported in Chapter 5, in which some aspects of the cyclopolymerization of non-conjugated olefins are considered. In the context of this work, new considerations regarding the modified Green-Rooney mechanism arise. Finally, Chapter 6 addresses some pending questions about the nature of the reactive intermediate and the processes which compete with propagation in polymerizations catalyzed by the *ansa*-cyclopentadienyl(amido)-scandium derivatives " $(\text{Cp}^*\text{SiNR})\text{ScR}(\text{PMe}_3)$ ".

## REFERENCES

1. Ziegler, K.; Holzkamp, E.; Martin, H. *Angew. Chem.* **1955**, *67*, 541.
2. (a) Collman, J. P.; Hegedus, L. S.; Norton, J. R.; Finke, R. G. *Principles and Applications of Organometallic Chemistry*. University Science Books: Mill Valley, California, **1987**, p. 577-617.  
 (b) Kaminsky, W.; Sinn, H., eds, *Transition Metals and Organometallics as Catalysts for Olefin Polymerization*. Springer-Verlag: Berlin, **1988**.  
 (c) Boor, Jr., J. *Ziegler-Natta Catalysts and Polymerizations*. Academic Press: New York, **1979**.
3. Barbé, P. C.; Cecchia, G.; Noristi, L. *Adv. Polym. Sci.* **1986**, *81*, 1-81, is a good, comprehensive review of the literature concerning  $MgCl_2$ -supported catalyst systems.
4. (a) Zefirova, A. K.; Shilov, A. E. *Dokl. Acad. Nauk SSSR* **1961**, *136*, 599.  
 (b) Dyachkovskii, F. S.; Shilova, A. K.; Shilov, A. E. *J. Polym. Sci., Part C* **1967**, *16*, 2333.
5. (a) Breslow, D. S.; Newburg, R. *J. Am. Chem. Soc.* **1959**, *81*, 81.  
 (b) Long, W. P.; Breslow, D. S. *J. Am. Chem. Soc.* **1960**, *82*, 1953.
6. (a) Cossee, P. *J. Catal.* **1964**, *3*, 80.  
 (b) Arlman, E. J.; Cossee, P. *J. Catal.* **1964**, *3*, 99.
7. (a) Watson, P. L. *J. Am. Chem. Soc.* **1982**, *104*, 337.  
 (b) Watson, P. L.; Roe, D. C. *J. Am. Chem. Soc.* **1982**, *104*, 6471.
8. (a) Tebbe, F. N.; Parshall, G. W. *J. Am. Chem. Soc.* **1971**, *93*, 3793.  
 (b) Guggenberger, L. J.; Meakin, P.; Tebbe, F. *J. Am. Chem. Soc.* **1974**, *96*, 5420.
9. Green, M. L. H.; Mahtab, R. *J. Chem. Soc., Dalton Trans.* **1979**, 262. This paper is notable for the unmistakable note of exasperation with which the authors note the lack of olefin insertion for the group 6 cationic (olefin)alkyl complexes reported!

10. (a) Ivin, K. J.; Rooney, J. J.; Stewart, C. D.; Green, M. L. H.; Mahtab, J. R. *J. Chem. Soc., Chem. Commun.* **1978**, 604.  
 (b) Green, M. L. H. *Pure Appl. Chem.* **1978**, 100, 2079.
11. (a) Ivin, K. J. "Olefin Metathesis." Academic Press: London; New York, 1983.  
 (b) Grubbs, R. H. In "Comprehensive Organometallic Chemistry," Wilkinson, G., Ed. Pergamon Press, Ltd.: Oxford, 1982, Vol. 8, pp 499-551.
12. Turner, H. W.; Schrock, R. R.; Fellmann, J. D.; Holmes, S. J. *J. Am. Chem. Soc.* **1983**, 105, 4942.
13. (a) Soto, J.; Steigerwald, M. L.; Grubbs, R. H. *J. Am. Chem. Soc.* **1982**, 104, 4479.  
 (b) Clawson, L.; Soto, J.; Buchwald, S. L.; Steigerwald, M. L.; Grubbs, R. H. *J. Am. Chem. Soc.* **1985**, 107, 3377.
14. Long, W. P.; Breslow, D. S. *Liebigs Ann. Chem.* **1975**, 463-469.
15. (a) Sinn, H.; Kaminsky, W. *Adv. Organomet. Chem.* **1980**, 18, 99.  
 (b) Kaminsky, W.; Miri, M.; Sinn, H.; Woldt, R.; *Makromol. Chem., Rapid Commun.* **1985**, 4, 417.
16. Wild, F. R. W. P.; Wasiucionek, M.; Huttner, G.; Brintzinger, H. H. *J. Organomet. Chem.* **1985**, 288, 63-67.
17. Kaminsky, W.; Külper, K.; Brintzinger, H. H.; Wild, F. R. W. P. *Angew. Chem., Int. Ed. Engl.* **1985**, 97, 507.
18. (a) Pino, P.; Cioni, P.; Wei, J. *J. Am. Chem. Soc.* **1987**, 109, 6189.  
 (b) Pino, P.; Galimberti, M. *J. Organomet. Chem.* **1989**, 370, 1.  
 (c) Waymouth, R.; Pino, P. *J. Am. Chem. Soc.* **1990**, 112, 4911.  
 (d) Pino, P.; Cioni, P.; Galimberti, M.; Wei, J.; Piccolrovazzi, N. in "Transition Metals and Organometallics as Catalysts for Olefin Polymerization," Kaminsky, W.; Sinn, H., eds., Springer-Verlag, NY, 1988, p. 269.



19. (a) Röhl, W.; Brintzinger, H. H.; Rieger, B.; Zolk, R. *Angew. Chem., Int. Ed. Engl.* **1990**, *29*, 279.  
(b) Erker, G.; Nolte, R.; Aul, R.; Wilker, S.; Krüger, C.; Noe, R. *J. Am. Chem. Soc.* **1991**, *113*, 7594.
20. Eisch, J. J.; Piotrowski, A. M.; Brownstein, S. K.; Gabe, E. J.; Lee, F. L. *J. Am. Chem. Soc.* **1985**, *107*, 7219.
21. Jordan, R. F. *Adv. Organomet. Chem.* **1991**, *32*, 325-387, and references therein.
22. Hlatky, G. G.; Turner, H. W.; Eckman, R. R. *J. Am. Chem. Soc.* **1989**, *111*, 2728.
23. Jeske, G.; Lauke, H.; Mauermann, H.; Sweptson, P. N.; Schumann, H.; Marks, T. J. *J. Am. Chem. Soc.* **1985**, *107*, 8091.
24. (a) Weber, S.; Chien, J. C. W.; Hu, Y. In *Transition Metals and Organometallics as Catalysts for Olefin Polymerization*, W. Kaminsky and H. Sinn, Eds. Berlin: Springer-Verlag, **1988**, p. 45.  
(b) Chien, J. C. W.; Wu, J. C. *J. Polym. Sci., Polym. Chem. Ed.* **1982**, *20*, 2461.
25. Zakharov, V. A.; Makhtarulin, S. I.; Polyboyarov, V. A.; Anufrienko, V. F. *Makromol. Chem.* **1984**, *185*, 1781.
26. (a) Baulin, A. A.; Novikova, Ye. I.; Mal'kova, G. A.; Maksimov, V. L.; Vyshirskaya, L. I.; Ivanchev, S. S. *Vysokomol. Soyed.* **1980**, *A22*, 181.  
(b) Kashiwa, N.; Yoshitake, J. *Makromol. Chem.* **1984**, *185*, 1133.
27. (a) Burger, B. J.; Santarsiero, B. D.; Trimmer, M. S.; Bercaw, J. E. *J. Am. Chem. Soc.* **1988**, *110*, 3134.  
(b) Doherty, N. M.; Bercaw, J. E. *J. Am. Chem. Soc.* **1985**, *107*, 2670.
28. (a) Thompson, M. E.; Baxter, S. M.; Bulls, A. R.; Burger, B. J.; Nolan, M. C.; Santarsiero, B. D.; Schaefer, W. P.; Bercaw, J. E. *J. Am. Chem. Soc.* **1987**, *109*, 203.  
(b) Burger, B. J.; Thompson, M. E.; Cotter, W. D.; Bercaw, J. E. *J. Am. Chem. Soc.* **1990**, *112*, 1566.

## Chapter 2

### Ethylene Oligomerization by Permethylscandocene Alkyl Complexes: Product Studies of Ethylene Oligomers.<sup>1</sup>

**Abstract:** Low-molecular weight oligomers were prepared by treatment of ethylene with  $\text{Cp}^*_2\text{ScR}$  ( $\text{R}$  = methyl, ethyl, propyl). The distribution of alkane products was measured *via* gas chromatography, and was modelled according to kinetic data obtained in a prior study. Product distributions support the claim that  $\text{Cp}^*_2\text{ScR}$  complexes catalyze the living polymerization of ethylene at sufficiently low temperatures. Slow initiation by  $\text{Cp}^*_2\text{ScRCH}_2\text{CH}_3$  is attributed to a ground-state  $\beta$ -agostic interaction. A model complex containing a similar interaction was prepared and the location of the agostic C-H bond confirmed by a deuterium-labelling experiment.

---



|  |    |
|--|----|
| I. INTRODUCTION.....   | 13 |
| II. RESULTS.....   | 14 |
| III. DISCUSSION .....  | 18 |
| Oligomer Product Distributions .....                                 | 18 |
| IR Characterization of a Ground-State $\beta$ -Agostic C-H bond..... | 21 |
| IV. CONCLUSIONS.....   | 22 |
| EXPERIMENTAL SECTION .....   | 23 |
| REFERENCES.....  | 26 |

## I. INTRODUCTION

Permethylscandocene alkyl complexes catalyze the polymerization of ethylene in the absence of a co-catalyst. Extensive kinetics experiments have been carried out on both the olefin insertion step and the reverse, chain-transfer step,  $\beta$ -hydride elimination.<sup>1,2</sup> The rates of insertion of ethylene into the scandium-carbon bonds of the series of complexes  $\text{Cp}^*_2\text{ScR}$  ( $\text{R} = \text{H}$ ,  $\text{CH}_3$  (1),  $\text{CH}_2\text{CH}_3$  (2),  $\text{CH}_2\text{CH}_2\text{CH}_3$  (3)) were followed by  $^{13}\text{C}$ -NMR at  $-78^\circ\text{C}$ . Even at this low temperature, insertion into the scandium-hydride bond occurs too quickly to be observed on the NMR time scale. The rate constants obtained for the other insertion reactions are reproduced below.

**Table I. Second-order rate constants for the reaction of ethylene with  $\text{Cp}^*_2\text{ScR}$  complexes<sup>1,2</sup>**

| R  | $k_2$ ( $-80^\circ\text{C}$ ) ( $\text{M}^{-1} \text{sec}^{-1}$ ) |
|--|---|
| $^{13}\text{CH}_3$                       | $8.1(2) \times 10^{-4}$   |
| $^{13}\text{CH}_2^{13}\text{CH}_3$       | $4.4(2) \times 10^{-4}$   |
| $\text{CH}_2\text{CH}_2^{13}\text{CH}_3$ | $6.1 \times 10^{-3}$  |

The slow insertion rate for 1 relative to 3 can be rationalized on the basis of ground-state bond-strength effects.<sup>3</sup> The scandium-carbon bond in the propyl ligand is effectively weakened by repulsive steric interactions with the  $\text{Cp}^*$  ligand system and by the inductive effects of the substitution of one hydrogen in the methyl derivative by a more electron-donating ethyl substituent. The surprisingly slow insertion observed in the case of 2 is attributed to an agostic interaction<sup>4</sup> between scandium and a  $\beta$  C-H bond in the ground state of this complex. That is, the electron-deficient scandium center in this molecule is stabilized by electron donation from the  $\beta$ -C-H bond. This stabilization is not expected to be available to 3 due to the additional steric bulk of the propyl ligand. That is, the agostic conformation would require orientation of the methyl group toward a  $\text{Cp}^*$  ring. This

argument applies equally to all alkyl groups longer than ethyl. It follows that all insertions into  $\text{Cp}^*_2\text{Sc}(\text{CH}_2)_n\text{CH}_3$  ( $n \geq 2$ ) should occur at the same rate. This assumption, together with the observation that  $\text{Cp}^*_2\text{ScR}$  complexes are stable to  $\beta$ -hydride elimination at  $-78^\circ\text{C}$ , suggested that the permethylscandocene system could be a "living" catalyst for ethylene polymerization under appropriate conditions.

The term "living" polymer was first coined by Szwarc<sup>5</sup> to describe the anionic polymerization of styrene, but the essential kinetics had been presented by Flory<sup>6</sup> years earlier in a discussion of ethylene oxide polymerizations. The essential features of such a system are (a) that no termination or chain-transfer steps occur under polymerization conditions, (b) that all propagation steps are equally probable, i.e., have the same rate constant,<sup>7</sup> and (c) that initiation be instantaneous relative to propagation. If these conditions are met, the average length of the polymer may be directly calculated by the ratio of monomer units consumed to catalyst molecules, and the distribution of products is governed by Poisson statistics. We set out to determine whether in fact all of these conditions were met in the case of permethylscandocene alkyls by studying the distributions of ethylene oligomers obtained from treatment of  $\text{Cp}^*_2\text{ScR}$  with small amounts of ethylene. We anticipated that oligomerizations initiated with **3** would result in Poisson distributions of products, and that we would be able to model the product distributions obtained from **1** and **2** using the previously obtained rate constants from ethylene insertion into these complexes (*vide supra*).

## II. RESULTS

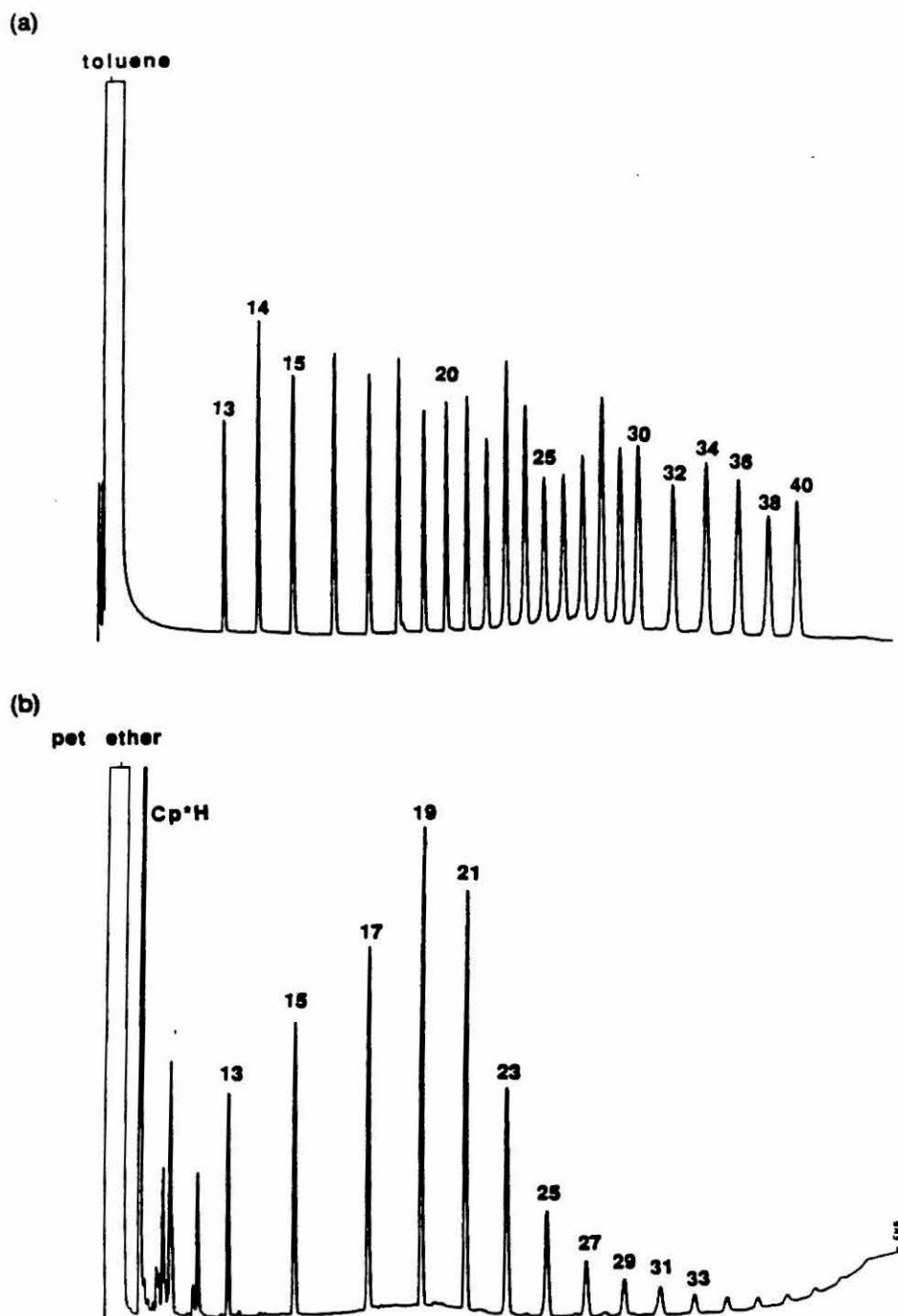
Product distributions from the reaction of permethylscandocene alkyls with ethylene have been measured by gas chromatography. The data were quantitated by comparison with external standards. Alkanes of fewer than thirteen carbons were obscured by solvent and pentamethylcyclopentadiene-associated peaks. The range of observable products was limited to alkanes of fewer than fifty carbons by the maximum operating temperature of the column. Product distributions are thus normalized to the amount of alkane within this molecular weight range. Samples were typically prepared by treating 0.05 mmol of the appropriate scandium alkyl complex with 40 equivalents of ethylene at  $-78^\circ\text{C}$  in 1 mL of solvent (toluene or petroleum ether).

After removal of excess ethylene to a Toepler pump, the oligomerizations were quenched with excess methanol, yielding alkane products. The scandium was hydrolyzed to the oxide with  $\text{H}_2\text{O}$  and the organics were extracted for GC analysis.

The reaction of **3** with ethylene produces only alkanes with odd numbers of carbons. Figure 1 shows chromatograms of a typical reaction mixture and of a mixture of alkane standards. In Figure 2 the quantitated data from a series of reactions are plotted along with Poisson distributions (*vide infra*) based on the number of equivalents of ethylene consumed (as determined by Toepler pump measurements). At conversions slightly higher than those shown, *ca.* ten equivalents of ethylene consumed, the heavier alkyls begin to precipitate from the reaction mixture and agreement with Poisson statistics suffers accordingly.

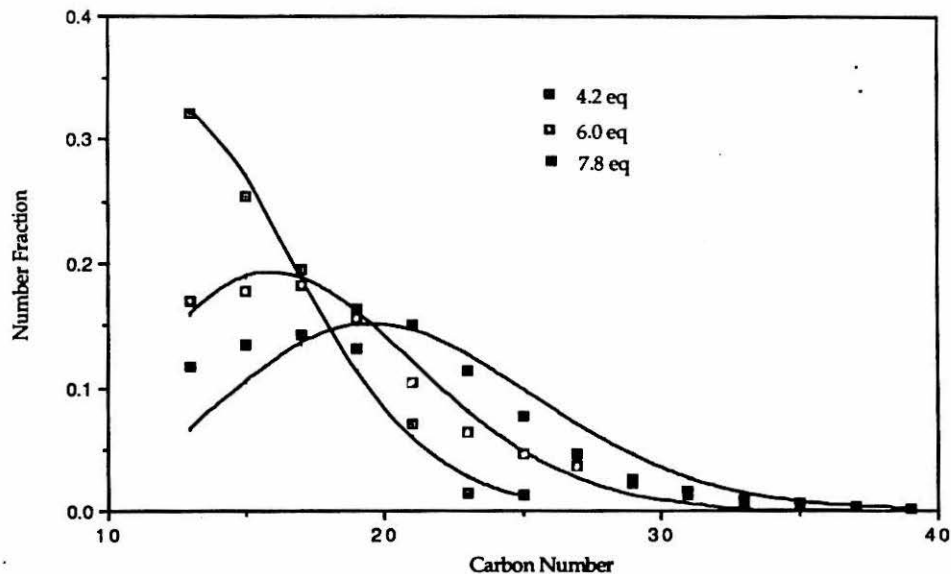
The effect of the alkyl substituent in the initiating complex was examined by comparing the product distributions obtained by allowing the propyl complex **3** and the methyl complex **1** to consume identical amounts of ethylene, as shown in Figure 3. As in the case of oligomerization initiated by **3**, the reaction of ethylene with **1** produces only alkanes with an odd number of carbons. Experiments conducted with **2** as the initiating species resulted in precipitation of product after consumption of four equivalents of ethylene; the product distribution obtained after consumption of two equivalents of ethylene is shown in Figure 4.

**Figure 1. (a) Sample chromatogram of alkane standards. (b) Sample chromatogram of reaction mixture<sup>a</sup>**

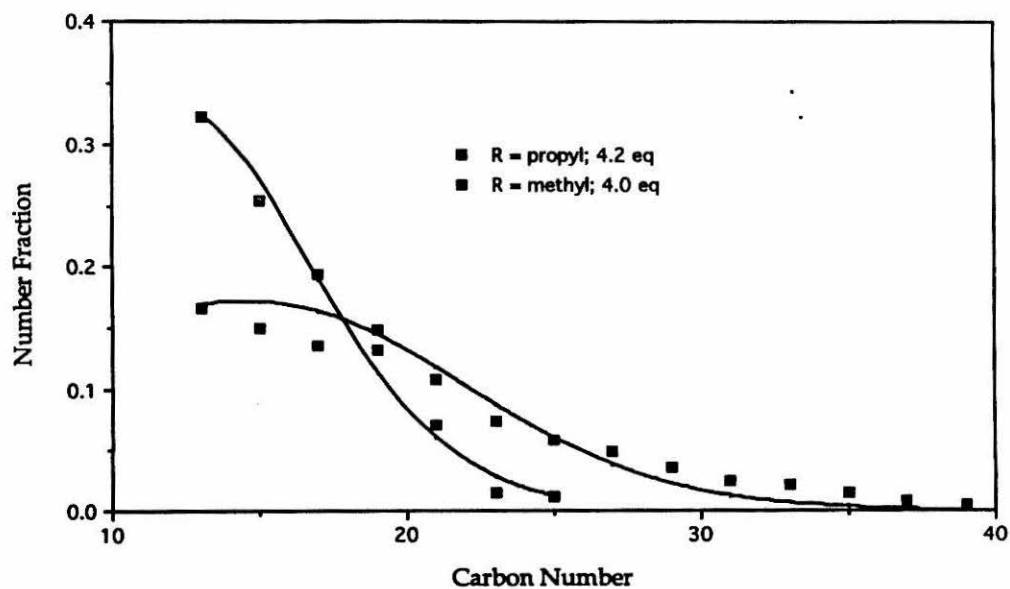


<sup>a</sup>Numerals indicate the number of carbons in the eluting alkane.

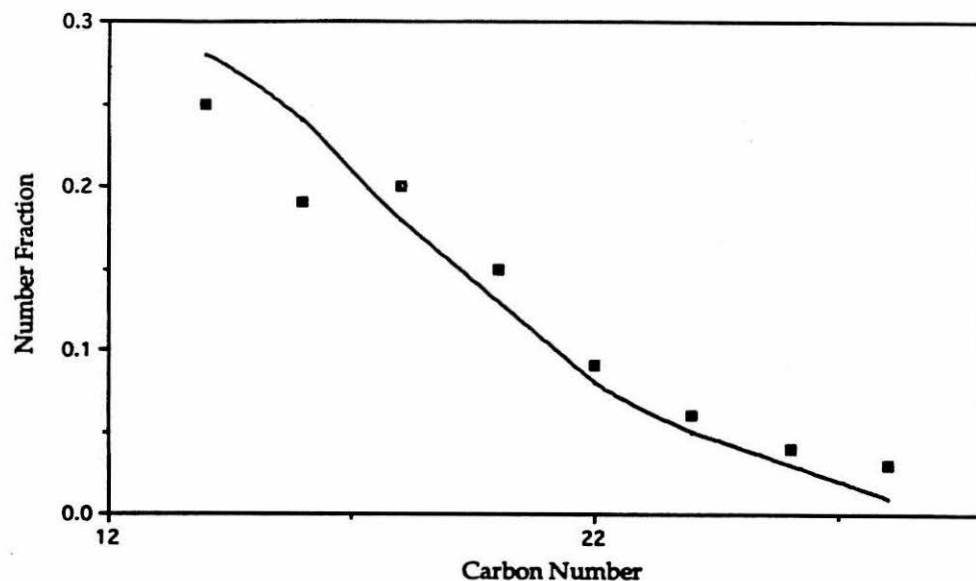
**Figure 2. Molecular weight distribution of alkanes prepared by treatment of 3 with varying amounts of ethylene**



**Figure 3. Molecular weight distribution of alkanes prepared by treatment of 1 and 3 with approximately equal amounts of ethylene**



**Figure 4. Molecular weight distribution of alkanes prepared by treatment of 2 with two equivalents of ethylene**



### III. DISCUSSION

#### Oligomer Product Distributions

The distributions of products resulting from the oligomerization of ethylene by permethylscandocene alkyls have been examined at low levels of ethylene consumption. Under the conditions examined, these complexes qualify as truly "living" catalysts for ethylene oligomerization. A living catalyst system has been defined as one in which chain propagation occurs at the same rate regardless of chain length<sup>15</sup> and without competition from termination or chain transfer pathways.<sup>14</sup> In this case, the relevant primary steps are ethylene insertion into a Sc-C bond and  $\beta$ -hydride elimination to form a free alkene and  $\text{Cp}^*_2\text{ScH}$ . The question of whether chain transfer occurs competitively with chain propagation may conveniently be addressed by initiating oligomerization with an alkyl containing an odd number of carbons, e.g.,  $\text{Cp}^*_2\text{ScCH}_2\text{CH}_2\text{CH}_3$  (3) and  $\text{Cp}^*_2\text{ScCH}_3$  (1). Insertion of ethylene into such an alkyl produces an alkyl with an odd number of carbons.  $\beta$ -Hydride elimination would yield  $\text{Cp}^*_2\text{ScH}$ , which can undergo insertion to form  $\text{Cp}^*_2\text{ScCH}_2\text{CH}_3$ . Further insertion would lead to products with an even number of carbons. Via gas chromatography we have unambiguously

determined that oligomerization of ethylene at  $-78^{\circ}\text{C}$  by **3** and **1** produces only alkanes with an odd number of carbons (Figure 1). No chain transfer occurs under these conditions. In contrast, the same experiment at  $-40^{\circ}\text{C}$  produces predominantly alkanes with an even number of carbons, indicating that chain transfer is a major pathway at this temperature.

If the additional mechanistic criterion is met that the initiation step is faster than, or at least as fast as, the propagation step, the distribution of products is governed by the Poisson distribution function<sup>14</sup> and may be described as "monodisperse." Because our GC analysis does not allow us to measure the amounts of all species present, e.g., alkanes with fewer than thirteen carbons, we cannot calculate meaningful polydispersity indices based on these data. We chose therefore to demonstrate monodispersity in these systems by direct comparison of the product distribution to a Poisson distribution based on the amount of ethylene consumed. As shown in Figure 2, agreements between the data and the Poisson function (both normalized to the observable product range) is good when reaction is initiated with **3**, at conversions of up to eight equivalents of ethylene. Thus the assumption that the rate of insertion into alkyls with three or more carbons is independent of chain length is substantiated. In addition, the fact that the molecular weight distribution can be calculated solely on the basis of the monomer/catalyst ratio indicates that all scandium centers are active in the polymerization. If high molecular weight samples of polyethylene are prepared at  $-78^{\circ}\text{C}$ , no oligomeric products are found in the supernatant upon workup, indicating that no chain transfer occurs even after long reaction times, regardless of the molecular weight distribution. Chain termination in this system occurs only when a long-chain alkyl complex precipitates from solution. This does not result in the initiation of a new chain.

Theoretical product distributions for oligomerizations initiated by **1** and  $\text{Cp}^*_2\text{ScCH}_2\text{CH}_3$  (**2**) cannot be calculated using the Poisson function, since in these cases the first insertion is slower than subsequent insertions (*vide supra*). The effect of the ratio of initiation rate to propagation rate in living systems was elucidated over thirty years ago by Gold.<sup>8</sup> Qualitatively, the expectation is that as the initiation rate becomes slower, the distribution broadens and favors longer chain products (molecules initiated early in the



reaction consume a disproportionately high amount of monomer). We use the experimental rate constants to predict the oligomer distributions in these cases, performing simple iterative calculations on the concentrations of all species over small time intervals until a specified amount of ethylene is consumed. Figure 3 (solid lines) shows the distribution calculated in this fashion for oligomerization for an ethylene consumption of 4.2 equivalents relative to scandium. Agreement between the experimental data and the predicted distributions is good. This comparison vividly depicts the effect of the initiation rate on a living polymerization, even at very low monomer conversion. Similarly good agreement between observation and theory is obtained with oligomerization initiated by **2**, under conditions where the solution remains homogeneous, e.g., consumption of approximately two equivalents of ethylene (Figure 4). The predominance of products corresponding to ten or more insertions of monomer at such a low level of monomer conversion is a particularly dramatic illustration of the inertness of the agostically stabilized bonding arrangement in **2**.

The product distributions of ethylene oligomerizations by  $\text{Cp}_2\text{TiCl}_2$ /chloroalkylaluminum systems at low conversions have been studied by several groups.<sup>9</sup> At cool temperatures (typically -5 to 10°C for the titanium systems) and low conversions, polyethylene formation appears to proceed by a living mechanism. Höcker and Saeki<sup>9b</sup> used gel permeation chromatography to measure molecular weight distributions of oligomers formed by treatment of  $\text{Cp}_2\text{TiCl}_2/\text{Et}_2\text{AlCl}$  with small amounts of ethylene. They found excellent agreement with Poisson distributions calculated on the basis of the measured value of  $M_w$ . NMR and IR evidence indicated the absence of vinyl endgroups. Agreement with Poisson statistics holds only as long as the system remains homogeneous, i.e., until precipitation of the ethylene oligomers begins. Additionally, overexposure of the Ti complex to the Al cocatalyst leads to slow, irreversible reduction of the active Ti(IV) species to an inactive Ti(III) species. These observations are consistent with the results of several later studies on similar systems.<sup>9d-f</sup> Höcker and Saeki also examined the oligomeric products obtained from a  $\text{TiCl}_4/\text{EtAlCl}_2$  system. In this case, significant chain transfer occurred, as evidenced by the presence of vinyl end-groups and broad molecular weight distributions. Although detailed mechanistic studies at the molecular level have not been performed,

suppression of termination events at low temperatures must also be responsible for the "living" polymerization of propylene reported by Doi and co-workers for vanadium/aluminum catalysts at  $-60\text{ }^{\circ}\text{C}$ .<sup>10</sup>

### IR Characterization of a Ground-State $\beta$ -Agostic C-H bond.

The  $\beta$ -agostic ground state of **2** was inferred in prior work from IR data of this compound. NMR data were less convincing and, unfortunately, crystallographic analysis of this compound was limited by disorder. Low-frequency IR stretches at 2593, 2503, and  $2440\text{ cm}^{-1}$  were attributed to the agostic C-H bond. This assignment could not be verified by isotopic substitution (e.g., by preparation of  $\text{Cp}^*_2\text{ScCH}_2\text{CD}_3$ , etc.) because rapid  $\beta$ -elimination leads to label scrambling in this system. Similar low-frequency modes had been observed in a related butenyl complex,  $\text{E-Cp}^*_2\text{Sc-(C(CH}_3\text{)C(H)CH}_3)$  (**4**).<sup>11</sup> This observation was confirmed, and the deuterium-labeled isotopomer  $\text{Cp}^*_2\text{Sc(C(CH}_3\text{)C(D)CH}_3)$  (**4-d**<sub>1</sub>) was prepared. Selected IR bands for these complexes are reported in the Table II. The low-frequency stretching and bending modes are clearly associated with the vinylic C-H bond. Thus it is clear that it is this  $\beta$ -C-H bond (and not an  $\text{sp}^3$  bond at the  $\beta$ -methyl group) which participates in the agostic interaction.

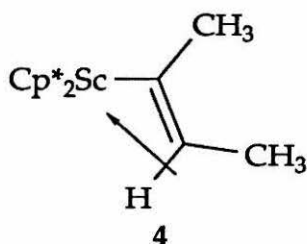


Table II: IR data for  $\text{Cp}^*_2\text{Sc(C(CH}_3\text{)C(X)CH}_3)$  (**4** and **4-d**<sub>1</sub>)

| Assignment            | X = H                 | X = D                 |
|-----------------------|-----------------------|-----------------------|
| $\nu_{\text{C-X}}$    | $2618\text{ cm}^{-1}$ | $1960\text{ cm}^{-1}$ |
| $\delta_{\text{C-X}}$ | $1314\text{ cm}^{-1}$ | $948\text{ cm}^{-1}$  |

The structurally similar propenyl complex  $\text{Cp}^*_2\text{Sc}(\text{C}(\text{H})=\text{C}(\text{H})\text{CH}_3)$  does not show low-frequency (agostic) IR modes, and the  $^1\text{H}$ -NMR resonance of the  $\beta$ -vinyl proton (5.25 ppm) is very different from that of the agostic proton in **4** (3.78 ppm). Presumably the  $\text{sp}^2$  framework is not intrinsically conducive to the formation of agostic interactions due to the wide bond angles associated with it. That is, with  $120^\circ$  angles about both carbons, the vinyl C-H bond is too far away from scandium for favorable overlap to occur. In the case of **4**, however, steric interactions between the  $\beta$ -methyl group and the bis(cyclopentadienyl) ligand array force the vinylic C-H bond deeper into the "wedge," resulting in better overlap and an observable agostic interaction. (This observation was an early occurrence of an agostic interaction which depended at least as much on the constraints of the ligand array as on the strength of the interaction itself, a theme which will become important in Chapters 3 and 5.)

#### IV. CONCLUSIONS

Our results with the scandium model system are in good agreement with product distributions of ethylene oligomerizations by  $\text{Cp}_2\text{TiCl}_2$ /chloroalkylaluminum systems (*vide supra*). It thus appears that the one-component scandium system is a good model for Ti/Al-based Ziegler catalysts, especially those based on cyclopentadienyl ligands. These product distribution studies not only demonstrate the applicability of our earlier kinetic studies to actual polymerizations performed with scandium catalysts, but they also strengthen the argument that kinetic and mechanistic information obtained from these very simple systems is qualitatively applicable to the much more complicated classical Ziegler systems.

## EXPERIMENTAL SECTION

### General Considerations

GC analyses were conducted on a Perkin-Elmer 8410 equipped with a flame ionization detector and an RSL-150 (Alltech) column. Alkanes used as standards for GC analysis--tridecane, tetradecane, pentadecane, hexadecane, heptadecane, ocatdecane, nonadecane, eicosane, heneicosane, docosane, tricosane, tetracosane, pentacosance, hexacosane, heptacosane, octacosane, nonacosane, tricontane, dotriacontane, tetratriacontane, hexatriacontane, octatriacontane and tetracontane (all Sigma)--were used as received.

$\text{Cp}^*_2\text{ScCH}_2\text{CH}_2\text{CH}_3$ ,  $\text{Cp}^*_2\text{ScCH}_2\text{CH}_3$ , and  $\text{Cp}^*_2\text{ScCH}_3$  were prepared as described previously,<sup>12b</sup> except that the products were isolated in greatly reduced yield ( $\approx 30\%$ ) by cooling concentrated petroluem ether solutions to  $-78^\circ\text{C}$  and removing the supernatant via cannula or filtration.

### Product Studies: Sample Preparations

The oligomerization experiments were carried out in a reaction vessel consisting of a small bulb ( $\approx 1$  mL) connected *via* a short (1-2") length of 6mm tubing to a  $90^\circ$  teflon valve (Kontes or Fischer-Porter) and a 24/40 ground glass joint. The volume of the 6mm tubing was  $\approx 1$  mL. A reaction vessel with a small overhead volume was used to encourage condensation of ethylene. The vapor pressure of ethylene at  $-78^\circ\text{C}$  is  $\approx 3.5$  atm;<sup>19</sup> the amount of ethylene (2 mmol) used in these reactions would result in a pressure of ca. 50 atm in a 1 mL volume. Thus, ignoring solution thermodynamics, we expect less than 10% of the added ethylene to exist in the gas phase at the beginning of reaction. The initial concentration of ethylene can be estimated at 1.8-1.9 M.

$\text{Cp}^*_2\text{ScR}$  (typically 16-20 mg) was loaded into the vessel described above and solvent (toluene or petroleum ether,  $\approx 1$  mL) was distilled onto the solid. The solution was frozen at  $-196^\circ\text{C}$  and ethylene was condensed into the vessel from a calibrated gas volume. The solution was warmed to  $-78^\circ\text{C}$  in a dry ice/acetone bath and stirred for 15-45 minutes. Volatiles were then removed

at  $-78^{\circ}\text{C}$  to a  $-196^{\circ}\text{C}$  trap and ultimately collected and measured via Toepler pump.

The oligomerizations were quenched with methanol, yielding exclusively alkanes as the oligomeric products. After hydrolysis of the scandium to the oxide with water (aqueous HCl was found to complicate GC analysis by encouraging decomposition of the  $\text{Cp}^*\text{H}$  residue), the organic products were extracted into toluene or petroleum ether. The product solutions were dried over  $\text{MgSO}_4$  before GC analysis.

#### Product Studies: GC Analysis

The GC conditions used were as follows. The injection port temperature was  $430^{\circ}\text{C}$ , the detector temperature,  $350^{\circ}\text{C}$ . Each run began with the oven at  $80^{\circ}\text{C}$ , where it was held for one minute. The temperature was then ramped at  $10^{\circ}\text{C}/\text{min}$  to  $130^{\circ}\text{C}$ . The oven was held at this temperature for one minute before resuming a  $10^{\circ}\text{C}$  ramp to  $320^{\circ}\text{C}$ . A final isothermal time (typically 1-5 minutes) sufficient to bring about complete elution of the products was then observed.

Accurate quantitative chromatography of the heavy alkanes produced in these reactions required some precautions, notably the high injector port temperature and a careful injection technique. Specifically, the syringe needle was held in the injector port for approximately thirty seconds after injection to allow the needle to come to thermal equilibrium and prevent it acting as a coldfinger. If this precaution is not taken, the heavier alkanes condense onto the syringe needle and are withdrawn along with it from the injection port, leading to anomalously and irreproducibly low integration values for the corresponding peaks in the GC trace.

Quantitation of the data was performed by calculation of response factors from analysis of an external standard solution. The response factors were periodically checked and redetermined as necessary. For alkanes where no standard was available, the value of the response factor was interpolated or extrapolated.

### Preparation of E-Cp\*<sub>2</sub>Sc(C(CH<sub>3</sub>)C(H)CH<sub>3</sub>)

In a glass bomb, a toluene solution of Cp\*<sub>2</sub>ScCH<sub>3</sub> (369 mg, 1.12 mmol) was treated with H<sub>2</sub> (4 atm, rm temp) for 30 min. Volatiles were removed from the reaction mixture at -78°C and a slight excess of 2-butyne was condensed into the reaction vessel from a calibrated gas volume. The resulting solution was transferred to a frit and filtered. Repeated attempts to obtain crystals were unsuccessful. An oily orange solid was obtained by removal of volatiles from a pentane solution (149 mg, 36%). E-Cp\*<sub>2</sub>Sc(C(CH<sub>3</sub>)C(D)CH<sub>3</sub>) was prepared by an entirely analogous procedure, except that D<sub>2</sub> was used in place of H<sub>2</sub>. <sup>2</sup>H- and <sup>1</sup>H-NMR showed that deuterium was located in the vinylic position, with an incorporation of approximately 80%. In addition, some deuterium incorporation into the Cp\* rings was observed.

## REFERENCES

1. This work has been published as part of Burger, B. J.; Thompson, M. E.; Cotter, W. D.; Bercaw, J. E. *J. Am. Chem. Soc.* **1990**, *112*, 1566.
2. Burger, B. J. Ph.D. Thesis, California Institute of Technology, 1987.
3. (a) Bulls, A. R.; Bercaw, J. E.; Manriquez, J. M.; Thompson, M. E. *Polyhedron* **1988**, *7*, 1409-1428.  
(b) Bruno, J. W.; Marks, T. J.; Morss, L. R. *J. Am. Chem. Soc.* **1983**, *105*, 6824.
4. (a) Thompson, M. E. Ph.D. Thesis, California Institute of Technology, 1985.  
(b) Thompson, M. E.; Baxter, S. M.; Bulls, A. R.; Burger, B. J.; Nolan, M. C.; Santarsiero, B. D.; Schaefer, W. P.; Bercaw, J. E. *J. Am. Chem. Soc.* **1987**, *109*, 203-219.  
(c) Brookhart, M.; Green, M. L. H.; Wong, L. *Prog. Inorg. Chem.* **1988**, *36*, 1.
5. Szwarc, M.; Levy, M.; Milkovich, R. *J. Am. Chem. Soc.* **1956**, *78*, 2656.
6. Flory, P. J. *J. Am. Chem. Soc.* **1940**, *62*, 1561.
7. Sequentially slower rate constants would yield the same result; it is important only that no step be faster than one which precedes it.
8. Gold, L. *J. Chem. Phys.* **1958**, *28*, 91.
9. (a) Waters, J. A.; Mortimer, G. A. *J. Polym. Sci., Part A-1* **1972**, *10*, 895.  
(b) Höcker, H.; Saeki, K. *Makromol. Chem.* **1971**, *148*, 107.  
(c) Reichert, K. H. *Angew. Makromol. Chem.* **1970**, *13*, 177.  
(d) Cihlár, J.; Mejzlik, J.; Hamrik, O.; Hudec, P.; Majer, J. *Makromol. Chem.* **1980**, *181*, 2549.  
(e) Fink, G.; Zoller, W. *Makromol. Chem.* **1981**, *182*, 3265.  
(f) Fink, G.; Schnell, D. *Angew. Makromol. Chem.* **1982**, *105*, 15.
10. (a) Doi, Y.; Nunomura, M.; Ohgizawa, N.; Soga, K. *Makromol. Chem., Rapid Commun.* **1991**, *12*, 245-249.  
(b) Doi, Y.; Keii, T. *Adv. Polym. Sci.* **1986**, *73/74*, 201.

11. Thompson, M. E. Unpublished results.



## Chapter 3

### Investigations of the Magnitude of Steric and $\alpha$ Deuterium Kinetic Isotope Effects in a Carbon-Carbon Bond-Forming Reaction of a Permethylscandocene Complex.<sup>1</sup>

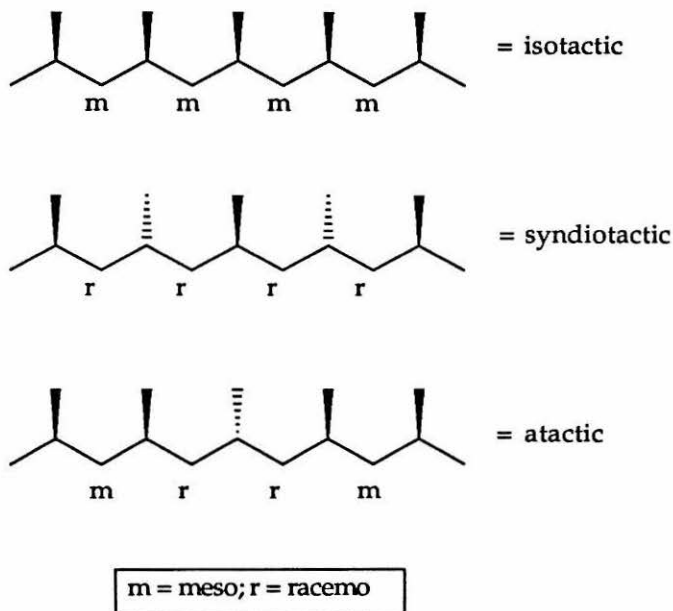
**Abstract:** No measurable isotope effect is observed in the reaction of  $(\text{Cp}^*-\text{d}_{15})_2\text{Sc}-\text{CH}_3$  (**1a**) with  $\text{CD}_3\text{C}\equiv\text{CCH}_3$  to yield a mixture of  $(\text{Cp}^*-\text{d}_{15})_2\text{Sc}-\text{C}(\text{CD}_3)\text{C}=\text{C}(\text{CH}_3)_2$  (**2a**) and  $(\text{Cp}^*-\text{d}_{15})_2\text{Sc}-\text{C}(\text{CH}_3)\text{C}=\text{C}(\text{CH}_3)(\text{CD}_3)$  (**2b**) ( $\text{2b:2a} = 1.01 \pm 0.02 : 1$ ). Thus steric repulsions between the 2-butyne methyl group and the scandium-bound methyl group are not sufficiently severe to give rise to a measurable steric deuterium kinetic isotope effect. Similarly, **1a** reacts with  $\text{CH}_3\text{C}\equiv\text{CCH}_3$  at approximately the same rate as does  $(\text{Cp}^*-\text{d}_{15})_2\text{Sc}-\text{CD}_3$  (**1b**), producing a mixture of  $(\text{Cp}^*-\text{d}_{15})_2\text{Sc}-\text{C}(\text{CH}_3)\text{C}=\text{C}(\text{CH}_3)_2$  (**2c**) and  $(\text{Cp}^*-\text{d}_{15})_2\text{Sc}-\text{C}(\text{CH}_3)\text{C}=\text{C}(\text{CD}_3)(\text{CH}_3)$  (**2d**) ( $k_{2c}/k_{2d} = 1.02 \pm 0.07$ ). The implication from the latter finding is that a  $[\text{Sc}-(\eta^2\text{-CH}_2\text{-H})]$   $\alpha$  agostic interaction is likely *not* present in the transition state for 2-butyne insertion into the scandium methyl bond of **1**. The latter reaction was monitored by both NMR and IR spectroscopies. A convenient method for the determination of the composition of methane isotopomers by gas-phase infra-red spectroscopy is reported.

|  |    |
|--|----|
| I. INTRODUCTION.....                     | 30 |
| II. RESULTS AND DISCUSSION .....         | 37 |
| Steric Deuterium Isotope Effects.....    | 37 |
| $\alpha$ -Deuterium Isotope Effects..... | 39 |
| III. CONCLUSIONS .....                   | 44 |
| EXPERIMENTAL SECTION .....               | 46 |
| REFERENCES .....                         | 50 |

## I. INTRODUCTION

From a commercial perspective, one of the most important contributions of Ziegler/Natta polymerization has been the introduction of a completely new kind of product: stereoregular poly( $\alpha$ -olefins). Intellectually, the extreme stereoregularity with which some Ziegler/Natta catalysts operate has provided much of the motivation for the intense study these catalysts have received. The three general structures which have been recognized are illustrated below. Isotactic polyolefins, in which consecutive chiral carbon centers bear a meso relationship to one another, have been the most commercially useful. Syndiotactic polyolefins, which consist of concatenated racemo units, have been less accessible.<sup>2</sup> Polyolefins which have no stereoregularity are referred to as atactic. Polypropylene with isotacticities of better than 99% can be prepared, making Ziegler/Natta polymerization easily one of the most highly stereoregular reactions outside of nature.

Scheme I. Stereoisomers of polypropylene.



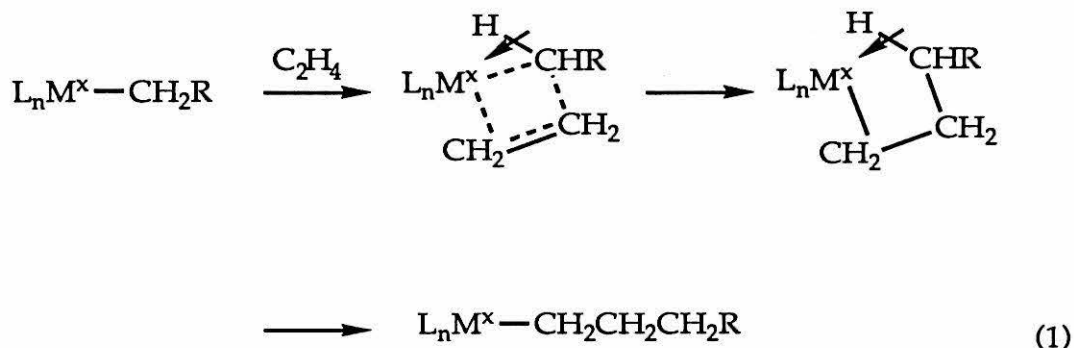
In order to understand this remarkable selectivity, one needs to know something about the geometrical requirements of the transition states involved in the carbon-carbon bond-forming, propagation step, since it is this step which will set the stereochemistry for a given repeat unit. The Cossee-

Arlman picture of direct C=C insertion into a M-C bond,<sup>3</sup> discussed in some detail in Chapter 1, provides a partial picture of the relevant transition state, but as it concerns itself exclusively with the four atoms at which bonds are either made or broken, it does not imply a particular rationale for stereochemical induction. Rather, it provides a set of basic transition-state characteristics with which any such rationale must be consistent.

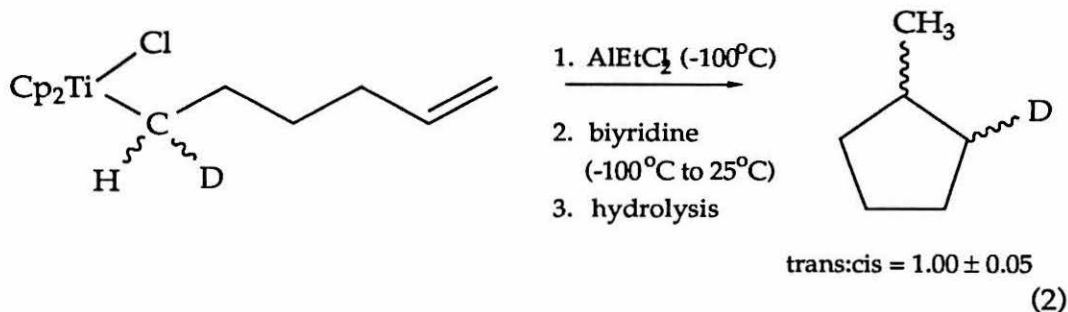
Two very recent studies--one from this group of a single-component Ziegler-Natta type system<sup>4</sup>, the other by Krauledat and Brintzinger of a zirconocene/methylalumoxane system<sup>5</sup>--suggest that the Cossee-Arlman mechanism may not always provide a complete description of olefin insertion. Specifically, it appears that an agostic interaction between the metal center and an  $\alpha$  C-H bond in the growing chain, a modification first suggested by Rooney and Green<sup>6</sup>, may play an important role in stabilizing the transition state for olefin insertion. This observation has important consequences for understanding tacticity control, as it rigidly defines a particular transition-state geometry for the growing alkyl chain. In metallocene-based catalysts, if an  $\alpha$  C-H agostic interaction is required for carbon-carbon bond formation, the  $\beta$ -carbon on the growing chain is constrained to lie out of the plane bisecting the two cyclopentadienyl units, a prediction which contradicts simple steric intuition. The geometrical constraints associated with the  $\alpha$ -agostic interaction will be looked at in more detail later in this chapter. However, the agostic effect is apparently not general.<sup>4,8</sup> It is therefore important to probe the scope of the effect, and eventually to understand the factors which favor or discourage it.

The so-called "agostic" M-C-H bond was discussed in Chapter 1, where such a interaction involving a C-H bond  $\beta$  to scandium was invoked to explain the relative inertness of the scandium-carbon bond in  $\text{Cp}^*_2\text{ScCH}_2\text{CH}_3$ . A similar interaction involving an  $\alpha$ -C-H bond was invoked in 1983 by Rooney, and by Brookhart and Green, in a modified version of the "Green/Rooney" mechanism for Ziegler-Natta olefin polymerization. These authors originally suggested that carbon-carbon bond formation occurred via  $\alpha$ -elimination from a metal alkyl, producing a carbene(hydride) species, followed by 2+2 addition and subsequent reductive elimination (see Chapter 1). When formal  $\alpha$ -elimination is impossible, as is the case with  $\text{Cp}^*_2\text{ScR}$

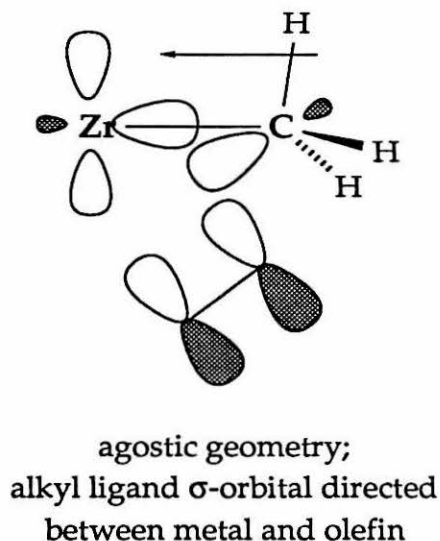
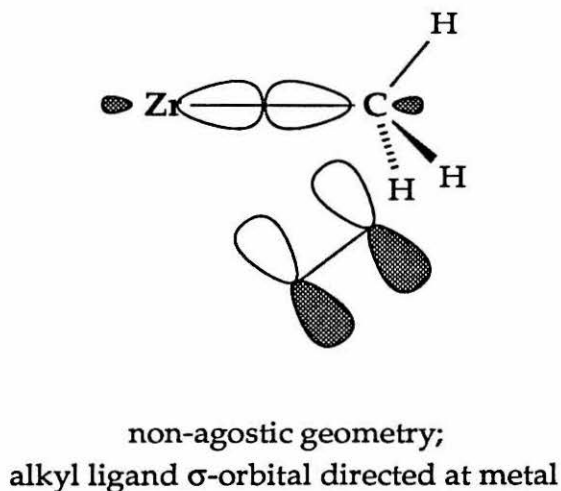
derivatives, Rooney, Brookhart, and Green suggested that a "partial" elimination--essentially the formation of an agostic interaction--could provide some electronic stabilization to the metal center during bond formation (Equation 1).



Although commonly referred to as the "modified Green-Rooney" mechanism, this suggestion is perhaps best considered as a perturbation of the Cossee-Arlman mechanism. It does not directly contradict any of the basic features of the Cossee-Arlman picture; rather, it adds to them an additional, stereochemical constraint. Tests for the validity of this mechanism have therefore been stereochemical in nature. The first experimental test was conducted by Grubbs, Clawson and co-workers for a homogeneous titanium/aluminum system.<sup>7</sup> These workers devised an isotopic labelling experiment based upon the intramolecular carbon-carbon bond forming reaction shown in Equation 2. When the unreactive chloro(alkenyl)titanium complex is activated with an alkylaluminum reagent, the pendant double bond inserts to form, upon workup, a mixture of methylcyclopentanes. Grubbs asserted that any deviation from a 1:1 mixture of cis and trans isomers would be indicative of selection between the  $\alpha$ -H and D substituents for the agostic position in a "modified Green-Rooney" transition state. No such deviation was observed, and the modified Green-Rooney mechanism seemed to have been dismissed. Indeed, the idea that a C-H bond could be an important  $\sigma$ -donor in systems where the role of olefin adducts had not been firmly established must have seemed unlikely on the ground of simple basicity arguments.



However, in 1990, Brintzinger and co-workers began working on a set of modified Hückel calculations that provided a tempting rationale for the viability of the modified Green-Rooney transition state.<sup>8</sup> Brintzinger's work suggested that the effect of an  $\alpha$ -agostic interaction might not be as much to datively stabilize the transition metal center as to increase the orbital density in the region where the new carbon-carbon bond is to be made. As the cartoon below suggests, the agostic effect appeared to be important in terms of increasing carbon-carbon overlap in the transition state. With this new conceptual approach to the problem, reinvestigation of the modified Green-Rooney mechanism appeared warranted.



The Brintzinger calculations were particularly compelling as they seemed to provide a justification for the growing body of evidence that extreme coordinative unsaturation--effectively two spatially accessible, empty, metal-based orbitals--was required to make an early transition metal complex

reactive toward Ziegler-Natta polymerization. For instance, although the neutral, 14-electron permethylscandocene alkyl system polymerizes ethylene, neutral, 16-electron zirconocene chloro(alkyl) species do not, even though they are formally electron-deficient and possess an empty orbital which could in principle support an olefin adduct.<sup>9</sup> Cationic, 14-electron zirconocene alkyl complexes are reactive olefin polymerization catalysts.<sup>10</sup> Why should there be an apparent need for an "extra" orbital? The answer, "to accomodate an agostic interaction in the transition state," began to seem reasonable. As theorists continue to attempt to rationalize and codify the lessons of stereochemical induction in homogenous systems,<sup>11</sup> efforts are also being made to parlay this information into reasonable models for reactive sites in heterogeneous catalysis.<sup>12</sup> If the requirement for  $\alpha$ -agostic assistance in bond formation is a reasonable possibility, it is important to determine whether it is real and general.

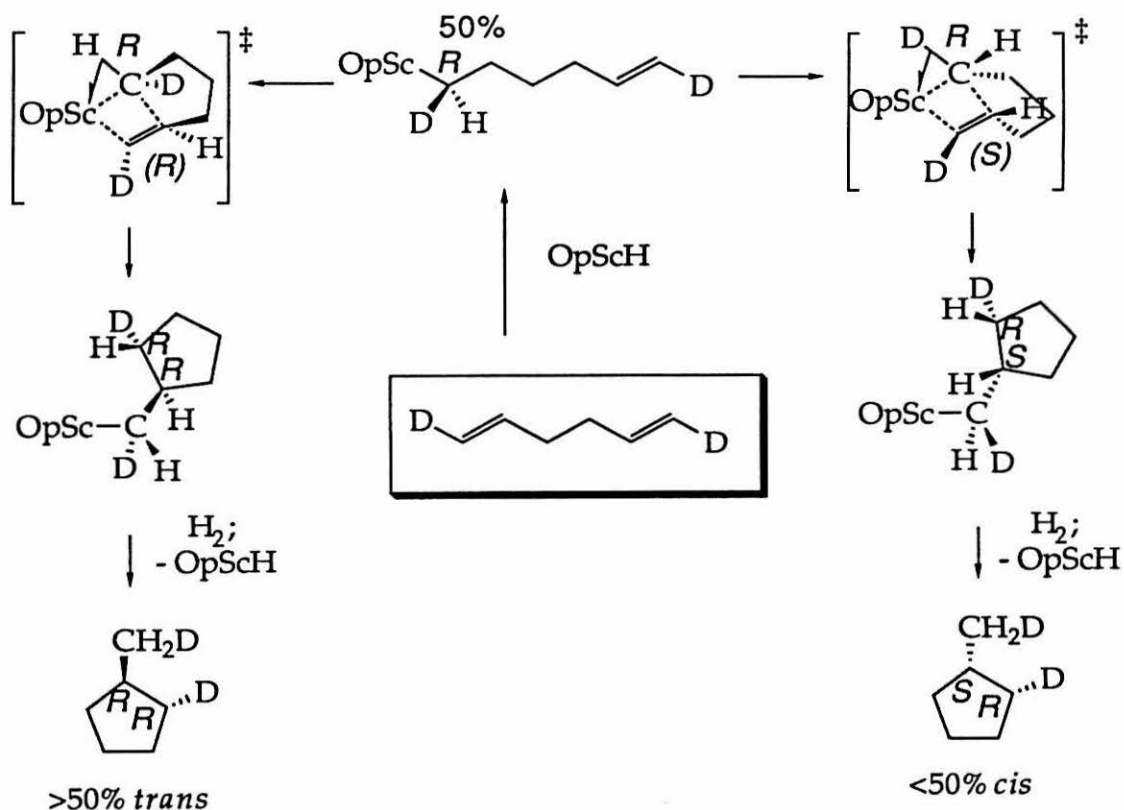
In 1990, Piers and Bercaw<sup>4</sup> performed a catalytic version of Grubbs' and Clawson's stoichiometric cyclization experiment. The ansa-scandocene derivative  $[(C_5Me_4)_2SiMe_2]ScH)_2$ , or "OpScH," was known to catalyze both the dimerization of simple  $\alpha$ -olefins (*e.g.*, propene, hexene) and the cyclization of  $\alpha,\omega$ -dienes (*e.g.*, 1,5-hexadiene, bis(allyl)methylamine, diallylsulfide).<sup>13</sup> The isotopically-labelled substrate *trans*, *trans*-1,6-dideuterio-1,5-hexadiene was prepared and cyclized to a mixture of methylcyclopentane-*d*<sub>2</sub> isomers. The ratio of *trans*- to *cis*-methylcyclopentane-*d*<sub>2</sub> was found to be approximately 1.2:1.

The proposed mechanism for this cyclization proceeds through an intermediate structure reminiscent of Grubbs' titanium alkenyl species. A detailed examination of the cyclization transition states available to the deuterated version of this intermediate (Scheme II) provides a rationale for the *cis*/*trans* perturbation anticipated by Grubbs and observed by Piers and Bercaw.

The preferred transition state for cyclization incorporates two important assumptions. The first of these is that light hydrogen rather than deuterium preferentially occupies the agostic position. This assumption is based upon zero-point energy arguments, assuming that the terminal C-H bond possesses a higher vibrational frequency than the bridging, agostic

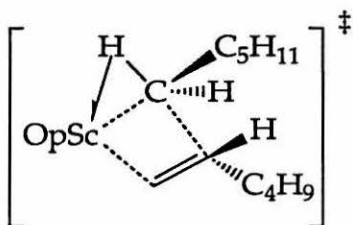
position.<sup>14</sup> The second, equally important assumption is that when the pendant double bond presents itself to the metal-carbon  $\sigma$ -bond for insertion, the carbon framework assumes a conformation such that the [5,4] bicyclic ring system, formed as the system passes through the four-center transition state discussed in Chapter 1, adopts an exclusively *cis* geometry as drawn. If the *trans*-[5,4] form were preferred, the isotope effect would be observed in the opposite direction; that is, an excess of *cis*-d<sub>2</sub>-methylcyclopentane would be observed. To the extent that the *trans*-[5,4] form is allowed, the observed isotope effect must be attenuated. Since the observed isotope effect,  $\approx 1.2$ , is normal for secondary isotope effects in general, any attenuation of the natural effect is assumed to be minor.<sup>15</sup>

**Scheme II. Origin of isotopic perturbation of stereochemistry for hexadiene hydrocyclization.**





A similar effect was observed in the hydrodimerization of 1-*d*-1-hexene by the same catalyst system. In this case, in order to explain the direction of the observed isotope effect one must make the assumption that the alkyl substituents avoid one another as shown below, if the assumption that hydrogen occupies the agostic site preferentially is to be taken as valid.



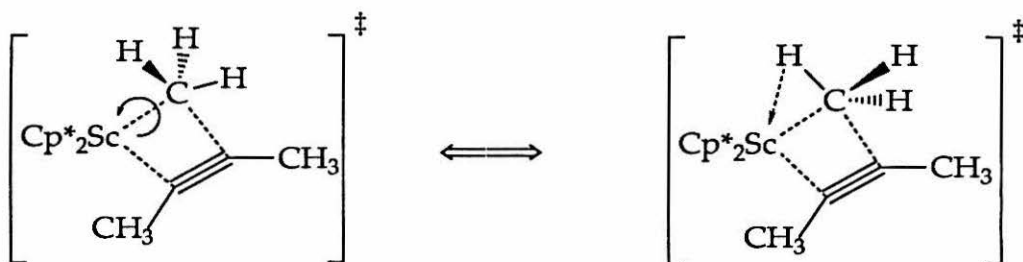
The odd history of the modified Green-Rooney mechanism became even more perplexing when Brintzinger and co-workers adapted the Piers-Bercaw experiment to the technically important zirconocene/methylaluminoxane system. While a significant isotope effect was observed for hydrodimerization chemistry,<sup>5</sup> no such effect manifested itself in the case of hydrocyclization.<sup>16</sup>

The evidence for (or against)  $\alpha$ -agostic assistance thus rests on the observation (or failure to observe) an "isotopic perturbation of stereochemistry,"<sup>7</sup> measured as an H/D isotope effect in the cyclization or hydrodimerization of singly- $\alpha$ -deuterium-labeled substrates. Of course, an observed isotope effect is often open to more than one interpretation. We have considered the possibility that the "isotopic perturbation of stereochemistry" might have arisen from a steric isotope effect rather than an  $\alpha$ -agostic interaction. The lower zero-point energy of the C-D bond relative to the C-H bond makes the former a "tighter" bond and effectively a smaller unit. The steric distinction is only marginal but can lead to observable differences in the rates of reactions which proceed via extremely crowded transition states<sup>17</sup>.

A further concern is that interpretation of the hydrodimerization and hydrocyclization results requires the invocation of a transition state in which a geometry conducive to an agostic interaction is required by conformational constraints independent of the agostic interaction itself. In other words, the [5,4] bicyclic transition state invoked for hydrocyclization forces an  $\alpha$ -C-H

bond to occupy a region of space already occupied by an empty, metal-based orbital. Similarly, in the case of hydrodimerization the requirement that the two alkyl groups--on the growing chain and the incoming olefin--avoid one another in the transition state could enforce or encourage a similar  $\alpha$ -C-H bond placement.

The question which arises from these observations is whether these particular configurational requirements drive the observed selection between agostic C-H vs. C-D, or whether the agostic interaction is an inherent requirement for carbon-carbon bond formation in these model complexes. In order to examine this question, we chose to look for  $\alpha$ -agostic assistance in intermolecular carbon-carbon bond-forming reactions across a scandium-methyl bond using small substrates. The methyl ligand was chosen because it should not be subject to any particular geometrical constraints.



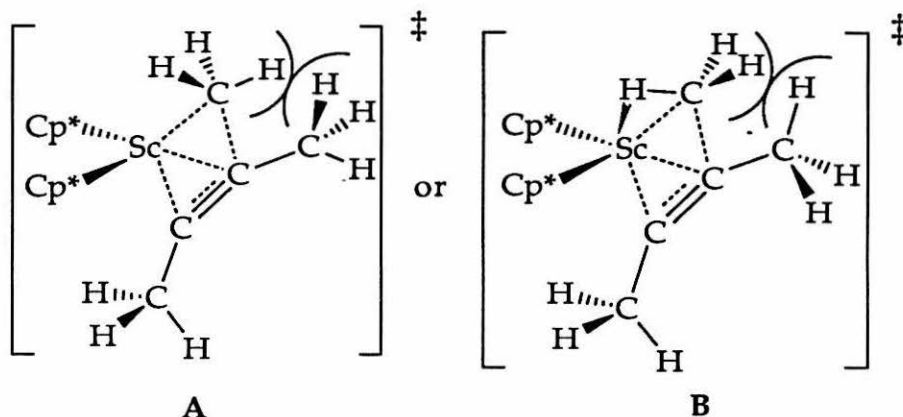
Once again, 2-butyne is an appropriate choice for the inserting ligand because of its relatively small size and clean, stoichiometric reactivity. These experiments are, on paper, inversions of those designed to probe for steric effects.

## II. RESULTS AND DISCUSSION

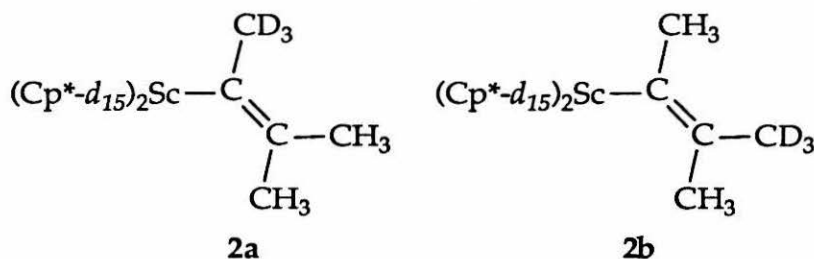
### Steric Deuterium Isotope Effects

To test whether this steric difference could reasonably account for the results attributed to an  $\alpha$ -agostic effect, we chose a carbon-carbon bond forming reaction at scandium in which steric crowding in the region of the  $\alpha$ -carbon is maximized: insertion of 2-butyne into the Sc-C bond of  $(\text{Cp}^*-\text{d}_{15})_2\text{Sc}-\text{CH}_3$ , **1a**, ( $\text{Cp}^* = \eta^5\text{-C}_5(\text{CH}_3)_5$ )<sup>18</sup>. Since 2-butyne is a linear molecule, the methyl groups on the acetylenic carbons must lie in the same

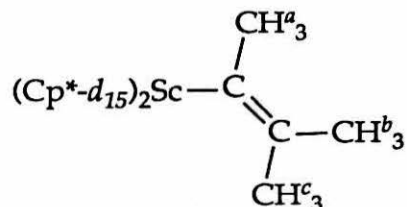
plane as the Sc-CH<sub>3</sub> unit in either transition state for insertion, conventional (A) or  $\alpha$  agostic (B).



When 2-butyne-1,1,1-*d*<sub>3</sub>, CD<sub>3</sub>C≡CCH<sub>3</sub>,<sup>19</sup> is allowed to react with **1a**, two regioisomeric products are expected:



If steric interactions between the alkyne methyl groups and the scandium-bound methyl group are sufficiently severe, **2a** and **2b** will be formed in unequal amounts, with **2b** being slightly preferred due to the decreased steric demand of the CD<sub>3</sub> group relative to the CH<sub>3</sub> group. The relative amounts of **2a** and **2b** in the product mixture can be determined by integrating the <sup>1</sup>H-NMR resonances of methyl groups (CH<sup>a</sup><sub>3</sub>, CH<sup>b</sup><sub>3</sub>, CH<sup>c</sup><sub>3</sub>) which are cleanly resolved at 400 MHz:



If **2a** and **2b** form in a 1:1 ratio, these integrals will appear in the ratio 1.50 : 1.50 : 3.00; deviation from this ratio should be indicative of a steric isotope effect.

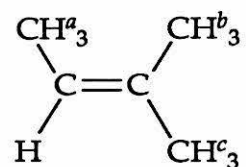
**1a** was treated with 2-butyne-1,1,1-*d*<sub>3</sub> in C<sub>6</sub>D<sub>6</sub> in a sealed NMR tube. The relative integrations of methyl groups *a* : *b* : *c* were 1.50 : 1.48 : 3.00, indicating that no isotopic perturbation of regiochemistry occurs, at least to the limits of NMR detection. Thus, steric repulsions between the 2-butyne methyl group and the scandium-bound methyl group are not sufficiently severe to give rise to a measurable steric deuterium kinetic isotope effect. By extension, we conclude that the kinetic deuterium isotope effects previously attributed to  $\alpha$ -agostic interactions in olefin insertions<sup>4,5</sup> are unlikely to be due to steric interactions. The transition state for olefin insertion necessarily positions the olefinic substituents out of the equatorial plane of the [Cp<sub>2</sub>M-R] moiety, away from [M-R] and into the cyclopentadienyl ligands. Hence, steric interactions between the reacting metal alkyl and olefin substituents should be considerably less than those between the metal alkyl and [C-CH<sub>3</sub>] in 2-butyne insertion.

### $\alpha$ -Deuterium Isotope Effects

We next examined this reaction for evidence of  $\alpha$ -agostic assistance in the transition state, by means of an internal competition experiment between (Cp\*-*d*<sub>15</sub>)<sub>2</sub>Sc-CH<sub>3</sub> (**1a**) and (Cp\*-*d*<sub>15</sub>)<sub>2</sub>Sc-CD<sub>3</sub> (**1b**) for unlabeled 2-butyne. If an  $\alpha$ -agostic interaction plays a significant role in determining the transition state energy, one would expect **1a** to react more quickly than **1b**, given the preference for H to occupy a bridging site.<sup>20</sup> That is, an agostic effect should manifest itself as an isotope effect  $k_{\text{CH}_3}/k_{\text{CD}_3} > 1$ . Furthermore, should steric interactions between the scandium methyl group and the pentamethylcyclopentadienyl ligands be severe enough, an inverse isotope effect ( $k_{\text{CH}_3}/k_{\text{CD}_3} < 1$ ) would be observed.

We chose to monitor this reaction by treating an equimolar mixture of **1a** and **1b** with varying amounts of 2-butyne (0.25, 0.44 and 0.62 equivalents) and subsequently cleaving the [Sc-C(CH<sup>*a*</sup><sub>3</sub>)C=C(CH<sup>*b*</sup><sub>3</sub>)(CY<sup>*c*</sup><sub>3</sub>)] (Y = H, D) groups from scandium in situ with water, thereby generating the corresponding 2-methyl-2-butenes, the concentrations of which were measured directly by

$^1\text{H}$  NMR at 500 MHz. The ratio of product olefins may be calculated from the integration of the  $\text{CH}^c_3$  resonance relative to the sum of the  $\text{CH}^a_3$  and  $\text{CH}^b_3$  integrations.



The normalized methyl integrations at these three stages are given in Table I. An isotope effect of essentially unity was observed ( $k_{2c}/k_{2d} = 1.02 \pm 0.07$ ). As can be seen, not only does the resonance for  $\text{CH}^c_3$  integrate to the value of 1.50 expected for no isotope effect, but, importantly, it does not change systematically with percent completion.

**Table I. Normalized methyl integrations for 2-methyl-butenes obtained from hydrolysis of 2c and 2d.**

| Percentage completion | Relative integration of $\text{CH}^c_3$ | Total relative integration of $\text{CH}^a_3$ and $\text{CH}^b_3$ . <sup>a</sup> | $\frac{[\text{CH}_3(\text{CH}_3)\text{C}=\text{CHCH}_3]}{[\text{CH}_3(\text{CD}_3)\text{C}=\text{CHCH}_3]}$ | $k_{2c}/k_{2d}^b$ |
|-----------------------|---|--|---|-------------------|
| 25                    | $1.50 \pm 0.03$                         | 6.00   | $0.99 \pm 0.04$   | $1.01 \pm 0.04$   |
| 44                    | $1.44 \pm 0.04$                         | 6.00   | $0.92 \pm 0.05$   | $1.10 \pm 0.06$   |
| 62                    | $1.53 \pm 0.04$                         | 6.00   | $1.03 \pm 0.05$   | $0.96 \pm 0.05$   |

<sup>a</sup> Defined as 6.00.

<sup>b</sup> Calculated according to the method described by Ingold and Shaw.<sup>21</sup>

This reaction can also be monitored by integrating the  $^1\text{H}$  NMR resonances due to the methanes produced by hydrolysis of the unreacted  $\text{Sc-CY}_3$  groups. The ratio of  $\text{CH}_4$  to  $\text{CH}_3\text{D}$  thus obtained is invariant over all examined levels of conversion, consistent with the absence of a significant

isotope effect. However, the observed ratio is not 1:1, but rather varies from 1:1.2 to 1:1.4, depending upon the manner in which the spectra were recorded. We do not understand the source of this apparent systematic error in the integrations of these methanes in solution (spectra were acquired with a relaxation delay of 5-10  $T_1$ 's to eliminate saturation effects; integrals were invariant over this range of relaxation delays), although it may be due to the very different peak shapes (singlet vs. septet).

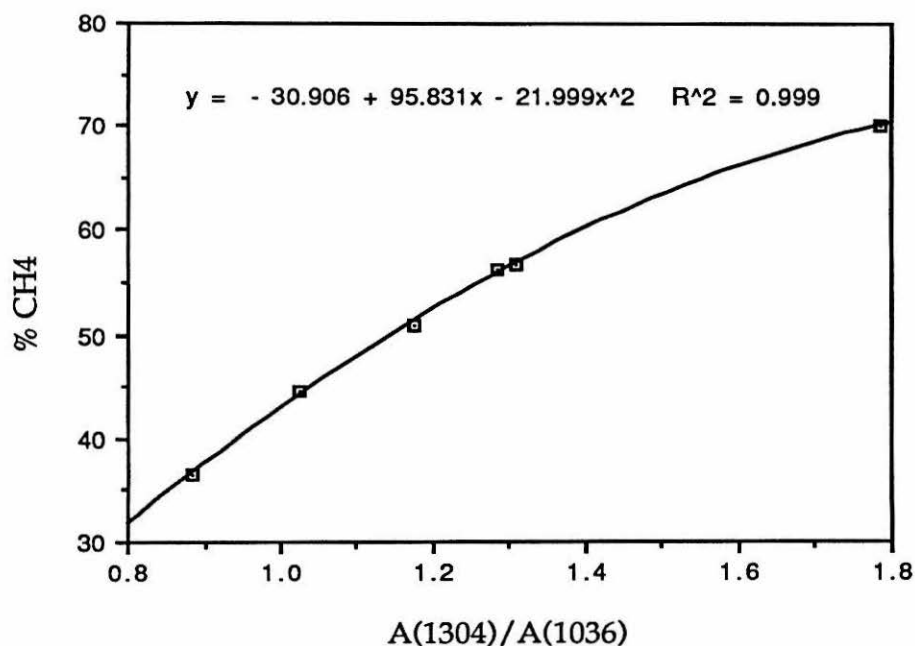
Nevertheless, and particularly in light of the scatter evident in Table I, we considered it desirable to monitor this external competition reaction by analysis of both the products produced and the residual starting materials. We thus sought a method for methane isotopomer analysis which was independent of NMR. Infra-red spectroscopic analysis of the methane mixture in the gas phase seemed a likely choice. Most of the C-H and C-D stretching and bending modes of methane and methane- $d_3$  are well-resolved from one another. Figures 1 and 2 illustrate the dependence upon composition of the relative intensities of selected bands due to each component of methane isotopomer mixtures (see Experimental for details of the construction of these calibration curves). These empirical calibration curves were used to determine the relative concentrations of methanes in gas mixtures prepared in the same manner described above, i.e., treatment of an equimolar mixture of **1a** and **1b** with varying amounts of 2-butyne (0.25, and 0.54 equivalents) followed by hydrolysis, and collected on a Toepler pump. These data are presented in Table II. Once again, no evidence of a non-unity isotope effect is observed.

**Table II. Relative concentrations of methanes obtained from hydrolysis of 2c and 2d.**

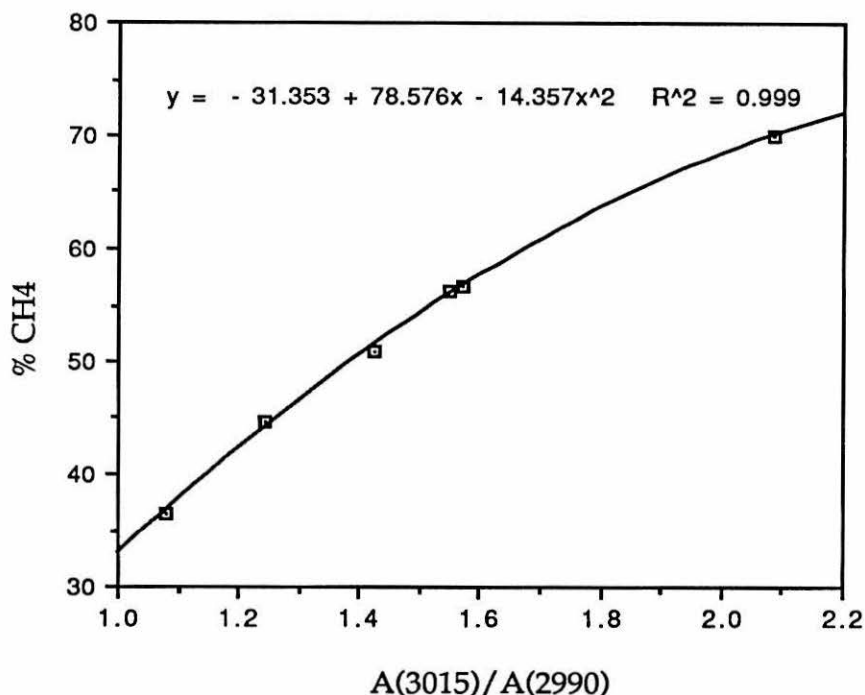
| Percent conversion | $[\text{CH}_4]_i/[\text{CHD}_3]_i$ | $[\text{CH}_4]_f/[\text{CHD}_3]_f$ | $k_H/k_D$       |
|--------------------|------------------------------------|------------------------------------|-----------------|
| 28.2               | $0.93 \pm 0.04^a$                  | $1.00 \pm 0.04$                    | $0.93 \pm 0.06$ |
| 54.0               | $1.07 \pm 0.04$                    | $1.09 \pm 0.04$                    | $0.97 \pm 0.07$ |

<sup>a</sup>Errors are calculated assuming a 1% error in percent composition from IR measurement.

**Figure 1. Methane isotopomer composition as a function of C-H/C-D bending ratios.**



**Figure 2. Methane isotopomer composition as a function of C-H stretching ratios.**



The most straightforward conclusion we may draw from the observation that **1a** and **1b** react with 2-butyne with rates that are essentially the same is that the process proceeds by way of the conventional Cossee-Arlman transition state **A**. There is, however, reason to question whether  $k_{2c}/k_{2d}$  should differ substantially from 1, even if the  $\alpha$  agostic transition state **B** were followed. The earlier experiments designed to probe for  $\alpha$  agostic assistance in the hydrocyclization of 1,5-hexadiene and 1,7-heptadiene and hydrodimerization of 1-deutero-1-hexene<sup>22</sup> differ somewhat from the one used here. Since the  $\alpha$  carbon atom was singly labeled with deuterium, those experiments utilized an *internal* H vs. D competition, whereas 2-butyne competes *externally* for **1a** or **1b** (i.e. 2-butyne must choose between molecules). Moreover, should transition state **B** operate, **1b** would have two



spectator deuteriums in addition to the one involved in the  $\alpha$  agostic interaction. Since 2-butyne competes externally for **1a** or **1b**, no isotope effect would be in evidence if the rate determining step is coordination of 2-butyne, rather than C-C bond formation. The very large, negative entropy of activation ( $\Delta S^\ddagger = -36(2)$  e.u.) and relatively small enthalpy of activation ( $\Delta H^\ddagger = 9.7(3)$  kcal·mol<sup>-1</sup>) associated with this process<sup>5b</sup> does make rate-determining 2-butyne coordination appear plausible. In the experiments utilizing an internal H *vs.* D competition an isotope effect is expected even if olefin coordination also is rate limiting. With regard to the possible effects of the two spectator deuteriums on  $k_{2c}/k_{2d}$ : to the extent that the  $\alpha$  agostic interaction rehybridizes the  $\alpha$  carbon atom from  $sp^3$  towards  $sp^2$ , a normal secondary deuterium kinetic isotope effect ( $k_H/k_D > 1$ ) from each is expected.<sup>23</sup> Thus, the isotope effect on the  $\alpha$  agostic hydrogen, also expected to be normal, should be reinforced by these secondary effects.

### III. CONCLUSIONS

The experimentally determined isotope effect,  $k_{2c}/k_{2d} = 1.02 \pm 0.07$ , does strongly imply a Cossee-Arlman transition state (A) for 2-butyne insertion. As discussed above, only if 2-butyne insertion is rate limiting, could  $\alpha$  agostic assistance occur with no observable kinetic deuterium isotope effect. Whereas these experiments have not unambiguously established whether or not  $\alpha$  agostic assistance accompanies this process, they suggest that it does not. The interpretation alluded to in the introduction to this chapter, that  $\alpha$ -agostic assistance tends to become kinetically important where the agostic configuration is favored by other factors, is one which will reappear in the discussion of hexadiene cyclopolymerization in Chapter 5. In that case, the steric demands of a polymeric substituent in a cyclization event apparently override an inherent disposition toward agostic assistance.

The experiments described in the present chapter have clearly shown that steric effects (both with the 2-butyne methyl group and the Cp\*-d<sub>15</sub> ligands)<sup>24</sup> are *not* sufficiently severe to give rise to a measurable steric deuterium isotope effect in alkyne insertion, and by extension, in alkene insertion reactions for these scandium alkyls.

Table III.  $^1\text{H}$ -NMR data for selected compounds.

| Compound/Conditions   | Assignment  | $\delta$ (ppm)    | J (Hz)                          |
|---|---|-------------------|---------------------------------|
| $\text{Z}-(\text{Cp}^*-d_{15})_2\text{Sc}-$<br>$\text{C}(\text{CH}_3)=\text{C}(\text{CH}_3)\text{CH}_3$<br><br>400 MHz $^1\text{H}$<br><br>$\text{C}_6\text{D}_6$ | $\text{Cp}^*-d_{14}$                                      | 1.80 (p)          | $^3\text{J}_{\text{H-D}} = 2.1$ |
|   | $-\text{C}(\text{CH}_3)=\text{C}(\text{CY}_3)\text{CH}_3$ | 1.89 (s)          |                                 |
|   | $-\text{C}(\text{CX}_3)=\text{C}(\text{CH}_3)\text{CH}_3$ | 1.12 (q)          | $^4\text{J}_{\text{H-H}} = 1.5$ |
|   | $-\text{C}(\text{CX}_3)=\text{C}(\text{CY}_3)\text{CH}_3$ | 1.52 (m)          |                                 |
| $\text{Z}-\text{CH}(\text{CX}_3)=\text{C}(\text{CY}_3)\text{CH}_3$<br><br>(X = H, Y = D;<br>X = D, Y = H)   | $\text{H}-\text{C}(\text{CX}_3)=$                         | $\approx 5.2$ (m) |                                 |
|   | $\text{CX}_3$   | 1.52 (d of q)     | 6.8 (d)<br>1.6 (q)              |
|   | $\text{CY}_3$   | 1.51 (d)          | 1.5                             |
|   | $\text{CH}_3$   | 1.64 (m)          |                                 |

## EXPERIMENTAL SECTION

### General considerations

All manipulations were performed under vacuum or inert atmosphere unless explicitly noted otherwise. Solvents were distilled from Na/benzophenone or 4Å activated molecular sieves and stored over Na/benzophenone or "titanocene".  $\text{Cp}^*\text{ScCH}_3$ ,  $\text{Cp}^*\text{ScCD}_3$ ,  $(\text{Cp}^*-\text{d}_{15})_2\text{ScCH}_3$ ,  $(\text{Cp}^*-\text{d}_{15})_2\text{ScCD}_3$ , and  $\text{CH}_3\text{CCCD}_3$  were prepared as described elsewhere. NMR spectra were obtained on JEOL GX-400 and Bruker WM-500 spectrometers. IR spectra were obtained on a Perkin-Elmer 1600 FTIR instrument.

### Steric Isotope Effect Experiments

$(\text{Cp}^*-\text{d}_{15})_2\text{ScCH}_3$  (47.2 mg, 0.131 mmol) was weighed into a 5-mL round-bottom flask which was sealed to a 5mm Kontes teflon valve.  $\text{C}_6\text{D}_6$  ( $\approx$  0.5 mL) was distilled onto the solid from titanocene and  $\text{CH}_3\text{CCCD}_3$  was added by vacuum transfer (323 Torr in 6.9 mL, 0.120 mmol). The reaction was warmed to room temperature and stirred for five minutes. All volatiles were then removed in vacuo. In a dry box, the oily solid residue was redissolved in  $\text{C}_6\text{D}_6$  (0.5 mL) and pipetted into a sealable NMR tube. The tube was sealed on the vacuum line. Solid  $[(\text{Cp}^*-\text{d}_{15})_2\text{Sc}]_2\text{O}$  was visible in the tube, and was separated from the solution *via* centrifuge. The  $^1\text{H}$ -NMR spectrum was recorded at 400 MHz with a 15 second pulse delay. Integrations were found to be invariant for pulse delays greater than 10 seconds.

### External Competition Experiments with NMR Analysis

In a dry box  $(\text{Cp}^*-\text{d}_{15})_2\text{ScCH}_3$  (50.2 mg, 0.139 mmol) and  $(\text{Cp}^*-\text{d}_{15})_2\text{ScCD}_3$  (50.8 mg, 0.140 mmol) were weighed into separate vials.  $\{\text{Sc}\}\text{CH}_3$  was dissolved in  $\text{C}_6\text{D}_6$  (500  $\mu\text{L}$ ) and transferred by pipet into the vial containing  $\{\text{Sc}\}\text{CD}_3$ . The first vial was rinsed with 2 500  $\mu\text{L}$  portions of  $\text{C}_6\text{D}_6$ , which were added to the second vial, bringing the total volume to 1500  $\mu\text{L}$ . All solids dissolved to give a sharp, yellow solution. An aliquot (370  $\mu\text{L}$ ) was transferred to a sealable NMR tube and frozen in liquid nitrogen.  $\text{H}_2\text{O}$  (9 Torr in 107.8 mL, 0.052 mmol) was then frozen into the tube, which was first sealed and then thawed to room temperature. In this way, no methanes were

formed until after the tube was sealed. Gas evolution was observed as the solution thawed, and a precipitate was deposited.

The rest of the solution was transferred to an "oligomerizer" (see Chapter 2), degassed and stirred overnight with 2-butyne (141 Torr in 6.9 mL, 0.0525 mmol, 0.25 equivalents) before being quenched in identical fashion to the reference sample. The same procedure was used to prepare references and samples for treatment with different amounts of 2-butyne as indicated in Table 2.

$^1\text{H}$ -NMR spectra were obtained at 500 MHz, using 16 pulses and a long relaxation delay of 400 seconds.<sup>25</sup> Several independently-phased integrations were obtained for each spectrum and averaged to obtain the values in Table 2.

### Standardization Curves for IR Determination of Methane Isotopomers

Solid  $\text{CH}_3\text{Li}\cdot\text{LiBr}\cdot(\text{Et}_2\text{O})_x$  was obtained by evaporation of a commercial solution (Aldrich) to dryness. Solid  $\text{CD}_3\text{Li}\cdot\text{LiI}\cdot(\text{Et}_2\text{O})_x$  was prepared by treatment of  $\text{CD}_3\text{I}$  with lithium metal and evaporating to dryness the clear solution obtained after filtration of the excess lithium. These solids were separately titrated by quenching a weighed amount ( $> 100$  mg per run) with  $\text{H}_2\text{O}$ , added to a frozen toluene slurry by vacuum transfer, and collecting the evolved methanes on a Toepler pump. IR analysis of the methanes evolved did not reveal contamination of either  $\text{CH}_4$  or  $\text{CD}_3\text{H}$  with other isotopomers of methane.

Reservoir bulbs of methane and methane- $d_3$  were prepared by quenching slurries of ca. 1 g of the appropriate alkyllithium reagent in toluene with a large excess of  $\text{H}_2\text{O}$  in 100-mL flasks sealed with Kontes valves. On the Toepler pump, a quantity of  $\text{CD}_3\text{H}$  was collected into the small (11.7 mL) volume, the pressure in this volume was noted, and the rest of the pump was evacuated. An additional amount of  $\text{CH}_4$  was then collected into the volume containing the previously collected  $\text{CD}_3\text{H}$ , the total volume was noted, and the rest of the pump was again evacuated. The two gases were thoroughly mixed by cycling them through the Toepler pump for at least fifteen minutes. The gas mixture was then collected once more in the small volume and the pressure was adjusted carefully to  $150 \pm 3$  Torr, and the rest of

the pump was again evacuated. An IR gas cell was attached to the Toepler pump and evacuated. The gas mixture was admitted to the cell by the shortest possible path, the equilibrated pressure in the cell and Toepler pump volume now being only a few Torr and not susceptible to accurate measurement via manometer.

This procedure of equilibrating the same total pressure with the same IR cell by the same path in each run allows the precise preparation of identical cell pressures from run to run. The relative intensities of the IR bands of interest were found to be dependent on total cell pressure.

### External Competition Experiments with IR Analysis: 2-Butyne

The general procedure is described for one experiment. Other determinations were performed in the same manner.

$\text{Cp}^*_2\text{ScCH}_3$  (153.0 mg, 0.463 mmol) and  $\text{Cp}^*_2\text{ScCD}_3$  (153.6 mg, 0.461 mmol) were weighed into separate vials and each was dissolved in toluene (1.00 mL). These solutions were then combined in a third vial. The original vials were washed with toluene (2 x 0.500 mL washings) making a total solution volume of 4.00 mL, nominally 0.231 M in Sc and 50.1 mol-%  $\text{Cp}^*_2\text{ScCH}_3$ .

Because  $\text{Cp}^*_2\text{ScCH}_3$  is frequently contaminated with small amounts of unreactive  $(\text{Cp}^*_2\text{ScO})_2$ , the ratio of  $\text{Cp}^*_2\text{ScCH}_3$  and  $\text{Cp}^*_2\text{ScCD}_3$  in the stock solution was measured by quenching an aliquot (0.500 mL, nominally 0.115 mmol) with  $\text{H}_2\text{O}$  and collecting the evolved gases (0.103 mmol) on the Toepler pump for IR analysis. After the total amount of gas had been collected and recorded, the pressure in the small Toepler pump volume (11.7 mL) was adjusted to 150 Torr and the gas mixture was admitted to a gas-phase IR cell as described above. The relevant IR intensities were as follows:  $A(3015) = 0.1196$ ,  $A(2990) = 0.0825$ ,  $A(1304) = 0.0769$ ,  $A(1036) = 0.0650$ . By comparison to the calibration curves described above, the mole fraction of  $\text{CH}_4$  was determined to be 51.6%.

To a second aliquot (0.930 mL) of this stock solution 2-butyne (0.104 mmol, 0.54 equivalents) was added by condensation from a calibrated gas bulb. The reaction mixture was allowed to stir overnight before quenching

with water and collecting the evolved gases as described above. Only 140 Torr could be collected into the small Toepler pump volume, or 93.3 % of the pressure at which the IR determination method had been calibrated. The relevant IR intensities were as follows:  $A(3015) = 0.0979$ ,  $A(2990) = 0.0688$ ,  $A(1304) = 0.0657$ ,  $A(1036) = 0.0541$ . By comparison to the calibration curves, the mole fraction of  $\text{CH}_4$  was determined to be 52.2%. As discussed above, while the error in overall pressure must have a Beer's law effect on the absolute intensities observed, the error in intensity ratios is expected to be less subject to variance over small differences in pressure, and the data were retained.

## REFERENCES

1. A portion of this work has been published. Cotter, W. D.; Bercaw, J. E. *J. Organomet. Chem.* **1992**, *417*, C1-C6.
2. (a) Ewen, J. A.; Jones, R. L.; Razavi, A.; Ferrara, J. D. *J. Am. Chem. Soc.* **1988**, *110*, 6255.  
(b) Doi, Y.; Keii, T. *Adv. Polym. Sci.* **1986**, *73/4*, 201.
3. (a) Cossee, P. *J. Catal.* **1964**, *3*, 80. (b) Arlman, E.J.; Cossee, P. *J. Catal.* **1964**, *3*, 99.
4. Piers, W.E.; Bercaw, J. E. *J. Am. Chem. Soc.* **1990**, *112*, 9406-7.
5. Krauledat, H.; Brintzinger, H.H. *Angew. Chem. Int. Ed. Engl.* **1990**, *29*, 1412-1413.
6. (a) Laverty, D. T.; Rooney, J. J. *J. Chem. Soc., Faraday Trans.* **1983**, *79*, 869-878.  
(b) Brookhart, M.; Green, M. L. H. *J. Organomet. Chem.* **1983**, *250*, 395.  
(c) Brookhart, M.; Green, M. L. H.; Wong, L. *Prog. Inorg. Chem.* **1988**, *36*, 1.
7. Clawson, L.; Soto, J.; Buchwald, S.L.; Steigerwald, M.L.; Grubbs, R.H. *J. Am. Chem. Soc.* **1985**, *107*, 3377-78.
8. Prosenc, M.-H.; Janiak, C.; Brintzinger, H. H. *Organometallics*, submitted for publication.
9. (a) Teuben, J. H., in *Fundamental and Technological Aspects of Organo-f-element Chemistry*, T. J. Marks and J. L. Fragãla, eds., Dordrecht: Reidel, 1985, p. 195.  
(b) Green, M. L. H.; Mahtab, R. *J. Chem. Soc., Dalton Trans.* **1979**, 262.  
(c) Guggenberger, L. J.; Meakin, P.; Tebbe, F. *J. Am. Chem. Soc.* **1974**, *96*, 5420.
10. Jordan, R. F. *Adv. Organomet. Chem.* **1991**, *32*, 325-387, and references therein.



11. (a) Venditto, V.; Guerra, G.; Corradini, P.; Fusco, R. *Polymer* **1990**, *31*, 530-537.  
(b) Cavallo, L.; Guerra, G.; Oliva, L.; Vacatello, M.; Corradini, P. *Polymer Comm.* **1989**, *30*, 16-19.
12. Corradini, P.; Busico, V.; Cavallo, L.; Guerra, G.; Vacatello, M.; Venditto, V. *J. Mol. Catal.* **1992**, *74*, 433.
13. Bunel, E.; Burger, B. J.; Bercaw, J. E. *J. Am. Chem. Soc.* **1988**, *110*, 976.
14. Calvert, R. B.; Shapley, J. R. *J. Am. Chem. Soc.* **1978**, *100*, 7726.
15. This second assumption will be examined in detail in Chapter 5.
16. Brintzinger, H. H. Unpublished results.
17. For a complete discussion of steric kinetic isotope effects treating both theory and experimental evidence, see Melander, L; Saunders, W.H., Jr. *Reaction Rates of Isotopic Molecules*, Wiley, New York, N.Y., 1980, pp. 189-197.
18. Thompson, M.E.; Baxter, S.M.; Bulls, A.R.; Burger, B.J.; Nolan, M.C.; Santarsiero, B.D.; Schaefer, W.P.; Bercaw, J.E. *J. Am. Chem. Soc.* **1987**, *109*, 203.
19. Whitesides, G.M.; Ehmman, W.J. *J. Am. Chem. Soc.* **1969**, *91*, 3800-3807..
20. Calvert, R.B.; Shapley, J.R. *J. Am. Chem. Soc.* **1978**, *100*, 7726-7727.
21. Ingold, C. K.; Shaw, F. R. *J. Chem. Soc.* **1927**, 2918.
22. Preliminary experiments reveal that  $\{(\eta^5\text{-C}_5\text{Me}_4)_2\text{SiMe}_2\}\text{ScH}(\text{PMe}_3)$ , like the  $\text{Cp}_2\text{ZrCl}_2/\text{MAO}$  system reported by Krauledat and Brintzinger (ref. 5), catalyzes hydrodimerization of 1-deutero-1-hexene preferentially to *erythro*-5-deuteromethyl-6-deuteroundecane. Piers, W.E.; Bercaw, J.E. Unpublished results.
23. Reference 17, Chapter 6.



24. There is a remote possibility that the steric interactions between [Sc-CY<sub>3</sub>] (Y = H, D) and Cp\*-d<sub>15</sub> ligands give rise to an inverse  $k_{2c}/k_{2d}$  which precisely offsets (or nearly so) the normal  $\alpha$  agostic  $k_{2c}/k_{2d}$  !

25. The relaxation times ( $T_1$ ) of methane isotopomers in solution are extremely long,  $\approx$  20 seconds for CH<sub>4</sub> and up to 50 seconds for CHD<sub>3</sub>.

(a) Raj, T.; Borah, B.; Riddle, R. M.; Bryant, R. G. *J. Solution Chem.* **1981**, *10*, 741-744.

(b) Gerritsma, C. J.; Oosting, P. H.; Trappeniers, N. J. *Physica* **1971**, *51*, 381.

## Chapter 4

### Polymerization of Conjugated Dienes with (Cyclopentadienyl)-amidoscandium Alkyl Complexes

**Abstract:** The polymerization of conjugated dienes by  $[(Cp^*SiNR)ScR']_2$  ( $R' = n$ -propyl,  $n$ -butyl) is slow but can produce a very nearly monodisperse product with an unusual microstructure. 1,2-insertion predominates, with two sequential 1,2-insertions leading to a rapid cyclization event. Vinylcyclopentane units account for approximately 40% of the mass of polybutadiene prepared by this method. Another 40% of repeat units are of the 1,4-insertion type, with a *cis:trans* ratio of about 1:3. Isolated allyl complexes with terminal substituents are found to adopt an anti configuration in solution; monomer insertion into the  $\eta^1$  form of this isomer presumably accounts for the relative prevalence of *trans*-1,4 repeat units. Allyl complexes can be independently synthesized by treatment of  $[(Cp^*SiNR)ScH(PMe_3)]_2$  (1) with allenes. The allyl complexes which have been isolated retain an equivalent of trimethylphosphine and are thus 16-electron compounds and inert to further insertion chemistry. Butadiene is not polymerized by  $[(Cp^*SiNR)ScH(PMe_3)]_2$ . Rather, initial 1,2-insertion is followed by rapid ethylene elimination and formation of the ethylene-bridged dimer 3. By contrast, the formation of terminally-substituted allyl products in the reaction of alkyl complexes with butadiene must proceed by a kinetically preferred 2,1-insertion in order to account for the observed regiochemistry.

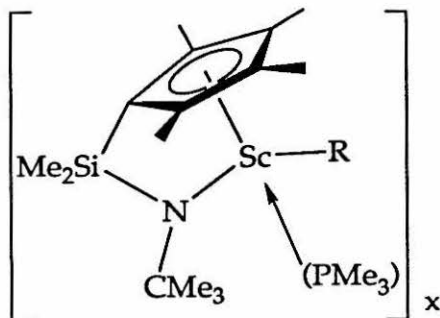
|   |    |
|---|----|
| I. INTRODUCTION .....   | 55 |
| II. RESULTS AND DISCUSSION.....                                 | 60 |
| Allylic Polymerization of Conjugated Dienes.....                | 60 |
| Preparation of Allyl Complexes.....                             | 65 |
| An Unusual Carbon-Carbon Bond Breaking Reaction .....           | 70 |
| Reactivity of the Ethylene-Bridged Dimer 3 with Butadiene ..... | 75 |
| III. CONCLUSIONS .....  | 75 |
| EXPERIMENTAL SECTION .....                                      | 80 |
| REFERENCES .....  | 84 |

## I. INTRODUCTION

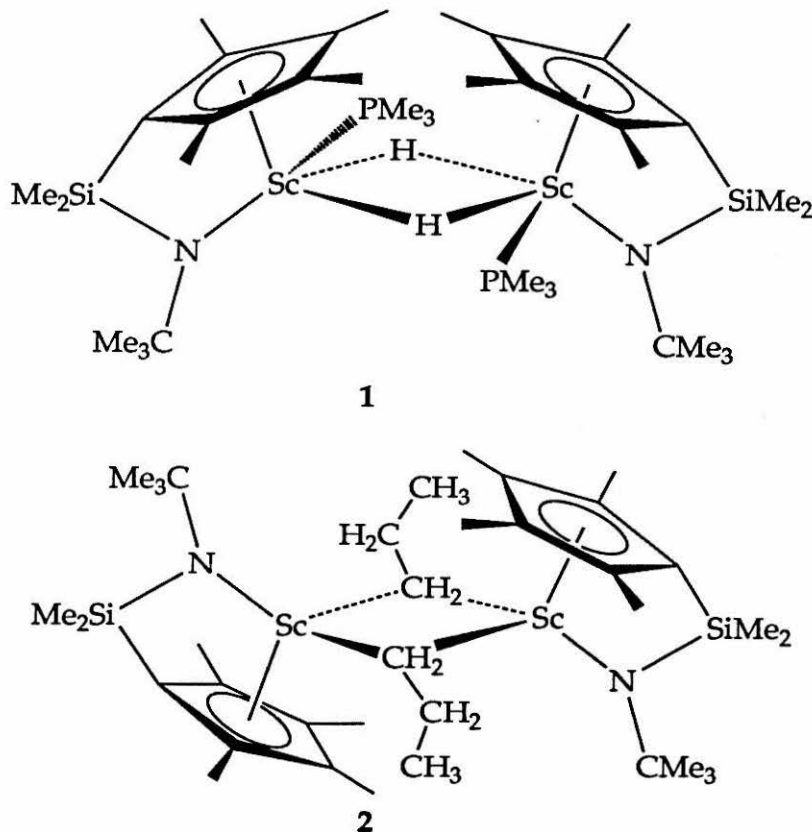
Ethylene polymerization and reactions which mimic it provide opportunities to study the most basic aspects of carbon-carbon bond formation during Ziegler-Natta catalysis. While issues concerning the regiochemistry and stereochemistry of this step are interesting in their own right, meaningful questions about them cannot be posed without some knowledge of the fundamental bond-making and bond-breaking chemistry. Chapters 2 and 3 described experiments which contribute to the basic picture we use to understand this process; however, the organometallic complexes described in Chapters 2 and 3 do not catalyze carbon-carbon bond forming reactions with substrates other than ethylene and some alkynes, and are thus unsuitable for the study of reactions where stereo- or regioselectivities can become important.

In the introduction to Chapter 3, a modified scandocene complex, "OpScH," was discussed which catalyzes dimerization and cyclization reactions of  $\alpha$ -olefins and  $\alpha,\omega$ -dienes.<sup>1</sup> Particularly through the use of isotopic labelling studies, this complex has been used to highlight the role of  $\alpha$ -agostic interactions in carbon-carbon bond forming transition states.<sup>1c</sup> Since this phenomenon can in principle affect both the electronic and the steric characteristics of carbon-carbon bond forming reactions, its study is relevant to an understanding of both the orbital interactions and the underlying causes of stereoselectivity in such reactions.

Nevertheless, none of these complexes actually polymerize olefins more complex than ethylene. The first single-component organometallic system to do so was reported in 1990 by Shapiro and Bercaw.<sup>2</sup> A generalized drawing of these complexes is shown below.

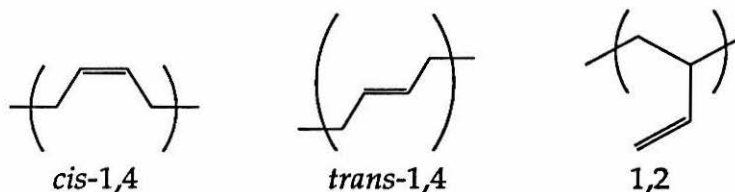


To date all structurally characterized derivatives have been dimeric in the solid state. Both phosphine-supported ( $R = H$ ) (1) and phosphine-free ( $R =$  propyl (2), butyl (3)) complexes are known.



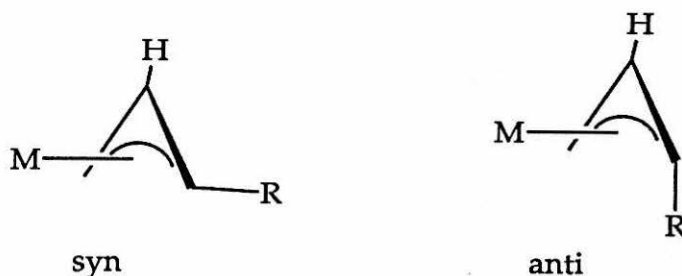
The  $[(\text{C}_5\text{Me}_4)\text{SiMe}_2\text{NCMe}_3]^{2-}$ , or "Cp\*SiNR" ligand is unique among the "ansa," or linked, cyclopentadienyl ligands in that it consists, not of two cyclopentadienyl units, but of a cyclopentadienyl ring linked to an amido moiety. This modification makes Cp\*SiNR derivatives less electronically and sterically saturated than their metallocene counterparts. Presumably both of these effects are important in the increased reactivity of this system toward the otherwise recalcitrant  $\alpha$ -olefins, though it would appear that steric relief is the more important factor.<sup>3</sup> Indeed, although the reactive intermediate in these polymerizations is thought to be a 12-electron, monomeric, base-free ("naked") scandium alkyl complex, this is not known with absolute certainty. It is possible, though it seems counterintuitive, that the 14-electron phosphine adducts (isoelectronic, though now far from isostructural with  $\text{Cp}^*_2\text{ScR}$ ) are reactive toward olefin insertion. This issue will be explored in Chapter 6.

The Cp\*SiNR derivatives exhibit broader catalytic activity than was at first appreciated. Specifically, as this chapter describes, they promote the polymerization of conjugated dienes to polymers containing the "1,4-" insertion unit characteristic of rubber. As complex as the mechanistic possibilities involved in  $\alpha$ -olefin polymerization are, diene polymerization presents an even more elaborate puzzle. Polymeric derivatives of the simplest conjugated diene, 1,3-butadiene, can contain three distinct repeat units in significant amounts, two of which (*cis*-1,4-, and *trans*-1,4-polybutadiene) are distinguished regiochemically from the third (1,2-polybutadiene) and stereochemically from one another.



Because of the enormous commercial importance of conjugated diene polymers, particularly *cis*-1,4-polybutadiene and *cis*-1,4-polyisoprene (artificial rubber), an arsenal of heterogeneous catalysts for the production of these polymers has been developed which rivals in range the  $\alpha$ -olefin polymerization catalysts.<sup>4</sup> Industrially, catalysts based on titanium, cobalt, and nickel have been the most useful for the production of *cis* polymers.

In general, the molecular characteristics of diene polymerization, especially by early transition metals, are even more poorly understood than those of  $\alpha$ -olefin polymerization.<sup>5</sup> However, several mechanistic points are widely agreed upon, if not in terms of their absolute importance, then at least in terms of their relevance as points of departure for mechanistic debate. First, it is in general assumed that a transition-metal catalyzed 1,4-diene polymerization must pass through a metal-allyl intermediate. Depending upon their substitution patterns and the metal ligand array, metal-allyl species can exist as a complicated mixture of isomers; the simplest distinction, *syn*/*anti* isomerism for a monosubstituted metal allyl, is illustrated below. The terms describe the relationship between the proton on the central allyl carbon and the substituent on a terminal carbon. Many mechanisms which attempt to describe stereoselection in 1,4-diene polymerization invoke an energetic distinction (usually steric) between *syn* and *anti* metal allyls to explain the predominance of either *trans*- or *cis*-1,4- repeat units in the polymer.



Second, most mechanistic discussions have assumed that a monomer adduct plays a crucial role in setting the regio- and/or stereochemistry. For example, a diene is capable of either bidentate or monodentate coordination to a transition metal; the former mode of binding is strongly suggestive of the 1,4-cis repeat unit, while the latter can be construed to resemble both the 1,4-trans- or 1,2- repeat units. If the geometry of the pre-coordinated ligand is assumed to be retained after carbon-carbon bond formation then it is relatively easy to construct mechanisms in which stereoselection occurs when monomer first coordinates to metal.



As is the case in  $\alpha$ -olefin polymerization, a general mechanistic solution to all the problems of bond-formation requirements, regioselection and stereoselection is unlikely to materialize. A reasonable mechanism for nickel-catalyzed polymerization is unlikely to reveal very much about titanium-catalyzed polymerization, and vice versa. Largely through the work of Teyssié,<sup>58</sup> diene polymerization by late transition metals is more thoroughly understood than is the case for early transition metals. This is because simple nickel complexes catalyze these polymerizations without the complicating presence of a co-catalyst. By studying the microstructure of 1,4-polybutadiene produced by allylnickel trifluoroacetate in the presence and absence of Lewis bases, Teyssié concluded that the stereoselective step was in fact monomer coordination. In the absence of Lewis bases, two coordination sites at a square planar Ni(II) center are available and bidentate monomer coordination is possible. The polymer produced under these conditions is predominantly cis. When a Lewis base such

as triphenylphosphite blocks one of these sites, monodentate coordination of butadiene is proposed to account for the formation of predominantly trans-1,4-polybutadiene.

Although titanium-based Ziegler-Natta catalysts have been used for the production of cis-polybutadiene since 1964<sup>6</sup> molecular-level mechanistic work in the area is almost totally lacking. Binary ( $\text{LnCl}_3/\text{AlR}_3$ ) lanthanide-based catalysts for the production of high-cis polybutadiene were first reported by Chinese workers in 1964.<sup>7</sup> Though the stereochemical properties of these catalysts were favorable, they received little attention for many years due to their relatively low reactivity. Since the report in 1980 of improved reactivity for some ternary systems (e.g.,  $\text{LnCl}_3/\text{AlR}_3/\text{R'OH}$ )<sup>8</sup>, lanthanide catalysts—in particular, those based on neodymium—have received renewed attention from several groups.<sup>9</sup> Lanthanide catalysts are unique for their ability to make high-cis polymer with substituted dienes. They frequently promote living polymerization as demonstrated by the preparation of block co-polymers and functionalized polymers. In addition, unlike titanium, cobalt, or nickel catalysts, the stereoselectivities of lanthanide catalysts show only a weak dependence on factors such as counterion and solvent. Some attempts at mechanistic interpretation of these catalysts have been made, but competent single-component model systems have not been synthesized.

Our hope in examining the polymerization of dienes with the  $\text{Cp}^*\text{SiNR}$  system was that by using well-defined, single-component catalysts we might begin to understand the preferred modes of reactivity for early transition metal and lanthanide Ziegler-Natta diene polymerization catalysts. At least one might hope to learn which questions are the relevant ones to ask. For example, what catalyst characteristics influence 1,2-/1,4- regioselectivity? If 1,4-polymerization occurs, at what point along the reaction coordinate is the cis/trans isomerism for a particular repeat unit set? Does one need to consider the possibility of a carbon-carbon bond forming reaction directly from a  $\pi$ -allyl complex, or can one assume that all  $\pi$ -allyls react via their  $\sigma$ -allyl isomers and thus treat all bond-forming events approximately as olefin insertion across a metal-carbon  $\sigma$ -bond? What termination steps, if any, will be important?

We have not been able to address these questions with any degree of completeness in this work. What we have been able to do is to demonstrate the



complexity involved in homogeneous diene polymerizations with these early transition metal derivatives. Our exploration of this chemistry has been characterized by unexpected reactivity, manifested in polymer microstructure and in model reactions. Yet it will also be shown that these organoscandium catalysts maintain a strong preference to treat conjugated dienes as if they were merely peculiarly substituted  $\alpha$ -olefins. Looked at from certain perspectives, some initially confusing aspects of this chemistry begin to seem almost familiar.

## II. RESULTS AND DISCUSSION

### Allylic Polymerization of Conjugated Dienes

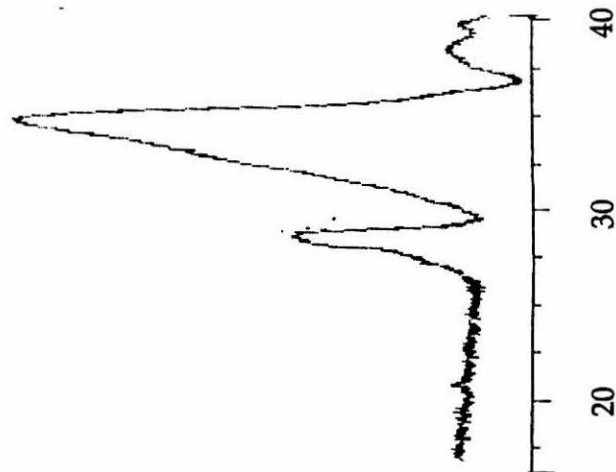
At room temperature, the phosphine-free alkyl dimers  $[(Cp^*SiNR)Sc(CH_2CH_2CH_3)_2]$  (2) and  $[(Cp^*SiNR)Sc(CH_2CH_2CH_2CH_3)_2]$  (3) catalyze the slow polymerization of butadiene and isoprene. Both 1,2 and 1,4 repeat units are present in significant amounts (*vide infra*). Molecular weights (*vs.* polystyrene) from the high oligomer (5,000 to 9,000) to the low polymer range (20,000-30,000) have been obtained with product yields of about 60%.

The molecular-weight distributions of several of these polymers shown in Figure 1 vary in systematic and informative ways. When poly(butadiene) is prepared from  $[(Cp^*SiNR)ScR]_2$  in neat monomer or at high levels of conversion in dilute solution, broad, bimodal molecular-weight distributions result, as shown in Figure 1a. This is consistent with extensive cross-linkage of poly(butadiene) via further reaction of 1,2- units (*i.e.*, pendant vinyl groups) as shown in Scheme 1a. The degree of cross-linking can be controlled. When butadiene is polymerized under conditions which encourage propagation and discourage the formation of large concentrations of polymer functionality, *e.g.*, low conversion in concentrated monomer solution, polymer with a narrow molecular-weight distribution (polydispersity index = 1.4) is obtained.

**Figure 1. Gel permeation chromatographs of polydienes prepared with scandium alkyl complex 2**

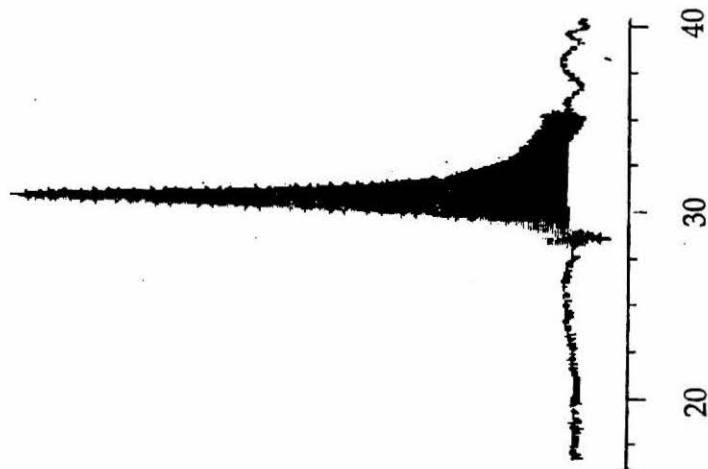
(a) polybutadiene from a dilute solution at high conversion

$M_n = 155,000; 4600$   
 $PDI = 1.14; 1.89$



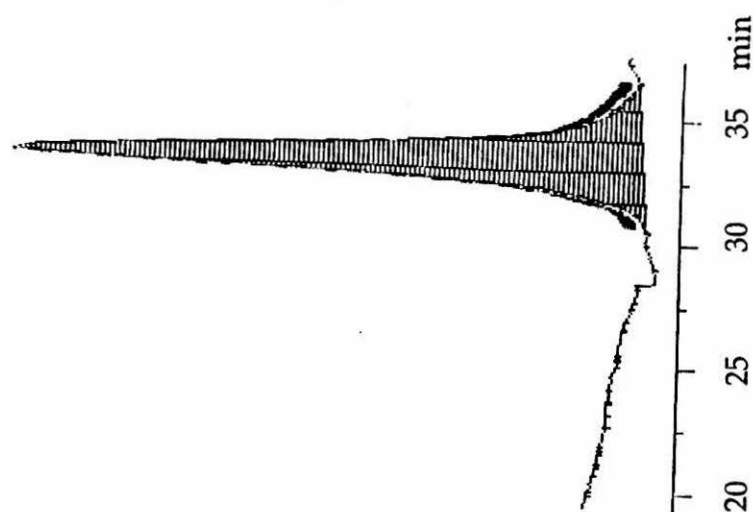
(b) polybutadiene from a concentrated solution at low conversion

$M_n = 22,000$   
 $PDI = 1.48$



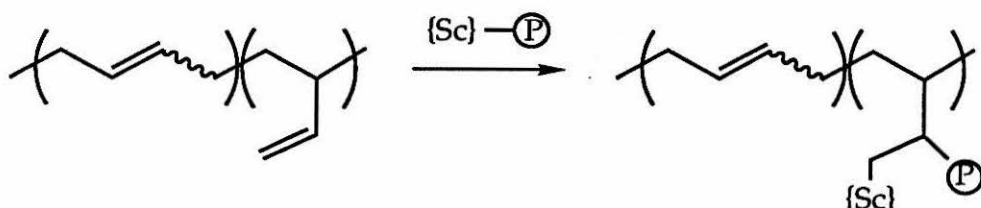
(c) polyisoprene prepared as in (a)

$M_n = 4800$   
 $PDI = 1.23$

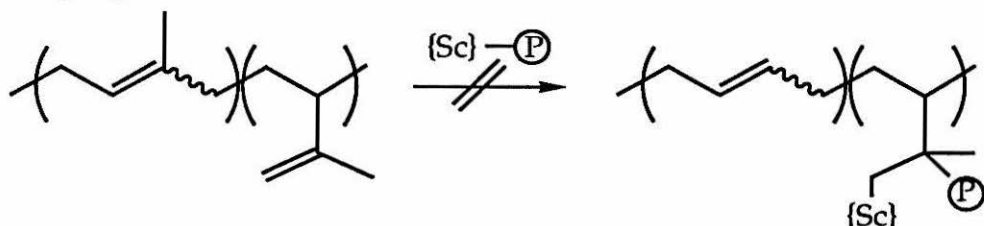


**Scheme I. Mechanisms for cross-linking in diene polymerization.**

- (a) Cross-linkage in butadiene polymerization *via* dangling vinyl groups.



- (b) Cross-linkage inhibited in isoprene polymerization by  $\beta,\beta$ -disubstitution at dangling olefin.



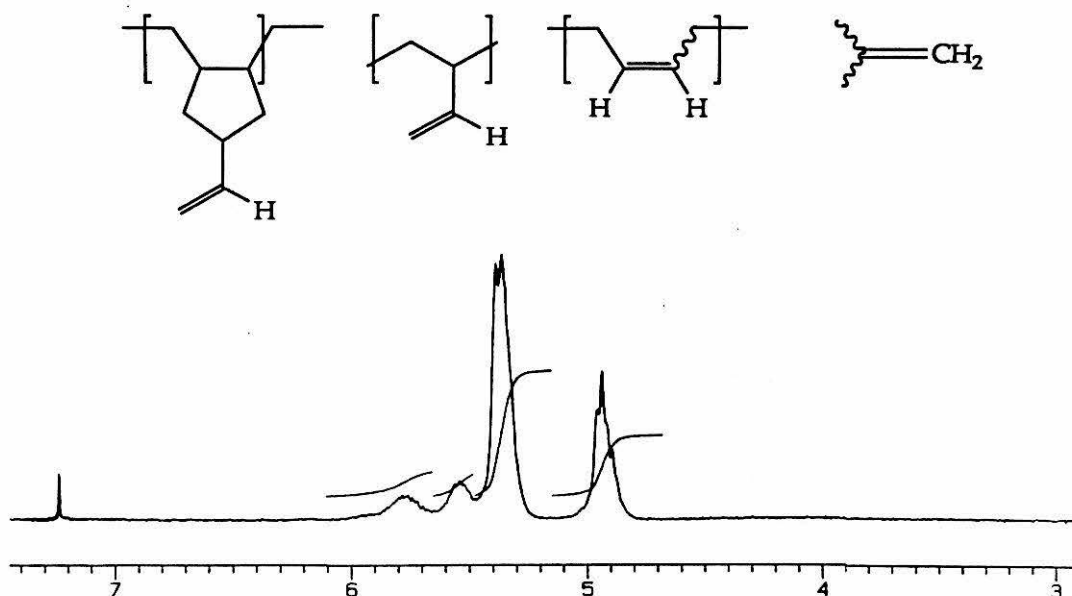
As is the case with simpler scandocene derivatives, **2** is extremely inert to the insertion of geminally disubstituted olefins across the scandium-carbon bond.<sup>2b</sup> If cross-linking is actually responsible for the molecular-weight distributions exemplified in Figure 1a, one would therefore expect markedly narrower distributions for polyisoprene. That is, as Scheme Ib suggests, the pendant olefin units in polyisoprene should show a greatly reduced tendency to participate in cross-linking reactions, compared to their less-substituted counterparts in polybutadiene. A GPC trace of polyisoprene prepared from a 1.3 M toluene solution of isoprene with a five-day reaction time is shown in Figure 1c. This polyisoprene is clearly unimodal and has an extremely low polydispersity index of 1.2. As expected, little or no cross-linking is present. A polydispersity index near 1.0 is also consistent with the absence (or at least suppression) of termination and chain-transfer reactions.  $\beta$ -Hydride elimination is a facile chain-transfer step in  $\alpha$ -olefin polymerization by **2** and **3**, which must proceed through scandium-alkyl intermediates. The absence of chain-transfer here suggests that the resting state of the catalyst is the  $\eta^3$ -allyl form, from which  $\beta$ -hydride elimination cannot occur. This conclusion is also consistent with the

generally slower polymerization observed for dienes vis-a-vis  $\alpha$ -olefins, since  $\eta^3$ -allylic intermediates would be 14-electron compounds. There is substantial evidence that carbon-carbon bond formation in this system requires a 12-electron scandium center (see Chapter 6).

$^1\text{H}$ -NMR spectroscopy is a convenient tool for determining the ratio of 1,2- to 1,4-repeat units in polybutadiene, as the olefinic protons in these two regioisomers have very different chemical shifts. Since this method relies on the presence of olefinic protons, polymer samples without significant cross-linkage were used, e.g., the low-dispersity polybutadiene sample whose molecular-weight distribution is shown in Figure 1b. The  $^1\text{H}$ -NMR spectrum of this polymer is shown in Figure 2. The low-field olefinic resonance is not attributable to either 1,4- or 1,2- repeat units.<sup>10,11</sup> Quack and Fetters<sup>11</sup> have observed this additional multiplet in the proton spectrum of polybutadiene prepared by alkyllithium-initiated anionic diene polymerization and attribute it to the vinylcyclopentyl repeat unit shown. This assignment is reasonable, at least for the polymers reported in this work, as the proposed structure can be formed via two sequential 1,2- insertions of butadiene, followed by a cyclization step analogous to 1,5-hexadiene cyclopolymerization (Scheme II).  $\text{Cp}^*\text{SiNR}$  derivatives of scandium are efficient catalysts for the latter reaction (see Chapter 5). By integration of these vinyl proton resonances, the 1,4-/1,2-/cyclopentyl repeat unit ratio is found to be approximately 2:1:1 by mass, or 2:1:2 by moles of monomer. The cis-1,4/trans-1,4 ratio is determined by integration of the olefinic  $^{13}\text{C}\{^1\text{H}\}$ -NMR signals<sup>12</sup> to be approximately 1:3.

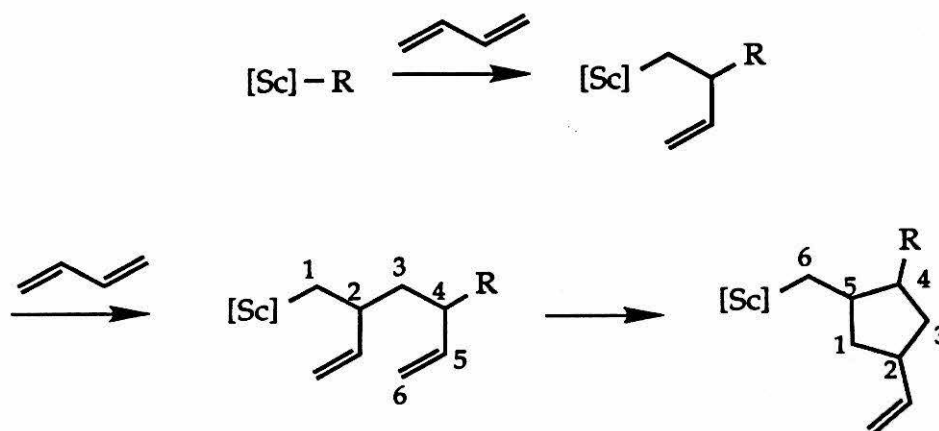
These data allow for complete regio- and stereochemical assignment of the polymer microstructure as shown in Table I. The presence of a vinylcyclopentyl repeat unit receives additional support from the internal consistency of these figures. That is, about 60 % of the insertion events are calculated to have been 1,2-insertions. Of these, another 60 % (or about 40 % of total insertions) were followed by a second 1,2-insertion and subsequent, fast cyclization.

**Figure 2. Partial  $^1\text{H}$ -NMR of polybutadiene showing the olefinic region.<sup>a</sup>**



<sup>a</sup>The four resonances at  $\approx 5.7$ , 5.55, 5.35 and 4.9 are due respectively to the four types of olefinic proton illustrated above.


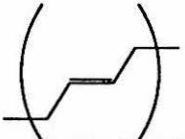
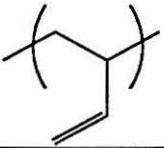
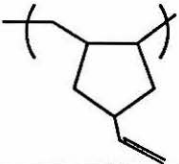
**Scheme II. Formation of vinylcyclopentyl repeat units.**



$[(\text{Cp}^*\text{SiNR})\text{ScH}(\text{PMe}_3)]_2$  (**1**) does not initiate polymerization of butadiene or isoprene at room temperature. Temperatures of  $80^\circ\text{C}$  or higher are required to initiate polymerization with this catalyst precursor. Under these conditions, the

organoscandium species are not stable, but decompose to form a clean, isolable species with NMR properties suggesting a phosphinomethanide structure. This decomposition product has also been observed in  $\alpha$ -olefin polymerization mixtures.<sup>2b</sup> Unfortunately, while this decomposition product is crystalline, single crystals suitable for X-ray analysis could not be obtained and its identity remains uncertain.

**Table I. Stereochemical assignments for polybutadiene**

| Insertion type     | Structure   | Characteristic NMR resonance             | ~mol-% in narrow-MWD poly(BD) |
|--------------------|---|--|-------------------------------|
| <i>cis</i> -1,4-   |    | 128.8-129.5 $\delta$ ( $^{13}\text{C}$ ) | 10                            |
| <i>trans</i> -1,4- |    | 129.5-130.2 $\delta$ ( $^{13}\text{C}$ ) | 30                            |
| linear 1,2-        |   | 5.55 $\delta$ ( $^1\text{H}$ )           | 20                            |
| cyclic 1,2-        |  | 5.8 $\delta$ ( $^1\text{H}$ )            | 20<br>(40 mass-%)             |

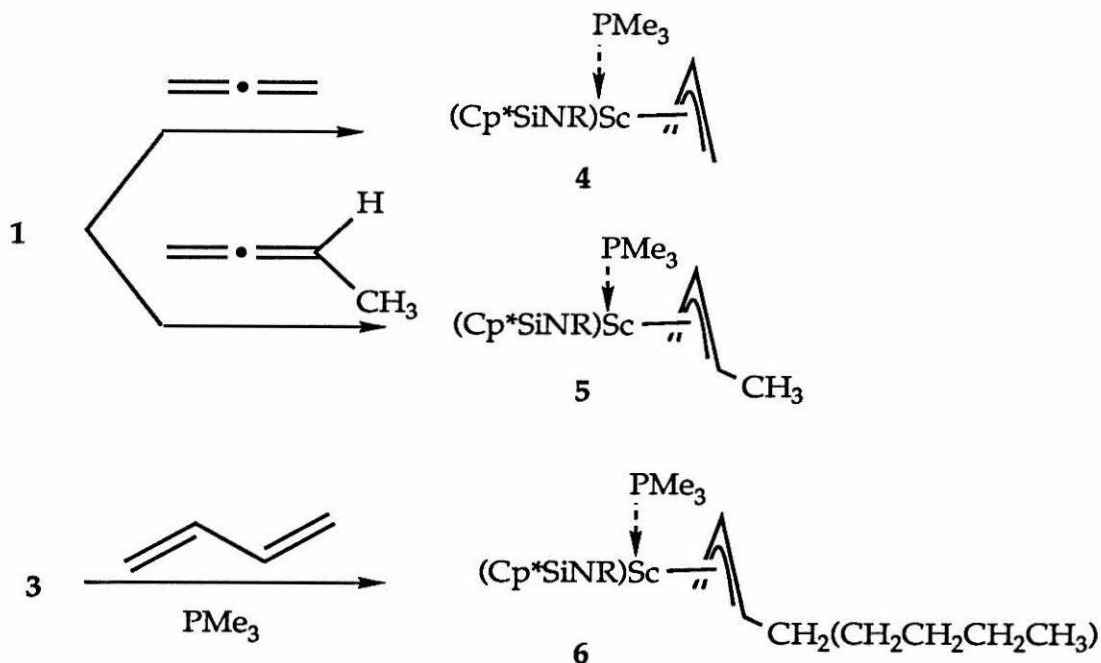
### Preparation of Allyl Complexes

Although **1** does not react with butadiene or isoprene to form allylic species (vide infra), these are readily prepared either by treatment of **1** with allenes or, perhaps somewhat surprisingly in view of the results above, by treatment of alkyl complexes **2** and **3** with 1,3-butadiene. Interestingly, when **3** is treated with 1,3-butadiene in the presence of 1/2 equivalent of  $\text{PMe}_3$ , the only

product isolated is  $(\text{Cp}^*\text{SiNR})\text{Sc}[\eta^3\text{-CH}_2\text{CHCHCH}_2(\text{CH}_2\text{CH}_2\text{CH}_2\text{CH}_3)]\cdot\text{PMe}_3$ , in nearly quantitative yield relative to phosphine.

Complexes 4-6 are well characterized by NMR and all can be prepared in reasonable yield. Regrettably, satisfactory elemental analysis was only obtained for 5. The  $^1\text{H}$ -NMR spectrum of 5 resembles those of both the bis(pentamethylcyclopentadienyl) analog<sup>13</sup> and 6. All share resonances attributable to a central allyl proton, one terminal allyl methylene group and one terminal allyl methine.

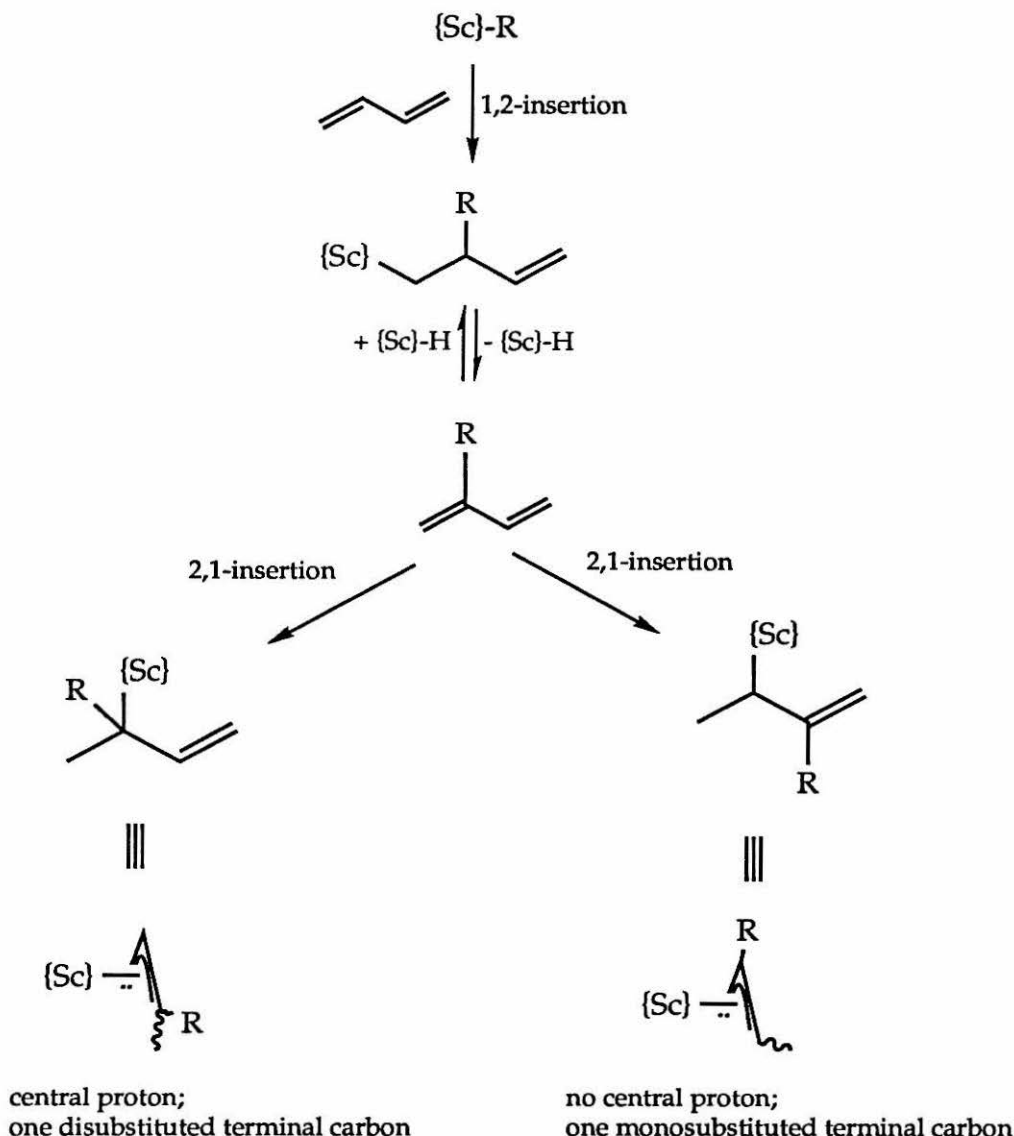
**Scheme III. Preparation of allyl complexes.**



The fact that the alkyl substituent in 6 resides at a terminal rather than central allyl carbon indicates that, contrary to what one might expect, 6 is possibly a kinetic rather than thermodynamic product. For steric reasons, 1,2-olefin insertion predominates for scandium-carbon bonds. That is, the organometallic fragment is placed at the least sterically hindered, terminal carbon of the olefin. As Scheme IV illustrates, 1,2-insertion of butadiene (which is in fact observed for the hydride complex 1, vide infra) followed by subsequent isomerization to the thermodynamically preferred allyl complex would place the alkyl substituent originally transferred from scandium at the central allyl carbon. This position in 6 is occupied by a proton, as indicated by the appearance in the  $^1\text{H}$ -NMR spectrum of a multiplet at 5.87  $\delta$ . Reasons for this apparent violation of

expected regiochemistry are not apparent (for an alternative mechanistic possibility which does not invoke a reversal of kinetic selectivity, *vide infra*).<sup>14</sup>

**Scheme IV. Regiochemistry of allyl formation by initial 1,2 insertion.**

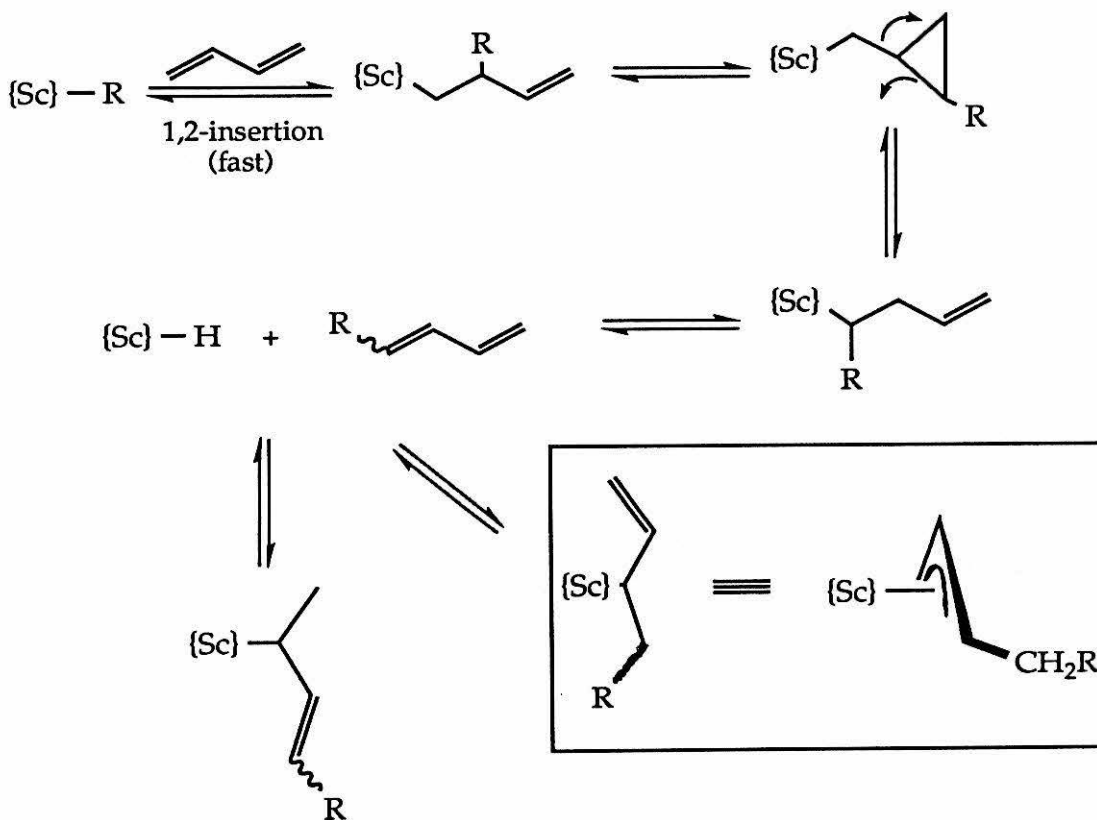


An alternative mechanism for the formation of terminally-substituted allyl complexes is shown in Scheme V. In this mechanism, the normal kinetic selectivity for 1,2-insertion of a singly-substituted carbon-carbon double bond across a scandium-carbon  $\sigma$ -bond is preserved. The first step in the effective migration of the alkyl group from the internal carbon on which it is initially placed to the terminal carbon on which it resides in the isolated product is

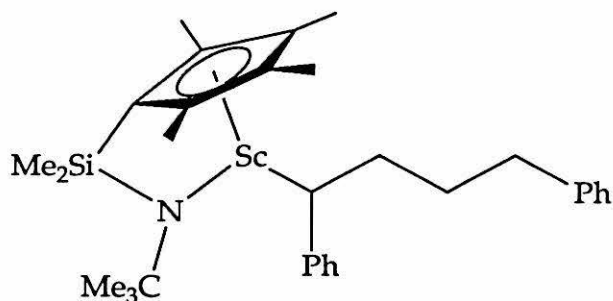


intramolecular cyclization to form an unstable cyclopropylmethyl complex. Ring-opening can occur degeneratively or productively; in the latter case, the alkyl group is transferred to the  $\alpha$ -carbon of a new alkyenyl species. Subsequent  $\beta$ -hydride elimination produces a transient scandium hydride and a new, terminally substituted diene, which can ultimately react by slow 2,1-insertion to give a pair of allyl complexes, only one of which is isolated. Like butadiene, the new diene would likely react many times by 1,2-insertion before allyl formation; this reaction manifold is omitted from Scheme V for clarity. Rapid cyclization and  $\beta$ -alkyl elimination of the type shown in Scheme V has been proposed to account for the observed scrambling of a  $^{13}\text{C}$  label from the terminal to the internal position in the formation of a crotyl complex from "OpScH(PMe<sub>3</sub>)" and 1- $^{13}\text{C}$ -butadiene.<sup>1a</sup>

**Scheme V.** Alternative mechanism for the formation of terminal allyl complexes.



It is interesting to note that a similarly counterintuitive selectivity has been previously observed for the insertion of styrene across a scandium alkyl bond supported by this ligand system.<sup>2b</sup> Thus reaction of **1** with two equivalents of styrene proceeds by 1,2-insertion of the first styrene equivalent across the scandium hydride bond, as expected. The second equivalent undergoes 2,1-insertion across the new scandium-carbon bond, forming the benzyl complex shown below, which is inert to further insertion.



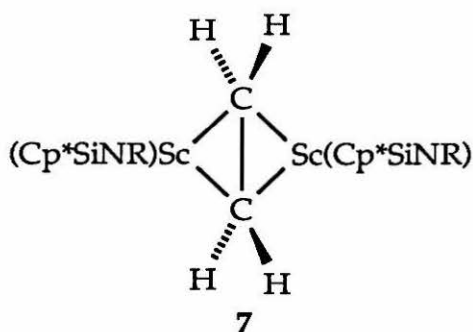
Allyl complexes **4-6** undergo rapid phosphine dissociation and  $\eta^3\text{-}\eta^1$  isomerization in solution as indicated by  $^1\text{H-NMR}$  spectroscopy. At ambient temperatures, the  $^1\text{H-NMR}$  spectra of **4-6** are typical of  $(\text{Cp}^*\text{SiNR})\text{ScR}'$  complexes with a vertical plane of symmetry. At 210 K the 500 MHz  $^1\text{H-NMR}$  spectrum of **5** indicates that this apparent symmetry has been broken. The signals of the ancillary  $\text{Cp}^*\text{SiNR}$  ligand are sharp at 210 K, while those of the allyl are broad. Dynamic phosphine dissociation processes are typically frozen out for  $(\text{Cp}^*\text{SiNR})\text{ScR}'$  complexes in this temperature regime. Further cooling reveals a second fluxional process which broadens all resonances. The second process cannot be frozen out, and presumably involves intramolecular isomerization of the allyl group.

Although they hydrogenate cleanly, compounds **4-6** are relatively inert to insertion chemistry. They do not react with 2-butyne at room temperature and decompose in the presence of 2-butyne when heated to 80°C. Finally, they promote the polymerization of ethylene, with rapid propagation and slow initiation. Thus, while treatment of **5** with 22 equivalents of ethylene in an NMR tube leads to the formation of solid polymer, the primary product visible by  $^1\text{H-}$

NMR after reaction is complete is unreacted **5**. The relative inertness of these species is entirely consistent with their formulation as 16-electron complexes.

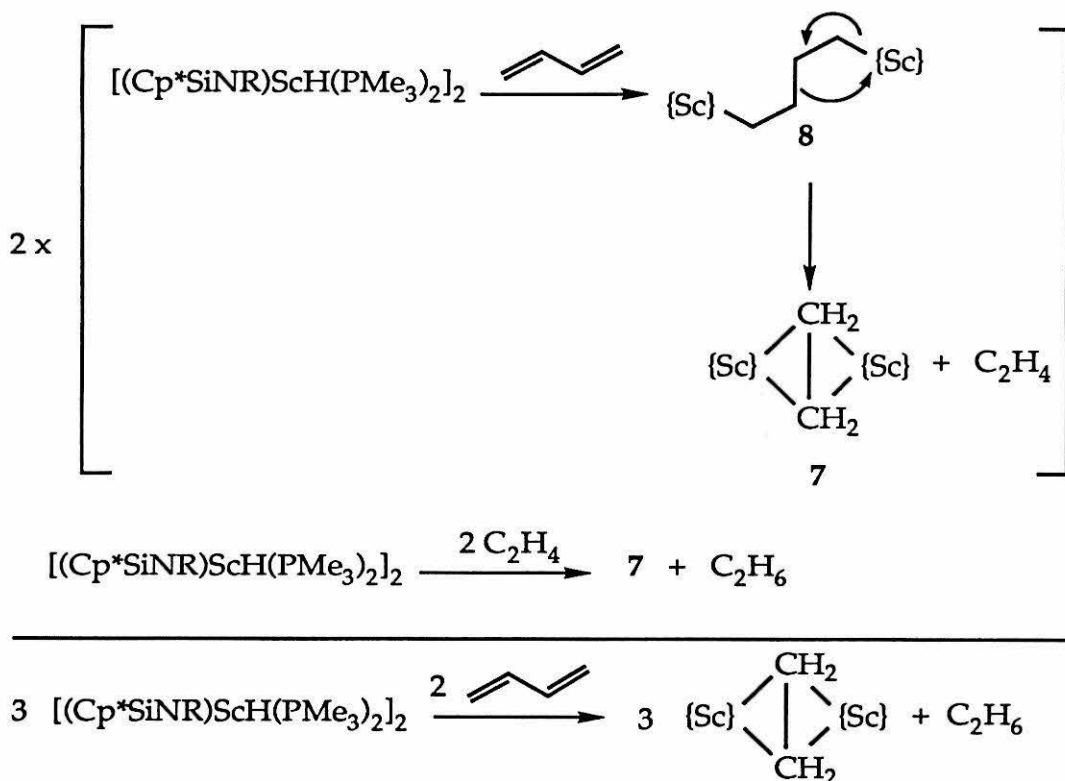
### An Unusual Carbon-Carbon Bond Breaking Reaction

Attempts to prepare the crotyl complex **5** from  $[(\text{Cp}^*\text{SiNR})\text{ScH}(\text{PMe}_3)]_2$  (**1**) and butadiene led instead to the isolation of the previously characterized ethylene-bridged dimer  $[(\text{Cp}^*\text{SiNR})\text{Sc}(\text{CH}_2\text{CH}_2)(\text{PMe}_3)]_2$  (**7**)<sup>15</sup> in 40% yield. Isoprene reacts in a similar fashion to produce **7** in lower yield, about 20%. The product of these reactions is unambiguously identified as **7** by its NMR spectrum—particularly the resonances of the ethylene protons—and by comparison of its unit cell parameters to those previously reported for **7**.

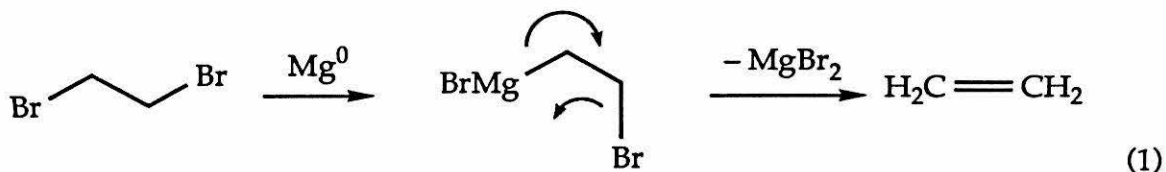


A proposed mechanism for the formation of **7** is shown in Scheme VI. Initial insertion of butadiene across the scandium-hydride bond must occur in the 1,2 sense, as 2,1-insertion would lead to the expected stable product **5**, which has been independently prepared (*vide supra*). Formation of a 1,4-discandabutane (**8**) followed by carbon-carbon bond cleavage leads to evolution of ethylene, which reacts with **1** to produce more **7** and ethane. The overall reaction was confirmed by the isolation via Toepler pump of ethane from the reaction of  $[(\text{Cp}^*\text{SiNR})\text{ScH}(\text{PMe}_3)]_2$  with 2/3 equivalent of butadiene.

**Scheme VI. Proposed Stoichiometry and Mechanism for Butadiene  
Fragmentation and Formation of 7**



The bond-cleavage reaction in Scheme VI can be considered a peculiar  $\beta$ -alkyl elimination reaction, or a special case of heterolytic fragmentation of organic compounds,<sup>16</sup> in which one scandium atom behaves as the electrofuge and the  $\gamma$ -carbon acts as the nucleofuge. Partial hydrogenation of butadiene to ethylene and ethane provides 94 kcal/mol of driving force.<sup>17</sup> Perhaps the simplest organometallic analog is the formation of ethylene from magnesium and 1,2-dibromoethane (Equation 1).<sup>8</sup>

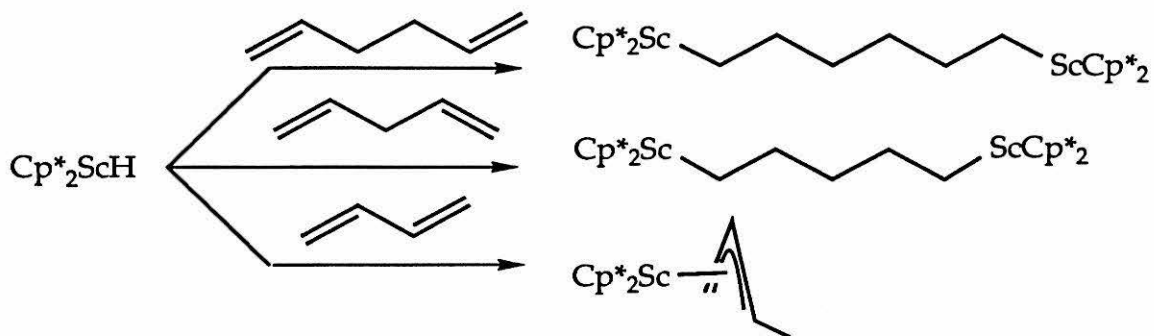


Hessen and Teuben<sup>18</sup> have observed that treatment of  $\text{CpVCl}(\text{PMe}_3)_2$  (generated in situ by reduction of  $\text{CpVCl}_2(\text{PMe}_3)_2$  with  $\text{Na/Hg}$ ) with the bifunctional Grignard reagent  $\text{BrMg}(\text{CH}_2)_4\text{BrMg}$  results in the formation of the ethylene complex  $\text{CpV}(\eta^2\text{-C}_2\text{H}_4)(\text{PMe}_3)_2$ . In this case, vanadium undergoes a formal change of oxidation state from +2 to either +1 (if the product is considered to be an ethylene adduct) or +3 (if the product is considered to be a vanadacyclopropane). One of the mechanisms proposed by these workers for fragmentation of the presumed 1,6-divanadahexane intermediate (Equation 2) is a radical rearrangement similar to the fragmentation reaction discussed above.



More detailed investigation of the mechanism of butadiene fragmentation by **1** met with little success. No intermediates could be observed when the reaction between **1** and butadiene was monitored by NMR at low temperatures, nor could an equilibrium between the proposed intermediates **8** and **7** be observed in the presence of ethylene (polyethylene formation was immediate, even at low temperatures). Attempts were made to prepare **7** by independently generating the 1,6-discandahexane **8**. Treatment of  $(\text{Cp}^*\text{SiNR})\text{ScCl}$  with  $\text{BrMg}(\text{CH}_2)_4\text{MgBr}$  yielded no clean products. This failure is not particularly surprising as the only alkylating agent known to react cleanly with  $(\text{Cp}^*\text{SiNR})\text{ScCl}$  is the extremely bulky  $\text{LiCH}(\text{SiMe}_3)_2$ . Nevertheless, formation of **7** coupled with evolution of ethane (and by extension ethylene) strongly implicates the formation of **8** and suggests that  $[(\text{Cp}^*\text{SiNR})\text{ScH}(\text{PMe}_3)]_2$  reacts with butadiene as if it were a bifunctional  $\alpha$ -olefin. This reactivity may be contrasted to that of  $\text{Cp}^*_2\text{ScH}$  with  $\alpha,\omega$ -diolefins (Scheme VII).<sup>13</sup> The non-conjugated olefins 1,5-hexadiene and 1,4-pentadiene react as bifunctional olefins—that is, each double bond reacts independently with a scandium-hydride bond to yield  $\alpha,\omega$ -discandaalkane products analogous to **8**. Butadiene reacts via formation of an allylic species.<sup>19</sup> A stable 1,6-dihafnahexane,  $\text{Cp}^*_2\text{Hf}(\text{H})\text{-CH}_2\text{CH}_2\text{CH}_2\text{CH}_2\text{Hf}(\text{H})\text{Cp}^*_2$  has been reported<sup>20</sup> from the reaction of excess  $\text{Cp}^*_2\text{HfH}_2$  with 1,3-butadiene. This reaction is not clean; the crotyl hydride species  $\text{Cp}^*_2\text{Hf}(\text{H})(\eta^3\text{H}_2\text{CCHC}(\text{H})\text{CH}_3)$  forms competitively. Relative yields of these 2,1- and 1,2- insertion products are not reported.

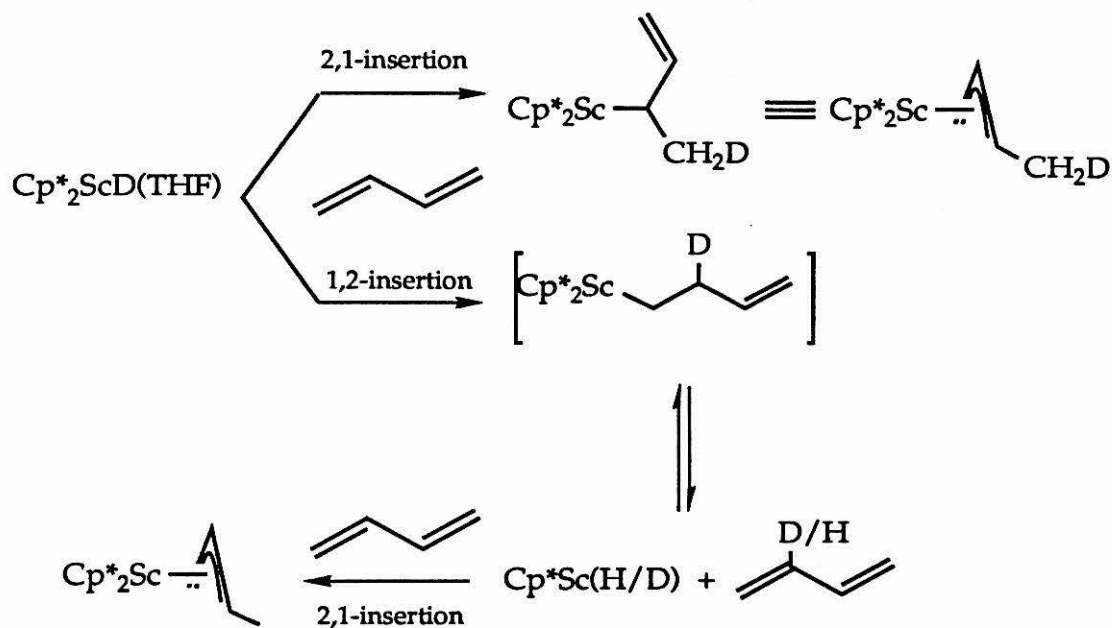
**Scheme VII. Reactivity of Cp\*<sub>2</sub>ScH with dienes.**



1,2-insertion of butadiene across the scandium hydride bond is the initial event in the formation of  $\text{Cp}^*\text{Sc}(\text{crotyl})$ . This was determined by the isotopic labelling experiment shown in Scheme VIII. Treatment of the isolable deuteride  $\text{Cp}^*\text{ScD}(\text{THF})$  with an excess of butadiene results in formation of the crotyl complex. If the product is formed by direct allyl formation via 2,1-insertion, deuterium should be placed exclusively in the methyl position. If the reaction pathway is initial 1,2-insertion followed by isomerization to the thermodynamically favored allyl, most of the deuterium label will be washed out by the excess of butadiene, and what remains will be scrambled about the four crotyl positions. The latter proves to be the case. As Figure 3 shows, only a small amount of deuterium incorporation into the methyl position is observed. No deuterium incorporation at the other sites can be detected. Initial insertion of butadiene across the Sc-D bond is therefore reversible. Since  $\beta$ -hydride elimination from allylic species is unfavorable (cf. the lack of chain-transfer processes during diene polymerization) even though these must be in a rapid  $\eta^1/\eta^3$  equilibrium, loss of the deuterium label is most consistent with initial 1,2-insertion of butadiene.

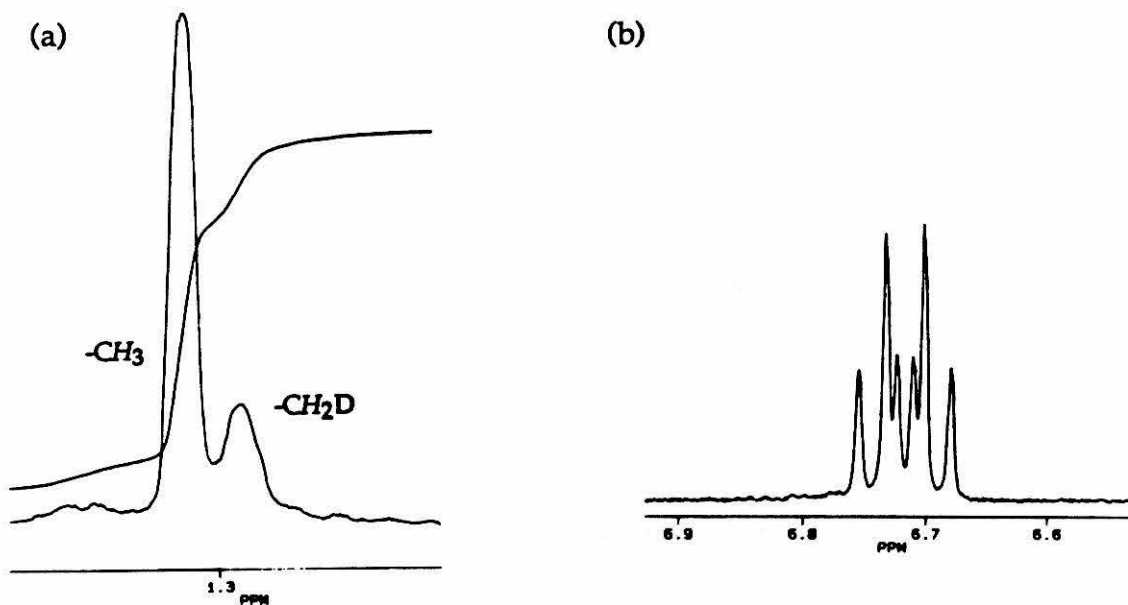
In the Cp\*SiNR case, the 1,2-insertion product **8** is unstable. Its formation is thus essentially irreversible and the kinetically disfavored 2,1-insertion which would lead to the expected allyl product never occurs. Although they display very different subsequent activities, the kinetically favored pathway for reaction of butadiene with both permethylscandocene hydride and **1** is 1,2-insertion. These results are consistent with our expectations based on  $\alpha$ -olefin reactivity, and highlight the unusual nature of the effective 2,1-insertions observed for scandium alkyl complexes **3** and **4** (*vide supra*).

**Scheme VIII. Reaction of  $\text{Cp}^*_2\text{ScD}(\text{THF})$  with butadiene.**



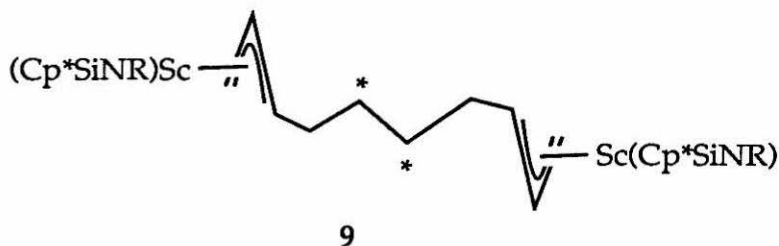
low levels of D incorporation  
possible at all sites except  
terminal methylene.

**Figure 3. Partial  $^1\text{H}$  NMR of the product of reaction between  $\text{Cp}^*_2\text{ScD}(\text{THF})$  and butadiene. (a) terminal methyl group decoupled at geminal proton; (b) central allylic proton showing undisturbed coupling to terminal methylene and methine protons.**



## Reactivity of the Ethylene-Bridged Dimer **3** with Butadiene

Because **7** is clearly the primary product when hydride **1** is treated with butadiene, the reactivity of **7** itself toward butadiene was investigated. Treatment of **7** with butadiene results in the isolation of a new allylic complex (**9**).



The assignment of **9** is consistent with the detection by NMR of one allylic unit per scandium, with  $^1\text{H}$ -NMR resonances which strongly resemble those of **5** and **6**. Furthermore, when  $7\text{-}^{13}\text{C}_2$  (labeled at the bridging carbons) is prepared and treated with butadiene, the carbon label is found in a unique, aliphatic methylenic site ( $\delta = 33.7$  ppm;  $^1\text{J}_{\text{C-H}} = 119$  Hz).

The formation of **9** from **7** clearly demonstrates that allylic species are ultimately formed when **1** is treated with excess butadiene. The inefficiency of **1** as a catalyst precursor is therefore due to the presence of trimethylphosphine rather than to the formation of **3** as a thermal sink. This is not surprising, as  $(\text{Cp}^*\text{SiNR})\text{Sc}(\eta^3\text{-allyl})(\text{phosphine})$  is a 16-electron complex. Assuming that the reactive intermediate is a 12-electron alkyl (or  $\eta^1\text{-allyl}$ ) species<sup>21</sup>, dissociation of phosphine, allylic rearrangement and intramolecular double-bond dissociation are required before propagation can take place.

## III. CONCLUSIONS

The phosphine-free scandium alkyl complexes  $[(\text{Cp}^*\text{SiNR})\text{Sc}(\text{R})]_2$  ( $\text{R} = \text{propyl, butyl}$ ) catalyze the slow polymerization of conjugated dienes to products which consist mostly, but not exclusively, of 1,2 repeat units, including an unusual cyclized derivative. Polymers with very narrow molecular weight distributions can be obtained, and while these polymerizations have not been rigorously shown to be "living," chain-transfer processes are clearly suppressed. The relative inertness of the allylic resting state of the catalyst provides favorable



chain-transfer properties to this polymerization at the expense of propagation rate.

The 1,4 repeat unit characteristic of rubber accounts for about 40% of the product. One assumption which informs this discussion but which has not been demonstrated is that 1,4-repeat units arise from allylic intermediates formed by 2,1-insertion of a diene across a scandium-carbon bond. A corollary assumption is that the intermediate scandium allyls react from the  $\eta^1$ -isomer, more or less as if they were alkyl complexes. Pathways involving direct hydrocarbyl transfer to the  $\delta$ -carbon of an inserting diene cannot be excluded, but are not preceded for early transition metals.

The factors which influence selection between 1,2- and 2,1-insertion are not clear from the experiments reported here, but some interesting variations in regioselectivity have been noted. Scandium-hydride bonds, both in this system and the parent permethylscandocene system, show an almost exclusive kinetic preference for 1,2-insertion. This pathway is reversible for permethylscandocene hydride; slower 2,1-insertion eventually leads to the observed, stable, allylic product. For the cyclopentadienyl(amido)scandium hydride **1**, initial 1,2-insertion is followed by rapid butadiene fragmentation and attendant formation of the ethylene-bridged dimer **7**. These reactions contrast sharply with those of scandium alkyl complexes **4-6** which, stoichiometrically and in the presence of phosphine, show a marked kinetic preference for 2,1-insertion which resembles that previously observed for styrene dimerization.

While organoscandium complexes have proven to be outstanding models for the reactive sites in Ziegler-Natta polymerization of  $\alpha$ -olefins, they do not appear to be satisfactory models for those titanium or lanthanide catalysts which produce high-cis polybutadiene. Although the  $\text{Cp}^*\text{SiNR}$  catalysts are sterically open relative to permethylmetallocenes, for example, it may be the case that the reactive sites for the much larger lanthanide metal catalysts are not well-modelled by a smaller metal in a moderately constrained environment. If monomer pre-coordination plays as important a role in lanthanide-catalyzed diene polymerization as it does in the nickel catalysts studied by Teyssié, the absence of f-electrons at scandium may also be an important limitation.

Table II. NMR data for selected compounds.

| Compound/<br>Conditions   | Assignment                          | $\delta$ (ppm) | J (Hz)                   |
|---|-------------------------------------|----------------|--------------------------|
| $(\text{Cp}^*\text{SiNR})\text{Sc}(\eta^3\text{-CH}_2\text{CHCH}_2) \bullet$<br>$\text{PMe}_3$<br><br>(4)<br><br>90 MHz $^1\text{H}$<br><br>toluene- $d_8$                                  | $\eta^3\text{-CH}_2\text{CHCH}_2$   | 5.91 (p)       | 13                       |
|   | $\eta^3\text{-CH}_2\text{CHCH}_2$   | 2.74 (d)       | 13                       |
|   | $\text{C}_5(\text{CH}_3)_4$         | 2.17 (s)       | $^3J_{\text{P-H}} = 2.9$ |
|   |                                     | 1.82 (s)       |                          |
|   | $\text{NC}(\text{CH}_3)_3$          | 1.13 (s)       |                          |
|   | $\text{P}(\text{CH}_3)_3$           | 0.87 (d)       |                          |
|   | $\text{Si}(\text{CH}_3)_3$          | 0.69 (s)       |                          |
| $\{\text{Sc}\}(\eta^3\text{-CH}_2\text{CHCHCH}_3) \bullet \text{PMe}_3$<br>$\{\text{Sc}\} = (\text{Cp}^*\text{SiNR})\text{Sc}$<br><br>(5)<br><br>400 MHz $^1\text{H}$<br><br>toluene- $d_8$ | $\eta^3\text{-CH}_2\text{CHCHCH}_3$ | 5.88 (m)       | 10.7                     |
|   | $\eta^3\text{-CH}_2\text{CHCHCH}_3$ | 3.52 (m)       |                          |
|   | $\eta^3\text{-CH}_2\text{CHCHCH}_3$ | 2.04 (br d)    |                          |
|   | $\text{C}_5(\text{CH}_3)_4$         | 2.24 (s)       |                          |
|   |                                     | 1.85 (s)       |                          |
|   | $\text{NC}(\text{CH}_3)_3$          | 1.19 (s)       |                          |
|   | $\text{P}(\text{CH}_3)_3$           | 0.76 (s)       |                          |
|   | $\text{Si}(\text{CH}_3)_3$          | 0.75 (s)       |                          |

Table II (continued).

| Compound/<br>Conditions   | Assignment                          | $\delta$ (ppm)       | J (Hz)               |
|---|-------------------------------------|----------------------|----------------------|
| $\{\text{Sc}\}(\eta^3\text{-CH}_2\text{CHCHCH}_3)\cdot\text{PMe}_3$<br>$\{\text{Sc}\} = (\text{Cp}^*\text{SiNR})\text{Sc}$<br>(5)<br>500 MHz $^1\text{H}$ ; 210 K<br>toluene- $d_8$                                   | $\eta^3\text{-CH}_2\text{CHCHCH}_3$ | 5.87 (br, m)         | 10.7                 |
|   | $\eta^3\text{-CH}_2\text{CHCHCH}_3$ | 3.47 (br)            |                      |
|   | $\eta^3\text{-CH}_2\text{CHCHCH}_3$ | 2.03 (br)            |                      |
|   | $\text{C}_5(\text{CH}_3)_4$         | 2.40 (s)             |                      |
|   |                                     | 2.10 (s)             |                      |
|   |                                     | 1.93 (s)             |                      |
|   |                                     | 1.76 (s)             |                      |
|   | $\text{NC}(\text{CH}_3)_3$          | 1.20 (s)             |                      |
|   | $\text{P}(\text{CH}_3)_3$           | 0.76 (s)             |                      |
|   | $\text{Si}(\text{CH}_3)_3$          | 0.87 (s)<br>0.78 (s) |                      |
| $\{\text{Sc}\}(\eta^3\text{-CH}_2\text{CHCHCH}_2\text{R}')\cdot\text{PMe}_3$<br>$\{\text{Sc}\} = (\text{Cp}^*\text{SiNR})\text{Sc}$<br>$\text{R}' = \text{n-propyl}$<br>(6)<br>400 MHz $^1\text{H}$<br>toluene- $d_8$ | $\eta^3\text{-CH}_2\text{CHCH-}$    | 5.87 (d of t)        | 11.8 (t)<br>14.1 (d) |
|   | $\eta^3\text{-CH}_2\text{CHCH-}$    | 3.51 (m)             | 11.7                 |
|   | $\eta^3\text{-CH}_2\text{CHCH-}$    | 2.04 (d)             |                      |
|   | $\text{C}_5(\text{CH}_3)_4$         | 2.22                 |                      |
|   |                                     | 1.87                 |                      |
|   | $\text{NC}(\text{CH}_3)_3$          | 1.19                 |                      |
|   | $\text{P}(\text{CH}_3)_3$           | 0.82 (d)             |                      |
|   | $\text{Si}(\text{CH}_3)_3$          | 0.72                 | 3.66                 |

Table II (continued).

| Compound/<br>Conditions  | Assignment                       | $\delta$ (ppm) | J (Hz)               |
|--|----------------------------------|----------------|----------------------|
| 6, continued   | $-\text{CH}_2\text{CH}_2-$ (R')  | 1.46 (br, m)   | 7                    |
|  | $-\text{CH}_3$ (R')              | 0.98 (t)       |                      |
| $\{\text{Sc}\}(\eta^3\text{-CH}_2\text{CHCH-CH}_2\text{CH}_2\text{-CH}_2\text{CH}_2\text{-}\eta^3\text{-CHCHCH}_2)\{\text{Sc}\} \bullet$<br>$(\text{PMe}_3)_2$<br>$\{\text{Sc}\} = (\text{Cp}^*\text{SiNR})\text{Sc}$<br>(9)<br>400 MHz $^1\text{H}$<br>$\text{C}_6\text{D}_6$ | $\eta^3\text{-CH}_2\text{CHCH-}$ | 5.95 (d of t)  | 12.0 (t)<br>14.9 (d) |
|  | $\eta^3\text{-CH}_2\text{CHCH-}$ | 3.60 (m)       | 8.7                  |
|  | $\eta^3\text{-CH}_2\text{CHCH-}$ | 2.32 (br)      |                      |
|  | $\text{C}_5(\text{CH}_3)_4$      | 2.28           |                      |
|  |                                  | 1.89           |                      |
|  | $\text{NC}(\text{CH}_3)_3$       | 1.23           |                      |
|  | $\text{P}(\text{CH}_3)_3$        | 0.78 (d)       |                      |
|  | $\text{Si}(\text{CH}_3)_3$       | 0.78           |                      |
|  | outer $\text{CH}_2^a$            | 2.10 (br)      | 8.7                  |
|  | inner $\text{CH}_2^a$            | 1.71 (br)      |                      |
| $9\text{-}^{13}\text{C}_2$<br>100 MHz $^{13}\text{C}$  | inner $^{13}\text{CH}_2^a$       | 33.7           | 119                  |

<sup>a</sup>Tentative assignment.

## EXPERIMENTAL SECTION

### General Considerations.

Unless otherwise noted, all manipulations were performed under anhydrous, anaerobic conditions on a high-vacuum line or in an inert atmosphere box. Organoscandium starting materials were prepared by previously reported routes. Gel permeation chromatography was performed on a Waters 150C GPC/HPLC eluting with toluene. NMR spectra were obtained on JEOL GX-400 and FX-90Q, and Bruker AM-500 instruments. IR spectra were recorded on a Perkin-Elmer 1600 FTIR.

The reaction of  $\text{Cp}^*\text{ScD}(\text{THF})$  with butadiene was conducted as described previously for  $\text{Cp}^*\text{ScH}(\text{THF})$ .<sup>13</sup>

### Polymerization of butadiene: High conversion/broad molecular weight distribution.

$[(\text{Cp}^*\text{SiNR})\text{Sc}(\text{CH}_2\text{CH}_2\text{CH}_2\text{CH}_3)_2]$  (8.9 mg, 0.012 mmol) was weighed into an NMR tube and dissolved in  $\text{C}_6\text{D}_6$  (0.5 mL). 1,3-Butadiene (179 Torr in 104 mL, 1.01 mmol, 54.6 mg, 84 equivalents) was added to the tube via vacuum transfer. After five days, the tube was cracked open and the viscous solution was pipeted into methanolic HCl. The precipitated polymer was collected and dried overnight in vacuo (31.0 mg, 57%).  $M_n$  (vs. polystyrene): 32,000; 8840. PDI: 1.14, 2.72.

### Polymerization of butadiene: Low conversion/narrow molecular weight distribution.

$[(\text{Cp}^*\text{SiNR})\text{Sc}(\text{CH}_2\text{CH}_2\text{CH}_3)_2]$  (9.4 mg, 0.014 mmol) was weighed into a glass bomb and dissolved in toluene (ca. 3 mL). 1,3-Butadiene (1.9 mL) was added via vacuum transfer. After 18 hours stirring at room temperature, the bomb was opened and the yellow solution was poured into methanolic HCl. The precipitated polymer was collected and dried in vacuo (38.9 mg).  $M_n$  (vs. polystyrene): 22,000. PDI: 1.5.

## Polymerization of isoprene.

$[(\text{Cp}^*\text{SiNR})\text{Sc}(\text{CH}_2\text{CH}_2\text{CH}_2\text{CH}_3)]_2$  (11.5 mg, 0.016 mmol) was weighed into an NMR tube and dissolved in  $\text{C}_6\text{D}_6$  (1 mL). Isoprene (231 Torr in 104 mL, 89 mg, 1.3 mmol) was added by vacuum transfer and the tube was sealed. After four days the tube was opened and the viscous solution was pipetted into methanolic HCl. The precipitated polymer was collected and dried overnight in vacuo (69.3 mg, 78.3 %).  $M_n$  (vs. polystyrene): 4800. PDI: 1.24.

## NMR tube preparation of $(\text{Cp}^*\text{SiNR})\text{Sc}(\eta^3\text{-allyl})(\text{PMe}_3)$ (4)

$[(\text{Cp}^*\text{SiNR})\text{ScH}(\text{PMe}_3)]_2$  (26.5 mg, 0.035 mmol) was weighed into an NMR tube and dissolved in toluene- $d_8$  (0.6 mL). Propadiene (193 Torr in 6.9 mL, 0.072 mmol) was added to the tube via vacuum transfer and the tube was sealed for analysis.

## NMR tube preparation of $(\text{Cp}^*\text{SiNR})\text{Sc}(\eta^3\text{-1-methylallyl})(\text{PMe}_3)$ (5)

$[(\text{Cp}^*\text{SiNR})\text{ScH}(\text{PMe}_3)]_2$  (10.2 mg, 0.0138 mmol) was weighed into an NMR tube and dissolved in cyclohexane- $d_{12}$  (0.5 mL). 1,2-Butadiene (Wiley Organics) was trap-to-trap distilled at  $-30^\circ\text{C}$  (76 Torr 6.9 mL, 0.0283 mmol) was added to the tube via vacuum transfer and the tube was sealed for analysis.

## Preparation of $(\text{Cp}^*\text{SiNR})\text{Sc}(\eta^3\text{-1-methylallyl})(\text{PMe}_3)$ (5)

$[(\text{Cp}^*\text{SiNR})\text{ScH}(\text{PMe}_3)]_2$  (957 mg, 1.29 mmol) was weighed into a frit assembly and dissolved in toluene (35 mL). 1,2-Butadiene (473 Torr in 104 mL, 2.66 mol) was added via vacuum transfer and the reaction mixture was stirred overnight at room temperature. The clear, yellow solution was concentrated to 25 mL and filtered. The solution was further concentrated to 15 mL, cooled to  $-78^\circ\text{C}$ , and cold-filtered (442 mg, 1.04 mmol, 40.3 %). Anal.: Found(Calc.) C: 60.85(62.09), H: 9.99(10.18) N: 4.01(3.29).

## Preparation of $(\text{Cp}^*\text{SiNR})\text{Sc}(\eta^3\text{-1-butylallyl})(\text{PMe}_3)$ (6)

$[(\text{Cp}^*\text{SiNR})\text{Sc}(\text{CH}_2\text{CH}_2\text{CH}_3)] \cdot (\text{PMe}_3)_{1/2}$  (348 mg, 0.924 mmol) was dissolved in toluene (10 mL) in a 15-mL glass bomb. 1,3-Butadiene (183 Torr in 104.2 mL, 1.03 mmol) was condensed into the bomb and the reaction mixture was warmed to room temperature. In a dry box, the bright yellow solution was

transferred to a frit assembly. Volatiles were removed in vacuo and the residual orange oil was triturated with three portions of petroleum ether. Cooling a concentrated petroleum ether solution afforded a bright yellow precipitate which was isolated by cold filtration (210 mg, 0.448 mmol, 48.5% vs. Sc, 97.0% vs.  $\text{PMe}_3$ ).

**Preparation of  $[(\text{Cp}^*\text{SiNR})\text{Sc}(\text{CH}_2\text{CH}_2)(\text{PMe}_3)]_2$  (**7**) from butadiene.**

$[(\text{Cp}^*\text{SiNR})\text{ScH}(\text{PMe}_3)]_2$  (522 mg, 0.71 mmol) was weighed into a glass bomb and dissolved in toluene. 1,3-Butadiene (251 Torr in 104.2 mL, 1.41 mmol) was added to the bomb via vacuum transfer and the reaction mixture was stirred for several minutes at room temperature. In a dry box, the yellow solution was transferred to a frit assembly. Volatiles were removed in vacuo leaving an orange oil. This was triturated with several portions of petroleum ether, eventually becoming a yellow solid. The pale, lemon yellow product was isolated from cold petroleum ether (200 mg, 0.52 mmol, 37%).

Single crystals were obtained by slowly cooling a toluene/petroleum ether solution of the product. Unit cell parameters were determined for one of these and were found to be identical to those previously determined for **3**<sup>2b</sup> prepared by another route.

**Reaction of  $[(\text{Cp}^*\text{SiNR})\text{ScH}(\text{PMe}_3)]_2$  with butadiene: Toepler pump collection of volatiles.**

$(\text{Cp}^*\text{SiNR})\text{ScH}(\text{PMe}_3)]_2$  (110 mg, 0.148 mmol) was weighed into a glass bomb and dissolved in toluene. 1,3-Butadiene (265 Torr in 6.9 mL, 0.099 mmol) was added to the bomb via vacuum transfer and the reaction mixture was stirred in an ice bath for three hours. The bomb was then opened to a cycling Toepler pump. The collected volatiles (270 Torr in 13.0 mL, 0.19 mmol) were transferred to an evacuated IR cell for analysis. The excessive amount of gas originated in a slow leak in the pump. IR ( $\nu_{\text{C-H}}$ ; collected gases): 3112 (w), 3104 (w), 3094 (w), 3085 (w), 3016 (m), 3005 (m), 2966 (s), 2953 (s), 2925 (s), 2894 (m), 2878 (m), 2852 (m). IR ( $\nu_{\text{C-H}}$ ; ethane): 3005 (m), 2968 (s), 2952 (s), 2931 (s) 2893 (m), 2879 (m). IR frequencies are all  $\pm 4.0 \text{ cm}^{-1}$ .

**Preparation of  $[(\text{Cp}^*\text{SiNR})\text{Sc}(\text{CH}_2\text{CH}_2)(\text{PMe}_3)]_2$  (**7**) from isoprene.**

$[(\text{Cp}^*\text{SiNR})\text{ScH}(\text{PMe}_3)]_2$  (489 mg, 0.66 mmol) was weighed into a glass bomb and dissolved in toluene. Isoprene (648 Torr in 37.8 mL, 1.32 mmol) was added to the bomb *via* vacuum transfer and the reaction mixture was stirred for several minutes at room temperature. In a dry box, the yellow solution was transferred to a frit assembly. Volatiles were removed *in vacuo* leaving an orange oil. This was triturated with several portions of petroleum ether, eventually becoming a yellow solid. The pale, lemon yellow product was isolated from cold petroleum ether (76 mg, 0.20 mmol, 15%).

**NMR tube preparation of 9- $^{13}\text{C}_2$ .**

$[(\text{Cp}^*\text{SiNR})\text{Sc}(\text{PMe}_3)]_2(^{13}\text{C}_2\text{H}_4)$  (9.1 mg, 0.012 mmol) was weighed into an NMR tube and dissolved in toluene (0.5 mL). 1,3-Butadiene (63 Torr in 6.9 mL, 0.023 mmol) was added to the tube *via* vacuum transfer and the tube was sealed for analysis. The natural-abundance compound was prepared in the same manner, using natural-abundance **7** as the starting material.



## REFERENCES

1. (a) Bunel, E.; Burger, B. J.; Bercaw, J. E.; *J. Am. Chem. Soc.* **1988**, *110*, 976.  
 (b) Piers, W. E.; Shapiro, P. J.; Bunel, E. E.; Bercaw, J. E. *Synlett* **1990**, 74.  
 (c) Piers, W. E.; Bercaw, J. E. *J. Am. Chem. Soc.* **1990**, *112*, 9406.
2. (a) Shapiro, P. J.; Bunel, E.; Schaefer, W. P.; Bercaw, J. E. *Organometallics* **1990**, *9*, 867.  
 (b) Shapiro, P. J. Ph.D. Thesis, California Institute of Technology, 1990.
3. The recently developed "BpYR" derivatives, isoelectronic with Cp\*<sub>2</sub>ScR, also polymerize  $\alpha$ -olefins. Coughlin, E. B.; Bercaw, J. E. *J. Am. Chem. Soc.* **1992**, *114*, 7606.
4. Extensive tabulations of catalyst composition vs. polymer structure can be found in Cooper, W.; Vaughan, G. *Prog. Polym. Sci.* **1967**, *1*, 93.
5. For reviews, see: (a) Reference 4.  
 (b) Arlman, E. J. *J. Catal.* **1966**, *5*, 178-189.  
 (c) Dolgoplosk, B. A.; Beilin, S. I.; Korshak, Yu. V.; Makovetsky, K. L.; Tinyakova, E. I. *J. Polym. Sci., Polym. Chem. Ed.* **1973**, *11*, 2569-2590.  
 (d) Furukawa, J. *Acc. Chem. Res.* **1980**, *13*, 1-6.  
 (e) Burford, R. P. *J. Macromol. Sci.-Chem.* **1982**, *A17*, 123-139.  
 (f) Porri, L. *Struct. Order Polym., Lect. Int. Symp.* **1981**, 51-62. This paper in particular provides a clear, cogent overview of the subject.  
 (g) Teyssié, Ph.; Hadjiandreou, P.; Julémont, M.; Warin, R. In *Transition-Metal Catalyzed Polymerizations*, R. P. Quirk, Ed. Cambridge: Cambridge University Press, 1988, pp 639-654.
6. Horne, S. E.; Gibbs, F.; Carlson, E. J. (Goodrich-Gulf Chem. Inc.), British Patent 827365, (1954).
7. Shen, Z.; Gong, Z.; Zhong, G.; Ouyang, J. *Sci. Sin. (Engl. Transl.)* **1964**, *13*, 1339.
8. Yang, J.; Hu, J.; Feng, S.; Pan, E.; Xie, D.; Zhong, C.; Ouyang, J. *Sci. Sin. (Engl. Transl.)* **1980**, *23*, 734.

9. (a) Cabassi, F.; Italia, S.; Ricci, G.; Porri, L. In *Transition Metal Catalyzed Polymerizations*, R. P. Quirk, Ed. Cambridge: Cambridge University Press, 1988, pp. 655-670.  
(b) Hsieh, H. L.; Yeh, G. H. C. *Ind. Eng. Chem. Prod. Res. Dev.* **1986**, *25*, 456-463.  
(c) Hsieh, H. L.; Yeh, H. C. *Rubber Chem. Technol.* **1985**, *58*, 117-145.  
(d) Yang, J.-H.; Tsutsui, M.; Chen, Z.; Bergbreiter, D. E. *Macromolecules* **1982**, *15*, 230-233.
10. Stehling, F. C.; Bartz, K. W. *Anal. Chem.* **1966**, *38*, 1467-1479.
11. Quack, G.; Fetters, L. J. *Macromolecules* **1978**, *11*, 369.
12. Conti, F.; Segre, A.; Pini, P.; Porri, L. *Polymer*, **1974**, *15*, 5.
13. Burger, B. J. Ph.D. Thesis, California Institute of Technology, 1987.
14. When **6** is prepared in situ in an NMR tube, it becomes clear that, while **6** is the major product, it is not the only product. A singlet appears in the midst of the  $\delta$  3.5 multiplet of **6**, which must arise from a minor product in which this proton—which by its chemical shift is an allyl proton in an anti position—is not coupled to a central allyl proton. This indicates that some of the allyl product which would arise from initial 1,2-insertion—with the alkyl substituent at the central allylic position—is formed, but is lost upon workup.
15. The preparation of **7** from **1** and ethylene has been previously reported. See Reference 2b.
16. Becker, K. B.; Grob, C. A. In *The Chemistry of Functional Groups*; Patai, S., Ed.; Wiley: New York, 1977; Supplement A, Part 2, 653-723.
17. Calculated from bond dissociation energies tabulated in Lowry, T. H.; Richardson, K. S. *Mechanism and Theory in Organic Chemistry*, New York: Harper and Row, 1981, 2nd edition, p. 146.
18. Hessen, B.; Meetsman, A.; van Bolhuis, F.; Teuben, J. H. *Organometallics* **1990**, *9*, 1925-1936,

19. The preparation of  $\text{Cp}^*_2\text{Sc}(\text{crotyl})$  uses isolated  $\text{Cp}^*_2\text{ScH}(\text{THF})$  as starting material; the other two reactions use  $\text{Cp}^*_2\text{ScH}$  generated in situ by hydrogenation of an alkyl starting material.
20. Bercaw, J. E.; Moss, J. R. *Organometallics* **1992**, *11*, 639-645.
21. See Reference 2b and Chapter 6.

## Chapter 5

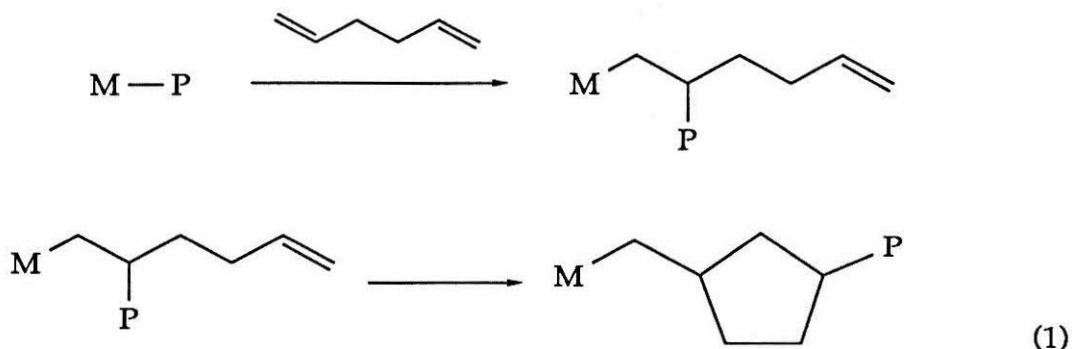
### Studies in the Mechanism of 1,5-Hexadiene Cyclopolymerization by Single-Component Organoscandium Catalysts

**Abstract:** Hydride and alkyl scandium complexes of the ansa-cyclopentadienyl(amido) ligand ( $\text{Cp}^*\text{SiNR}$ ) are efficient catalysts for the cyclopolymerization of 1,5-hexadiene. Molecular weight distributions with polydispersity indices approaching 1.0 can be obtained with certain catalyst precursors. The polydispersity is very sensitive to the presence of trimethylphosphine, and less sensitive to the nature of the initiating group. In contrast to  $\alpha$ -olefin polymerizations with the same catalyst system, good yields of polymeric product can be obtained after a few hours from a dilute solution of monomer. The difference in reactivity between  $\alpha$ -olefins and hexadiene is determined to arise from a suppression of termination and chain-transfer steps, rather than from an enhanced rate of propagation for hexadiene. The rate of  $\beta$ -hydride elimination could not be studied using conventional alkyne traps, as these alkylscandium complexes react with alkynes directly by C-H bond activation, forming allylic species or products arising from rearrangement of allylic species. Cyclopolymerization is not accompanied by a measurable  $\alpha$ -agostic isotope effect on the cyclization step. This observation strongly suggests that trans-fused [5,4]-bicyclic transition states are allowed for the cyclization step during polymerization.

|  |     |
|--|-----|
| I. INTRODUCTION .....  | 89  |
| II. RESULTS AND DISCUSSION.....  | 91  |
| Characteristics of the Polymerization with a Scandium Hydride as<br>Catalyst Precursor .....   | 91  |
| Polymerization with Scandium Alkyl Complexes as Catalyst<br>Precursors: Effect of Initiating Group and Phosphine.....                      | 93  |
| Polymer Stereochemistry .....  | 96  |
| Preparation and Reactivity of Cyclopentylmethyl Derivative 2 .....   | 97  |
| Copolymerization of Hexene and Hexadiene; Relative Kinetics of<br>Homopolymerization .....   | 98  |
| Attempts to Observe $\beta$ -Hydride Elimination via Trapping<br>Reactions of Scandium Hydride and Alkyl Complexes with<br>Alkynes .....   | 102 |
| Cyclopolymerization of <i>trans,trans</i> -1,6-Dideuterio-1,5-hexadiene:<br>Probing for $\alpha$ -Agostic Transition State Assistance..... | 105 |
| (i) A closer look at stereochemical induction .....  | 105 |
| (ii) Stereochemical analysis of deuteriopolymerization .....   | 108 |
| III. CONCLUSIONS .....   | 111 |
| EXPERIMENTAL SECTION .....   | 117 |
| APPENDIX: Analysis of $\alpha$ -Agostic Perturbation of Stereochemistry in<br>Hexadiene Cyclopolymerization .....                          | 123 |
| REFERENCES .....   | 126 |

## I. INTRODUCTION

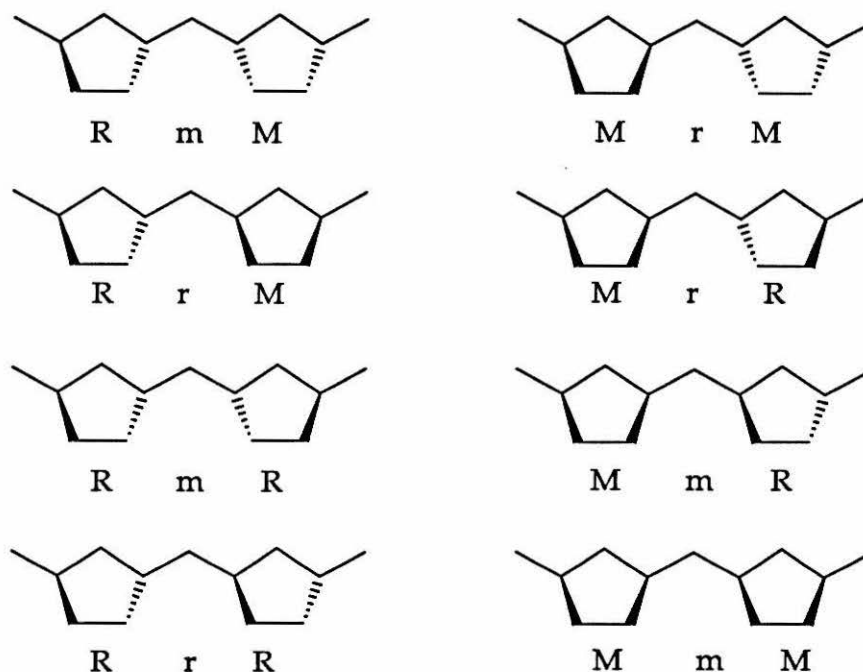
Marvel and Stille first demonstrated the cyclopolymerization of 1,5-hexadiene by classical Ziegler-Natta catalysts in 1958.<sup>1</sup> In its product and, most probably, in its mechanism, this reaction combines the intermolecular chemistry of  $\alpha$ -olefin polymerization with the intramolecular chemistry of hydrocyclization, each repeat unit being formed by the consecutive operation of these two steps as shown in Equation 1.



Recently, work from the Waymouth group revived interest in this unusual polymerization by demonstrating remarkable stereoselectivities when polymerization is initiated with zirconocene/methylalumoxane (MAO) catalysts.<sup>2</sup> As each repeat unit contains a 1,3-substituted cyclopentyl ring, each is subject to cis/trans isomerism. Resconi and Waymouth reported that a catalyst mixture derived from  $\text{Cp}_2\text{ZrCl}_2/\text{MAO}$  produced polymer rich in trans repeat units. When the catalyst precursor is  $\text{Cp}^*\text{ZrCl}_2$ , a reversal of stereoselectivity is observed, the resulting polymer being rich in cis repeat units. Subsequently, Coates and Waymouth reported that polymerization of 1,5-hexadiene with (ethylenebis(tetrahydroindenyl)) $\text{ZrCl}_2$  as catalyst precursor was highly selective both in terms of ring stereochemistry and of tacticity. In so doing, these workers provided a precise definition of tacticity and a complete triad analysis for these polymers (Scheme I).<sup>2b</sup>

**Scheme I. Stereochemical Triads for Poly(cyclohexadiene).**

M, m = meso; R, r = racemo.<sup>a</sup>



<sup>a</sup>Uppercase letters represent stereochemistry within rings; lowercase letters represent stereochemistry between rings.

The mechanistic interpretations of these selectivities that have appeared in the literature challenge some of the assumptions implicit in much of the work discussed in the previous chapters, particularly those assumptions regarding the constraints on transition state geometries for Ziegler-Natta cyclization. These questions will be considered at length in a later section of this chapter dealing explicitly with attempts to observe an isotopic perturbation of stereochemistry in hexadiene cyclopolymerization. In addition to our continuing interest in expanding the scope of organoscandium-catalyzed Ziegler-Natta polymerization, our uneasiness with some of these stereochemical ideas was a factor in motivating us to study this particular polymerization with single-component organoscandium catalysts.

## II. RESULTS AND DISCUSSION

### Characteristics of the Polymerization with a Scandium Hydride as Catalyst Precursor.

Our initial polymerization experiments suggested that hexadiene might be much more reactive than  $\alpha$ -olefins in the Ziegler-Natta polymerization catalyzed by  $[(Cp^*SiNR)ScH(PMe_3)]_2$  (1). Based on experience with the latter reaction, a slow polymerization in neat monomer was expected, so a small scale reaction with several milligrams of catalyst and approximately half a milliliter of monomer was set up in a septum-capped NMR tube. Within several seconds, the solution turned yellow and began to bubble. The NMR tube exploded. The dispersed product was unambiguously polymeric.

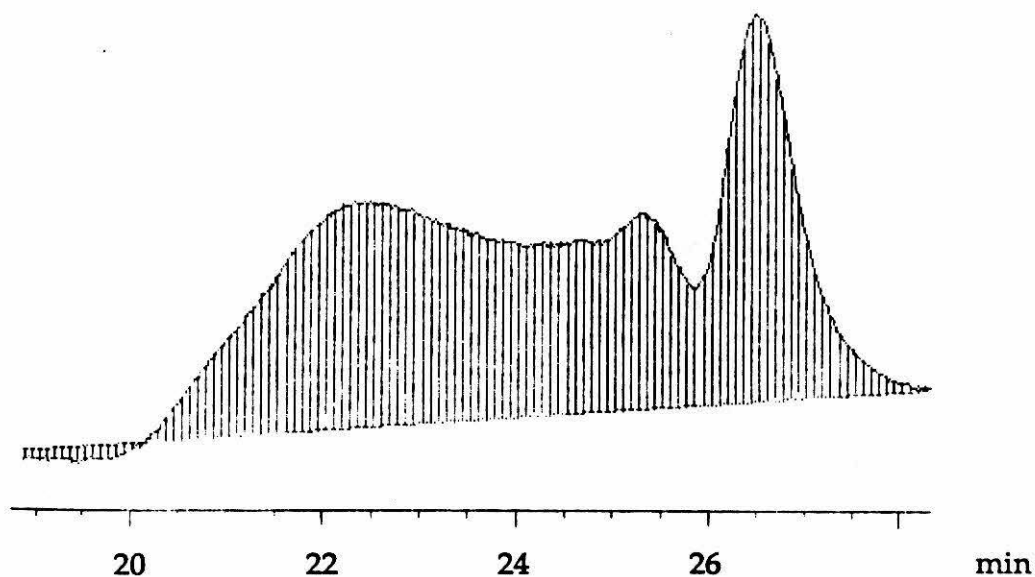
A polymerization conducted in a dilute toluene solution of monomer (3 mM, ca. 30 equivalents vs. catalyst) yielded a solid gel of polymer (69.5% mass recovery of monomer) after two hours at room temperature. The product swelled into toluene only with heat and sonication. The molecular weight distribution of the soluble fraction of this polymer was found by gel permeation chromatography (GPC) to be polymodal with a  $M_w$  of  $\approx 270,000$  (Figure 1a).<sup>3</sup> This result and the low solubility of the product suggest extensive cross-linking. A similar polymerization conducted at 10°C gave an intractable polymer, also presumable due to cross-linking.

Smooth conversion to polymer with good molecular weight characteristics was finally obtained when the polymerization was conducted by dropwise addition of a toluene solution of hexadiene (12.5 mL total volume, 1.7 M in hexadiene, 324 equivalents relative to Sc) to a toluene solution of catalyst (35 mL, 2 mM). Addition over one hour followed by one hour of stirring at room temperature yielded the polymer whose GPC is shown in Figure 1b. The polydispersity index is quite narrow, about 1.1, with a number-average molecular weight of about 16,000 vs polystyrene. The shoulder represents a small fraction with a maximum at twice the molecular weight of that of the main peak, indicating the presence of a small amount of cross-linkage in an otherwise nearly monodisperse polymer. The overall yield of polymer using this procedure was somewhat low, about 30%. No simple cyclization products were found by gas chromatography of volatiles.

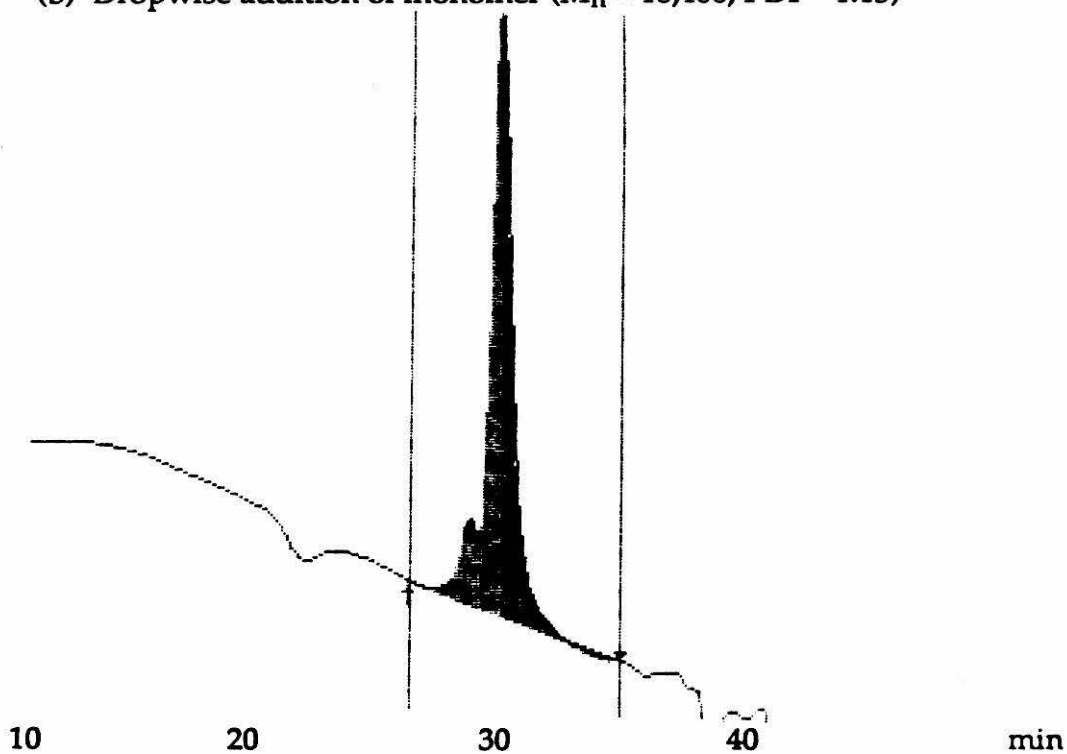


**Figure 1. Gel permeation chromatographs of poly(hexadiene) prepared with **1** as catalyst precursor.**

(a) Immediate addition of monomer ( $M_n \approx 100,000$ ; PDI  $\approx 2.5 - 3$ )



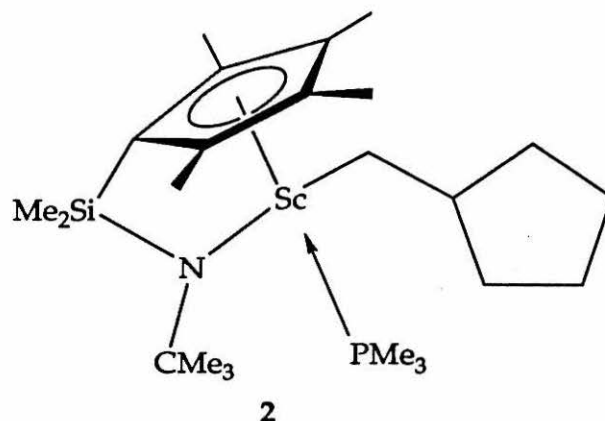
(b) Dropwise addition of monomer ( $M_n = 16,400$ ; PDI = 1.13)



By contrast, 1-pentene is a relatively poor substrate for polymerization by the same catalyst precursor. This polymerization proceeds only in neat solution, yielding an oligomeric product ( $M_n = 2900$ ) in 72% yield after 19 hours.<sup>4</sup> A turnover rate of  $50 [\text{Sc}]^{-1} \text{ hr}^{-1}$  is reported for pentene polymerization. Although the origin of this number is obscure, it is presumably based on molecular weight data. A turnover rate of  $100 [\text{Sc}]^{-1} \text{ hr}^{-1}$  can be calculated for the hexadiene polymerization on the same basis. Correcting for the statistical factor of two double bonds per hexadiene unit, these numbers are the same. However, for pentene this turnover rate reflects the reactivity of neat (9.12 M) pentene; for hexadiene, the same number derives from a solution three orders of magnitude more dilute. Repeated attempts to prepare poly(1-hexene) in dilute toluene solution according to the procedure described above for hexadiene did not produce isolable amounts of polymer. The relative polymerization reactivities of these monomers are pursued in more detail in a subsequent section of this chapter.

#### **Polymerization with Scandium Alkyl Complexes as Catalyst Precursors: Effect of Initiating Group and Phosphine.**

The cyclopentylmethylscandium species **2** can be prepared by treatment of the hydride with a concentrated solution of methylenecyclopentane in toluene (*vide infra*). The product of hexadiene polymerization using **2** as the catalyst precursor is a nearly monodisperse polymer, as demonstrated by the gel permeation chromatograph shown in Figure 2. The close resemblance between this polymer and that prepared via initiation by the hydride species **1** strongly suggests that initiation by **1** via formation of **2** proceeds more quickly than the subsequent propagation steps.



The scandium alkyl dimer  $[(Cp^*SiNR)Sc(CH_2CH_2CH_3)_2]$  (**3**) also initiates hexadiene polymerization. Under the same conditions described for polymerization by **1**, a 30% yield of polymer is again obtained after a total reaction time of two hours. The GPC of this soluble polymer is shown in Figure 3a. Though the molecular weight is again unimodal, the polymer is far from monodisperse, with a PDI of  $\approx 2.5$ . When **3** is used as catalyst precursor in the presence of an added equivalent of trimethylphosphine, however, the polydispersity of the product decreases to about 1.6 (Figure 3b).

**Figure 2. Gel permeation chromatograph of poly(hexadiene) prepared with **2** as catalyst precursor**

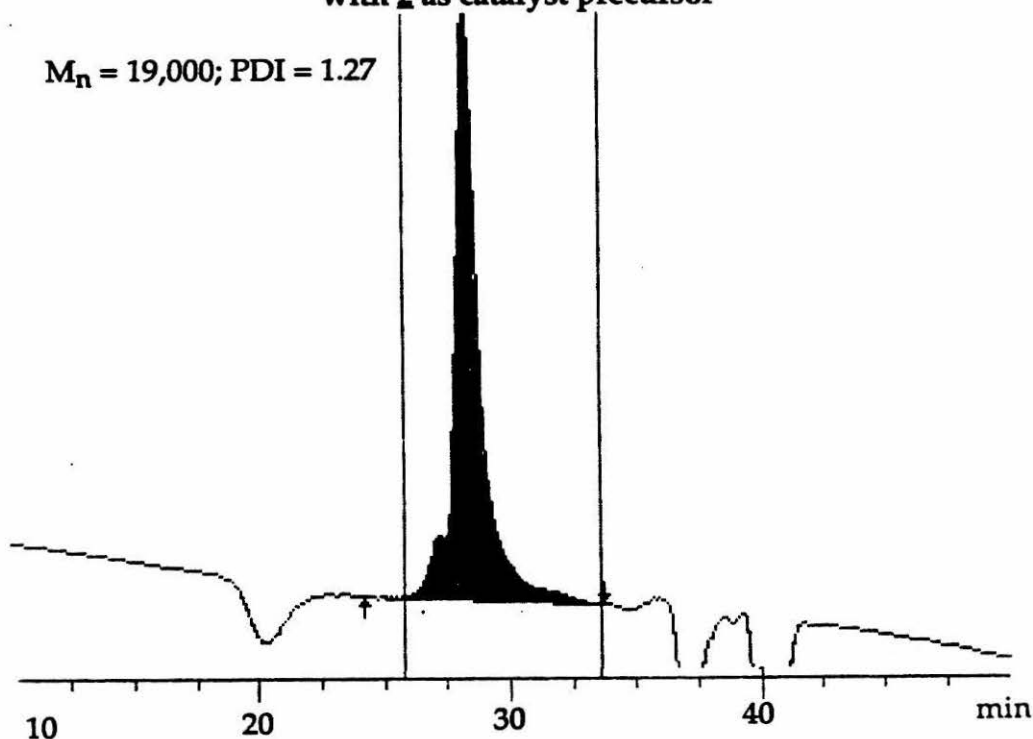
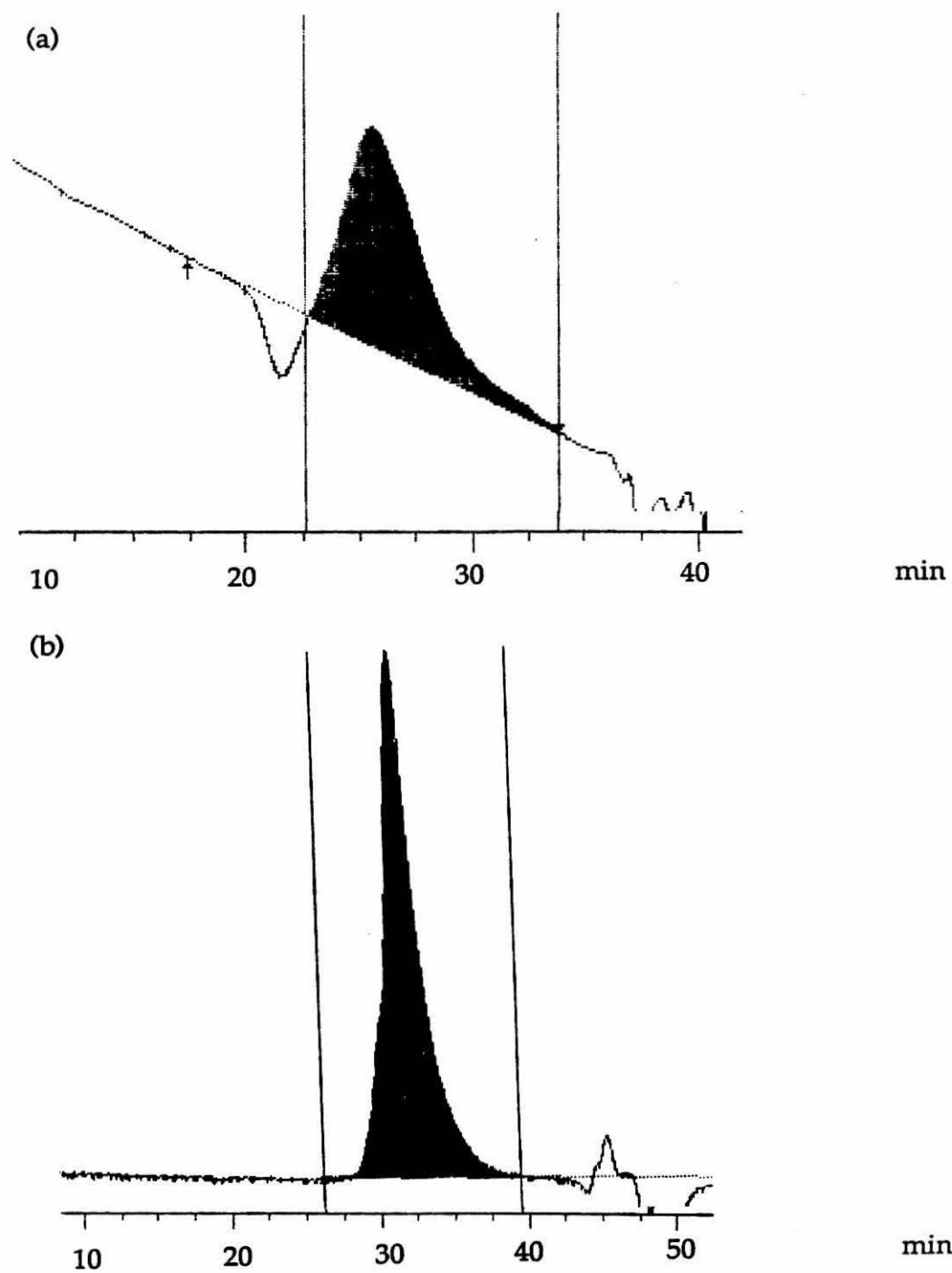


Figure 3. Gel permeation chromatographs of poly(hexadiene) prepared with **3** (a) and **3** + PMe<sub>3</sub> (b) as catalyst precursor



The variation of molecular weight distribution with catalyst precursor displays an interesting trend. In particular, the polydispersity of the product depends strongly on the presence or absence of trimethylphosphine while the influence of the initiating group is relatively weak. The attainment of polydispersities as low as 1.1 suggests that termination steps can be suppressed in this polymerization (polydispersity indices range from 1.7 to 2.2 for  $\alpha$ -olefin polymerizations by the same catalyst precursor).<sup>5</sup> Trimethylphosphine could plausibly influence the polydispersity index of the polymers simply by occupying an empty orbital at scandium which otherwise would be available to support  $\beta$ -hydride elimination. It is not clear why such an effect would be more pronounced for cyclopolymerization vis-a-vis linear  $\alpha$ -olefin polymerization. Unfortunately, attempts to study the  $\beta$ -hydride elimination reaction in detail by trapping the transient scandium hydride species were frustrated by unexpected reactivity of (Cp\*SiNR)ScR complexes with the intended trapping reagents (vide infra).

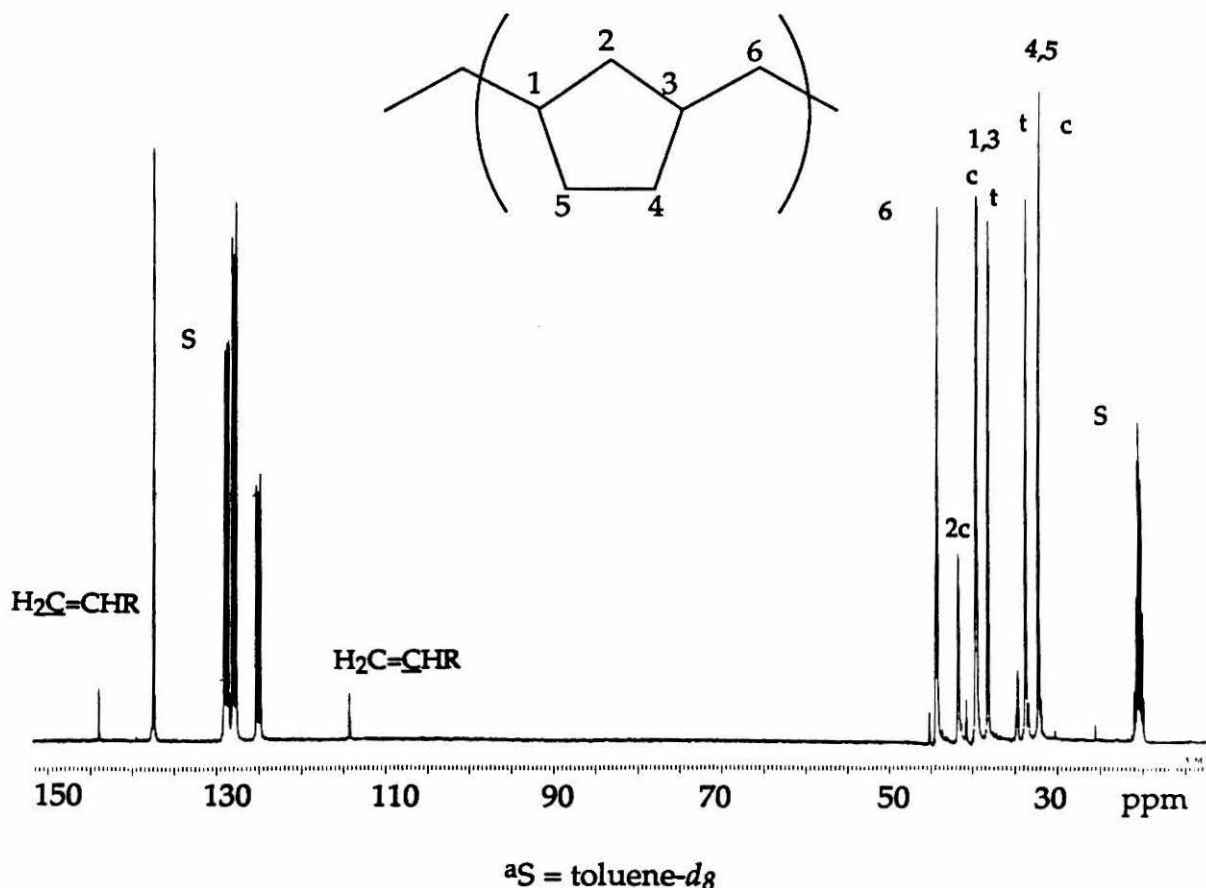
The rate of initiation can also affect polydispersity.<sup>5</sup> NMR evidence indicates that these alkyl complexes enter a rapid, complex equilibrium in the presence of trimethylphosphine.<sup>6</sup> By contrast, the <sup>1</sup>H-NMR spectrum of the phosphine-free propyl complex indicates a single, presumably dimeric structure which remains unchanged from -80 °C to 25 °C.<sup>7</sup> Although trimethylphosphine has been shown to inhibit propagation in  $\alpha$ -olefin polymerization,<sup>8</sup> the rate of *initiation* by **3** could be enhanced by phosphine if the dimeric form is appreciably less prone to dissociation than the phosphine-supported monomeric form. As will be seen in Chapter 6, dimerization occurs to a very small extent in the presence of trimethylphosphine, if at all. That is, the association constant for phosphine binding is in general much larger than that for dimerization. This line of reasoning suggests that phosphine is unlikely to accelerate the rate of initiation. It is more probable that trimethylphosphine influences polydispersity by inhibiting  $\beta$ -hydride elimination.

### Polymer Stereochemistry

A typical <sup>13</sup>C{<sup>1</sup>H}-NMR spectrum of one of these polymers is shown in Figure 4. Resonances which can be attributed to uncyclized monomer units account for < 10% of the overall signal intensity. A modest excess of *cis*-fused rings is observed. Expanding previous work by Cheng and Khasat,<sup>9</sup> Waymouth

and Coates<sup>2b</sup> have developed an NMR method for determining the tacticity of hexadiene cyclopolymers as defined in Scheme 2 (*vide supra*). Using their methodology, the polymers prepared in this work can be determined to be completely atactic (see Experimental Section).

Figure 4.  $^{13}\text{C}\{^1\text{H}\}$ -NMR spectrum of low-dispersity poly(hexadiene)<sup>a</sup>

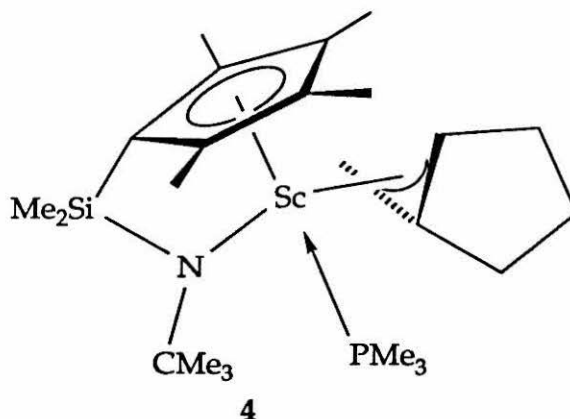


### Preparation and Reactivity of Cyclopentylmethyl Derivative 2

Treatment of 1 with a concentrated solution of methylenecyclopentane in toluene leads primarily to the formation of the scandium cyclopentylmethyl derivative 2. The instability of 2 in solution precludes Signer molecular weight analysis. The  $^1\text{H}$ -NMR spectrum of 2 is extremely fluxional at room temperature, while at least three forms are detectable at  $-80^\circ\text{C}$ . However, in the fast-exchange limit  $^1\text{H}$ -NMR clearly shows the expected doublet for the  $\alpha\text{-CH}_2$  on the cyclopentylmethyl substituent. In addition, an allylic species 4 can be present as

a minor impurity. This impurity is apparently inactive toward polymerization since hexadiene is converted to nearly monodisperse, unimodal polymer using **2** contaminated with < 10% **4**.

When **2**, contaminated with **4**, is treated with  $H_2$  in toluene- $d_8$  solution, the hydride dimer **1** and methylcyclopentane are the only products observed in the  $^1H$ -NMR spectrum, indicating that both **2** and **4** must be derivatives of **1** and a dehydromethylcyclopentane. **4** can be cleanly isolated from the reaction of **1** with methylenecyclopentane in a concentrated petroleum ether solution. The  $^1H$ -NMR spectrum of isolated **4** is consistent with the allylic structure below.



**4** is almost certainly formed by the reaction of **2** with excess methylenecyclopentane, *via*  $\sigma$ -bond metathesis at the allylic position.

### Copolymerization of Hexene and Hexadiene; Relative Kinetics of Homopolymerization

The apparent disparity in turnover numbers for pentene and hexadiene polymerization noted in the previous section led us to examine the relative polymerization kinetics of these monomers more closely. If hexadiene is polymerized more rapidly than normal  $\alpha$ -olefins, the nature of the acceleration would be of interest. To distinguish between an acceleration based on inherent differences in reactivity between the two monomers (hexadiene and  $\alpha$ -olefin), on the one hand, and organometallic intermediates (scandium-cyclopentylmethyl

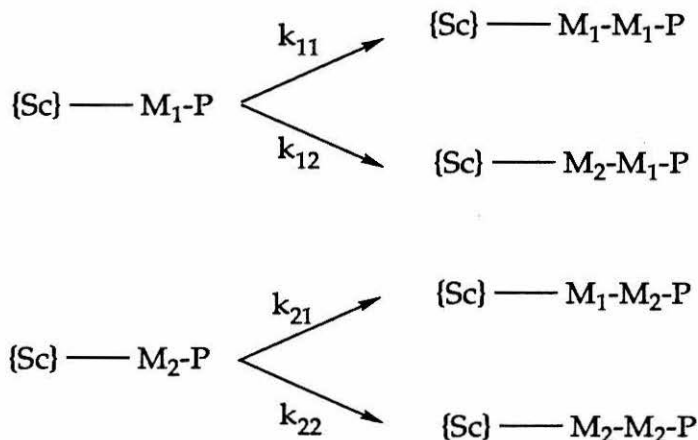
and  $\beta$ -branched scandium alkyl species) on the other, copolymerization and the kinetics of monomer consumption were examined.

A solution of hexene and hexadiene (present in a molar ratio of 0.95:1) was treated with **1** as described above for homopolymerizations. The reaction mixture was not quenched directly. Rather, all volatiles (solvent and residual monomer) were removed from the reaction mixture in vacuo and examined by gas chromatography. A  $^{13}\text{C}\{^1\text{H}\}$  NMR spectrum of the polymer (64% yield based on monomer) was recorded. It qualitatively showed the product to contain both cyclic and linear units. A more reliably quantitative assay of the amount of each monomer consumed was obtained by gas chromatography. The composition of the residual monomer mixture was found to be 71% hexene to 30% hexadiene. From these data and the polymer yield, the polymer composition is calculated to be 64% hexadiene to 36% hexene. From the monomer ratio present in the feed it is possible to calculate the expected product composition at any time during polymerization, assuming that the reaction is pseudo-first order in both monomers, and allowing for a statistical doubling of the reaction rate of hexadiene. At 64% conversion, the expected polymer composition is 68% hexadiene to 32% hexene.<sup>10</sup> Copolymerization of these monomers, therefore, proceeds without any apparent selectivity for hexadiene.

Either of two possibilities can account for this lack of selectivity. The simplest would be that there is in fact no reactivity difference between hexadiene and hexene, which seems to contradict the rather large reactivity difference implied in the turnover numbers, molecular weights, and yields noted in the previous section of this chapter. Alternatively it is possible that there is a reactivity difference, not between the monomers as such, but between the reactive organometallic species that derive from them, assuming that these intermediates react at the same rate with either monomer ( $k_{11} \approx k_{12} > k_{21} \approx k_{22}$  in Scheme II).



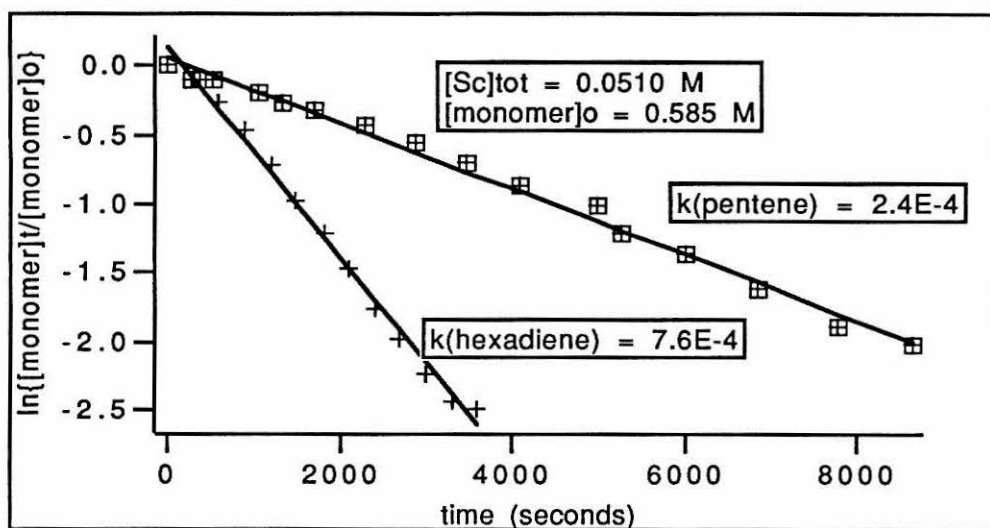
## Scheme II. Copolymerization rate constants.



$\text{M}_1$  = hexadiene;  $\text{M}_2$  = pentene or hexene

To distinguish between these two possibilities, the kinetics of monomer consumption for hexadiene and 1-pentene were directly compared (1-pentene was used instead of 1-hexene because it was the basis of a prior, extensive kinetic study of this catalyst system). When approximately 10 equivalents of either monomer are treated with 1 in toluene-*d*<sub>8</sub> at 31±1°C, clean pseudo-first order disappearance of monomer is observed over several half-lives as shown in Figure 5. The observed rate constant for pentene consumption,  $k_{\text{obs}} = 2.4 \times 10^{-4} \text{ sec}^{-1}$ , differs only by a factor of two from the value obtained in prior work for the same value of  $[\text{Sc}]_0$ ,  $k_{\text{obs}} \approx 9 \times 10^{-5} \text{ sec}^{-1}$ . The extreme susceptibility of these organometallic complexes to adventitious decomposition could conceivably account for this discrepancy, since any decomposition during sample preparation would lead to a lower observed rate constant. In any event, oligomerization of hexadiene with the same catalyst stock solution proceeds with an observed rate constant ( $7.6 \times 10^{-4} \text{ sec}^{-1}$ ) approximately a factor of three times faster than pentene polymerization. This represents an insignificant acceleration over the statistical factor of two.

Figure 5. Monomer Consumption Kinetics for 1,5-Hexadiene and 1-Pentene with Scandium Hydride **1** at  $T = 31 \pm 1^\circ\text{C}$ .



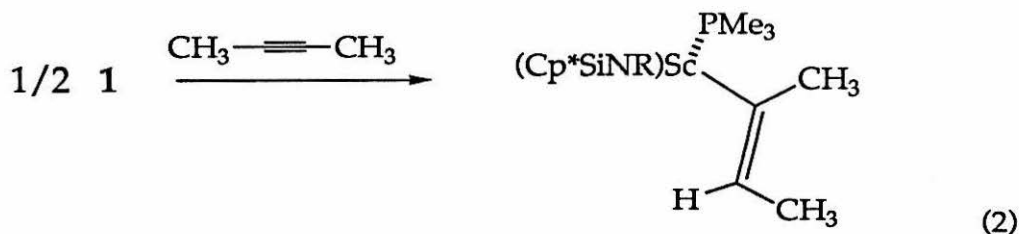
This result is somewhat surprising. Comparison of the gross features of hexadiene polymerization to those of  $\alpha$ -olefin polymerization suggested a much more striking difference in reactivity. From the kinetic data presented in Figure 5, meaningful turnover numbers can be calculated for both processes. At an olefin concentration of ca. 0.5 M, turnover numbers of  $27 \text{ Sc}^{-1} \text{ hr}^{-1}$  for hexadiene and  $8.5 \text{ Sc}^{-1} \text{ hr}^{-1}$  for pentene are derived.

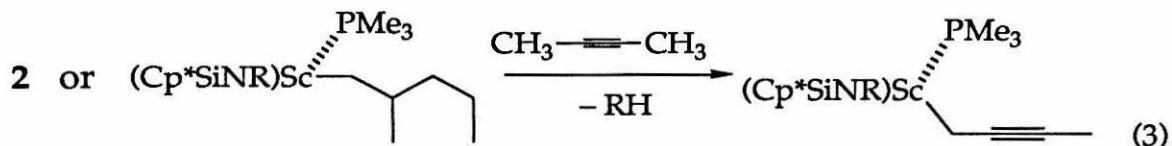
It thus appears that the "exceptional" reactivity of hexadiene in this system derives more from a suppression of termination steps than from any striking difference in propagation rates. Propagation is first-order in monomer, whereas chain transfer (by  $\beta$ -hydride or  $\beta$ -alkyl elimination) should be zero-order in monomer. The propagation rate constants for the two polymerizations are nearly identical. Chain transfer from an  $\alpha$ -olefin polymerization intermediate remains competitive with propagation even in neat monomer, whereas chain transfer is almost completely suppressed for cyclopolymerization at monomer concentrations  $10^3$  more dilute. This indicates that the chain-transfer rate constant (or sum of chain-transfer rate constants) is significantly more than three orders of magnitude greater for the former polymerization than for the latter.

## Attempts to Observe $\beta$ -Hydride Elimination *via* Trapping Reactions of Scandium Hydride and Alkyl Complexes with Alkynes

The experiments described in the previous sections clearly indicate that the major difference between  $\alpha$ -olefin polymerization and  $\alpha,\omega$ -diolefin polymerization with these organoscandium catalysts resides in the termination and chain-transfer reactivity rather than in propagation. It was therefore of interest to try to observe, kinetically characterize and compare the  $\beta$ -hydride elimination reaction, which we presume to be the major chain-transfer pathway, from the organometallic intermediates involved in each polymerization. Previous studies in this group<sup>11</sup> have shown that the hydride species generated by  $\beta$ -H elimination from the related alkyl complexes  $\text{Cp}^*_2\text{ScR}$  ( $\text{R} = \text{CH}_2\text{CH}_3$ ,  $\text{CH}_2\text{CH}_2\text{CH}_3$ , etc.) can be trapped by reaction with 2-butyne, generating the corresponding *E*-2-butenyl derivative. In the permethylscandocene system, 2-butyne reacts only with the transient hydride and not with the alkyl complexes themselves unless, as in the case of  $\text{Cp}^*_2\text{ScCH}_3$ ,  $\beta$ -H elimination is not possible, in which case slow insertion of the alkyne across the scandium-carbon bond occurs. The butenyl complexes do not react with excess 2-butyne.

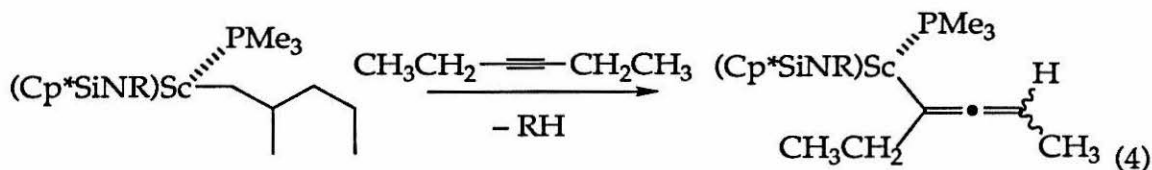
2-Butyne reacts with 1 in the expected way to produce a 2-butenyl complex (Equation 2). However, treatment of 2 with 2-butyne leads, not to formation and subsequent trapping of the hydride, but to (formal) " $\sigma$ -bond metathesis" at the  $\text{sp}^3$  carbon of the alkyne, generating methylcyclopentane and a scandium propargyl species (Equation 3). The 2-methylpentyl derivative  $[(\text{Cp}^*\text{SiNR})\text{Sc}(\text{CH}_2\text{CH}(\text{CH}_3)\text{CH}_2\text{CH}_2\text{CH}_3)]\cdot\text{PMe}_3$  also reacts via activation of the propargylic C-H bond.





If **2** and  $[(\text{Cp}^*\text{SiNR})\text{Sc}(\text{CH}_2\text{CH}(\text{CH}_3)\text{CH}_2\text{CH}_2\text{CH}_3)]\cdot\text{PMe}_3$  undergo  $\beta$ -hydride elimination in solution, either the reverse process--e.g., methylenecyclopentane insertion into the transient scandium hydride bond--must be very much faster than 2-butyne insertion, or the observed C-H activation must be very much faster than  $\beta$ -hydride elimination. The latter appeals to us, because the insertion of a  $\beta,\beta$ -disubstituted olefin across the scandium hydride bond in  $[(\text{Cp}^*\text{SiNR})\text{ScH}(\text{PMe}_3)]_2$  is slow,<sup>4</sup> although 2-butyne insertion is by no means instantaneous in this system, requiring several minutes for completion.

2-Butyne is thus not a useful trapping reagent for the  $\text{Cp}^*\text{SiNR}$  system. 3-Hexyne was considered as an alternative trapping reagent in the hopes that the secondary propargylic hydrogens would be less accessible than the primary propargylic hydrogens in 2-butyne. Although normal insertion of the alkyne was observed in the reaction of 3-hexyne with **1**, treatment of  $[(\text{Cp}^*\text{SiNR})\text{Sc}(\text{CH}_2\text{CH}(\text{CH}_3)\text{CH}_2\text{CH}_2\text{CH}_3)]\cdot\text{PMe}_3$  with 3-hexyne led once again to propargylic C-H bond activation. In this case, the observed product is allenic rather than propargylic (Equation 4).<sup>12</sup> The propargyl intermediate apparently rearranges by migration of scandium to the  $\text{sp}$   $\beta$ -carbon.  $(\text{Cp}^*\text{SiNR})\text{ScR}$  derivatives react directly with allenes to form allyl complexes rather than allenic derivatives of the type observed here (see Chapter 4).



Because they react directly and rapidly with scandium-carbon bonds, alkynes bearing propargylic hydrogens are clearly unsuitable for trapping transient hydrides in the  $\text{Cp}^*\text{SiNR}$  system. An attempt to use diphenylacetylene, which has no propargylic hydrogens, was also unsuccessful. Although diphenylacetylene reacts with  $[(\text{Cp}^*\text{SiNR})\text{ScH}(\text{PMe}_3)]_2$  to give the expected insertion product, the reaction is extremely slow, with a half-life of several hours when the acetylene is present in modest excess.

$[(\text{Cp}^*\text{SiNR})\text{Sc}(\text{CH}_2\text{CH}(\text{CH}_3)\text{CH}_2\text{CH}_2\text{CH}_3)]\cdot\text{PMe}_3$  does not react cleanly with diphenyl-acetylene, either in the presence of several equivalents of the alkyne or in a ca. 3 M toluene- $d_8$  solution of diphenylacetylene (analogous to the conditions used for the trapping of transient  $\text{Cp}^*_2\text{ScH}$  by 2-butyne). The product of insertion into a transient hydride is not visible in the reaction mixture. NMR provides no evidence of olefin release; rather, 2-methylpentane appears to be among the products.

The mechanism by which these unexpected products are likely to be formed is worth comment. Organoscandium complexes typically activate C-H bonds via a four-center mechanism termed " $\sigma$ -bond metathesis".<sup>13</sup> This reaction is favored at carbon-hydrogen bonds with high s-character and is best thought of as occurring at a covalent scandium-carbon bond. However, there is no evidence of activation of the solvent ( $\text{C}_6\text{D}_6$ )  $\text{sp}^2$  bonds on the time-scale of reaction with the  $\text{sp}^3$  bonds of 2-butyne. Attributing these propargylic activation reactions to  $\sigma$ -bond metathesis is therefore problematic.

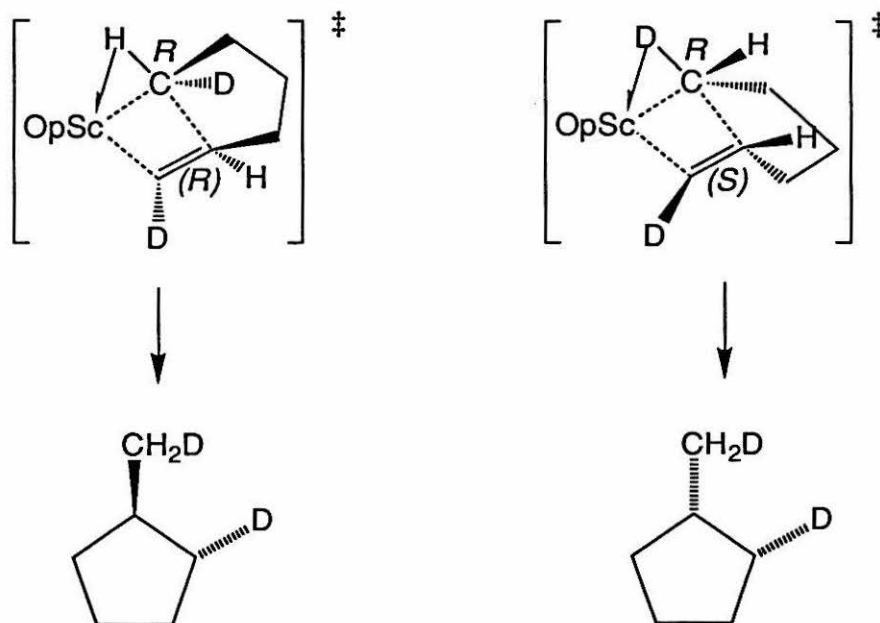
Chemists have known of the susceptibility of propargylic C-H bonds to metalation since 1888, when Favorskii reported the base-catalyzed isomerization of terminal to internal acetylenes.<sup>14</sup> In fact, it is possible to remove all four protons from propyne with butyllithium.<sup>15</sup> Propargylic activation by the scandium alkyl derivatives described here may be better described as a classical metalation, i.e., acid-base, reaction rather than as a  $\sigma$ -bond metathesis reaction as such. Further support for this view is provided in the allenic rearrangement shown in Equation 4. Propargyl carbanions are known to rearrange to thermodynamic mixtures of alkyne and allene isomers.<sup>14b,15</sup>

In any case, because they did not provide an effective means of observing  $\beta$ -hydride elimination, these reactions were not pursued, though the propargylic activations and rearrangement to an allenic species are clearly intrinsically interesting.

## Cyclopolymerization of *trans, trans*-1,6-Dideuterio-1,5-hexadiene: Probing for $\alpha$ -Agostic Transition State Assistance

### (i) A closer look at stereochemical induction in Ziegler-Natta cyclization chemistry.

The introduction to Chapter 1 of this thesis discussed several mechanisms for carbon-carbon bond formation which have been proposed over the years. In that chapter, it was suggested that the direct-insertion, or "Cossee-Arlman" mechanism seemed most consistent with the bulk of experimental evidence for most important catalyst systems. In Chapter 2, evidence for the operation of the "modified Green-Rooney" mechanism, involving so-called  $\alpha$ -agostic assistance in the bond-forming transition state, was discussed, and it was noted that reactions with particular configurational constraints, such as cyclizations and dimerizations of moderately bulky olefins, have provided most of the positive evidence for this mechanism. For example, in the case of the hydrocyclization of 1,5-hexadiene by "OpScH", the direction of the observed perturbation required the postulate that the 5,4 ring system, formed by the bonds being made and broken in the transition state, adopts a *cis* conformation. Indeed, if the corresponding *trans*-[5,4] conformation were degenerate with its *cis* counterpart,  $\alpha$ -agostic stabilization of the transition state would be kinetically invisible.



slightly favored



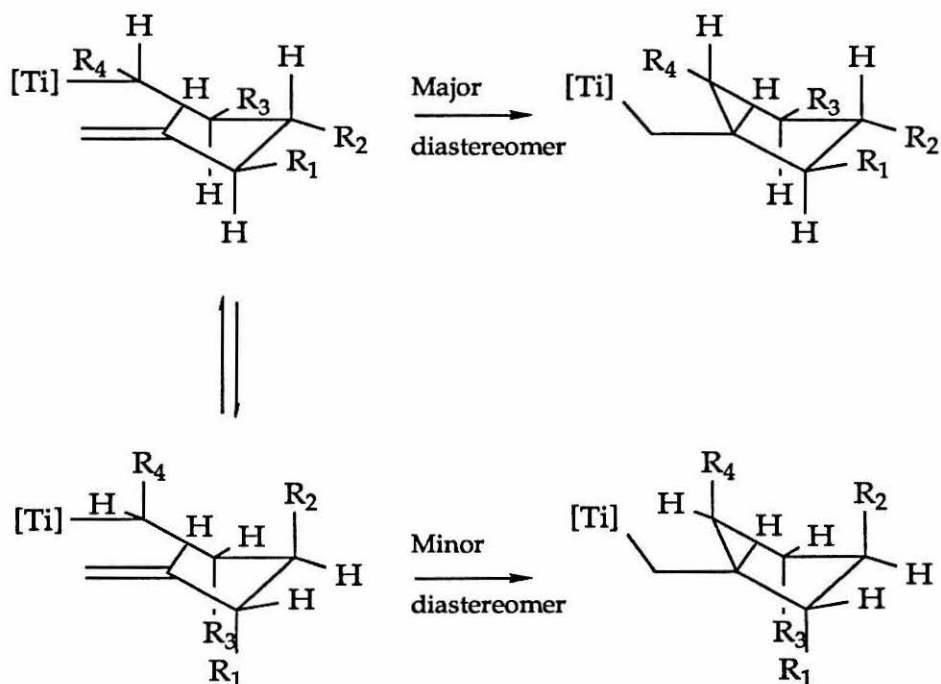
The expectation that the pseudo bicyclic transition state ("pseudo" because some of the bonds which constitute the skeleton are being formed or broken) should assume a *cis*-fused geometry is founded in conformational intuition stretching back to the early days of conformational analysis. In 1935 it was already noted that *cis* fusion of small (four- or five-membered) alicyclic rings should be greatly favored over *trans* fusion. While *trans*-[5,4] ring systems were unknown at the time, *trans*-bicyclo[3.3.0]octan-3-one had been prepared and its heat of combustion found to be 28.5 kJ/mol greater than for the *cis* isomer.<sup>16</sup> The first derivatives of *trans*-bicyclo[3.2.0]heptane were not prepared until 1964.<sup>17</sup> Current estimates of the strain engendered by *trans* fusion of the bicyclo[3.2.0]heptane skeleton have been derived by MM2 calculations and partially verified by electron diffraction measurements. For the parent hydrocarbon,  $\Delta\Delta H_f^\circ \approx 5.5$  kJ/mol<sup>18,19</sup>, which implies an equilibrium distribution of 9:1 (*cis* : *trans*). The electron diffraction data are consistent with a ratio of this magnitude. The ring strain in bicyclo[3.2.0]heptane is not exclusively associated with the four-membered ring, since bicyclo[3.3.0]octane rings show a similar preference for *cis*-fusion (*vide supra*).

Although one would not expect a transition state structure to experience the full strain energy associated with a model alicyclic compound, in many cases the preference for *cis* fusion in the transition state for a Ziegler-Natta cyclization event is apparently quite strong. Stille has studied stoichiometric ring-closures at Ziegler-Natta active titanium centers of the type employed by Grubbs<sup>20</sup> (see Chapter 2). When methyl groups are present on the incipient ring in any one of the positions R<sub>1</sub>-R<sub>4</sub> in Scheme III, cyclization proceeds with high diastereomeric excesses, ca., 92%.<sup>21</sup> The mechanism invoked by Stille involves two assumptions, one explicit and one implicit. Stille explicitly assumes that alkyl substituents on cyclizing substrates will tend to occupy equatorial positions in the incipient five-membered ring. Implicitly, by considering only the "envelope" conformation of cyclopentane, he restricts his cyclization transition states to those with *cis*-fused [5,4] pseudo bicyclic rings.<sup>22</sup> In fact, it is easy to show that the inclusion of competitive *trans*-fused transition states leads to a prediction of no diastereoselectivity.

The MM2 picture of bicyclo[3.2.0]heptane suggests a credible explanation for the apparently rigid enforcement of a *cis*-fused transition state. In *cis*

-bicyclo[3.2.0]heptane, the four-membered ring is calculated to be very nearly planar. By contrast, the four-membered ring in *trans*-bicyclo[3.2.0]heptane is extremely puckered. The important orbitals in the transition-state for ring formation in a  $d^0$  metallocene environment are coplanar;<sup>23</sup> recent calculations indicate that the only deviations from planarity in an acyclic transition state arise from weak steric interactions between nearly eclipsed C-H bonds.<sup>24</sup> Overlap between the four atoms involved in the bond-making and -breaking process will be diminished to the extent that they deviate from a coplanar arrangement. Thus the apparently strong preference for a *cis*-fused transition state can be considered to arise more from consideration of orbital overlap than from ring strain per se.

Scheme III. Stille's Mechanism for Diastereoselectivity in Five-membered Ring Closure.



Stille's stoichiometric studies provide a useful context in which to consider the diastereoselectivity observed by Waymouth and Resconi for cyclopolymerization of hexadiene to predominantly *trans* repeat units by



$\text{Cp}_2\text{ZrCl}_2/\text{MAO}$ . In both cases a transition state with a *cis* [5,4]bicyclic ring and equatorial placement of substituents (methyl or polymer) leads to the observed predominant product. The striking reversal of selectivity, resulting in a predominance of *cis* repeat units in the polymer, observed when  $\text{Cp}^*\text{ZrCl}_2/\text{MAO}$  is used as catalyst precursor is attributed by Waymouth to a change in transition state geometry from a *cis*-fused to a *trans*-fused [5,4]bicyclic ring system.<sup>25</sup> In the face of both the Stille experiments and the hydrocyclization experiments of Bercaw and Brintzinger, this explanation appears somewhat *ad hoc*. At the very least it is clear that the factors which determine stereoselectivity in hydrocyclization and cyclopolymerization remain incompletely described.

(ii) Stereochemical analysis of deuteriopolymerization

The cyclopolymerization of 1,5-hexadiene appeared to provide an ideal opportunity to observe the modified Green-Rooney mechanism at work in an actual polymerization reaction. Because the  $\text{Cp}^*\text{SiNR}$  catalysts show an almost complete lack of stereoselectivity in cyclopolymerization (*vide infra*), any experimental perturbations (e.g., those expected from  $\alpha$ -deuterium isotope effects) were expected to be more readily observable than they would be in an already selective reaction.

We first sought to determine whether the  $\text{Cp}^*\text{SiNR}$  catalysts would show a secondary isotope effect in the well-examined hydrocyclization reaction. In collaboration with Timothy A. Herzog, it was found that in the presence of four atmospheres of dihydrogen,  $[(\text{Cp}^*\text{SiNR})\text{ScH}(\text{PMe}_3)]_2$  cleanly catalyzes the hydrocyclization of 1,5-hexadiene. No oligomeric products are observed by NMR. When *trans, trans*-1,6-dideuterio-1,5-hexadiene is used as the substrate, the expected stereochemical perturbation is observed ( $k_{\text{H}}/k_{\text{D}} = 1.209 \pm 0.015$ ).<sup>26</sup> These observations demonstrate that the "modified Green-Rooney" mechanism can operate for catalysts based on the  $\text{Cp}^*\text{SiNR}$  ligand array. They further imply that the transition state for ring closure proceeds through the expected *cis*-fused [5,4]bicyclic transition state.

The appendix traces the stereochemical results expected from the operation of agostic stabilization in both the propagation and cyclization steps; these two effects are independent of one another. An agostic interaction in the propagation step affects tacticity, while an agostic interaction during cyclization

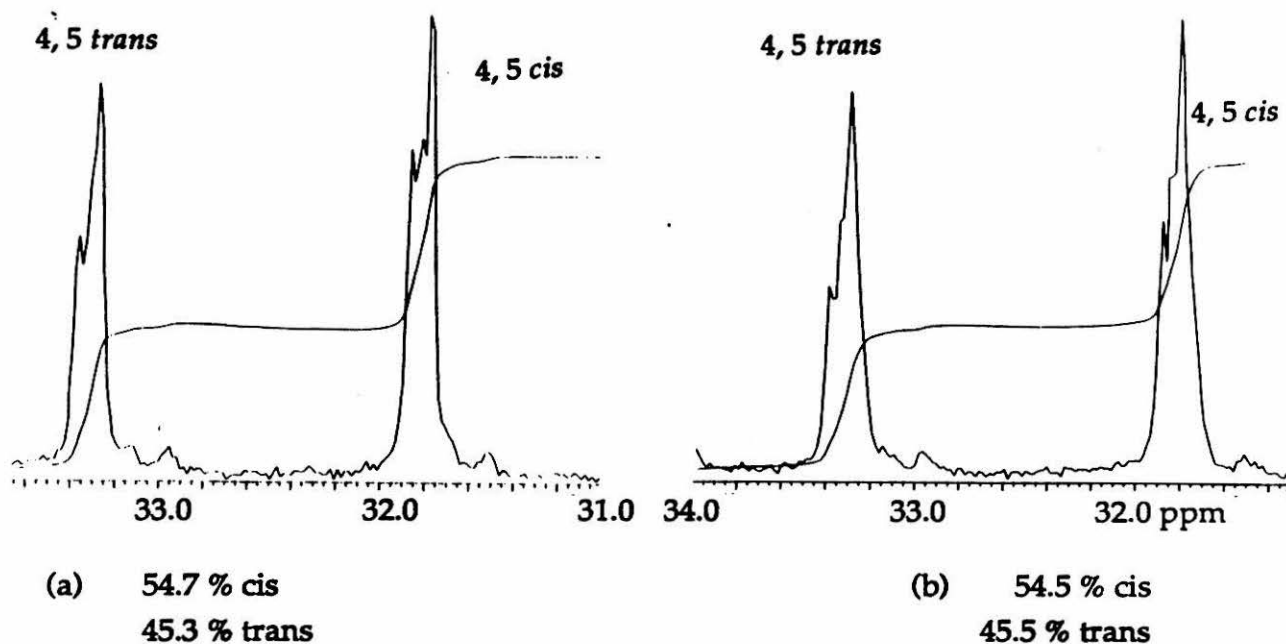
affects the cis/trans stereochemistry of the five-membered rings. The predicted effect on the ring stereochemistry is a consequence of the presumed isotope effect, of the trans, trans arrangement of deuterium on the substrate olefin, and of the presumed restriction of the transition state [5,4] ring system to an exclusively cis configuration. Single enantiomers of the important transition states are shown in Figure 7 (*vide infra*). It is worth emphasizing that, if the transition state occurs via the cis-[5,4] bicyclic ring system shown, the transition states (T and its enantiomer) leading to trans rings in the polymer will always have light hydrogen in the "agostic" position, whereas those (C and its enantiomer) leading to cis rings will always have deuterium in the "agostic" position. If the agostic effect makes an important contribution to the energies of these transition states, the former must be of lower energy than the latter.

Furthermore, in addition to perturbing the cis/trans disposition of the deuterium atoms about the rings, an agostic isotope effect should also perturb the stereochemistry of the polymeric carbon skeleton (a quite fortunate event since the deuterium spectrum of the labelled polymer is broad and uninformative). We chose, therefore, to analyze the problem by comparison of the  $^{13}\text{C}$ -NMR spectra of polymers prepared from labeled and unlabeled monomer. Partial  $^{13}\text{C}\{^1\text{H}\}$ -NMR spectra of deuterated and undeuterated polymer are shown in Figure 6. In each case the cis/trans ratio is very nearly unity.<sup>27</sup> Polymerization of 1,6-dideuterio-1,5-hexadiene does not result in a perturbation in the stereochemistry of the product.

It follows that competition between the transition states T and C does not determine the stereochemistry of the polymer. One of the assumptions from which these transition states were derived must be discarded. Because the corresponding hydrocyclization chemistry proceeds with a substantial secondary kinetic deuterium isotope effect, it is implausible to suggest that such an effect is inherently untenable. The most reasonable conclusion is to discard the assumption that the pseudo-[5,4] ring system in the transition state is constrained to adopt a cis geometry. The range of possible transition states when trans-[5,4]bicyclic transition states are allowed is shown in Figure 7. Now transition states T and T' lead to the formation of trans rings in the polymer. One of these (T) possesses agostic hydrogen and the other (T') agostic deuterium. A similar situation holds for the transition states C and C' that lead to cis rings. Even if an

agostic stabilization effect is important, this set of transition states predicts that it should be kinetically invisible, with the pairs T and C', and T' and C effectively cancelling one another. Note that T and C' are related to one another by a reversal of the enantioface of the inserting olefin, as are C and T'.

Figure 6. Partial  $^{13}\text{C}\{^1\text{H}\}$ -NMR spectra of (a) deuterated and (b) undeuterated polymers.

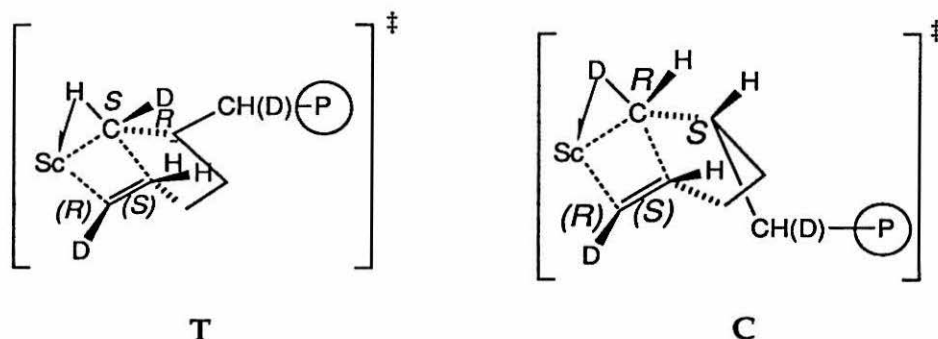


The results of this deuteriopolymerization study support the implicit assumption of Waymouth and co-workers that ring-strain considerations are less important to the determination of transition-state energy than the conformational requirements of the polymeric side-chain. Where no such side-chain exists, as in hydrocyclization, the *cis*-[5,4]bicyclic transition state is more stable than its *trans* counterpart, and agostic stabilization of the transition state becomes kinetically visible. With a sufficiently bulky substituent, as in polymerization, any strain

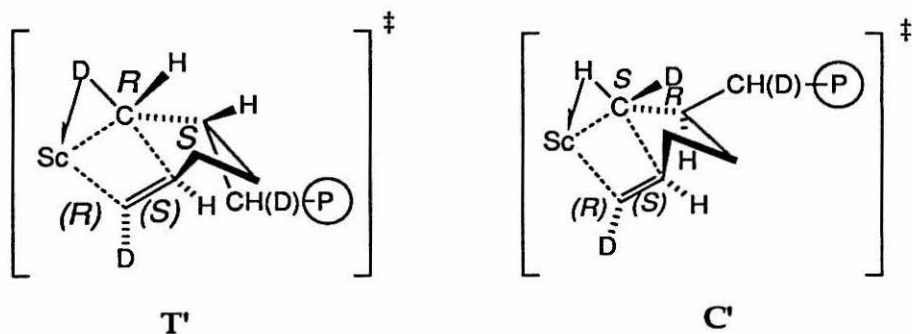
energy inherent in a trans-[5,4]bicyclic ring arrangement is not sufficient to override the preference of that substituent for an equatorial position in the forming ring, and agostic stabilization of the transition state becomes kinetically invisible.

**Figure 7. Transition states for the cyclization step in hexadiene polymerization.**

(a) Transition states with cis-fused [5,4] ring system



(b) Transition states with trans-fused [5,4] ring system



### III. CONCLUSIONS

The (Cp\*SiNR)Sc- system provides a variety of effective single-component catalysts for diene cyclopolymerization. The molecular weight properties of the hexadiene polymers are strongly influenced by the choice of catalyst precursor.

The presence of trimethylphosphine is of particular importance in determining the molecular-weight characteristics of the product. Hexadiene cyclopolymerization is more efficient than  $\alpha$ -olefin polymerization (in terms of both polymer yield and molecular weight) with the same catalysts, although a comparison of the propagation rates for these monomers reveals them to be nearly identical.

Attempts were made to study  $\beta$ -hydride elimination from model intermediate complexes because of the suppression of termination and chain transfer processes. Unfortunately, no suitable trapping reagents for the transient hydride species were found. The reaction of one of these  $(\text{Cp}^*\text{SiNR})\text{ScR}(\text{PMe}_3)_2$  complexes with 3-hexyne provided unexpected access to a scandia(allene) complex.

In contrast to similar hydrocyclizations, the stereochemistry of cyclopolymerization is not perturbed by deuteration of the substrate. This observation suggests that cis/trans selection during polymerization arises from a partitioning between a more complex manifold of transition states than in the case of hydrocyclization. In particular, transition states in which the 5,4 ring system composed of the incipient ring and the atoms involved in bond-making and bond-breaking adopts a trans configuration, as invoked by Waymouth and co-workers in the cyclopolymerization of hexadiene by  $\text{Cp}^*_2\text{ZrCl}_2/\text{MAO}$ , appear to be important here as well.

Table I. NMR Data for Selected Compounds

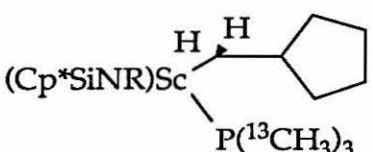
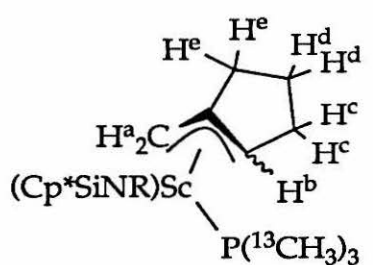
| Compound/Conditions   | Assignment   | $\delta$ (ppm)   | J (Hz)  |
|---|--|--|---|
| <br><p>2</p> <p>300 MHz <math>^1\text{H}</math><br/> <math>\text{C}_6\text{D}_6</math><br/>           rm temp</p>  | <p><math>\text{C}_5(\text{CH}_3)_4</math></p> <p><math>\text{NC}(\text{CH}_3)_3</math></p> <p><math>\text{Si}(\text{CH}_3)_2</math></p> <p><math>\text{P}(^{13}\text{CH}_3)_3</math></p> <p><math>\alpha\text{-CH}_2</math><br/>(diastereotopic)</p> | <p>2.36 (br s)<br/>           1.18 (br s)<br/>           1.95 (br s)<br/>           1.88 (br s)</p> <p>1.43 (s)</p> <p>0.64 (s)<br/>           0.81 (s)</p> <p>0.65 (d of q)</p> <p>0.0 - 0.04 (m)</p> | <p><math>^3\text{J}_{\text{P-H}} = 4</math><br/> <math>^1\text{J}_{\text{C-H}} = 125</math></p> |
| <br><p>4</p> <p>400 MHz <math>^1\text{H}</math><br/> <math>\text{C}_6\text{D}_6</math><br/>           rm temp</p> | <p><math>\text{C}_5(\text{CH}_3)_4</math></p> <p><math>\text{NC}(\text{CH}_3)_3</math></p> <p><math>\text{Si}(\text{CH}_3)_2</math></p> <p><math>\text{P}(\text{CH}_3)_3</math></p> <p><math>\text{H}^a</math></p> <p><math>\text{H}^b</math></p>    | <p>2.24 (s)<br/>           1.90 (s)</p> <p>1.19 (s)</p> <p>0.76 (s)</p> <p>0.078 (d)</p> <p>2.06 (br s)<br/>           3.82 (br s)</p>   | <p><math>^3\text{J}_{\text{P-H}} = 3.3</math></p>   |

Table I (continued).

| Compound/Conditions  | Assignment                                     | $\delta$ (ppm)                       | J (Hz)                              |
|--|--|--------------------------------------|-------------------------------------|
| 4, continued   | H <sup>c</sup> , H <sup>e</sup>                | 2.60 (br d of t)<br>2.34 (br d of t) |                                     |
|  | H <sup>d</sup>                                 | 1.87 (br m)                          |                                     |
| (Cp*SiNR)Sc-<br>C(CH <sub>3</sub> <sup>a</sup> )=C(H <sup>c</sup> )CH <sub>3</sub> <sup>b</sup><br><br>300 MHz <sup>1</sup> H<br><br>C <sub>6</sub> D <sub>6</sub> , rm temp | C <sub>5</sub> (CH <sub>3</sub> ) <sub>4</sub> | 1.93 (s)<br>$\approx$ 2.25 (br)      |                                     |
|  | NC(CH <sub>3</sub> ) <sub>3</sub>              | 1.33 (s)                             |                                     |
|  | Si(CH <sub>3</sub> ) <sub>2</sub>              | 0.720 (s)<br>0.730 (s)               |                                     |
|  | P(CH <sub>3</sub> ) <sub>3</sub>               | $\approx$ 0.8 (br)                   |                                     |
|  | H <sup>c</sup>                                 | 5.126 (m)                            |                                     |
|  | CH <sub>3</sub> <sup>b</sup>                   | 1.80 (d)                             | 5.5 Hz                              |
|  | CH <sub>3</sub> <sup>a</sup>                   | 2.06 (d)                             | 1 Hz                                |
| (Cp*SiNR)Sc-CH <sub>2</sub> CCCH <sub>3</sub><br><br>300 MHz <sup>1</sup> H<br><br>C <sub>6</sub> D <sub>6</sub> , rm temp   | C <sub>5</sub> (CH <sub>3</sub> ) <sub>4</sub> | 2.24 (s)<br>1.87 (s)                 |                                     |
|  | NC(CH <sub>3</sub> ) <sub>3</sub>              | 1.23 (s)                             |                                     |
|  | Si(CH <sub>3</sub> ) <sub>2</sub>              | 0.79 (s)                             |                                     |
|  | P(CH <sub>3</sub> ) <sub>3</sub>               | 0.72 (d)                             | <sup>2</sup> J <sub>P-H</sub> = 3.9 |
|  | Sc-CH <sub>2</sub> -                           | 2.36 (br q)                          | $\approx$ 2.3                       |
|  | ScCH <sub>2</sub> CCCH <sub>3</sub>            | 1.98 (t)                             | 2.6                                 |

Table I (continued).

| Compound/Conditions  | Assignment    | $\delta$ (ppm)                               | J (Hz)              |
|--|---------------|--|---------------------|
| (Cp*SiNR)Sc-<br>$C(CH_2^aCH_3^b)=C(H^c)CH_2^d-CH_3^3$<br><br>300 MHz $^1H$<br><br>$C_6D_6$ , rm temp | $C_5(CH_3)_4$ | not located<br>(extremely broad)             |                     |
|  | $NC(CH_3)_3$  | 1.34 (s)                                     |                     |
|  | $Si(CH_3)_2$  | 0.738 (s)                                    |                     |
|  | $P(CH_3)_3$   | $\approx 0.8$ (br)                           |                     |
|  | $H^a, H^d$    | not located                                  |                     |
|  | $H^b, H^e$    | 1.13 (t)<br>0.99 (t)                         | 6.0<br>6.0          |
|  | $H^c$         | 4.82 (m)                                     |                     |
| (Cp*SiNR)Sc-<br>$C(CH_2^aCH_3^b)=C=C(H^c)CH_3^d$<br><br>300 MHz $^1H$<br><br>$C_6D_6$ , rm temp      | $C_5(CH_3)_4$ | 2.37 (s)<br>2.21 (s)<br>1.99 (s)<br>1.82 (s) |                     |
|  | $NC(CH_3)_3$  | 1.23 (s)                                     |                     |
|  | $Si(CH_3)_2$  | 0.74 (s)<br>0.84 (s)                         |                     |
|  | $P(CH_3)_3$   | 0.79 (d)                                     | $^2J_{P-H} = 3.3$   |
|  | $H^a$         | not located                                  |                     |
|  | $H^b$         | 1.30 (t)                                     | 7.1                 |
|  | $H^c$         | 3.82 (m)                                     | $^5J_{Ha-Hc} = 5.5$ |
|  |               |  |                     |
|  |               |  |                     |



Table I (continued).

| Compound/Conditions | Assignment     | $\delta$ (ppm) | J (Hz)                     |
|---------------------|----------------|----------------|----------------------------|
| (continued)         | H <sup>d</sup> | 1.55 (d)       | $^3J_{\text{Hc-Hd}} = 6.0$ |

## EXPERIMENTAL SECTION

### General Considerations

All manipulations were performed using standard dry box or high-vacuum techniques, except as noted. All solvents were purified as described in previous chapters. Olefins were obtained from Aldrich and purified by distillation from  $\text{CaH}_2$  or  $\text{LiAlH}_4$ .

NMR spectra were recorded on JEOL GX-400 and GE QE-300 instruments using standard  $^1\text{H}$  and  $^{13}\text{C}\{^1\text{H}\}$  acquisition parameters. Gel permeation chromatography was performed on a Waters ALC/GLC eluting with toluene. Gas chromatography was performed on a Perkin-Elmer 8410 instrument.

Catalysts were prepared as described elsewhere, except for **2**, which is described below. *trans,trans*-1,6- $d_2$ -1,5-Hexadiene was a generous gift from Timothy A. Herzog.

### Polymerization of 1,5-Hexadiene: Dry Box Method

In a representative experiment, the catalyst (**1**, 24 mg, 0.065 mmol) was weighed into a 100-mL Schlenk flask in a dry box, and dissolved in toluene (35 mL). Also in the dry box, a pressure-equalizing addition funnel was charged with hexadiene (2.5 mL, 21.1 mmol, 324 eq) and toluene (10 mL), attached to the Schlenk flask and sealed with a ground glass stopper. The monomer solution was added dropwise with stirring over one hour (subsequent experiments indicated that addition need not be so slow for good polymerization behavior). The reaction mixture was allowed to stir for an additional hour before the assembly was removed from the dry box. The solution was quenched with methanol (1 mL) and poured into methanol (300 mL, acidified with 4 drops of concentrated HCl) to precipitate the product.<sup>28</sup> The product was filtered and dried in vacuo (290 mg, 20%).

Although effective, this procedure was unacceptable for frequent use, as it involves the manipulation of a volatile, reactive liquid (1,5-hexadiene) in a dry box normally reserved for the exclusion of such materials.

## Polymerization of 1,5-Hexadiene and 1-Hexene: Vacuum Line Method

Because the polymerizations are best performed under conditions of high dilution, a method was sought which would fully exploit the rigorous exclusion of air and water possible on a high vacuum line. Indeed, less rigorous techniques (e.g., syringe transfer of monomer solution to an addition funnel under argon flush) frequently led to the decomposition of the catalyst. In order to allow both the catalyst and the monomer solutions to be prepared under high vacuum conditions, a graduated, airless addition funnel in which the pressure equalization arm had been equipped with a teflon Kontes valve was used. With the valve closed, volatile liquids could be vacuum-transferred into the funnel by swabbing it with dry ice/acetone slurry. Any material in the flask beneath remained undisturbed.

A typical procedure involved weighing the catalyst (3, 14.3 mg, 0.021 mmol) into a 100-mL round-bottom flask in the dry box, and attaching the flask to the addition funnel described above. In turn, the upper joint of the addition funnel was then equipped with a calibrated gas volume which could be directly attached to a high-vacuum port. The entire apparatus was evacuated and the funnel was isolated from the flask by closing both the addition and the pressure equalization valves. Toluene (25 mL) was condensed into the funnel, where the volume could be measured, then allowed to drain into the flask. The catalyst solution was then cooled to  $-78^{\circ}\text{C}$ . Trimethylphosphine (234 Torr in 3.3 mL, 0.042 mmol) was admitted to the gas bulb and then condensed into the cold catalyst solution. In order to harvest any residual phosphine vapor, an additional aliquot of toluene (5 mL) was condensed into the funnel and drained into the catalyst solution below. A final aliquot of toluene (20 mL) was condensed into the addition funnel. 1,5-Hexadiene (1.50 mL, 0.013 mmol) was condensed into a graduated finger, then vacuum-transferred into the addition funnel. The entire apparatus was then allowed to warm to room temperature and was shaken gently to mix the catalyst solution. The monomer solution was added dropwise with stirring to the catalyst solution over a period of 15 minutes and allowed to stir at room temperature for a total of three hours. The product was isolated as described above (430 mg, 41.4 %).

### **$^{13}\text{C}$ -NMR Analysis of Hexadiene Polymers**

Tacticity information was derived from  $^{13}\text{C}\{^1\text{H}\}$ -NMR spectra obtained in  $\text{CDCl}_3$  at  $40^\circ\text{C}$ . Assignments were made according to the method of Coates and Waymouth.<sup>2b</sup>

**Table II.  $^{13}\text{C}\{^1\text{H}\}$ -NMR Stereochemical analysis of a representative poly(hexadiene) sample.<sup>a</sup>**

| Chemical Shift | Assignment           | Intensity<br>(% of total) | Calculated<br>Intensity <sup>b</sup> |
|----------------|----------------------|---------------------------|--------------------------------------|
| 33.87          | RmM or RrM           | 12.1                      | 12.4                                 |
| 33.83          | RmR                  | 13.3                      | 10.1                                 |
| 33.78          | RrR and (RmM or RrM) | 18.5                      | 22.5                                 |
| 32.32          | MrM                  | 16.7                      | 15.1                                 |
| 32.30          | MrR or MmR           | 17.8                      | 12.4                                 |
| 32.24          | MmM and (MrR or MmR) | 21.7                      | 27.5                                 |

<sup>a</sup>100 MHz spectrum obtained on JEOL GX-400.

<sup>b</sup>Calculated for atactic polymer with cis:trans ratio of 55 % : 45 %.

While the experimental values do not precisely match the calculated values for a completely atactic polymer, the deviations are minor and are not systematic.

### **Polymerization of 1,6- $d_2$ -1,5-hexadiene**

Using the vacuum-line method described above, a solution of 1,6- $d_2$ -1,5-hexadiene (1.0 mL, 8.2 mmol) in methyl-cyclohexane (9.0 mL) was added dropwise to a solution of **1** (20.5 mg in 1.0 mL methylcyclohexane). After stirring for 5 hours at room temperature, the volatiles were transferred to a Schlenk pot

and retained for future use. The residual polymer was worked up by dissolution in toluene and precipitation with methanol (140 mg, 20.2 %).

### **Copolymerization of Hexadiene and Hexene**

1-Hexene (0.50 mL, 4.0 mmol) and 1,5-hexadiene (0.50 mL, 4.2 mmol) were allowed to polymerize in methylcyclohexane and with a 24 hour reaction time, otherwise following the vacuum-line procedure described above up to the point of polymer workup. At the end of the reaction time, all volatiles were vacuum-transferred to a separate flask for GC analysis. Fresh toluene was condensed onto the residue, and the normal workup procedure was followed. After precipitation, filtration and drying in vacuo, the product was a sticky goo (435 mg, 63.7 %).

### **Kinetics of Monomer Consumption for Hexadiene and Pentene Polymerization**

A stock solution was prepared in a dry box by dissolving **1** (28.4 mg, 0.0382 mmol) and ferrocene (40.4 mg, 0.217 mmol) in toluene (1.500 mL; 0.145 M in ferrocene, 0.0510 M in total scandium). Aliquots (0.500 mL) of this solution were transferred by syringe to NMR tubes equipped with J. Young valves. On a vacuum line, the NMR tubes were degassed and frozen in liquid N<sub>2</sub>. Monomer (hexadiene or pentene) was added by condensation from a calibrated gas bulb (hexadiene: 52 Torr in 104 mL, 0.29 mmol; pentene: 51 Torr in 104 mL, 0.29 mmol). The tubes were thawed and immediately placed in a dry ice/acetone slurry. <sup>1</sup>H NMR spectra were obtained at 300 MHz in a 31±1 °C probe. The tubes were removed from the dry ice slurry and warmed to room temperature immediately before being placed in the probe.

### **Preparation of **2****

**1** (423 mg, 1.14 mmol) was weighed into a 25-mL round-bottom flask and slurried in toluene (5 mL). Methylenecyclopentane (0.5 mL, 4.8 mmol) was added by vacuum transfer via a graduated finger, and the mixture was stirred at room temperature for two hours. Toluene was removed from the yellow solution, leaving behind a yellow oil. This was triturated several times with petroleum ether, eventually yielding a yellow solid. The yellow, powdery product was isolated by cold filtration from petroleum ether (137 mg, 0.302

mmol, 26.5 %). The crude material was recrystallized from petroleum ether as a cream-colored, microcrystalline solid (75 mg, 0.172 mmol, 15.1 %), contaminated with ca. 10% **4**.

**2-<sup>13</sup>C<sub>3</sub>** was prepared free of allylic impurity using P(<sup>13</sup>CH<sub>3</sub>)<sub>3</sub>, a more dilute reaction solution (100.8 mg **1** in 5 ml toluene), a smaller excess of methylenecyclopentane (3.5 equivalents) and a shorter reaction time (one hour). The carbon label was incorporated for use in experiments not reported here.

#### Preparation of (Cp\*SiNR)Sc(CH<sub>2</sub>CHCH<sub>2</sub>CH<sub>2</sub>CH<sub>2</sub>CH<sub>2</sub>)•P(<sup>13</sup>CH<sub>3</sub>)<sub>3</sub>

(Cp\*SiNR)Sc(CH<sub>2</sub>CHCH<sub>2</sub>CH<sub>2</sub>CH<sub>2</sub>CH<sub>2</sub>)•P(<sup>13</sup>CH<sub>3</sub>)<sub>3</sub> (**2-<sup>13</sup>C<sub>3</sub>**) was prepared for use in NMR experiments which are not reported in this thesis. The preparation is reported here because **2-<sup>13</sup>C<sub>3</sub>** was prepared free of contamination by **4-<sup>13</sup>C<sub>3</sub>**. Slightly lower concentrations and shorter reaction times were used to discourage the secondary formation of allylic impurities.

To a toluene solution (5 mL) of the labeled hydride precursor [(Cp\*SiNR)ScH(P<sup>13</sup>CH<sub>3</sub>)<sub>3</sub>]<sub>2</sub> (100.8 mg, 0.269 mmol) was added by vacuum transfer an excess of methylenecyclopentane (≈100 μL, ≈0.95 mmol). The reaction mixture was stirred for one hour at room temperature, yielding a clear, yellow solution which, upon removal of volatiles, became a yellow oil. A solid was obtained by trituration with four portions of petroleum ether (5 mL). The product was isolated by recrystallization from cold petroleum ether (40.5 mg, 0.089 mmol, 33%). No allylic impurities were observed in the NMR spectrum of the product.

#### NMR tube reactions of **2**: Hydrogenation

A small sample of **2** (7.1 mg) was dissolved in benzene-*d*<sub>6</sub> and sealed in an NMR tube under 4 atmospheres H<sub>2</sub>.

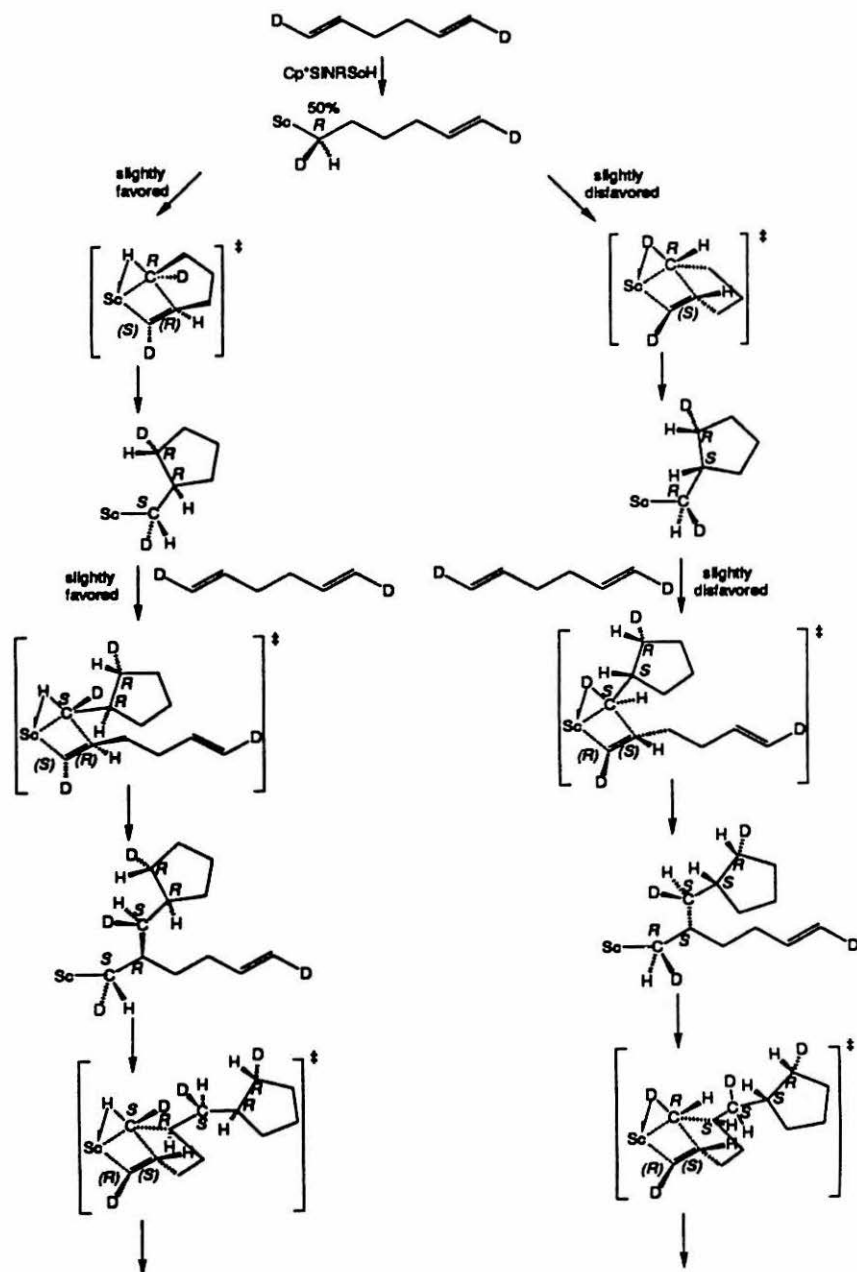
#### NMR tube reactions of **2**: 2-Butyne

Samples of **2** (ca. 7 mg) were dissolved in benzene-*d*<sub>6</sub> and cyclohexane-*d*<sub>12</sub> in separate NMR tubes. 2-Butyne (48 Torr in 6.9 mL, 0.018 mmol) was added to each tube and the tubes were sealed for NMR analysis.

## Preparation of **4**

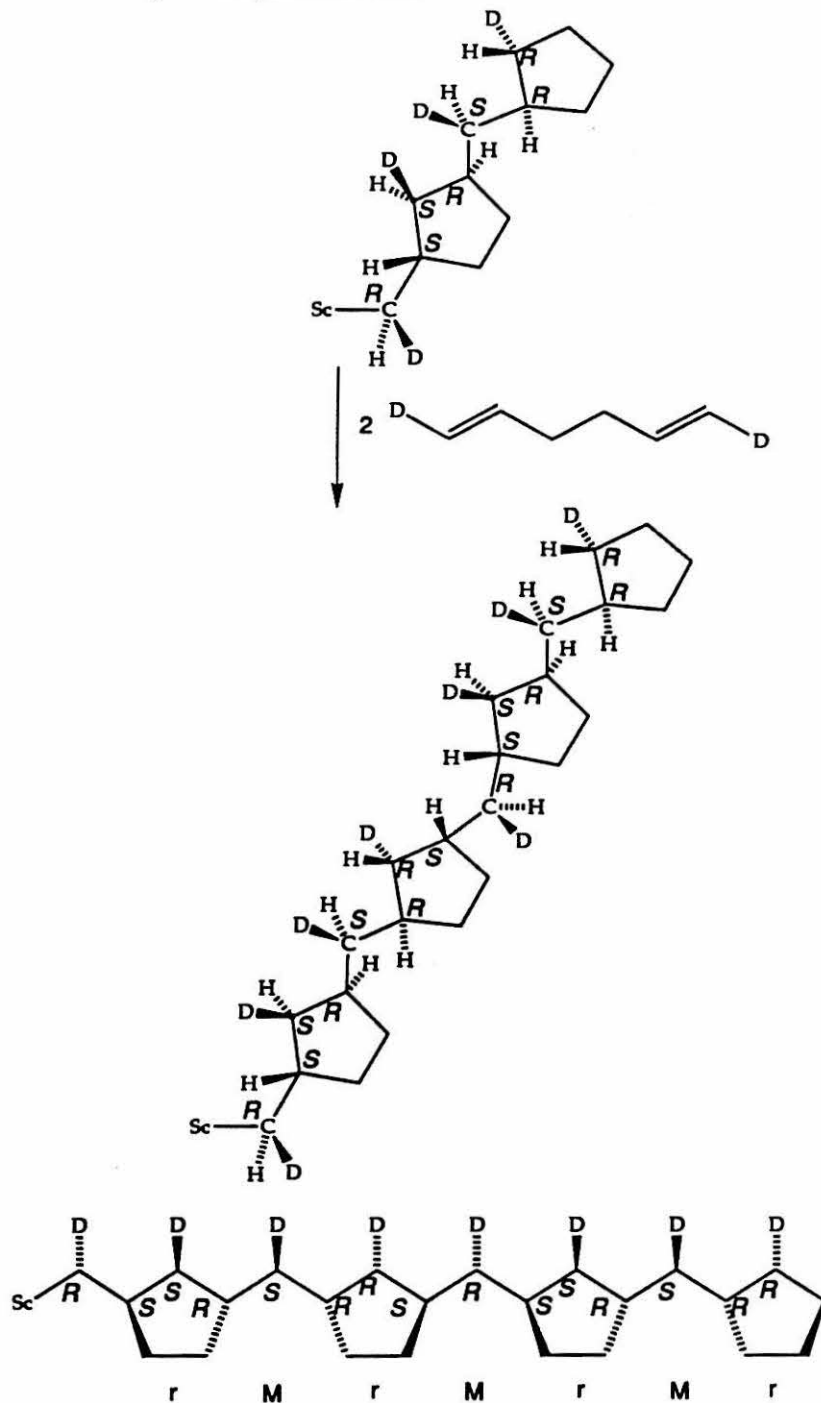
$[(\text{Cp}^*\text{SiNR})\text{ScH}(\text{PMe}_3)]_2$  (1.015 g, 2.73 mmol) was weighed into a 50-mL round-bottom flask and slurried in petroleum ether (15 mL). Methylenecyclopentane (1.0 mL, 9.6 mmol) was added by vacuum transfer by way of a graduated coldfinger, and the mixture was stirred at room temperature for over five hours. The yellow solution was concentrated and cooled to precipitate the product as a yellow microcrystalline solid, isolated by cold filtration, and washed twice with fresh petroleum ether. A second crop was obtained (total yield: 472.8 mg, 1.045 mmol, 51.5 %).

**Appendix: Analysis of  $\alpha$ -Agostic Perturbation of Stereochemistry in Hexadiene Cyclopolymerization (assuming a cis-fused transition state geometry)**





Most favored pathway, continued.





## REFERENCES

1. (a) Marvel, C. S.; Stille, J. K. *J. Am. Chem. Soc.* **1958**, *80*, 1740.  
 (b) Marvel, C. S.; Garrison, Jr., W. E. *J. Am. Chem. Soc.* **1959**, *81*, 4737.  
 (c) Butler, G. B. *Acc. Chem. Res.* **1982**, *15*, 370.  
 (d) Butler, G. B. In *Comprehensive Polymer Science*; Allen, G.; Bevington, J. C. Eds.; Pergamon Press: Oxford, 1989; p 423.
2. (a) Resconi, L.; Waymouth, R. M. *J. Am. Chem. Soc.* **1990**, *112*, 4953.  
 (b) Coates, G. W.; Waymouth, R. M. *J. Am. Chem. Soc.* **1991**, *113*, 6270.
3. All molecular weight data are *vs.* polystyrene. A Viscotek chromatograph for the determination of absolute molecular weights by viscometric GPC has recently been acquired by Caltech but is not operational at the time of writing. Samples have been submitted for analysis, however. Absolute molecular-weight data will greatly aid in interpreting some of the data presented in this chapter.
4. Shapiro, P. J. Ph.D. Thesis, California Institute of Technology, 1990.
5. See Chapter 1 and references therein.
6. See Chapter 6.
7. Reference 4, p. 26.
8. Reference 4, p. 109.
9. Cheng, H. N.; Khasat, N. P. *J. Appl. Polym. Sci.* **1988**, *35*, 825.
10. The slight deviation from a statistical 2 : 1 composition reflects the fact that the ratio of monomer concentrations is not identically 1.
11. Burger, B. J.; Thompson, M. E.; Cotter, W. D.; Bercaw, J. E. *J. Am. Chem. Soc.* **1990**, *112*, 1566.
12. It is possible that this product is an  $\eta^3$ -propargyl complex rather than a simple scandia(allene) as drawn. See, for example, (a) Casey, C. P.; Yi, C. S. *J.*

*Am. Chem. Soc.* **1992**, *114*, 6597; (b) Gotzig, J.; Otto, H.; Werner, H. *J. Organomet. Chem.* **1985**, *287*, 247.

13. Thompson, M. E.; Baxter, S. M.; Bulls, A. R.; Burger, B. J.; Nolan, M. C.; Santarsiero, B. D.; Schaefer, W. P.; Bercaw, J. E. *J. Am. Chem. Soc.* **1987**, *109*, 205-219.

14. (a) Favorskii, A. E. *J. Prakt. Chim.* **1888**, *37*, 417.

(b) For a review of propargylic metalation chemistry, see Klein, J., in Patai, S., ed., *The Chemistry of the Carbon-Carbon Triple Bond*, Chichester: John Wiley and Sons, 1978, Volume 1, Chapter 9, pp. 343-379.

15. (a) West, R.; Carney, P. A.; Mineo, I. C. *J. Am. Chem. Soc.* **1965**, *87*, 3788.

(b) West, R.; Jones, P. C. *J. Am. Chem. Soc.* **1969**, *91*, 6156.

16. Barrett, J. W.; Linstead, R. P. *J. Chem. Soc.* **1935**, 436-442. The energy unit as reported is 6.8 kg•cal.

17. (a) Meinwald, J.; Tufariello, J. J.; Hurst, J. J. *J. Org. Chem.* **1964**, 2914.

(b) Meinwald, J.; Anderson, P.; Tufariello, J. J. *J. Am. Chem. Soc.* **1966**, *88*, 1301.

18. Glen, R.; Gunderson, G.; Murray-Rust, P.; Rankin, D. W. H. *Acta. Chem. Scand.* **1983**, *A 37*, 853-863.

19. Somewhat less straightforward calculations have also been reported for the bridgehead-substituted derivative 1,5-diphenylbicyclo[3.2.0]heptane ( $\Delta\Delta H_f^\circ \approx 11.7$  kJ/mol). However, these calculations do not correlate well with experimental thermochemistry on these compounds, for reasons which remain speculative. See Roth, W. R.; Lennartz, H.-W.; Doering, W. von E.; Birladeanu, L.; Guyton, C. A.; Kitagawa, T. *J. Am. Chem. Soc.* **1990**, *112*, 1722.

20. Clawson, L.; Soto, J.; Buchwald, S.L.; Steigerwald, M.L.; Grubbs, R.H. *J. Am. Chem. Soc.* **1985**, *107*, 3377-78.

21. Young, J. R.; Stille, J. R. *Organometallics* **1990**, *9*, 3022-3025.

22. The conformational terminology used by the various authors cited in this discussion is not uniform. This note is intended to explicitly state what certain words mean in this thesis and what is inferred to have been meant in the works cited. Cyclopentane can exist in a  $C_s$  conformation commonly called the "envelope" conformation, and a  $C_2$  conformation commonly called the "chair" or "half-chair." In bicyclic systems, cis-fusion rigidly enforces the "envelope" form, which possesses approximate  $C_s$  symmetry. Trans-fusion fixes a five-membered ring in the "chair" form, which then possesses approximate  $C_2$  symmetry. The following sets of terms are roughly equivalent: cis-fused [5,4] bicyclic ring system =  $C_s$  = envelope; trans-fused [5,4] bicyclic ring system =  $C_2$  = chair or half-chair. These distinctions are emphasized here because standard terminology is violated in the important paper by Resconi and Waymouth, reference 2a. These authors unfortunately employ terminology more appropriate for the description of six-membered rings; thus the  $C_2$  "half-chair" conformation becomes "twist-boat" and, most confusing of all, the  $C_s$  "envelope" conformation is referred to as "chair."

23. Lauher, J. W.; Hoffman, R. *J. Am. Chem. Soc.* **1976**, *98*, 1729-1742.

24. Kawamura-Kuribayashi, H.; Koga, N.; Morokuma, K. *J. Am. Chem. Soc.* **1992**, *114*, 2359.

25. It would be extremely interesting to know whether the stoichiometric reactions reported by Stille demonstrate a corresponding reversal of selectivity upon moving from a titanocene- to a permethyltitanocene-based catalyst precursor.

26. Herzog, T. A. Unpublished results.

27. The NMR data cannot give an accurate determination of the absolute cis/trans composition of the polymer, since NOE and relaxation time effects on the relevant carbons are not accounted for explicitly. NMR polymer analysis is quite generally afflicted with this limitation. The observed cis/trans ratio for the polymers reported here varied from spectrometer to spectrometer, but on a given machine was reproducible to within a few percent.

28. When the methanol is not acidified, the product can precipitate as a latex.

## Chapter 6

### Examination of the Solution Dynamics of Intermediates in Organoscandium-catalyzed Ziegler-Natta Polymerization

**Abstract:** Variable-temperature  $^1\text{H}$ - and  $^{13}\text{C}\{^1\text{H}\}$ -NMR spectroscopy were used to examine the dynamic solution behavior of organoscandium Ziegler-Natta catalysts of the form  $(\text{Cp}^*\text{SiNR})\text{ScR}\cdot\text{PMe}_3$ .  $^1\text{H}$  spectroscopy of the 2-methylpentyl derivative **4** in the presence of excess  $\text{PMe}_3$  revealed no evidence of a bis(phosphine) adduct. Phosphine dissociation equilibria were observed by  $^{13}\text{C}$  spectroscopy of the carbon-labeled 2-methylpentyl ( $4\text{-}^{13}\text{C}_3$ ), propyl ( $6\text{-}^{13}\text{C}_3$ ), and isobutyl ( $5\text{-}^{13}\text{C}_3$ ) derivatives. Studies of the latter compound revealed one significant organoscandium species in addition to a phosphine-bound form. On the basis of symmetry arguments, it is proposed that this species is monomeric. While these observations are at variance with the prior suggestion that dimerization of the organometallic catalyst competes with propagation during olefin polymerization, they provide strong support for the primary importance of 12-electron, base-free, alkyl complexes as the reactive intermediates.

|  |     |
|--|-----|
| I. INTRODUCTION .....  | 132 |
| II. RESULTS.....   | 136 |
| Variable-Temperature $^1\text{H}$ -NMR Spectroscopy of 4 .....   | 136 |
| Measurement of Phosphine-Dissociation Equilibria .....   | 139 |
| III. DISCUSSION .....  | 146 |
| EXPERIMENTAL SECTION .....   | 161 |
| APPENDIX: Derivation of Equilibrium Expressions and Igor Routines for<br>Their Numerical Solution..... | 166 |
| REFERENCES .....   | 171 |

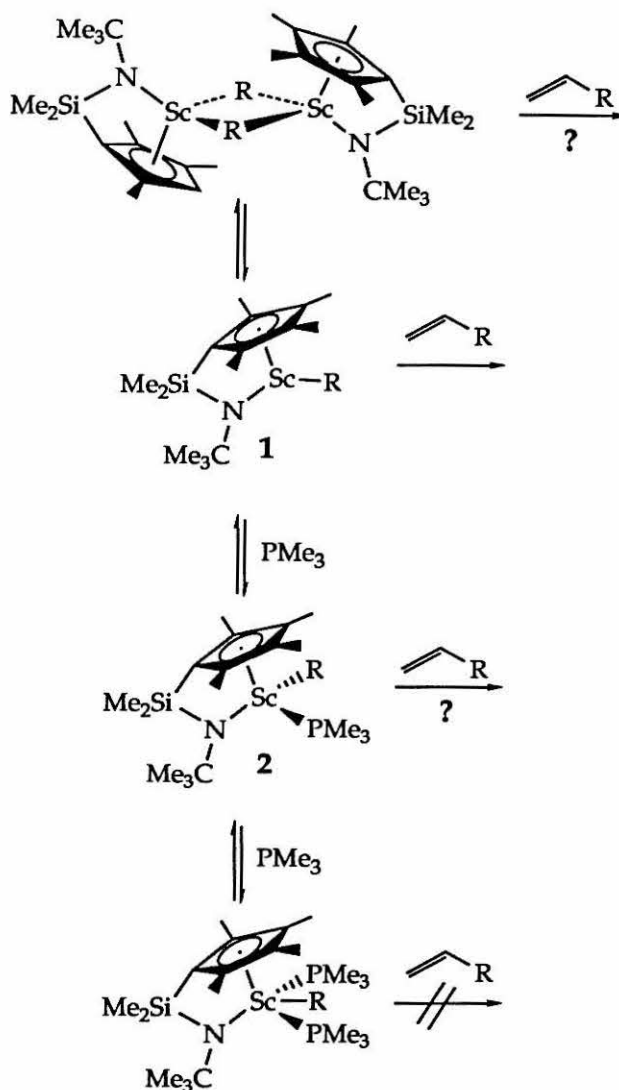


## I. INTRODUCTION

The two previous chapters have discussed some polymerization chemistry of organoscandium complexes supported by the linked cyclopentadienyl-amido ligand " $\text{Cp}^*\text{SiNR}$ ". These were the first single-component homogeneous catalysts for Ziegler-Natta polymerization of  $\alpha$ -olefins,<sup>1</sup> and were designed to be both sterically and electronically less saturated than fourteen-electron scandocene complexes. They remain the most reactive organoscandium derivatives for olefin polymerization.<sup>2</sup> With reactivity, at least in this case, has come complexity.  $(\text{Cp}^*\text{SiNR})\text{ScR}'$  complexes are not strictly "single-component" catalysts in one important sense: several forms of both catalyst precursor and reactive intermediate can exist in equilibrium with one another in solution. Unlike permethylscandocene derivatives, straight-chain  $(\text{Cp}^*\text{SiNR})\text{ScR}'$  derivatives (e.g.,  $\text{R}' = \text{propyl}$  and presumably butyl) are dimers in the solid state.<sup>1</sup> Shapiro, who first isolated these complexes, has shown that although trimethylphosphine is present during the synthesis of these complexes, this base is not retained in the solid state. Rapid phosphine exchange occurs when trimethylphosphine is added to a solution of the isolated alkyl dimers.<sup>1</sup>

The most likely solution structures for these compounds are shown in Scheme I. It was of particular interest for us to establish which of these was responsible for olefin polymerization. Shapiro addressed this question by examining the dependence of the rate of olefin polymerization on such variables as total scandium concentration and phosphine concentration. The observed behavior was complex and interpreted only with difficulty, but seemed to implicate the monomeric, base-free, twelve-electron species of general structure  $(\text{Cp}^*\text{SiNR})\text{ScR}'$  (1) as the most likely structure for the reactive intermediate. It was further concluded that this monomer existed in dynamic equilibrium not only with its phosphine-ligated precursor but also with a dimeric form.

**Scheme I. Some Possible Intermediates for Olefin Polymerization by  $(\text{Cp}^*\text{SiNR})\text{ScR}(\text{PMe}_3)$  Catalyst Precursors.**

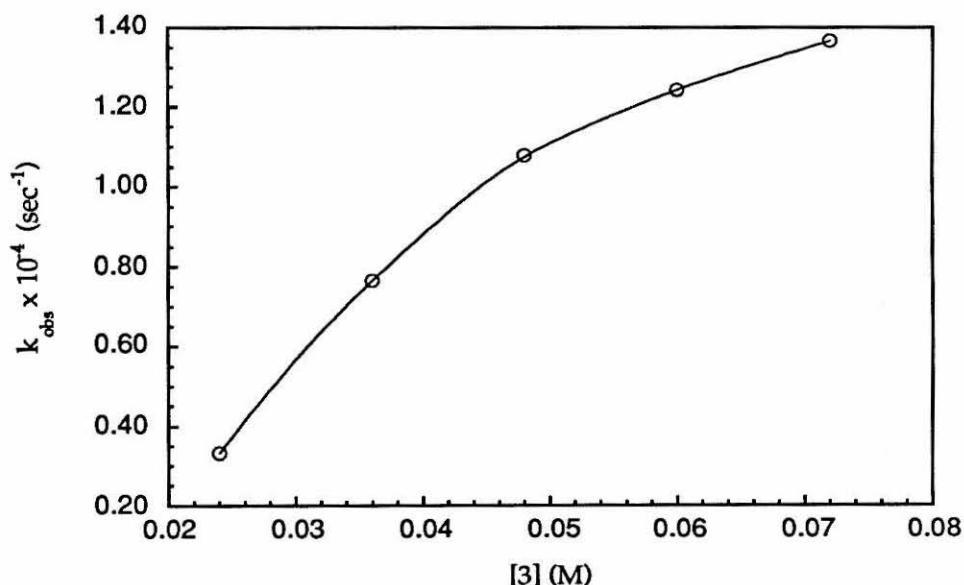


While these conclusions are intuitively satisfying, the data which support them present some cause for concern. It was clearly established that excess phosphine inhibits polymerization, but this fact alone is insufficient to implicate **1** as the reactive intermediate structure. **1** would certainly be the *most* reactive of the complexes shown in Scheme I, but it is not the only one which could conceivably react with olefins. For example, a phosphine-coordinated monomer of general structure  $(\text{Cp}^*\text{SiNR})\text{ScR}'(\text{PMe}_3)$  (**2**) would be a fourteen-electron species, isoelectronic with the ethylene polymerization catalyst precursor series

$\text{Cp}^*_2\text{ScR}$ ,<sup>3</sup> with similar lanthanide catalysts,<sup>4</sup> and with cationic zirconocene catalysts.<sup>5</sup> If **2** were an important, reactive intermediate, phosphine inhibition could still occur via a sixteen-electron bis(phosphine) adduct. Such adducts have been isolated for some of the cationic zirconocene catalyst precursors studied by Jordan and co-workers.<sup>6</sup>

The simplest evidence put forward for the intermediacy of **1** was the observation of saturation kinetics in 1-pentene polymerization by  $[(\text{Cp}^*\text{SiNR})\text{ScH}(\text{PMe}_3)_2]$  (**3**), indicating a dissociative pre-equilibrium step prior to olefin insertion. The original plot is shown in Figure 1a. This equilibrium was presumed to involve phosphine loss.

**Figure 1a. Dependence of Polymerization Rate on Catalyst Concentration, as Plotted in Reference 3.**



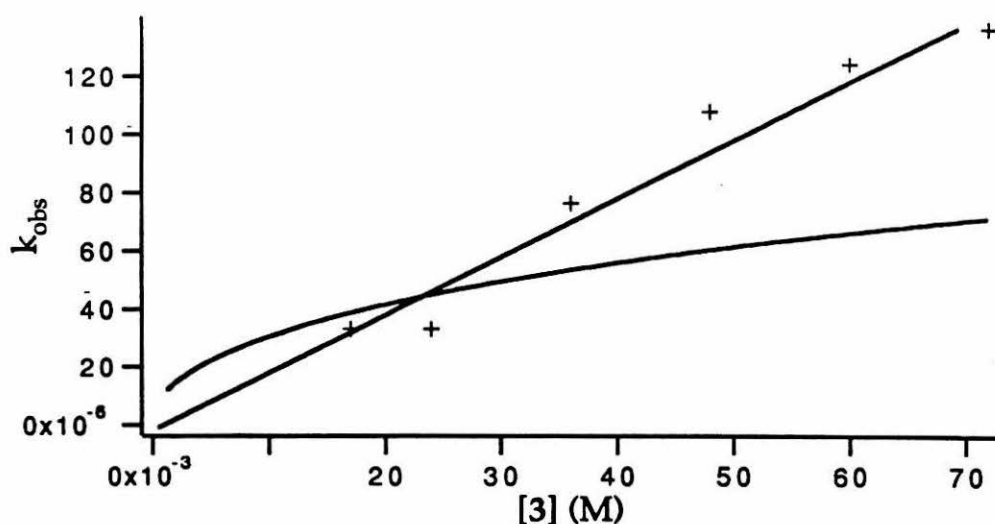
Examination of the plot upon which this argument was based, and the data from which the plot was constructed, indicates that an error of omission was committed. One point present in the data set does not appear in the plot; inclusion of this point and the origin diminishes the appearance of asymptotic

behavior.<sup>7</sup> A plot of the complete data set (Figure 1b) is fully compatible with simple first-order kinetics.

As the result of a series of kinetic experiments, including the one described above, Shapiro concluded that both phosphine association and dimerization competed effectively with propagation during  $\alpha$ -olefin polymerization, and reported a set of best values for the phosphine binding constant, dimerization constant and true second-order propagation rate constant. From these data, values of the observed rate constant  $k_{obs}$  can be calculated as a function of the total concentration of scandium complex in solution,  $[Sc]_0$  (see Discussion and Appendix for details of this calculation). This plot appears alongside the linear fit in Figure 1b. The dissociative picture very poorly describes the observed behavior. Unfortunately, as Shapiro recognized, this conclusion is unacceptable. Strict first-order kinetics simply are not possible in this reaction. Whatever the form of the reactive species, it cannot be static.

Interpretation of many key kinetics experiments required complicated data manipulation and some almost ad hoc assumptions. The chemically important difference between reaction from a manifold which includes dimerization processes and one which does not predicts only subtle changes in the kinetic observables. A more direct examination of the solution structures of the reactive intermediates seemed to be necessary. The primary goal in the present work was to elucidate the important equilibrium processes and the associated equilibrium constants for relevant organoscandium complexes in the presence of trimethylphosphine. Of particular interest was the question whether scandium alkyl complexes with  $\beta$ -branches--which most closely resemble the structures of actual polymerization intermediates--dimerize appreciably upon phosphine loss. In addition, we wished to establish the accessibility of bis(phosphine) adducts. These two questions bear directly upon the validity of **1** as an intermediate and upon the proper formulation of the rate law for polymerization.

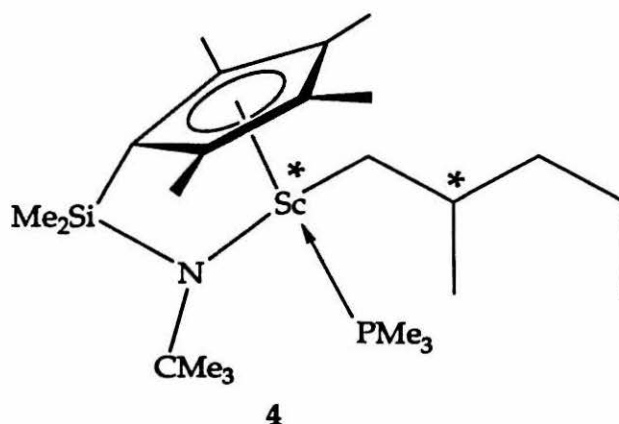
**Figure 1b. Dependence of Polymerization Rate on Catalyst Concentration, with Restored Data Points.**



## II. RESULTS

### Variable-Temperature $^1\text{H}$ -NMR Spectroscopy of **4**

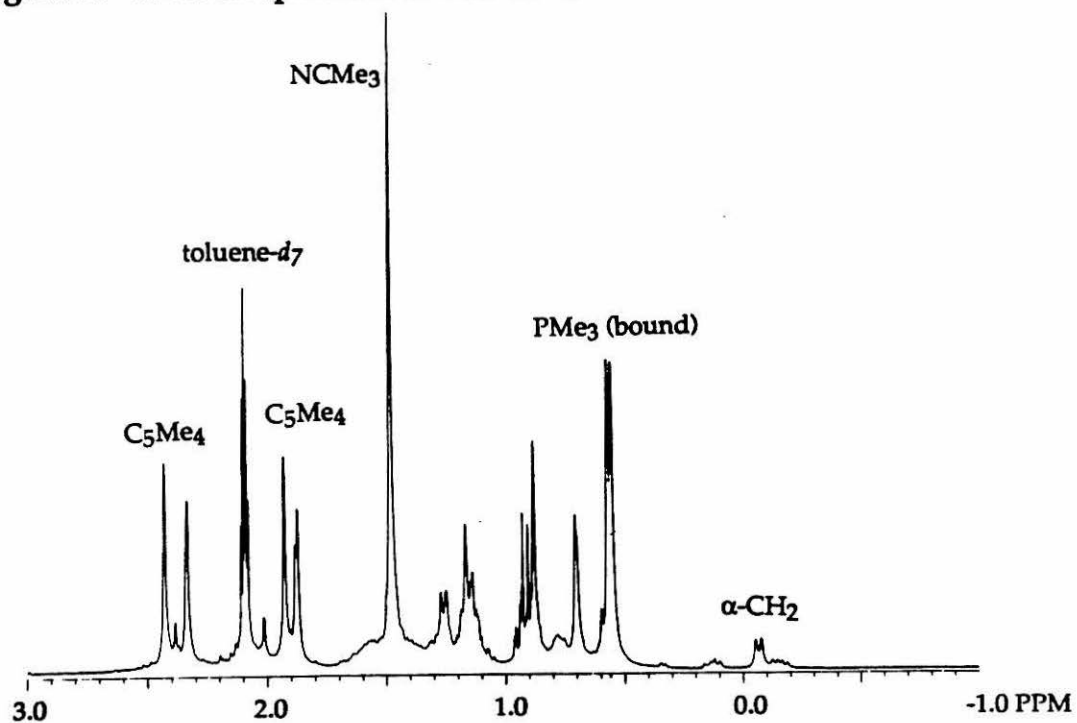
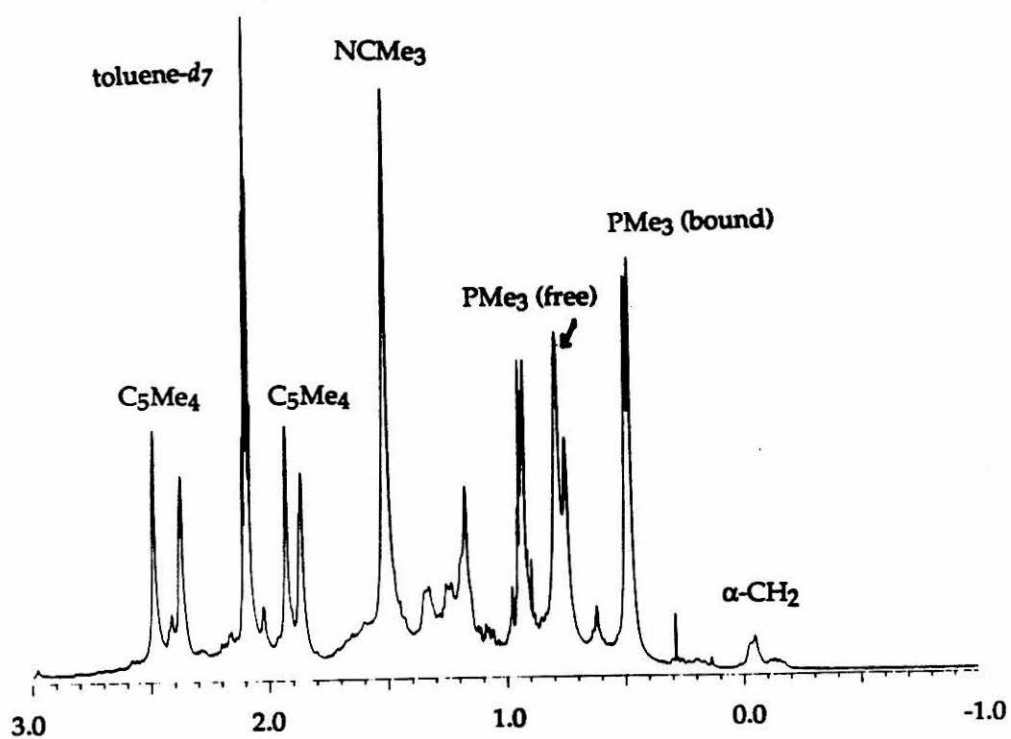
( $\text{Cp}^*\text{SiNR}$ ) $\text{Sc}[\text{CH}_2\text{CH}(\text{CH}_3)\text{CH}_2\text{CH}_2\text{CH}_3][\text{P}(\text{CH}_3)_3]$  (**4**) was chosen to model an active polymerization site, as its structure is that which would result from reaction of two molecules of propylene with scandium hydride **3**. The preparation of **4** by treatment of **3** with two equivalents of 2-methylpentene has been reported.<sup>1b</sup>



$^1\text{H}$ -NMR spectra of **4** were recorded between  $+75^\circ\text{C}$  and  $-80^\circ\text{C}$ . Figure 2 shows representative spectra at three different temperatures. Shapiro noted that

in the low-temperature limit **4** exists as a diastereomeric pair of complexes, presumably phosphine-bound monomers, in approximately equal amounts. As shown in the illustration above, **4** contains stereogenic scandium and carbon centers, and thus should exist as two diastereomers. This observation was corroborated by the present work. No resonances due to free trimethylphosphine or a phosphine-free scandium species could be detected in the complicated  $^1\text{H}$  spectrum.

As the temperature is raised above the slow-exchange limit, the resonances of the various ligands undergo characteristic changes. The trimethylphosphine doublet broadens, migrates downfield toward the chemical shift expected for free  $\text{PMe}_3$ , and then sharpens again. At no time can separate resonances for free and bound  $\text{PMe}_3$  be distinguished in the proton spectra. The methylene group directly bound to scandium shows a second-order  $\text{AA}'\text{X}$  pattern in the fast-exchange limit due to coupling between the two diastereotopic methylene protons and the adjacent methine proton. No coupling to phosphorus is observed. In the slow-exchange limit, two distinct methylene patterns appear, presumably one for each diastereomer. One of these is again an  $\text{AA}'\text{X}$  pattern; the second is a doublet, possibly due to an accidental degeneracy of chemical shift for the A and A' protons. Alternatively, the second diastereomer may still exhibit dynamic behavior at -80 K. The  $\text{Cp}^*\text{SiNR}$  ligand resonances in one diastereomer also display apparent accidental degeneracies in the slow-exchange spectra, both in the tetramethylcyclopentadienyl region and in the dimethylsilyl region. It is unlikely that the "second diastereomer" giving rise to these symmetrical patterns is actually a bis(phosphine) complex.  $^{13}\text{C}\{^1\text{H}\}$ -NMR spectroscopy of the phosphine carbons (vide infra) reveals a pair of diastereomers as well. The phosphine methyl carbon chemical shifts are almost identical; a bis(phosphine) complex would be expected to show a very different chemical shift for the phosphine carbons than a (mono)phosphine complex. The following section presents further evidence supporting the conclusion that neither of the major species observed in the proton spectra is a bis(phosphine) adduct.

**Figure 2.**  $^1\text{H}$ -NMR spectrum of **4** at  $-60^\circ\text{C}$ **Figure 3.**  $^1\text{H}$ -NMR spectrum of **4** + 1 equivalent  $\text{PMe}_3$  at  $-85^\circ\text{C}$ 

### Variable Temperature NMR Spectroscopy of 4 with Excess Phosphine

The  $^1\text{H}$ -NMR spectra of **4** were obtained in the presence of one additional equivalent of trimethylphosphine, again between +75 °C and -80 °C. Figure 3 shows the spectra obtained at the high and low temperature extremes. In the slow-exchange limit, the species observed are the same which appear in the absence of added phosphine. In addition, the high-temperature spectrum in Figure 2 is notable in that the fast exchange limit is not reached for all resonances, although the presence of additional phosphine is known to increase the rate of phosphine exchange.<sup>8</sup>

### **Measurement of Phosphine-Dissociation Equilibria**

These proton spectra are extremely complex. Most resonances overlap with their nearest neighbors, making accurate integrations impossible. Furthermore, we are not able to observe resonances unambiguously attributable to both a free and a bound form, either of phosphine or of the scandium-alkyl moiety. Accordingly, we opted to use  $^{13}\text{C}$ -NMR of appropriately labeled compounds for the purpose of measuring phosphine dissociation and/or dimerization equilibria. We expected that the larger chemical shift range of  $^{13}\text{C}$  (vis-a-vis  $^1\text{H}$ ) would allow us to completely freeze out the dynamic behavior of the system, and that the greatly simplified spectra resulting from the use of the labeled compounds would allow us to observe and integrate resonances arising from both free and bound trimethylphosphine and scandium complexes.

#### **(i) $(\text{Cp}^*\text{SiNR})\text{Sc}[\text{CH}_2\text{CH}(\text{CH}_3)\text{CH}_2\text{CH}_2\text{CH}_3][\text{P}(^{13}\text{CH}_3)_3]$ (**4- $^{13}\text{C}_3$** )**

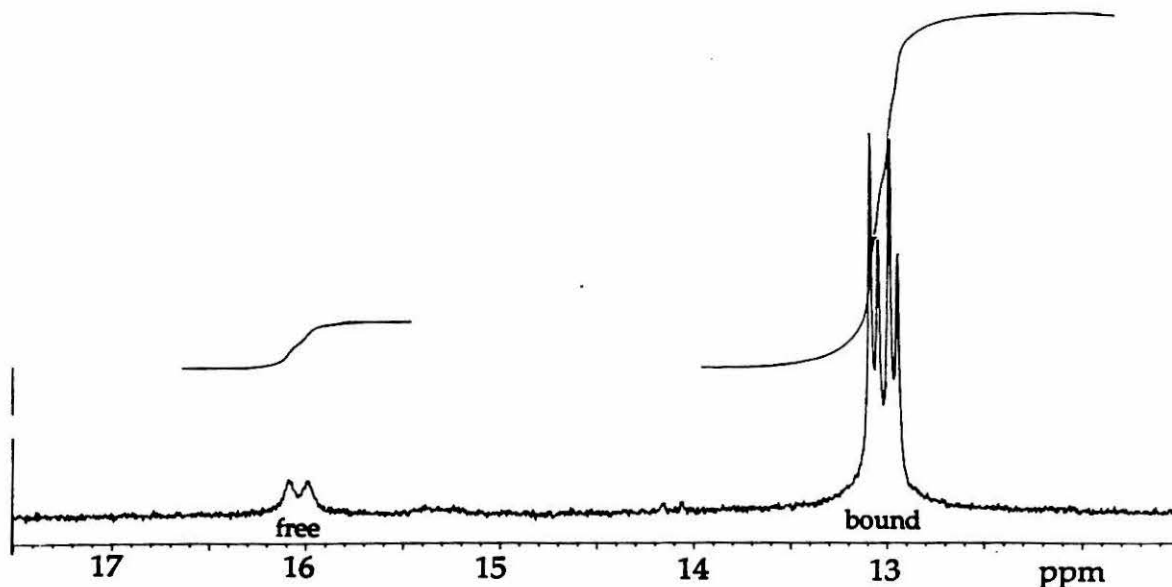
We chose first to examine the phosphine dissociation equilibrium in isolation from dimerization processes, by placing a carbon label exclusively on the phosphine. While this approach renders all phosphine-free complexes spectroscopically silent, it has the advantage that the  $^{13}\text{C}$  chemical shift of free phosphine can be independently determined. Resonances for free and bound phosphine can thus be assigned unambiguously in the variable-temperature spectra.

The  $^1\text{H}$  spectrum of **4- $^{13}\text{C}_3$**  is complicated but the strongly  $^{13}\text{C}$ -split pattern of the labeled phosphine is clearly visible. The 125 MHz  $^{13}\text{C}\{^1\text{H}\}$ -NMR



spectrum at room temperature shows only one broadened resonance for the phosphine methyl carbons. At low temperatures, however, free phosphine is clearly resolved 3 ppm downfield from the scandium-bound form. As shown in Figure 4, the bound phosphine carbons appear as two  $^1\text{J}_{\text{P-C}}$  doublets, providing further evidence that two diastereomers are present in roughly equal amounts.<sup>9</sup>

Figure 4. 125 MHz  $^{13}\text{C}\{^1\text{H}\}$ -NMR Spectrum of 4- $^{13}\text{C}_3$  (0.042 M) at 200 K.

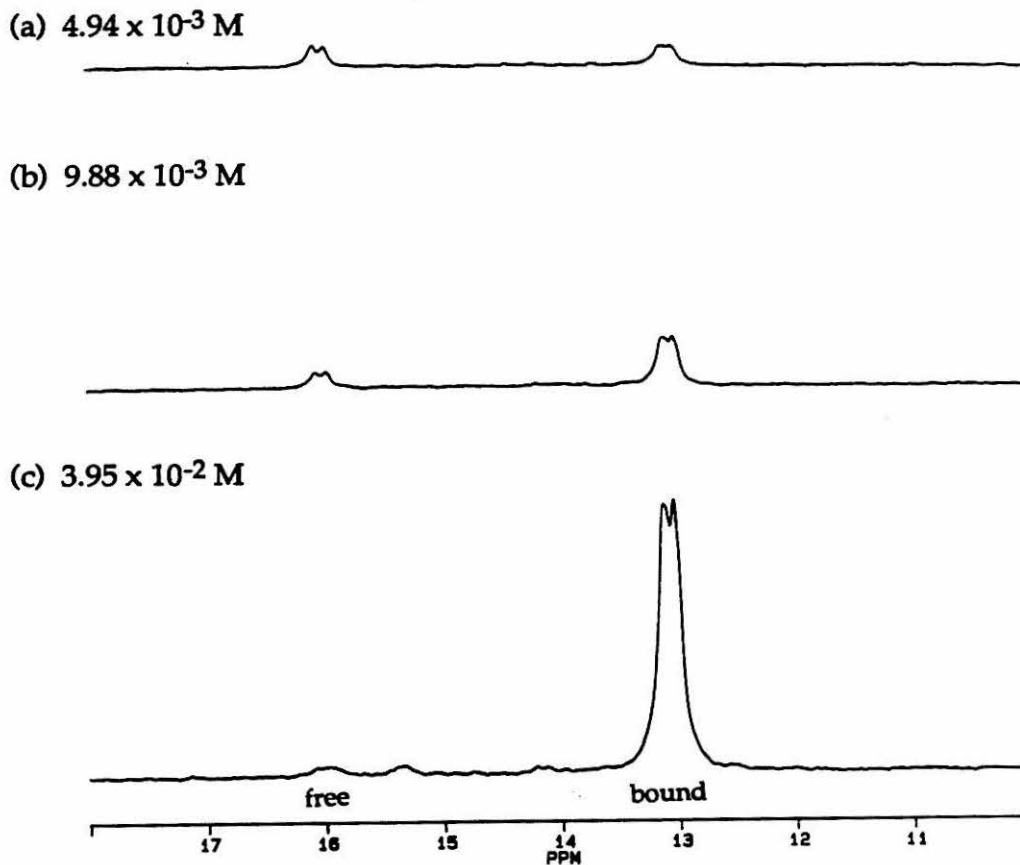


At a total scandium concentration of 0.04 M, the resonances due to free and bound phosphine are clearly resolved between 185 K and 220 K, though toward the high end of this temperature range the weaker signal of free phosphine already shows considerable broadening. The equilibrium composition of 10% free phosphine ( $[\text{PMe}_3]_{\text{free}} = 5 \text{ mM}$ ) to 90% bound phosphine ( $[\text{PMe}_3]_{\text{bound}} = 38 \text{ mM}$ ) does not vary significantly over this 35 K range. Because of this weak temperature dependence and the experimentally circumscribed temperature range, these data do not allow precise extrapolation of equilibrium behavior at typical polymerization temperatures, e.g., room temperature or above. However, the spread in the data over the given temperature range can be used to estimate an upper limit to the change in equilibrium constant between the experimentally accessible region and 298 K. Whether they are calculated assuming a monomeric or dimeric formulation for the phosphine-free scandium alkyl, equilibrium constants change by about a factor of two. The relation

$$\ln K_{\text{eq}} \propto 1/T$$

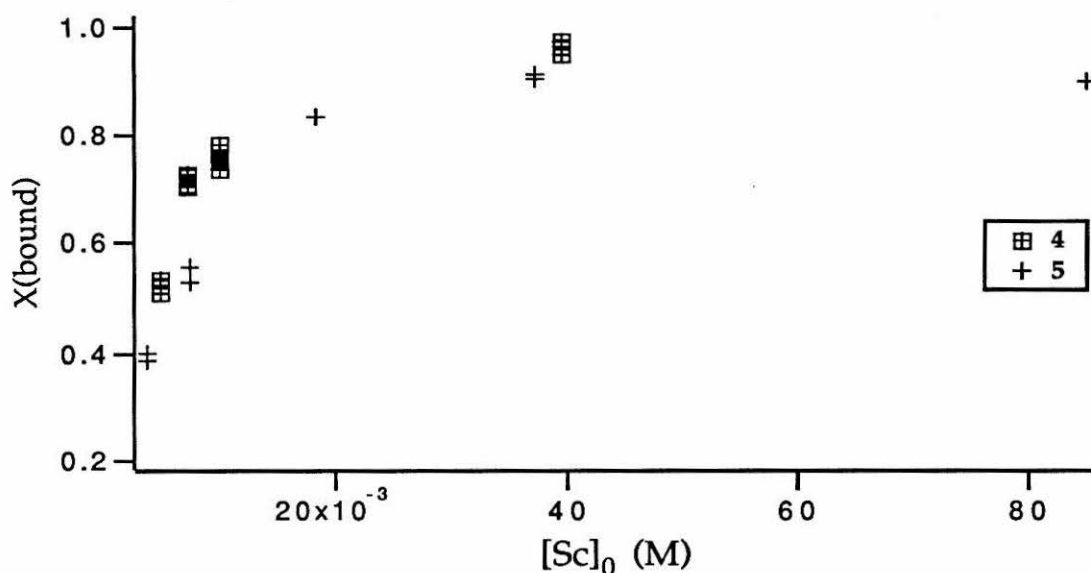
implies a change in  $K_{\text{eq}}$  of less than an order of magnitude between 200 and 298 K.

**Figure 5. 125 MHz  $^{13}\text{C}\{^1\text{H}\}$ -NMR Spectra for  $4\text{-}^{13}\text{C}_3$  in Dilute Solution at 200 K.**



The concentration dependence of the equilibrium composition of  $4\text{-}^{13}\text{C}_3$  in solution was examined using samples prepared by sequential dilutions of a stock solution. Representative spectra appear in Figure 5. The two diastereomeric phosphine doublets are not resolved in these spectra due to a combination of lower-quality shims and application of a 5 Hz line-broadening exponential. As can be seen in the data plotted in Figure 6 the fractional population of bound phosphine shows a strong dependence on  $[\text{Sc}]_0$ .

**Figure 6. Equilibrium Composition of Phosphine-Bound Scandium Alkyl Complexes as a Function of Total Scandium Concentration.**



(ii)  $(\text{Cp}^*\text{SiNR})\text{Sc}({}^{13}\text{CH}_2\text{CH}({}^{13}\text{CH}_3)_2 \cdot \text{P}(\text{CH}_3)_3)$  ( $5\text{-}^{13}\text{C}_3$ )

More direct information about the solution dynamics of the organometallic moiety was obtained via incorporation of a  $^{13}\text{C}$  label into an alkyl ligand at scandium. The isobutyl ligand in  $5\text{-}^{13}\text{C}_3$  was chosen primarily for ease of synthesis of the labeled olefin precursor, and for its close resemblance to the 2-methylpentyl group. In addition, the diastereotopic  $\gamma$ -methyl groups provided useful information about the symmetry of the complexes in solution.

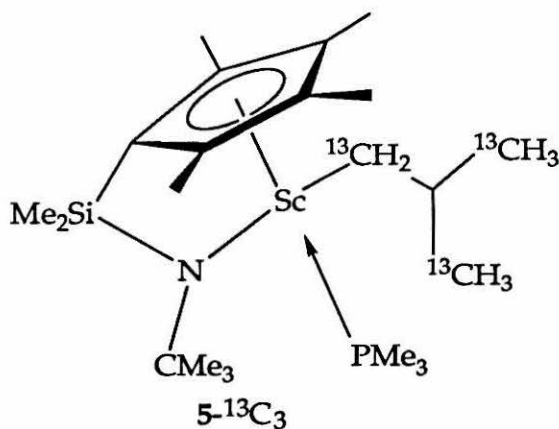
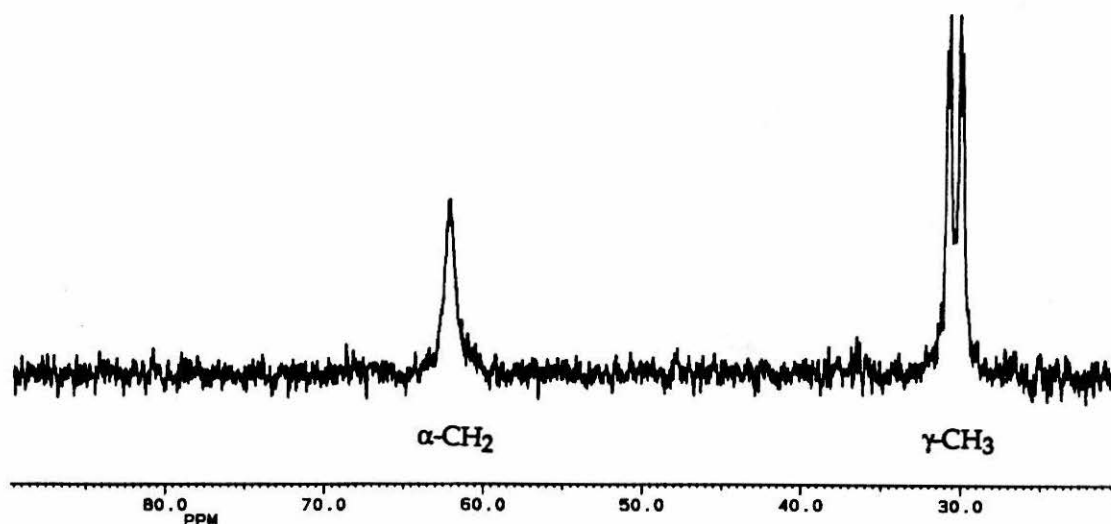


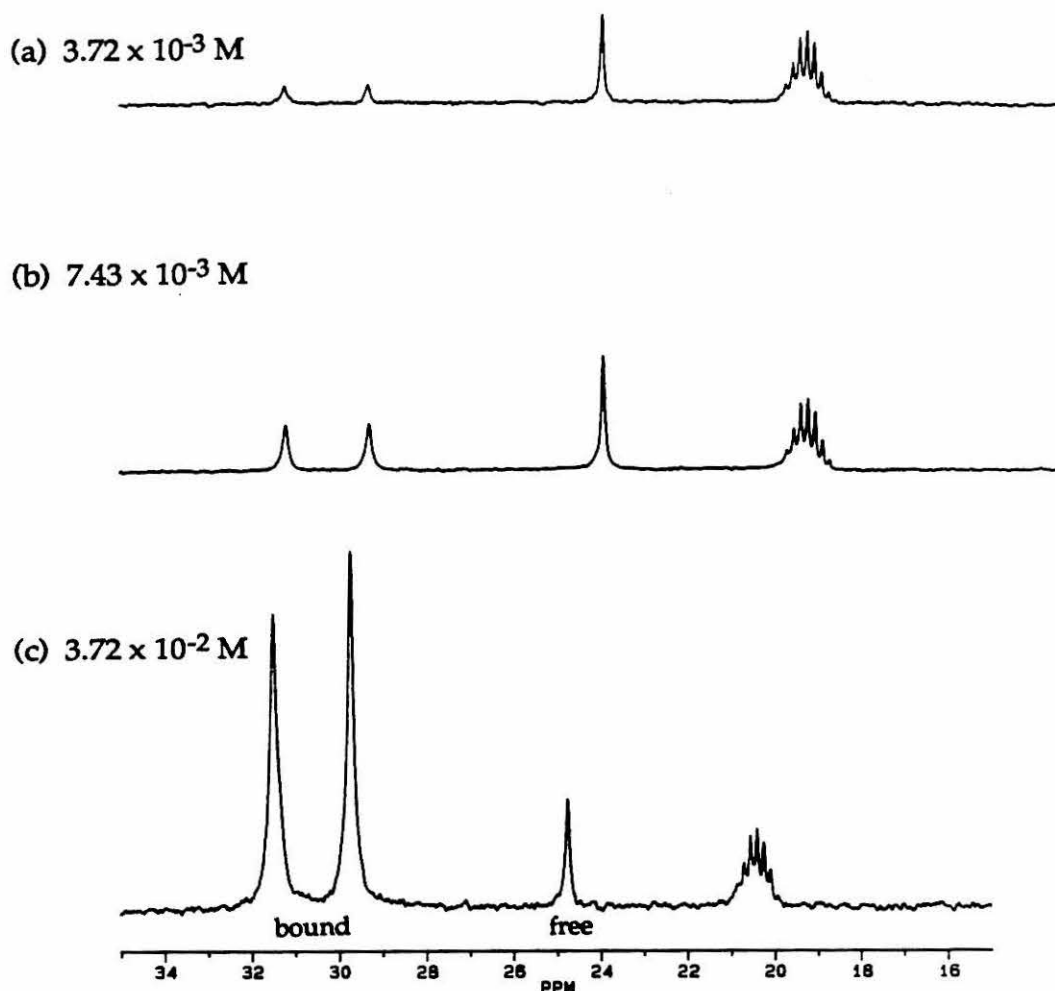
Figure 7. 125 MHz  $^{13}\text{C}\{^1\text{H}\}$ -NMR Spectrum of 5- $^{13}\text{C}_3$  at Room Temperature



The room temperature 125 MHz  $^{13}\text{C}\{^1\text{H}\}$ -NMR spectrum of this compound is shown in Figure 7. Because the tetracoordinate scandium is stereogenic, the labeled methyl carbons are diastereotopic in the phosphine-bound form. They appear as a pair of doublets (the smaller coupling is due to  $^3\text{J}_{\text{C-C}}$ ). The position of the  $\alpha$ -carbon is similar to that observed for other carbons bound to scandium. In dilute solutions at 200 K, a single additional resonance in the  $\gamma$ -carbon region is cleanly resolved, ca. 7 ppm upfield of the original pair of doublets ( $^3\text{J}_{\text{C-C}}$  coupling is not observed in these spectra due to the application of line-broadening). No corresponding  $\alpha$ -carbon resonance is observed. Figure 8 shows representative low-temperature spectra over the concentration range of interest.

By monitoring the  $\gamma$ -carbon resonances, a concentration profile of equilibrium composition for the isobutyl complex was constructed. Figure 6 shows the data for this (alkyl-labeled) complex alongside those for the (phosphine-labeled) 2-methylpentyl complex 4- $^{13}\text{C}_3$ . Agreement between these two structurally similar complexes is quite good.

**Figure 8. 125 MHz  $^{13}\text{C}\{^1\text{H}\}$ -NMR Spectra of  $5\text{-}^{13}\text{C}_3$  in Dilute Solution at 200 K.**



(iii)  $(\text{Cp}^*\text{SiNR})\text{Sc}(\text{CH}_2\text{CH}_2\text{CH}_3) \cdot \text{P}(^{13}\text{CH}_3)_3$  ( $6 \cdot \text{P}(^{13}\text{CH}_3)_3$ )

Because the propyl derivative **6** is isolated as a phosphine-free dimer, dimer formation must play an important role in the solution dynamics of this compound. With the hope of observing an illuminating difference between the equilibrium behavior of this complex vis-a-vis the 2-methylpentyl and isobutyl species discussed above, low-temperature  $^{13}\text{C}$ -NMR spectra of solutions of  $[(\text{Cp}^*\text{SiNR})\text{Sc}(\text{CH}_2\text{CH}_2\text{CH}_3)_2]$  in the presence of two equivalents of  $\text{P}(^{13}\text{CH}_3)_3$  (that is, one equivalent of phosphine per equivalent of scandium) were obtained.

Phosphine exchange for  $6 \cdot \text{PMe}_3$  is more rapid than for the 2-methylpentyl complex. At  $4 \times 10^{-2} \text{ M}$ , the  $^{13}\text{C}$ -NMR resonances due to free and bound

phosphine in the former system coalesce at  $\approx 240$  K, as opposed to 295 K for the latter. Even at lower concentrations, the two NMR signals are not baseline resolved, nor is the coupling constant  $^1J_{C-P}$  observed. Representative spectra appear in Figure 9. Regrettably, this broadening compromises the accuracy of NMR integrations. Nevertheless, reliable integrations were obtained by repeated cutting and weighing of the appropriate peaks. The data are plotted in Figure 10, alongside those for the  $\beta$ -branched alkyl complexes for comparison.

**Figure 9: 125 MHz  $^{13}C\{^1H\}$ -NMR Spectra for  $6 \cdot P(^{13}CH_3)_3$  at 200 K.**

(a)  $2.95 \times 10^{-3}$  M



(b)  $1.58 \times 10^{-2}$  M

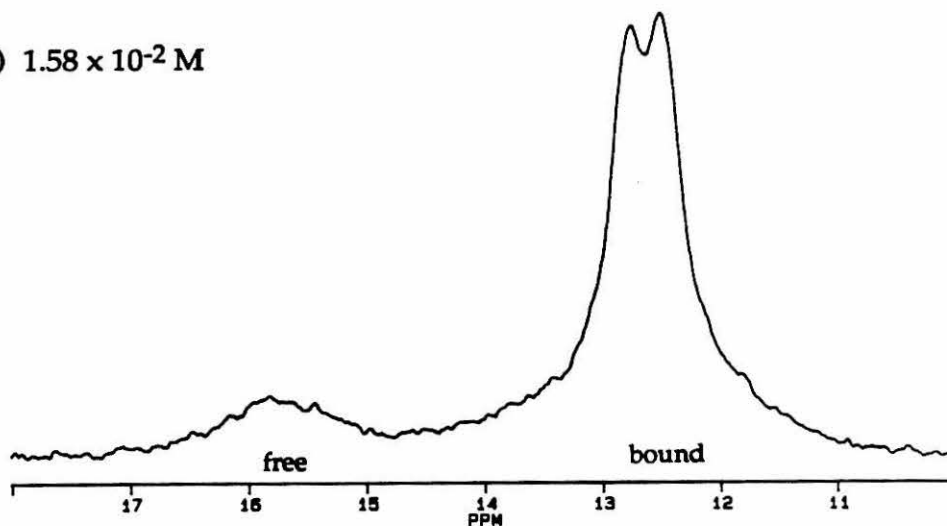
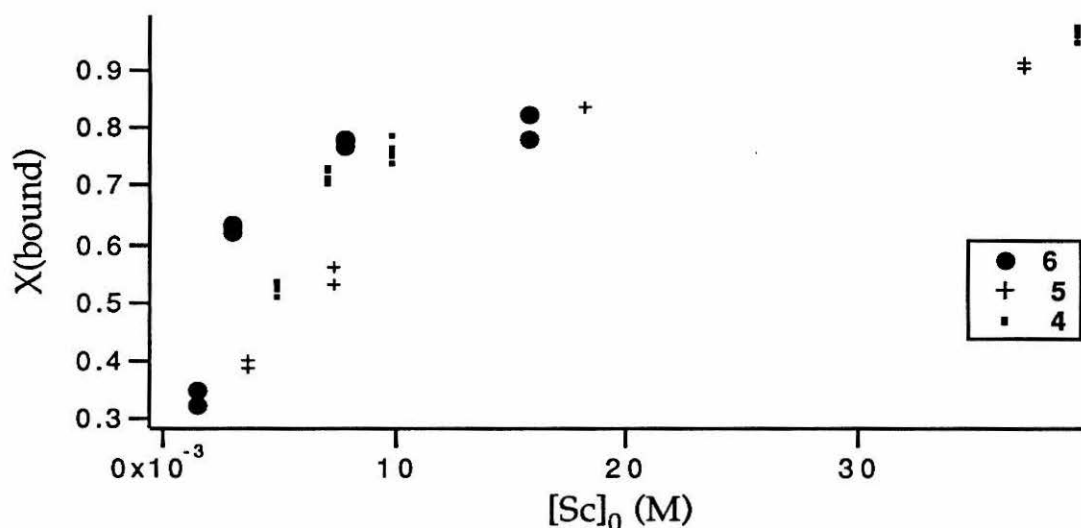


Figure 10. Equilibrium Composition of Phosphine-Bound Scandium Propyl Complex as a Function of Total Scandium Concentration



### III. DISCUSSION

Ultimately, it must be admitted that precise description of the solution behavior of these extremely electronically and sterically unsaturated complexes has eluded both kinetic and equilibrium analysis. However, several important aspects of these solution dynamics have been sorted out with some measure of confidence. The predominant equilibrium is one between a phosphine-bound scandium alkyl and a monomeric, phosphine-free scandium alkyl. The implications for the mechanism of  $\alpha$ -olefin polymerization by  $(\text{Cp}^*\text{SiNR})\text{ScR}'$  complexes is clear: the chain-propagating species is monomeric.

The simplest of the questions this work addresses is that of the importance of a bis(phosphine) adduct. A stable bis(phosphine) adduct is required to explain phosphine inhibition of polymerization *via* chain propagation from a phosphine-bound complex. In contrast to Jordan's observations for cationic zirconocene derivatives, we find no evidence for such a species in our system. This reaction pathway is thus effectively eliminated. The prior observation that phosphine exchange is associative for the scandium complexes indicates that the bis(phosphine) structure is accessible only as a transition state, not as a stable intermediate.

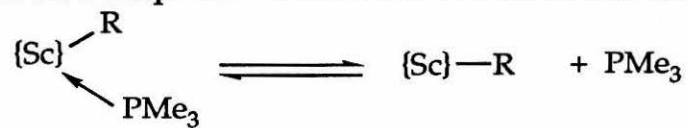
This result is in accord with observations of Jordan and co-workers for cationic zirconocene catalysts.<sup>5a</sup> Cations of general structure  $[\text{Cp}_2\text{Zr-R(PMe}_3)]^+$  undergo associative phosphine exchange. However, while bis(phosphine) adducts  $[\text{Cp}_2\text{Zr-R(PMe}_3)_2]^+$  can be isolated for sufficiently small R groups (hydride, methyl), no such adducts are observed with zirconium alkyl substituents larger than methyl.<sup>10</sup> A transient bis(phosphine)adduct can be observed for the phenyl derivative. For the zirconium compounds as for the scandium compounds described in this work, bis(phosphine) adducts of the higher alkyls are presumably destabilized by steric crowding.

The more difficult questions involve the behavior of the mono(phosphine) and phosphine-free complexes. Phosphine is obviously a competent ligand in this system, and phosphine coordination may be presumed to deactivate a catalytic center. Is phosphine coordination the only pathway to a dormant catalyst molecule, or does dimerization also compete with propagation? Going further, one could ask, is the dimer in fact the favored species in solution? Is it perhaps necessary to consider the dimer--instead of or in addition to the monomer--as the propagating intermediate?

Schemes II and III illustrate the two extreme equilibrium situations. In Scheme II, a phosphine-supported, monomeric scandium alkyl complex dissociates to free ligand and a "naked," monomeric alkyl complex, with a dissociation constant  $K_m$ . In Scheme III, the same initial complex dissociates to form a molecule of free ligand and one half of an alkyl bridged dimer analogous to the solid-state structure observed for the propyl derivative. This process is governed by dissociation constant  $K_d$ . Both of these are simplifications of the coupled equilibrium situation shown in Scheme IV, in which the initial complex undergoes phosphine dissociation yielding a "naked" alkyl complex which, in the reverse reaction, is competitively trapped by free ligand ( $K_1$ ) or by itself, forming the dimeric structure ( $K_2$ ).

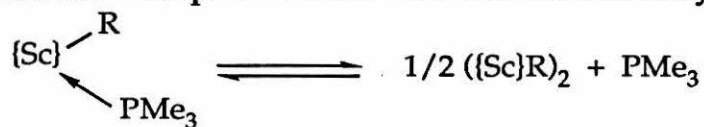


**Scheme II. Phosphine Dissociation to Monomeric Alkyl Complex.**



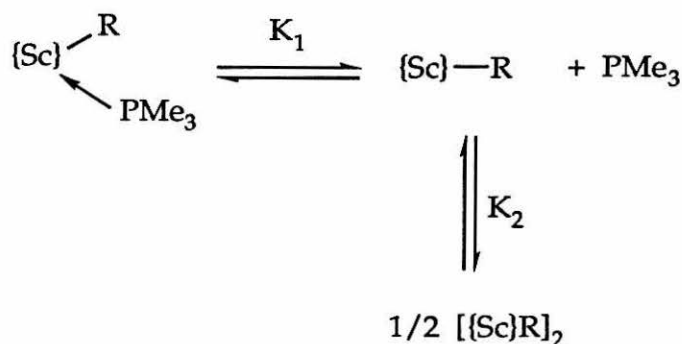
$$K_m = \frac{[\{\text{Sc}\}\text{R}] [\text{PMe}_3]}{[\{\text{Sc}\}\text{R}(\text{PMe}_3)]}$$

**Scheme III. Phosphine Dissociation to Dimeric Alkyl Complex.**



$$K_d = \frac{[(\{\text{Sc}\}\text{R})_2]^{1/2} [\text{PMe}_3]}{[\{\text{Sc}\}\text{R}(\text{PMe}_3)]}$$

**Scheme IV. Phosphine Dissociation with Coupled Dimerization  
Equilibrium.**



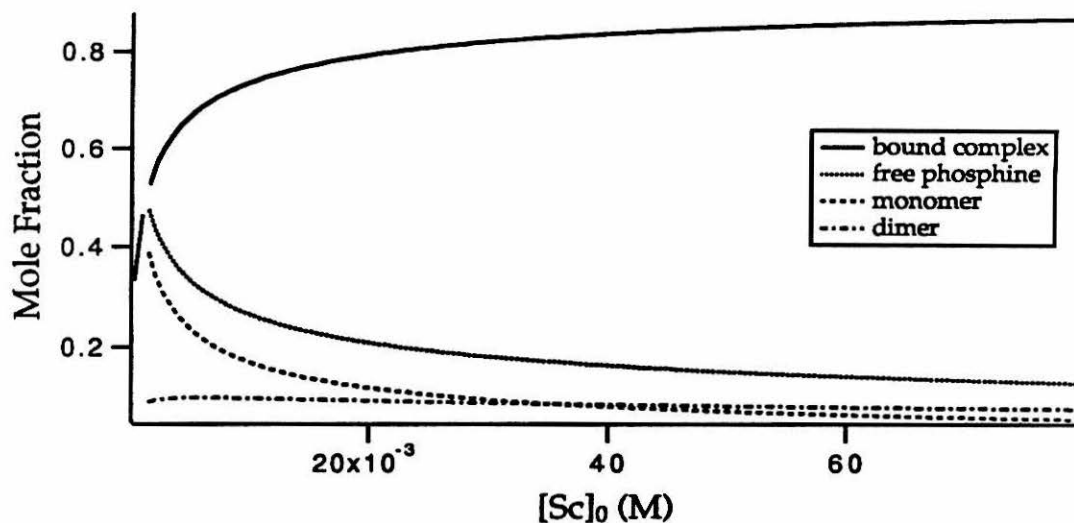
$$K_1 = \frac{[\{\text{Sc}\}\text{R}][\text{PMe}_3]}{[\{\text{Sc}\}\text{R}(\text{PMe}_3)]} ; K_2 = \frac{[[\{\text{Sc}\}\text{R}]_2]^{1/2}}{[\{\text{Sc}\}\text{R}]}$$

One relevant feature of the branched alkyl complexes 4 and 5 which is immediately striking is that, in contrast to the straight-chain alkyl derivatives  $[(\text{Cp}^*\text{SiNR})\text{Sc}(\text{CH}_2\text{CH}_2\text{CH}_3)_2]$  (6) and  $[(\text{Cp}^*\text{SiNR})\text{Sc}(\text{CH}_2\text{CH}_2\text{CH}_2\text{CH}_3)_2]$  (7), these are isolated as phosphine adducts. The procedure previously reported<sup>1b</sup> for the isolation of 4 omits a crucial step included in the work-up procedures reported for 6. The latter two are dissolved in petroleum ether and evaporated to dryness several times before finally being recrystallized. If this step is not performed, significant amounts of phosphine can be retained in the isolated product. That this step is not reported for the isolation of 4 raises the question whether the retention of phosphine in this complex is adventitious or intrinsic. Therefore, in preparing 4 and 5 for the work reported here, care was taken to follow precisely the procedures responsible for complete phosphine removal from 6. Even when the branched alkyl complexes are repeatedly dissolved and evaporated to dryness before isolation, one equivalent of trimethylphosphine is retained in the isolated product. To put it another way, 6 is capable of releasing phosphine and dimerizing on the preparative time-scale, whereas 4 and 5 are not. This difference could be attributed to either a larger phosphine binding constant or a smaller dimerization constant for the branched alkyl complexes with respect to their linear counterparts. A priori, the latter explanation makes

the most sense as one would expect the relative bulk of the branched alkyls to exacerbate steric crowding about the dimeric core and, perhaps, to discourage phosphine binding.

Shapiro's kinetic investigations suggested that phosphine dissociation and dimerization processes were competitive. Estimates for the equilibrium constants in Scheme III, obtained from kinetic measurements of monomer uptake, were reported ( $K_1 = 0.0006$  and  $K_2 = 13$ ).<sup>11</sup> Using these values it is possible to construct a profile of the expected equilibrium compositions of all species (bound complex, free phosphine, monomer and dimer) as functions of the overall scandium concentration  $[\text{Sc}]_0$  (for calculations, see Appendix). These are plotted in Figure 11 as the mole fractions of scandium in each form (allowing for two moles of scandium per mole of dimer).

Figure 11. Equilibrium Compositions Predicted from Kinetic Studies.<sup>12</sup>



If these predictions are accurate, both the monomer and the dimer are expected to be present in nearly equivalent amounts in an experimentally accessible range of  $[\text{Sc}]_0$  (20 to 40 x mM). In this range, they can be expected to account for roughly 15-20% of the total scandium present and thus should be observable by NMR, given a spectroscopic handle (e.g., a  $^{13}\text{C}$  label) on one of the ligands at scandium. In fact, for 5- $^{13}\text{C}_3$  only two species are observed—one

appearing as a 1:1 pair of  $\gamma$ -carbon resonances at 31.48 and 29.71 ppm, the other as a single resonance at 24.74 ppm. This observation excludes a series of coupled equilibria (Scheme IV) and indicates the operation of a single equilibrium process (Scheme II or III).

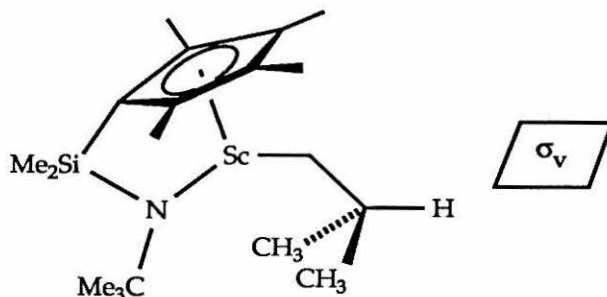
The 1:1 set of resonances is unambiguously assigned to the phosphine-bound alkyl complex. The  $\gamma$ -carbons are inequivalent as expected. More importantly, the dependence of the amount of this species on  $[\text{Sc}]_0$  correlates well with the amount of bound phosphine in studies of 4- $^{13}\text{C}_3$ .

The appearance of a single resonance for the  $\gamma$ -carbons of the phosphine-free species suggests that it is a monomer. As Scheme Va shows, the monomeric complex possesses a mirror plane which makes these methyl groups strictly equivalent. The most likely form for a putative dimer to take is that shown in Scheme Vb, with a trans-oid arrangement of  $\text{Cp}^*\text{SiNR}$  ligands about the dimeric core, as has been observed in the crystal structure of 6. Two rotamers are drawn: one with  $C_i$  and one with  $C_s$  symmetry. Neither of these symmetry elements relates the methyl groups labeled **a** and **b** to one another. The isobutyl methyl groups are thus diastereotopic in a dimeric isobutyl complex, and should display two distinct NMR resonances. Thus, the simplest explanation for the observation that only one resonance appears for the  $\gamma$ -methyl groups in the phosphine-free complex is that this species is monomeric.

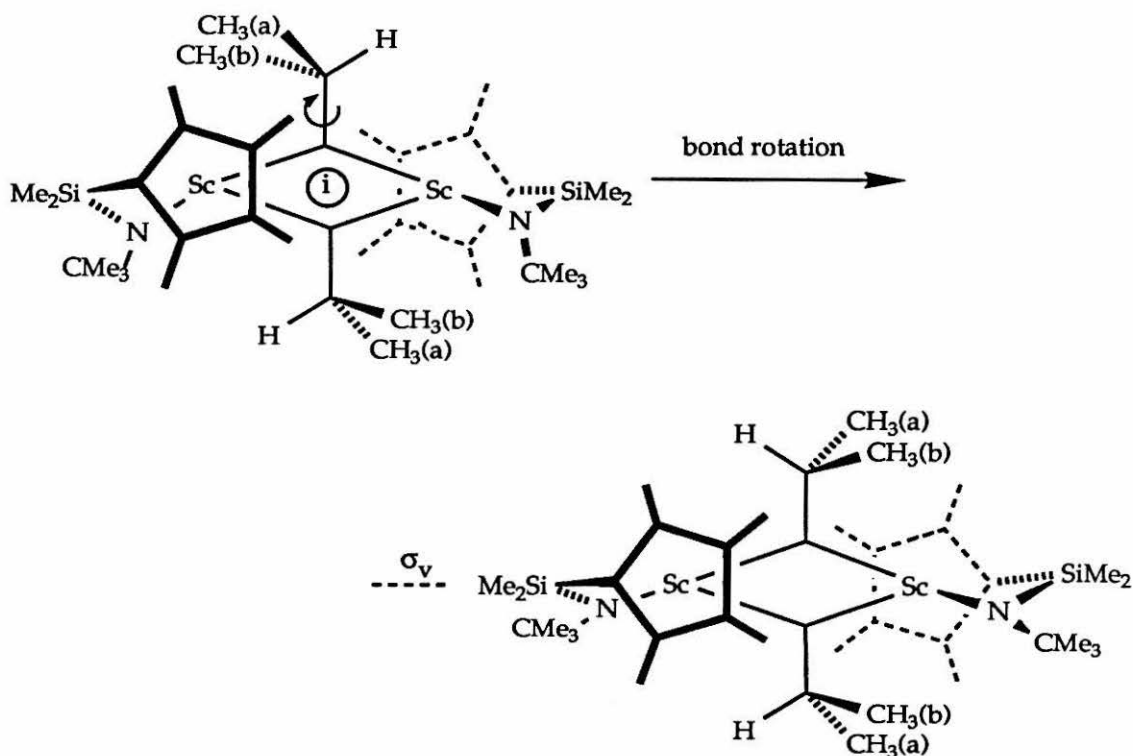
It is possible that this single resonance actually belongs to a dimer in which the diastereotopic methyl groups rapidly equilibrate. This requires that the dimeric unit break apart and reassemble after rotation about the  $\text{C}\beta\text{-C}\gamma$  bond—which again implies a series of coupled equilibria with the attendant prediction that an additional monomeric species should be observed. Finally, it must be recognized that accidental degeneracy of formally inequivalent carbons is always a possibility.

### Scheme V. Symmetry Properties of Phosphine-free Isobutyl Complexes.

(a) Equivalency of isobutyl methyl groups in monomer.



(b) Inequivalency of isobutyl methyl groups in dimer.



The absence of an  $\alpha$ -carbon resonance for the phosphine-free complex indicates a relatively strong coupling to the adjacent, quadrupolar scandium nucleus. It follows that the phosphine-free alkyl is more symmetric than the

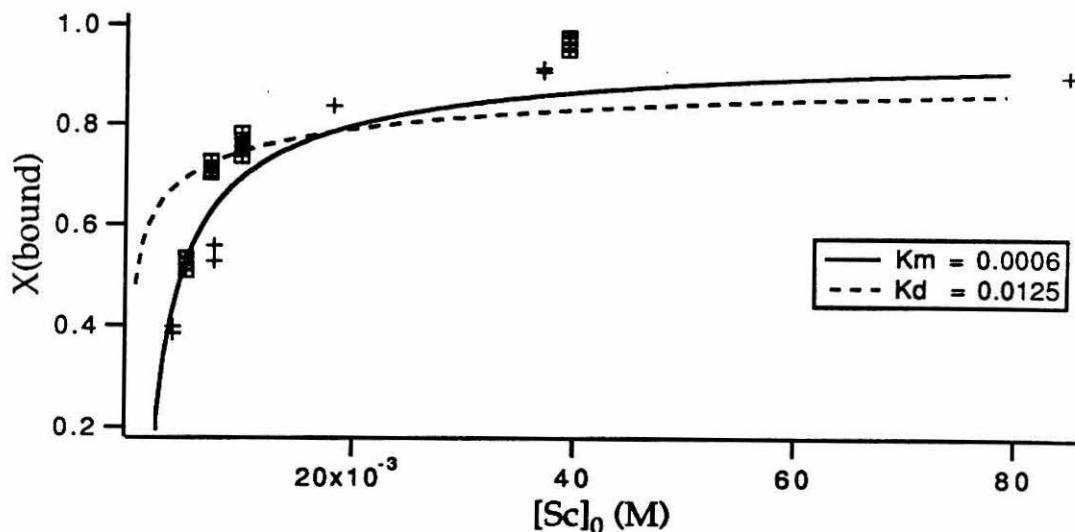
bound complex. As Scheme V shows, both the dimer and the monomer are of higher symmetry than the phosphine-bound form, so this observation is consistent with either formulation. One would expect coupling between scandium and a terminal carbon to be stronger than to a bridging carbon and, indeed, the  $\alpha$ -carbon resonance of the propyl dimer **6** (in the absence of phosphine) is clearly visible at  $\delta$  50.5. Thus, while it is not a strong criterion, the missing  $\alpha$ -carbon resonance is more consistent with a monomeric than a dimeric formulation for the phosphine-free form of **5**.

Interpreting the quantitative aspects of these NMR studies is a less straightforward matter. Our original intention was to compare the observed phosphine dissociation behavior with the equilibrium expressions in Schemes II-IV, hoping that one of these would describe the data much better than the other two. This did not prove to be the case and, perhaps not surprisingly, we were faced with much the same dilemma presented by the kinetic studies. Namely, it appeared that the mechanistic issues which most concerned us predicted very subtle differences in our observables. Variance in the NMR data was such that simply calculating equilibrium constants ( $K_m$  or  $K_d$ ) provided no clear distinction--both were equally bad. Fortunately, in light of the arguments above, the less definitive equilibrium data take on a supportive rather than a central role in analyzing this system. In order to extract some information from them, we tried a more global, qualitative approach to the equilibrium data.

Routines similar to those used to construct Figure 11 (see Appendix) were used to calculate predicted concentration profiles for both monomeric ( $K_m$ ; Scheme I) and dimeric ( $K_d$ ; Scheme II) equilibrium expressions. The best visual fits obtained are shown alongside the data in Figure 12. As expected, neither expression provides a spectacular fit.<sup>13</sup> However, the overall fit to the  $K_m$  expression is significantly better than that to  $K_d$ , particularly with regard to matching the slope of the curve in the low-concentration regime with the asymptotic behavior observed in the high-concentration regime. This semi-quantitative model of equilibrium behavior is consistent with the interpretation offered above for the NMR properties of the phosphine-free complex--namely, that for these  $\beta$ -branched alkyl derivatives, the phosphine-free form of the complex in solution is predominantly, if not exclusively, monomeric. The best

estimate of  $K_m$  which we can then extract from these data is that in Figure 10:  $6(3) \times 10^{-4} \text{ M}$ .<sup>14</sup>

**Figure 12. Equilibrium Data for  $\beta$ -Branched Alkyl Complexes, Plotted with Fits to Monomeric (Scheme II) and Dimeric (Scheme III) Equilibrium Expressions.**

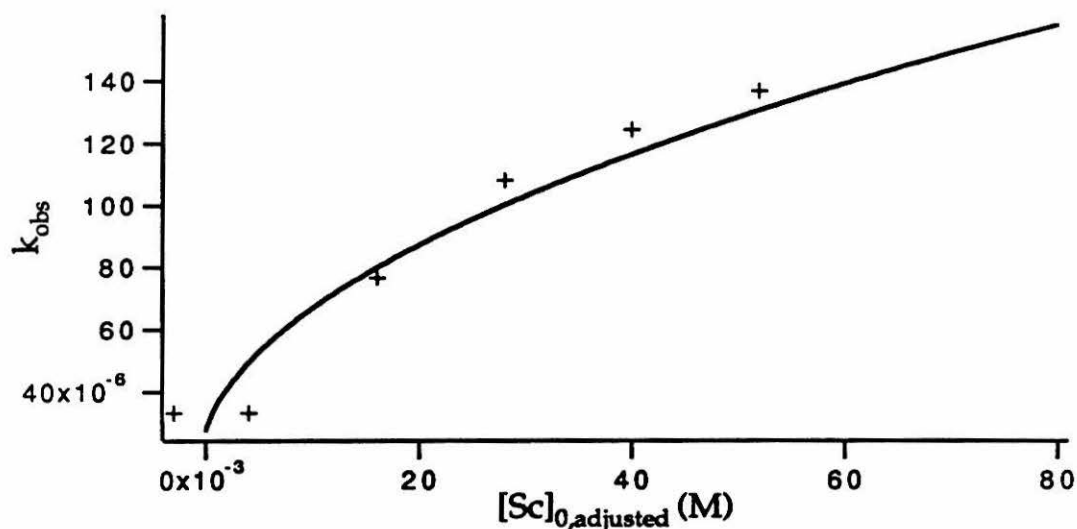


By extension of these studies of the simple  $\beta$ -branched alkyl complexes 4 and 5, it is concluded that the active intermediates in  $\alpha$ -olefin polymerization with  $(\text{Cp}^*\text{SiNR})\text{ScR}$  derivatives are twelve-electron monomers, and that—at least when phosphine is present—fourteen-electron, alkyl-bridged dimers are unlikely to affect polymerization chemistry, either as reactive intermediates or as inactive forms of the catalyst. In other words the "naked" alkyl is much more effectively trapped by phosphine than it is by itself. This notion is consistent with the more efficient donation expected from a phosphine lone-pair vis-a-vis a bridging  $\text{sp}^3$  carbon. These conclusions are at odds with those derived from the earlier kinetic work,<sup>15</sup> in which it was determined that dimerization processes should be competent to produce observable amounts of  $[(\text{Cp}^*\text{SiNR})\text{ScR}]_2$  at total scandium concentrations of ca.  $10^{-2} \text{ M}$ .

Figure 13 suggests one line of explanation for the apparent discrepancy. Contamination of the catalyst stock solution or diluent solvent (or both) from

which the samples in Shapiro's original kinetics experiments were prepared would result in generally lower  $[\text{Sc}]_0$  values than reported. The assumption that a plot of  $k_{\text{obs}}$  vs  $[\text{Sc}]_0$  should pass through the origin--which informs the construction of Figure 1b--would then be invalid. It would be fruitless to try to guess precisely how the reported  $[\text{Sc}]_0$  values should be altered. In Figure 13 they are merely shifted toward the origin. If it is also assumed that the values reported as [3] are actually representative of  $[\text{Sc}]_0$ , which introduces an error of a factor of two along the x-axis, a fit generated using a rate constant of  $0.018 \text{ M}^{-1}\text{sec}^{-1}$  (taken from reference 3) and a  $K_{\text{m}}$  of 0.0008 (estimated from this work) matches surprisingly well, suggesting that this may in fact be a reasonable explanation for the aberrant behavior shown in Figure 1a.

Figure 13. The Effect on Figure 1a of Altering  $[\text{Sc}]_0$ .



The equilibrium behavior of  $(\text{Cp}^*\text{SiNR})\text{Sc}(\text{CH}_2\text{CH}_2\text{CH}_3) \cdot \text{P}(\text{}^{13}\text{CH}_3)_3$  shows a somewhat different concentration profile than that of the  $\beta$ -branched alkyl complexes. In particular, although phosphine binding appears to approach the same approximate asymptote in the two cases,<sup>16</sup> the propyl complex binds phosphine more tightly at lower concentrations. This observation is consistent with the steric reasoning put forth above. The equilibrium composition (expressed as the mole fraction of bound trimethylphosphine) as a function of overall concentration is shown in Figures 14 and 15, along with fits obtained from the modelling routines.



Figure 14. Equilibrium Data for  $6 \cdot \text{P}(\text{}^{13}\text{CH}_3)_3$ , Plotted with Fits to Monomeric (Scheme II) and Dimeric (Scheme III) Equilibrium Expressions.

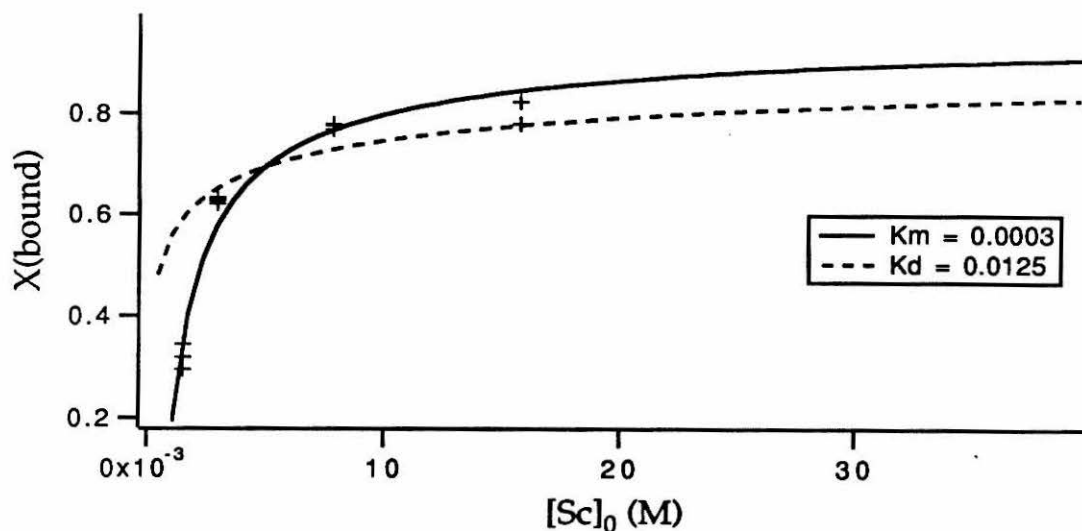
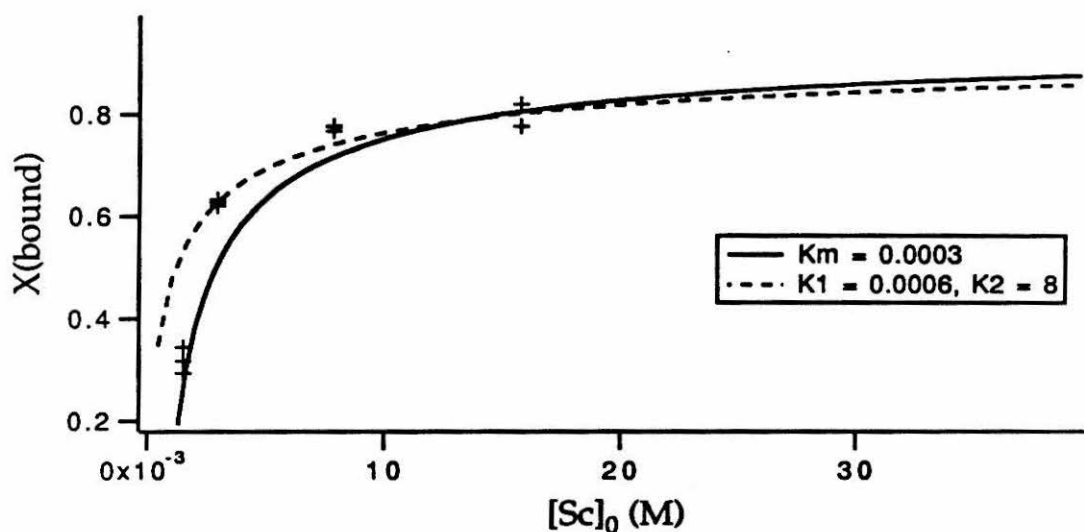


Figure 15. Equilibrium Data for  $6 \cdot \text{P}(\text{}^{13}\text{CH}_3)_3$ , Plotted with Fits to Monomeric (Scheme II) and Coupled (Scheme IV) Equilibrium Expressions.



Within reasonable limits set by the quality of the data, these phosphine dissociation equilibria are nearly equally well (or poorly) described by expressions assuming no dimerization and partial dimerization of the alkyl moiety upon phosphine loss. Somewhat surprisingly, given the preparative

chemistry of this compound, the least satisfactory fit is probably that derived from the dimeric equilibrium expression (Scheme III), though in the absence of data beyond  $[\text{Sc}]_0 = 2 \times 10^{-2} \text{ M}$ , it is hard to choose an appropriate value for the high-concentration asymptote. Although the propyl ligand does not carry the stereochemical information of an isobutyl ligand, studies of a derivative carrying a label on the propyl ligand would be of interest, if only to establish whether one or more phosphine-free species can be observed. Such studies would also allow for the examination of monomer/dimer equilibria in the absence of perturbing phosphine-dissociation processes.



Table I (continued).

| Compound/Conditions  | Assignment                                | $\delta$ (ppm)                                   | J (Hz)   |
|--|---|--|--|
| $4\text{-}^{13}\text{C}_3$ , continued   | $\alpha\text{-}^{13}\text{CH}_2$          | 0.05 -- 0.2<br>(br, m)                           |  |
|  | $\epsilon\text{-}^{13}\text{CH}_3$        | 1.05 (t)   | $^3J_{\text{H-H}} = 7.5$                                 |
| $4\text{-}^{13}\text{C}_3$<br>125 MHz $^{13}\text{C}$ , 200 K<br>$4.2 \times 10^{-2}$ M  | $\text{P}(^{13}\text{CH}_3)_3$<br>(free)  | 15.97<br>(br d)                                  | $^1J_{\text{P-C}} \approx 13$                            |
|  | $\text{P}(^{13}\text{CH}_3)_3$<br>(bound) | 12.96 (d)<br>12.92 (d)                           | $^1J_{\text{P-C}} = 12.63$<br>$^1J_{\text{P-C}} = 12.63$ |
| $\text{H}_2^{13}\text{C}=\text{C}(^{13}\text{CH}_3)_2$<br><br>75 MHz $^{13}\text{C}$   | $\text{H}_2^{13}\text{C}$                 | 4.70<br>(d of m)                                 | $^1J_{\text{C-H}} = 154.10$                              |
|  | $^{13}\text{CH}_3$                        | 1.60<br>(d of m)                                 | $^1J_{\text{C-H}} = 124.81$                              |
|  | $\text{H}_2^{13}\text{C}$                 | 24.07 (d)  | $^3J_{\text{C-C}} = 3$ Hz                                |
|  | $^{13}\text{CH}_3$                        | 111.13 (t)                                       | $^3J_{\text{C-C}} = 3$ Hz                                |
| $(\text{Cp}^*\text{SiNR})\text{Sc}(^{13}\text{CH}_2\text{C}-$<br>$(^{13}\text{CH}_3)_2) \cdot (\text{P}(\text{CH}_3)_3)$<br>$(5\text{-}^{13}\text{C}_3)$<br><br>300 MHz $^1\text{H}$ , rm temp | $\text{C}_5(\text{CH}_3)_4$               | 2.358 (s)<br>2.278 (s)<br>1.945 (s)<br>1.870 (s) |  |
|  | $\text{NC}(\text{CH}_3)_3$                | 1.426 (s)  |  |
|  | $\text{Si}(\text{CH}_3)_2$                | 0.802 (s)<br>0.629 (s)                           |  |
|  | $\text{P}(\text{CH}_3)_3$                 | 0.645 (br, s)                                    | $^2J_{\text{P-H}}$ not resolved                          |
|  |   |  |  |

Table I (continued).

| Compound/Conditions   | Assignment                               | $\delta$ (ppm)       | J (Hz)   |
|---|--|----------------------|--|
| 5- $^{13}\text{C}_3$ , continued.<br><br>75 MHz $^{13}\text{C}$   | $\alpha$ - $^{13}\text{CH}_2$            | -0.031<br>(d of m)   | $^1\text{J}_{\text{C-H}} = 103.31$                                   |
|   | $\gamma$ - $^{13}\text{CH}_3$            | 2.312<br>(d of m)    | $^1\text{J}_{\text{C-H}} = 116.56$                                   |
|   | $\alpha$ - $^{13}\text{CH}_2$            | 64 (br)              |  |
|   | $\gamma$ - $^{13}\text{CH}_3$            | 28.5 (d)<br>30.5 (d) | $^3\text{J}_{\text{C-C}} = 3$<br>$^3\text{J}_{\text{C-C}} = 3$       |
| (Cp*SiNR)Sc( $^{13}\text{CH}_2\text{C}-$<br>( $^{13}\text{CH}_3)_2$ )•(P(CH $_3$ ) $_3$ )<br>(5- $^{13}\text{C}_3$ )<br><br>125 MHz $^{13}\text{C}$ , 200 K | $\alpha$ - $^{13}\text{CH}_2$            | 61.34                | $(^3\text{J}_{\text{C-C}}$ obscured by<br>10 Hz line-<br>broadening) |
|   | $\gamma$ - $^{13}\text{CH}_3$<br>(bound) | 31.48<br>29.71       |  |
|   | $\gamma$ - $^{13}\text{CH}_3$<br>(free)  | 24.74                |  |

<sup>a</sup>All spectra were obtained in toluene-*d*<sub>8</sub>.

## EXPERIMENTAL SECTION

### General Considerations

All manipulations were performed under an inert atmosphere unless explicitly noted otherwise. NMR spectra were obtained on GE QE-300 and Bruker AM-500 spectrometers.

Triphenyl phosphite was dried and purified by vacuum distillation from  $\text{CaH}_2$ . Solvents for preparative work were distilled in vacuo or under an inert atmosphere from "titanocene" or sodium/benzophenone ketyl before use. Toluene- $d_8$  was purified by stirring overnight over activated 4Å molecular sieves and was stored over "titanocene".

### Preparation of Trimethylphosphine- $^{13}\text{C}_3$

The procedure described here represents a modification of a published, large-scale preparation of trimethylphosphine. Magnesium turnings (0.206 g) were slurried in anhydrous dibutyl ether (50 mL, Aldrich) in a 250-mL three-necked flask, equipped with a reflux condensor,  $\text{N}_2$  flush inlet, and stir bar. With the flask in a bath of room-temperature water, iodomethane- $^{13}\text{C}$  (20 g, 0.140 mmol) was added dropwise. The Grignard solution was then cooled to  $0^\circ\text{C}$ . An addition funnel was charged with dry triphenyl phosphite (11g, 0.035 mmol) and dibutyl ether (20 mL). This solution was added dropwise to the ice-cooled Grignard mixture.

When addition was complete, a distillation head was attached to the top of the reflux condensor and the ice bath was replaced with a heating mantle. The coils of the reflux condensor were filled with water, although water was not circulated through the coils continuously. The reaction mixture was then heated until dibutyl ether refluxed vigorously. The product phosphine was slowly liberated from the mixture and distilled (2.89 g, crude). During practice runs with non-labelled methyl iodide, several different distillation set-ups were tried. Use of a filled, non-circulating reflux condensor was found to facilitate the simultaneous maintenance of ether reflux while allowing the phosphine to distill. The crude product contained a small amount of dibutyl ether, and was distilled once more before use (1.88 g, 71% overall yield).

### Determination of the spin-lattice relaxation time for the methyl carbons in Trimethylphosphine- $^{13}\text{C}_3$

A solution of  $\text{P}(^{13}\text{CH}_3)_3$  in toluene- $d_8$ , sufficiently concentrated to allow for strong  $^{13}\text{C}\{^1\text{H}\}$  spectra to be obtained in eight scans, was prepared in a J. Young NMR tube. The automated routine INVRECX.AUR on a Bruker AM-500 was used to acquire a series of ten 64 K spectra with 32 K of zero-fill, using the 180- $\tau$ -90-observe inversion recovery pulse sequence. The variable  $\tau$  was allowed to vary from 0.012 sec to 60 sec. The following parameters were used: RG (receiver gain) = 20, S1 (NOE decoupler power) = 16H, S2 (observe decoupler power) = 4H, RD (minimum relaxation delay) = 60 seconds. The intensities of the  $\text{P}(^{13}\text{CH}_3)_3$  resonance in each spectrum were recorded, using the AI command to ensure the comparability of intensities between spectra. The same NMR conditions were used to measure eight data points at 200 K. Well-behaved exponential decay of intensity with time was observed. The relaxation time  $T_1$  was determined to be 16.9 seconds at room temperature and 2 seconds at 200 K.

### Preparation of $(\text{Cp}^*\text{SiNR})\text{Sc}[\text{CH}_2\text{CH}(\text{CH}_3)\text{CH}_2\text{CH}_2\text{CH}_3][\text{P}(\text{CH}_3)_3]$

$(\text{Cp}^*\text{SiNR})\text{Sc}[\text{CH}_2\text{CH}(\text{CH}_3)\text{CH}_2\text{CH}_2\text{CH}_3][\text{P}(\text{CH}_3)_3]$  was prepared as previously described, with a modified work-up procedure. After the solid product was isolated from the crude reaction mixture, it was dissolved in petroleum ether and evaporated to dryness four or five times before finally being isolated as a white powder from a cold, concentrated, petroleum ether solution. This procedure was employed in an attempt to force the liberation of phosphine from the product, as has been described for the related propyl and butyl derivatives. One equivalent of phosphine was invariably found in the isolated product.

### Preparation of $(\text{Cp}^*\text{SiNR})\text{Sc}[\text{CH}_2\text{CH}(\text{CH}_3)\text{CH}_2\text{CH}_2\text{CH}_3][\text{P}(^{13}\text{CH}_3)_3]$

$(\text{Cp}^*\text{SiNR})\text{Sc}[\text{CH}_2\text{CH}(\text{CH}_3)\text{CH}_2\text{CH}_2\text{CH}_3][\text{P}(^{13}\text{CH}_3)_3]$  was prepared as described for  $(\text{Cp}^*\text{SiNR})\text{Sc}[\text{CH}_2\text{CH}(\text{CH}_3)\text{CH}_2\text{CH}_2\text{CH}_3][\text{P}(\text{CH}_3)_3]$ , except that  $\text{P}(^{13}\text{CH}_3)_3$  was used in place of  $\text{P}(\text{CH}_3)_3$  during the preparation of the hydride precursor.

## Determination of the spin-lattice relaxation time for the phosphine methyl carbons in $(\text{Cp}^*\text{SiNR})\text{Sc}[\text{CH}_2\text{CH}(\text{CH}_3)\text{CH}_2\text{CH}_2\text{CH}_3][\text{P}(\text{CH}_3)_3]$

A sample of  $(\text{Cp}^*\text{SiNR})\text{Sc}[\text{CH}_2\text{CH}(\text{CH}_3)\text{CH}_2\text{CH}_2\text{CH}_3][\text{P}(\text{CH}_3)_3]$  (23.8 mg, 0.058 mmol) was dissolved in toluene (0.500 mL, 0.104 M) and sealed in an NMR tube for  $T_1$  analysis. Data were collected at 185 K. The concentration used here was significantly higher than that used in equilibrium measurements, to allow for good signal-to-noise with an 8-pulse accumulation. A line-broadening exponential of 3 Hz was applied to the FID's to enhance the signal-to-noise ratio. Otherwise, the NMR parameters and data work-up were the same as described above for  $\text{P}(\text{CH}_3)_3$ . The relaxation time  $T_1$  was determined to be 0.24 seconds.

## Preparation of $(\text{Cp}^*\text{SiNR})\text{Sc}[\text{CH}_2\text{CH}(\text{CH}_3)\text{CH}_2\text{CH}_2\text{CH}_3][\text{P}(\text{CH}_3)_3]$ samples for NMR analysis

A stock solution of  $(\text{Cp}^*\text{SiNR})\text{Sc}[\text{CH}_2\text{CH}(\text{CH}_3)\text{CH}_2\text{CH}_2\text{CH}_3][\text{P}(\text{CH}_3)_3]$  (18.1 mg; 0.0395 mmol) was prepared in toluene- $d_8$  (1.000 mL, 0.0395 M). Samples were prepared adding sample and diluent (volumes were measured by 100- or 1000- $\mu\text{L}$  Hamilton syringe, as appropriate) directly to sealable 5mm NMR tubes. These were frozen, degassed on the vacuum line, and sealed for analysis.

## In situ preparation of $(\text{Cp}^*\text{SiNR})\text{Sc}(\text{CH}_2\text{CH}_2\text{CH}_3)(\text{P}(\text{CH}_3)_3)$

$[(\text{Cp}^*\text{SiNR})\text{Sc}(\text{CH}_2\text{CH}_2\text{CH}_3)]$  was prepared as described elsewhere.<sup>1b</sup> A stock solution of this compound (19.2 mg; 0.0567 mmol) was prepared in toluene- $d_8$  (1.800 mL; 0.0315 M). One equivalent of phosphine was added in one of two ways. In the first method, the stock solution was measured into a sealable NMR tube via Hamilton syringe and diluted with toluene- $d_8$  to the desired concentration. The NMR tube was then attached to a calibrated gas volume (3.3 mL), by way of which, on the vacuum line,  $\text{P}(\text{CH}_3)_3$  was added to the tube in the desired amount. In the second method, a stock solution of  $\text{P}(\text{CH}_3)_3$  (0.050 mL; 0.0473 mmol) was prepared in toluene- $d_8$  (1.000 mL) and an aliquot of this solution (0.063 mL; 0.0284 mmol) was added to an aliquot of the organoscandium stock solution (900  $\mu\text{L}$ ; 0.0284 mmol). This solution was stored in a refrigerator in a dry box and diluted as needed into sealable NMR tubes for analysis.



### Preparation of 1,3,3-<sup>13</sup>C<sub>3</sub>-2-methylpropene

To a toluene (20 mL) solution of triphenylphosphine (3.22 g, 12.3 mmol) was added <sup>13</sup>CH<sub>3</sub>I (0.80 mL, 1.8 g, 12.6 mmol). The mixture was stirred overnight (on the benchtop). The precipitate was collected, dried in vacuo and removed to a dry box, where it was slurried in anhydrous diglyme (80 mL, Aldrich). Mineral oil-free KH (560 mg, 14 mmol) was added to the mixture. Under argon on a Schlenk line, the reaction mixture was heated to 100 °C, stirred overnight, and cooled to room temperature. Against an argon counterflow, 1,3-<sup>13</sup>C<sub>2</sub>-acetone (0.90 mL, 12.3 mmol) was added via syringe. Upon addition of acetone, the reaction mixture became noticeably warm. When it had cooled, it was degassed through a -185 °C (liquid nitrogen) trap. The condensed volatiles were distilled twice on a vacuum line from -60 °C (acetonitrile slurry) traps. The product was stored over lithium aluminum hydride in a glass bomb (521 mg, 70 %).

### Preparation of (Cp\*SiNR)Sc(<sup>13</sup>CH<sub>2</sub>CH(<sup>13</sup>CH<sub>3</sub>)<sub>2</sub>)•P(CH<sub>3</sub>)<sub>3</sub>

[(Cp\*SiNR)ScH(PMe<sub>3</sub>)]<sub>2</sub> (360 mg, 0.969 mmol) was dissolved in toluene (5 mL) in a 10-mL round-bottom flask on a "pencil" frit. 1,3,3-<sup>13</sup>C<sub>3</sub>-2-methylpropene was added via condensation from a calibrated volume (770 Torr in 33.5 mL, 1.39 mmol) and the reaction mixture was stirred at room temperature for one hour. Volatiles were removed and the product was isolated from petroleum ether solution. The isolated product was found to consist of ca. 20% [(Cp\*SiNR)ScH(PMe<sub>3</sub>)]<sub>2</sub>, so all solids were returned to the reaction vessel, redissolved in toluene (5 mL), treated with a further portion of 1,3,3-<sup>13</sup>C<sub>3</sub>-2-methylpropene (134 Torr in 33.5 mL, 0.243 mmol) and allowed to stir overnight at room temperature. Volatiles were removed to obtain a yellow oil which slowly deposited a crystalline solid. Recrystallization from petroleum ether afforded the product as a cream-colored microcrystalline solid (135.5 mg, 0.3147 mmol, 32.5 %).

### Determination of the spin-lattice relaxation time for the labeled alkyl carbons in (Cp\*SiNR)Sc<sup>13</sup>CH<sub>2</sub>CH(<sup>13</sup>CH<sub>3</sub>)<sub>2</sub>•P(CH<sub>3</sub>)<sub>3</sub>

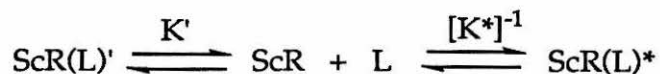
The relaxation time was determined as described above, using an 8.5 × 10<sup>-2</sup> M solution of the complex in toluene-*d*<sub>8</sub>. Good signal-to-noise ratios

were obtained after 8 scans and with the application of 5 Hz of line-broadening. The spectra were acquired at 245 K. At lower temperatures exchange broadening became severe enough to affect the signal-to-noise ratio. A relaxation time of approximately 0.5 seconds was determined for both the  $\alpha$ - and the  $\gamma$ -carbons.

## APPENDIX: Derivation of Equilibrium Expressions and Igor Routines for Their Numerical Solution.

I. Proof that the diastereomers of ScR(L) need not be considered independently.

For the following coupled equilibria,



$$K' = \frac{[\text{ScR}][\text{L}]}{[\text{ScR(L)'}]} \qquad K^* = \frac{[\text{ScR}][\text{L}]}{[\text{ScR(L)*}]}$$

where "ScR(L)'" and "ScR(L)\*" are diastereomers which are interconvertible by phosphine loss and coordination, one may define an overall equilibrium constant such that:

$$(K)^{-1} = (K')^{-1} + (K^*)^{-1} = \frac{[\text{ScR(L)'}]}{[\text{ScR}][\text{L}]} + \frac{[\text{ScR(L)*}]}{[\text{ScR}][\text{L}]} = \frac{[\text{ScR(L)'}] + [\text{ScR(L)*}]}{[\text{ScR}][\text{L}]}$$

Thus the concentrations [ScR] and [L] are related to the sum of diastereomer concentrations [ScR(L)] = [ScR(L)'] + [ScR(L)\*] in the proper way. It is therefore not necessary to explicitly include K' and K\* in the calculations which follow.

## II. Derivation of MonomerSolve

Solution of the equilibrium expression in Scheme II for [{Sc}R] as a function of [Sc]<sub>0</sub> produces the following quadratic equation.

$$[{\text{Sc}}\text{R}]^2 - 2K_m[{\text{Sc}}\text{R}] - K_m[{\text{Sc}}]_0 = 0$$

This equation can be used to plot either [{Sc}RL] or [{Sc}R] as simple functions using the following Igor routine,<sup>17</sup> where the waves "free" and "fbound" have been previously scaled to the concentration range of interest.

Macro MonomerSolve(Km)

Variable Km

Prompt Km, "Enter a phosphine dissociation constant: "

$$\text{free} = (2 * K_m + \sqrt{K_m^2 + 4 * K_m * x}) / 2$$

$$\text{fbound} = (x - \text{free}) / x$$

EndMacro

### III. Derivation of DimerCubicSolve

Solution of the equilibrium expression in Scheme III for  $[(\text{Sc})\text{RL}]$  in terms of  $[\text{Sc}]_0$  yields a cubic equation of the following form.

$$[(\text{Sc})\text{RL}]^3 + (2K_d^2 - 3[\text{Sc}]_0)[(\text{Sc})\text{RL}]^2 + 3[\text{Sc}]_0^2[(\text{Sc})\text{RL}] - [\text{Sc}]_0^3 = 0$$

This expression may be solved<sup>18</sup> over the range  $[\text{Sc}]_0 = [0.0005, 0.05]$  using the following Igor macro, where the appropriate waves (p1, a1, . . . , fbound) have been scaled appropriately.

Macro DimerCubicSolve(K)

Variable K

Prompt K, "Enter an equilibrium constant: "

$$p1 = (2 * K^2 - 3 * x)$$

$$q1 = 3 * x^2$$

$$r1 = -x^3$$

$$a1 = (3 * q1 - p1^2) / 3$$

$$b1 = (2 * p1^3 - 9 * p1 * q1 + 27 * r1) / 27$$

$$\text{prea2} = (-b1/2 + (b1^2/4 + a1^3/27)^{1/2})$$

if (prea2 < 0)

$$a2 = -(abs(-b1/2 + (b1^2/4 + a1^3/27)^{1/2}))^{1/3}$$

else

$$a2 = (-b1/2 + (b1^2/4 + a1^3/27)^{1/2})^{1/3}$$

endif

$$\text{preb2} = (-b1/2 - (b1^2/4 + a1^3/27)^{1/2})$$

if (preb2 < 0)

$$b2 = -(abs(-b1/2 - (b1^2/4 + a1^3/27)^{1/2}))^{1/3}$$

else

```

        b2=(-b1/2 - (b1^2/4 + a1^3/27)^(1/2))^(1/3)
    endif

    x1=a2+b2
    bound = x1-p1/3
    fbound=bound/x
EndMacro

```

### III. Derivation of CoupledCubicSolve.

Solution of the coupled equilibrium expressions in Scheme IV for  $[(\text{Sc})\text{RL}]$  in terms of  $[\text{Sc}]_0$  yields the following cubic equation.

$$[(\text{Sc})\text{RL}]^3 + (2K_1^2K_2^2 - K_1 - 3[\text{Sc}]_0)[(\text{Sc})\text{RL}]^2 + (3[\text{Sc}]_0^2 + K_1[\text{Sc}]_0)[(\text{Sc})\text{RL}] - [\text{Sc}]_0^3 = 0$$

This equation cannot be solved by any single technique<sup>16</sup> over all values of  $[\text{Sc}]_0$  on the appropriate range and for all interesting values of  $K_1$  and  $K_2$ . The two Igor macros which follow, applied simultaneously, will give complete (or nearly complete) solutions. (Note: where one of these routines fails for a given combination of  $K_1$ ,  $K_2$  and  $[\text{Sc}]_0$ , it will be because imaginary numbers are generated. Igor ignores imaginary numbers; thus the plots are not perturbed.)

Macro CoupledCubicSolve(K1,K2)

Variable K1, K2

Prompt K1, "Enter a phosphine dissociation constant: "

Prompt K2, "Enter a dimerization constant: "

$$p1 = (2*K1^2*K2^2 - K1 - 3*x)$$

$$q1 = (3*x^2 + K1*x)$$

$$r1 = -x^3$$

$$a1 = (3*q1 - p1^2)/3$$

$$b1 = (2*p1^3 - 9*p1*q1 + 27*r1)/27$$

$$\text{phi} = \text{acos}(-(b1/2)/\text{sqrt}(-a1^3/27))$$

$$\text{prefactor} = 2*\text{sqrt}(-a1/3)$$

```

x1=prefactor*cos(phi/3)
x2=prefactor*cos(phi/3 + 2*pi/3)
x3=prefactor*cos(phi/3 + 4*pi/3)

bound1 = x1-p1/3
bound2=x2-p1/3
bound3=x3-p1/3

fbound1=bound1/x
fbound2=bound2/x
fbound3=bound3/x
EndMacro

Macro CoupledCubicSolve2(K1,K2)
  Variable K1, K2
  Prompt K1, "Enter a phosphine dissociation constant: "
  Prompt K2, "Enter a dimerization constant: "

  p1 = (2*K1^2*K2^2 - K1 - 3*x)
  q1 = (3*x^2+K1*x)
  r1 = -x^3

  a1=(3*q1 - p1^2)/3
  b1=(2*p1^3 - 9*p1*q1 + 27*r1)/27

  prea2=(-b1/2 + (b1^2/4 + a1^3/27)^(1/2))
  if (prea2 < 0)
    a2 = -(abs(-b1/2 + (b1^2/4 + a1^3/27)^(1/2))^(1/3))
  else
    a2=(-b1/2 + (b1^2/4 + a1^3/27)^(1/2))^(1/3)
  endif

  preb2=      (-b1/2 - (b1^2/4 + a1^3/27)^(1/2))
  if (preb2 < 0)
    b2 = -(abs(-b1/2 - (b1^2/4 + a1^3/27)^(1/2))^(1/3))
  endif

```

```
else
    b2=(-b1/2 - (b1^2/4 + a1^3/27)^(1/2))^(1/3)
endif

x1=a2+b2
bound = x1-p1/3
fbound=bound/x
EndMacro
```

## REFERENCES

1. (a) Shapiro, P. J.; Bunel, E.; Schaefer, W. P.; Bercaw, J. E. *Organometallics* **1990**, *9*, 867.  
 (b) Shapiro, P. J. Ph.D. Thesis, California Institute of Technology, 1990.
2. A family of organoyttrium complexes has been developed recently which is capable of making polyolefins with higher molecular weights and high stereospecificities. Coughlin, E. B.; Bercaw, J. E. *J. Am. Chem. Soc.* **1992**, *114*, 7606.
3. (a) Thompson, M. E.; Baxter, S. M.; Bulls, A. R.; Burger, B. J.; Nolan, M. C.; Santarsiero, B. D.; Schaefer, W. P.; Bercaw, J. E. *J. Am. Chem. Soc.* **1987**, *109*, 205-219.  
 (b) Burger, B.J.; Thompson, M.E.; Cotter, W.D.; Bercaw, J.E. *J. Am. Chem. Soc.* **1990**, *112*, 1566-1577.
4. (a) Watson, P. L. *J. Am. Chem. Soc.* **1982**, *104*, 337.  
 (b) Watson, P. L.; Roe, D. C. *J. Am. Chem. Soc.* **1982**, *104*, 6471.  
 (c) Jeske, G.; Lauke, H.; Mauermann, H.; Sweptson, P.N.; Schumann, H.; Marks, T.J. *J. Am. Chem. Soc.* **1985**, *107*, 8091.
5. (a) Jordan, R. F. *Adv. Organomet. Chem.* **1991**, *32*, 325, and references therein.  
 (b) Hlatky, G. G.; Turner, H. W.; Eckman, R. R. *J. Amer. Chem. Soc.* **1989**, *111*, 2728.
6. (a) Jordan, R. F.; Bajgur, C. S.; Dasher, W. E.; Rheingold, A. L. *Organometallics* **1987**, *6*, 1041.  
 (b) Borkowsky, S. L.; Jordan, R. F.; Hinch, G. D. *Organometallics* **1991**, *10*, 1268.
7. The asymptote in this case is not a constant but a line with positive slope.
8. Associative ligand exchange is also observed in Jordan's related phosphine-supported cationic zirconocene alkyl complexes. See Reference 5a.
9. (a) Two doublets in trace amounts can be discerned between the major resonances. These cannot be identified; however, they are not observed to broaden or shift with temperature, and at lower concentrations they are not



observed, presumably due to the worsening signal-to-noise ratio.

(b) With regard to the discussion of the possibility of a bis(phosphine) adduct (vide supra): It could be argued that, because of the stereogenic center in the alkyl ligand, the two phosphines in such a complex would be diastereotopic and therefore subject to a formal non-degeneracy in chemical shift which would be expected to be slight--as is observed in the carbon resonance at 13 ppm.

However, since this accounts for almost all of the phosphine at most values of  $[Sc]_0$ , this conclusion is stoichiometrically impossible in the presence of only one equivalent of phosphine per scandium.

10. Similar chemistry is observed for THF adducts of zirconocene cations.

Jordan, R. F.; Bajgur, C. S.; Willett, R.; Scott, B. *J. Am. Chem. Soc.* **1986**, *108*, 7410.

11. Reference 1b, p. 108.

12. The discontinuities represent a region where the cubic function describing the equilibrium concentration of  $(Cp^*SiNR)ScR \cdot P(^{13}CH_3)_3$  cannot be solved by either of the routines used (see the appendix to this chapter).

13. Small experimental errors in the low-concentration regime lead to large errors in equilibrium constant, while the high-temperature regime is less susceptible to such errors.

14. The estimated error is derived by comparison of fits to several values of  $K_m$ .

15. It should be noted, however, that the phosphine dissociation constant derived from the earlier kinetic studies was also  $6 \times 10^{-4}$  M.

16. The extreme fluxionality of the propyl complex precludes equilibrium measurements at the high end of the concentration regime of interest, at least with the phosphine-labeled complex.

17. IGOR © 1988-1990, WaveMetrics, Lake Oswego, OR 97035.

18. Hodgman, C. D., Ed. "CRC Standard Math Tables." Chemical Rubber Publishing Company: Cleveland, OH, 1959, pp 358-359.